Sensitivity Analysis of Error in a Roof Membrane Temperature Model Versus Input Data

By

Mathew P. Dupuis, PE

A dissertation submitted in partial fulfillment of the requirements for the degree of

Doctor of Philosophy

(Civil and Environmental Engineering)

At the

University of Wisconsin – Madison

2014

Date of final oral examination: 3/7/2014

The dissertation is approved by the following members of the Final Oral Committee:

Jeffrey S. Russell, Professor, Civil and Environmental Engineering
Chin H. Wu, Professor, Civil and Environmental Engineering
Jae K. Park, Professor, Civil and Environmental Engineering
Bin Ran, Professor, Civil and Environmental Engineering
Patrick D. Eagan, Professor, The Nelson Institute

Abstract:

The use of thermal modeling of the building envelope has become a focal point in building research and building design. The consequences of inaccurate modeling in both fields can lead to poor conclusions and decisions, and it can lead to poor public policy and building designs.

One of the most fundamental decisions made when researchers begin to perform a simulation, using a model, is the selection of input variables for the model. While some of the required input variables have been widely published and are well understood, most are not published or available to the public. This forces the modeler, in research or in design, to decide to expend the resources necessary to measure these unknown variables or to approximate them with no knowledge of the inaccuracies that may result.

This dissertation examines roof membrane temperature model accuracy and its sensitivity to input variable error. In this study, a theoretical lumped capacitance roof membrane temperature model is developed for a building in Manhattan, Kansas. This model is validated against field membrane measurements collected from the building. An experimental analysis by the One Factor At a Time method is made by using the validated model to examine the model accuracy against input variable variation. Input variables studied in this experiment are Interior Temperature (T_I), Thermal Resistance (R), Solar Reflectivity ($\propto_{Solar}$), Insolation (G_{Solar}), Emissivity (ε), Long Wave Irradiance (G_{Long}), Convective Coefficient ($h_{Convection}$), Air Temperature (T_A), Specific Heat Capacity (C), Membrane Mass (U) and Data Sample Rate.

The results of this study provide guidance for researchers and designers on the importance of the studied variables. Specifically, this study produces a ranking for roof membrane temperature model accuracy against the input variables. Using the results of this study, researchers and designers can make educated choices about expending time and resources to quantify input variables for their models that may be unknown or poorly understood.

Table of Contents **Page**

Table of Contents (cont.) **Page**

Master List of Variables

$\propto_{Long}$	Long Wave Reflectivity (%)
$\propto_{Solar}$	Solar Reflectivity (%)
$\Delta_{\%Accuracy}$	Change in Accuracy (%)
Δt	Time period (s)
ΔT	Change in Temperature During Current Time Step (K)
ε	Emissivity (%)
σ	Stefan-Boltzmann constant (5.670373×10^{-8} W / m^2 ·K^4)
A	Unit Area (m^2)
C	Specific Heat Capacity (J/g·K)
E_{Roof}	Emitted Energy From the Roof Membrane (W/m^2)
G_{Solar}	Solar Insolation (W/m^2)
G_{Long}	Long Wave Irradiance (W/m^2)
$h_{Convection}$	Convective Coefficient (W/m^2 ·K)
k	Thermal Conductivity (W/m·K)
L	Roof System Thickness (m)
M	Mass (g)
P	Radiated power From a Surface (W/m^2)
$Percent\ Error_{OFAT}$	Percent Error from OFAT Analysis (%)
$Percent\ Error_{Validated}$	Percent Error from Validation Phase (%)
q''_{Net}	Net Heat flux (W/m^2)
$q''_{Convection}$	Convective Heat Flux (W/m^2)
$q''_{Conduction}$	Conduction Heat Flux (W/m^2)
$q''_{Radiation}$	Radiation Heat Flux (W/m^2)

Master List of Variables (cont.)

R	Thermal Resistance ($m^2 \cdot K/W$)
RH	Relative Humidity (%)
T	Temperature of the Emitting Surface (K)
T_A	Exterior Air Temperature (K)
T_D	Dew Point Temperature (C)
T_I	Interior Building Temperature (K)
$T_{Measured}$	Measured Roof Membrane Temperature (K)
T_{Model}	Model Predicted Roof Membrane Temperature (K)
T_n	Temperature and the End of Current Time Step (K)
T_{n-1}	Temperature at the End of the Previous Time Step (K)
T_S	Roof Membrane temperature (K)
U	Unit Membrane Mass (g/m^2)
W	Wind speed (m/s)

In Memoriam:

Dwight “Rick” L. Gwaltney, III (1949-2011)

This research project and efforts I have made herein are in memory of Rick Gwaltney. Rick was the owner of Diamond Roofing in Kansas where the field portion of this research project took place. Rick always treated me with far more respect than my age and position in life would suggest; a trait we all should strive to emulate more. From the first time I met Rick he genuinely impressed upon me the need to better the roofing industry, to give something back. To that end I hope he would have been proud of this study and the support he provided for it. Rick passed very unexpectedly and I never got a chance to truly thank him for the generosity he showed to me over the years. Thank you, Rick.

Chapter 1: Introduction

1.1 Background

From the early 1900's to the 1970's and 1980's, the predominant roof system used for low slope roofs (roofs with a slope of 10 degrees or less) was a built-up-roof (BUR). A BUR roof is composed multiple layers of a bitumen such as asphalt or coal tar and reinforced with staggered layers of reinforcement fabric. The BUR roof's redundant layers, resistance to mechanical damage, ease of repair, and potential for self-healing of damage served our society well for many decades. Photo 1-1 shows a BUR roof being constructed on the University of Wisconsin – Madison campus.

Photo 1-1 – A BUR roof system being installed on Chamberlin Hall on the University of Wisconsin - Madison campus.

In the 1970's, the United States experienced a dramatic increase in the cost of petroleum based products that carried over into the roofing industry, where the cost of asphalt, constituent to a built-up roof, increased as well. With the pressure of increased roofing costs, the roofing industry began to experiment with a new class of products from Europe as well as the United States. These products have become known as single-ply roof membranes. As the name implies, a single-ply roof membrane, unlike a BUR, is only comprised of a single layer of material. This material layer is a premanufactured polymer sheet. During the late 1970's and early 1980's, Polyvinyl Chloride (PVC) membranes from Europe as well as Ethylene Propylene Diene Monomer (EPDM) membranes from the United States began to see use. The two major

advantages of the single-ply membrane are lower unit prices for materials and labor, which means a lower overall unit cost for single-ply roofs when compared to BURs. However, while single-ply membranes do enjoy a lower overall cost, they have the disadvantage of being a single layer (non-redundant), susceptible to mechanical damage, and they can be more difficult to repair. Photo 1-2 shows a PVC single-ply membrane being installed on a building in Verona, Wisconsin.

Photo 1-2 – A PVC single-ply membrane being installed in Verona, WI. This membrane is termed “fully adhered” as it is installed with an adhesive to a gypsum based cover board. The side lap, by the worker’s foot, will subsequently be welded with a robotic hot air welder to produce a continuous waterproof membrane.

Even with these disadvantages, the single-ply membrane segment of the roofing market grew. Based on surveys of the United States roof market [1, 2], in1979 BUR roofing accounted for 85% of the new construction market and single-ply membranes only 5%. By 2011 these numbers have changed to single-ply membranes accounting for 64% of the market and BUR roofs accounting for less than 10%. Clearly the single-ply membrane is now the dominant roof system in the United States.

Beginning in the late 1990's, a new class of single-ply membrane was brought to the United States from Europe. This membrane is a mixture of Polypropylene and Polyethylene. This product is referred to as Thermoplastic Polyolefin, or TPO. The TPO single-ply membrane is marketed to have the advantages of both the PVC and EPDM roof membranes: TPO is a thermoplastic, so it can be heat welded like PVC, and it is offered at a low material cost to compete against EPDM membranes.

The early formulations of TPO membranes were marred with some very dramatic failures. The roofing industry learned from these failures that formulations of TPO membranes require chemical stabilizers to protect the base polymers of Polypropylene and Polyethylene from degradation by heat and ultraviolet radiation [3-5]. Photo 1-3 shows a degraded sample of TPO roof membrane taken from a roof in Texas.

Photo 1-3 A close up photo of a TPO membrane sample, from a roof in Texas. This TPO membrane was installed for approximately six months before the sample was taken. The polymeric component of the material has completely degraded exposing the reinforcing. This membrane was intended to provide over 20 years of service.

Whether because of market conditions, consumer demand, or contractor preference, in 2011 TPO roofing membrane became the predominant roofing membrane in the United States. As Table 1-1 for New Construction shows, EPDM single-ply membranes had the dominant market share in 2002. By 2011, TPO single-ply membranes assumed the dominant market position.

ROOF SYSTEM SALES FOR NEW CONSTRUCTION (%)						
ROOF SYSTEM	2012	2010	2008	2006	2004	2002
BUR	7.6	8.3	12.5	18.1	15.6	21.9
EPDM	24.4	25.7	29.6	27.0	29.0	28.1
PVC	10.9	9.2	8.7	5.7	8.2	5.8
TPO	31.3	28.5	22.3	16.3	10.4	9.1
METAL	8.9	9.7	10.2	9.5	8.4	7.2
MODIFIED BITUMEN	11.3	12.9	12.9	19.3	23.0	22.2

Table 1-1 Historical sales for roofing market share by roof system type (selected systems)

At the same time that TPO membranes were moving into the U.S. market, another important change was occurring in the U.S. roofing market, the concept of a “cool roof.” A “cool roof” is one that reflects away a large proportion of incoming solar radiation and emits a large portion of energy as a real body radiator. These two factors result in a roof membrane that effectively achieves a lower operating temperature when compared to a standard roof membrane that is situated identically. The concept of a “cool roof” has been embraced by proponents of energy conservation, as less heat energy is available to conduct into the building and thus less needs to be removed by the building’s cooling system. The use of highly reflective roof membranes, or “cool roofs,” has now been integrated into United Sates energy policy [6] and subsequently codified into model and local building codes.

1.2 Introduction

Since the beginning of the “cool roof” movement at the end of the last century, many studies have been conducted [7-12] of highly reflective roof membranes. These studies have almost exclusively focused on the effects that highly reflective roof membranes have on the energy consumption of buildings. Most studies have concluded that highly reflective membranes reduce building energy usage.

These studies and their conclusions are useful for decision makers to determine the best course of action for public policy. However, these studies do little for manufacturers who need to chemically design the roof membranes, building designers needing to do actual energy simulations and the forensic scientists analyzing roof system failures. When a structural engineer is asked to design a beam to carry a load, they need to know what the applied load will be. When chemists and engineers for a manufacturer sit down to design a single-ply roof membrane, they need to know what the applied loads will be. In the case of roof membranes, one of the important loads will be the service temperatures of the membrane.

There are tools now available to architects and engineers to assess building energy consumption. These tools, such as the Department of Energy Cool Roof Calculator and Oak Ridge National Labs Roof Savings Calculator, are both in use by designers to make design choices. Both of these tools assess the heating and cooling impacts roof membrane service temperatures will have on a building.

Roof membrane failures, like the one shown in Photo 1-3, result in large monetary losses for the building owner. In many cases, fault for the failure needs to be assigned by legal proceedings or other kinds of assessment. These failures are typically sorted into classes such as,

but not limited to, failure in manufacture, installation, design, or end use. Being able to forensically determine the service temperature that the roof membrane experienced prior to failure can be vital forensic information. Additionally, the failure of roof systems is not strictly limited to roof membrane failure. The failure of adhesives used to secure roof system components, roof insulation degradation, or even metal roof deck corrosion issues can all be more accurately determined with the knowledge of service temperatures of the roof system and its membrane.

The experimental determination of roof membrane service temperatures has been carried out in the past with mixed results[13, 14]. The most current generation of commercially available modeling programs, called Wärme und Feuchte Instationär and commonly referred to as WUFI, is a finite element analysis program that calculates transient heat and moisture movement for building envelope components. The WUFI program is impressive in its ability to analyze a variety of conditions right out of the box.

However, WUFI was originally developed for the hygrothermal analysis of mass wall systems. As such, this program has some limitations in its applicability to roof systems. Several of the available input variables for the WUFI program are limited in or not available for the user to control. Further complicating the use of programs like this is the lack of material properties built into the program or available in current literature. Concerns about input variables and material data carries over to other programs as well – especially programs used to evaluate building energy use. These programs also hinge on inputs from the user to achieve accurate outputs for decision making.

This issue leaves the end user of these programs in a quandary. Regardless of the end use of an energy or hygrothermal simulation, the accuracy of the output obviously hinges on the

accuracy of the inputs. However, there is a demonstrated lack of input data typically available. Therefore, the program operator may or may not be required to make educated guesses and approximations as to input variables. Typical situations have the program operator entering some variables that are well understood and other variables that are far less so, with little or no understanding of the impact these less understood variables will have on the accuracy of the results.

There currently is no guidance as to the error sensitivity of the program output to the variables required to perform thermal, hygrothermal, or energy simulations for roof systems. With important research, building envelope design decisions, construction cost decisions, forensic investigations, and even public policy decisions being weighted by these energy usage and hygrothermal simulations, it is necessary to study the influence of these variables.

1.3 Problem Statement.

Quantify the amount of error in predicted temperature that errors in the input variables will cause in a roof membrane temperature model.

References

1. Van Ryzin, G., *Reroofing To Highlight 1980 Market*, in *The Roofing Spec*. 1979. p. 42-44.

2. NRCA, *NRCA Market Survey 2011-2012*. 2012, National Roofing Concractors Association.

3. Delgado, A.H., et al. *Investigation of the effect of heat on specially formulated thermoplastic polyolefin (TPO) films by thermogravimetry, dynamic mechanical analysis, and fourier transform infrared spectroscopy*. in *6th International Symposium on Roofing Research and Standards Development, December 2, 2007 - December 2, 2007*. 2007. Tampa, FL, United states: American Society for Testing and Materials.

4. Delgado, A.H., et al. *Thermoplastic polyolefin roof membranes exposed in the western united states for seven years*. in *7th Symposium on Roofing Research and Standards Development, December 4, 2011 - December 5, 2011*. 2011. Tampa, FL, United states: American Society for Testing and Materials.

5. Xing, L. and T.J. Taylor. *Correlating accelerated laboratory, field, and thermal aging TPO membranes*. in *7th Symposium on Roofing Research and Standards Development, December 4, 2011 - December 5, 2011*. 2011. Tampa, FL, United states: American Society for Testing and Materials.

6. Office, U.S.G.P., *Federal Register.* 2012. **77**(96): p. 10.

7. Suehrcke, H., E.L. Peterson, and N. Selby, *Effect of roof solar reflectance on the building heat gain in a hot climate.* Energy and Buildings, 2008. **40**(Compendex): p. 2224-2235.

8. Wray, C. and H. Akbari, *The effects of roof reflectance on air temperatures surrounding a rooftop condensing unit.* Energy and Buildings, 2008. **40**(1): p. 11-28.

9. Synnefa, A., M. Santamouris, and H. Akbari, *Estimating the effect of using cool coatings on energy loads and thermal comfort in residential buildings in various climatic conditions.* Energy & Buildings, 2007. **39**(Copyright 2007, The Institution of Engineering and Technology): p. 1167-74.

10. Akbari, H., *Measured energy savings from the application of reflective roofs in two small non-residential buildings.* Energy, 2003. **28**(953-967).

11. Akbari, H., R. Levinson, and L. Rainer, *Monitoring the energy-use effects of cool roofs on California commercial buildings.* Energy and Buildings, 2005. **37**(Compendex): p. 1007-1016.

12. Konopacki, S. and H. Akbari. *Measured energy savings and demand reduction from a reflective roof membrane on a large retail store in Austin*. in *Society of Plastics Engineers, Vinyltec 2005, October 3, 2005 - October 5, 2005*. 2006. Philadelphia, PA, United states: Society of Plastics Engineers.

13. Wilkes, K.E., *Model for Roof Thermal Performance*. 1989, U.S. Department of Energy: Oak Ridge National Labs. p. 98.

14. Kunzel, H.M., *Simultaeous Heat and Moisture Transport in Building Components*, in *Fraunhofer Institute of Building Physics*. 1995, University of Suttgart: Suttgart, Germany. p. 65.

Chapter 2: Research Methodology

The study was broken into eight (8) phases of work.

2.1 Phase 1 – Problem Identification

The sole objective of this phase was to identify an active problem in the United States roofing industry. The problem, as discussed in Chapter 1, is a general lack of knowledge and information about the in service temperatures of single ply roofing membranes and, specifically, about the variables used to model them. Therefore, this project seeks to establish a validated model for predicting roof surface temperatures and then systematically to study the effects that deliberately introduced input errors have on the predicted membrane temperature against the measured values.

From Chapter 1

1.3 Problem Statement.

Quantify the amount of error in predicted temperature that error in the input variables will cause in a roof membrane temperature model.

2.2 Phase 2 – Existing Literature Review

A preliminary review was conducted of the available research. It is believed that the relevant literature was collected and reviewed. The results of the preliminary literature review are discussed in a Chapter 3 of this paper.

2.3 Phase 3 – Field Data Collection

In order to produce a model and validate it, the collection of actual field data was required. This field data was used as a basis for quantifiable comparisons against predicted values from a mathematical model. This phase of work involved the design, procurement, and installation of a data acquisition system to collect field data. This system was required to:

1. Collect roof membrane temperatures at a user specified sampling interval.
2. Collect roof top meteorological data, to include air temperature, relative humidity, wind speed, wind direction, short wave infrared radiation, and long wave infrared radiation at a user specified sampling interval.
3. Remain flexible enough to accommodate additions and or modifications to the original configuration.

The test site was predetermined by other parties. The system would be installed at the Manhattan, Kansas facility of Diamond Roofing. This location is unique in that Diamond Roofing had installed eight (8) different roof systems to include (3) white thermoplastic polyolefin (TPO), a white ethylene propylene diene monomer (EPDM), a black EPDM, a grey

polyvinyl chloride (PVC), a white polymer-modified bitumen (mod bit), and a standing seam metal roof system, all of which were installed on a single building and over a common interior air space. An elevated view of this roof is shown in Photo 2-1.

This building with the numerous collection of roof systems utilizing the same fully adhered attachment method, with the same roof cross section of structural and insulating components, over the same interior space offered a unique opportunity for the purposes of this study. By utilizing this building with these attributes the study can control and eliminate variables that are routinely introduced into other studies [1, 2]

Details of the field data collection system are discussed in Chapter 4 of this paper.

Photo 2-1 An overall view of the Manhattan, Kansas test bed facility.

2.4 Phase 4 – Roof Membrane Temperature Model

The construction of a closed form time step roof membrane temperature model for the membranes present at the Manhattan, Kansas facility was Phase 4 of the work. The basic components of the model are terms for heat transfer via conduction, convection, and radiation.

These terms and the subsequent model were assembled from the treatments within a traditional heat transfer text [3], combined with information within additional research papers[4-6].

As will be discussed in the literature review of Chapter 3, several efforts have been made to produce roof membrane temperature models. The efforts vary from simple analytical to extremely complex theoretical finite element approaches. In the previous studies, little, if any, accuracy was gained with increasingly complex routes. The optimum approach appears to be a closed form analytical model with an emphasis placed on the accuracy of inputs and coefficients, the focus of this study.

The measured inputs for this study were interior building temperature, exterior air temperature, wind speed, incoming short wave infrared, incoming long wave infrared, and roof surface temperature from the previous time step. Other model inputs include material properties such as membrane mass, membrane specific heat, membrane infrared emissivity, membrane short wave infrared reflectance, and roof system thermal resistance. The convective coefficient for convective heat transfer was also required for the roof membrane temperature model.

2.5 Phase 5 – Roof Membrane Temperature Model Validation

This phase focuses on validating the roof surface temperature model from Phase 4. The output from the roof membrane temperature model is compared to the actual temperatures recorded from Phase 3. The output from the previous time step is used to calculate the output for the following time step. If there were a flaw in the model, it would be clearly evident, as it is run in

comparison to the Phase 3 data for an entire day; the 8,640 successive calculations would diverge quickly.

A calculation of percent error, shown below in Equation 2-1, for predicted versus measured temperature is the metric used for validating the model.

$$\boldsymbol{Precent\ Error} = \frac{|\boldsymbol{T_{Measured}} - \boldsymbol{T_{Model}}|}{\boldsymbol{T_{Measured}}} \boldsymbol{X100}$$

Equation 2-1 Formula for Percent Error.

Where:

$T_{Measured}$ = Field Measured Temperature (K)

T_{Model} = Model Predicted Temperature (K)

2.6 Phase 6 - Calculation of Predictive Model Baseline Error

In order to establish a point of reference for the next phase, the validated model was used to tabulate the composite percent error for all membranes and days in the population.

2.7 Phase 7 - Calculation of Model Error Sensitivity for Model Inputs

Using the baseline cumulative percent error from Phase 6, the problem statement can be investigated. The One Factor At a Time (OFAT) method of sensitivity analysis was used. Each of the input radiation variables, meteorological variables and the measured material properties for the roof membrane temperature model were individually manipulated by 20% of their

measured values. The resulting change in percent error is tabulated against the variable manipulated.

The variables investigated are:

1. Interior Temperature (T_I)
2. Thermal Resistance (R)
3. Solar Reflectivity ($\propto_{Solar}$)
4. Insolation (G_{Solar})
5. Emissivity (ε)
6. Long Wave Irradiance (G_{Long})
7. Convective Coefficient ($h_{Convection}$)
8. Air Temperature (T_A)
9. Specific Heat (C)
10. Membrane Mass (U)

References

1. Akbari, H., *Measured energy savings from the application of reflective roofs in two small non-residential buildings.* Energy, 2003. **28**(953-967).

2. Akbari, H., R. Levinson, and L. Rainer, *Monitoring the energy-use effects of cool roofs on California commercial buildings.* Energy and Buildings, 2005. **37**(Compendex): p. 1007-1016.

3. Incropera, et al., *Fundamentals of Heat and Mass Transfer*. 6th Edition ed. 2007: Wiley. 995.

4. Hoglund, B.I., G.P. Mitalas, and D.G. Stephenson, *Surface temperatures and heat fluxes for flat roofs.* Building Science, 1967. **2**(1): p. 29-36.

5. Rose, W.B., *White Roofs and Moisture in the US Desert Southwest*, in *Buildings X*. 2007, Oak Ridge National Labs: Clearwater Beach, Florida.

6. Wilkes, K.E., *Model for Roof Thermal Performance*. 1989, U.S. Department of Energy: Oak Ridge National Labs. p. 98.

3 Literature Review

A part of this research was a review of available literature on the subject matter. More literature was acquired and studied than represented here, and approximately half of the works reviewed proved relevant to the subject matter of this author's research. The following is a brief review of the relevant literature.

As discussed in previous chapters, the quantifications of errors in temperature modeling of the service temperature of a roof is the goal of this study. Therefore, the literature reviewed focuses on the topics of building science, physics, and heat transfer. Building science is a recently derived label for the study of the building envelope (e.g. roofs, walls, windows, doors, etc.) and how it functions over the life of the building. In the end, building science will be the main categorization for this study. The treatment of heat transfer is a foundation for this study. Much of the literature reviewed focuses heavily on the heat transfer concept; they generally explore energy savings and lower building temperatures by utilizing highly solar reflective or "cool" coatings. The heat transfer concept for this study is very similar but will require additional manipulation to reach the study goal.

In Building Science, the concept of different materials with different operating temperatures versus solar insolation is not a new idea. In 1929 Houghton [1] observed the temperature and solar absorptivity of various building materials. Later, Goodman [2] conducted experiments with various building materials, putting forth an early attempt at modeling the heat transfer that takes place. The 1960's and 1970's provided new studies. Hoglund [3] made an excellent effort to model heat flux through a roof system. His calculated results trended well with the measured response, but they were systematically off from the measured by almost constant

amounts. The error in Hoglund's work appears to be based on issues with assumptions made in the long wave radiation balance between the roof surface and atmosphere.

In 1979, Michell [4] explored the possibilities of using selective surfaces for building cooling. Michell's results proved that selective surfaces are of little value for cooling, over a blackbody. However, this work has value in that it represents one of the first published pieces quantifying night time radiative cooling for roof membranes. Prior to Mitchell's study, the phenomenon was known [3] but apparently never quantified for the roof.

The 1980's brought several new studies. In 1981 Abrantes [5] produced one of the early works in computerized building energy modeling. In this work he stated that the exterior air temperature, wind direction, wind speed, and incident radiation on the roof were the only external inputs needed. The paper lacks detail in the calculations and results, but still represents an early heat transfer analysis by computer.

Nayak et al. [6] looked at different passive ways to keep roofs in India cool. In order to evaluate the different methods, they produced a heat transfer model for the roof in the indefinite form. This model was manipulated with concepts such as shading, roof ponding, green roofing, and reflective techniques. The green roof proved the most successful theoretical technique for reducing heat flow through the roof. Interestingly, this work also appears to represent one of the earliest works quantifying the benefits of green roofing.

1986 brought a study by Flynn [7]. In this study, three (3) buildings in the San Diego area were instrumented for temperature and data recorded before and after the application of a reflective roof coating. Previous studies that dealt with material reflectivity, such as those conducted by Houghton and Goodman, identified the material's ability to sustain lower temperatures by reflecting incident solar radiation. Flynn's study was of a full-scale field experiment with reflective materials on a roof.

In the late 1980's Oak Ridge National Labs made an attempt to create a roof temperature model. This model, called STAR (Simplified Transient Analysis of Roofs), was published by Wilkes [8] in 1989. The theoretical treatment of the conduction, convection, and radiation terms are very similar to the approach used in the present study. However, a lack of accurate material properties and an underestimation of the radiation terms seem to have plagued the Wilkes model. In the conclusion, Wilkes claims that the model was successfully validated. However, the data presented in the paper suggests otherwise. The model achieved parity between the experimental and recorded roof membrane temperature for very short periods during the day. At other points in the day, the model tended to routinely under predict the temperature extremes, day and night, by 10°F - 15°F.

In the 1990's the concept of cool roofing was formally introduced. Cool roofing materials are those that have a high reflectance to solar loads and high emissivity in the long infrared range. Berdahl [9] provides a very thorough review of reflectivity of various roof coatings and membranes. His work also included an in depth look at the effects surface roughness has on the reflectivity of the material. Al-Turki [10] looked at the impact increasing roof stone ballast can have on energy savings. Al-Turki focused on the variables of ballast mass over area and size of the stone. Akridge [11] made an experimental study on the application of a cool roof coating, finding a 27% peak air conditioning energy reduction near Atlanta, GA. Yarbrough [12] made theoretical calculations for the use of cool roof coatings. His calculations found up to a 60% reduction in heating and cooling loads.

In 1995 a seminal piece of work was published in Germany by Künzel [13] as a doctoral dissertation at the University of Stuttgart. This work focused on the mathematical model behind the current WUFI (Wärme und Feuchte Instationär) finite element analysis program for hygrothermal analysis. As discuss in chapter 1, this program was developed for mass wall systems. The mathematical model behind WUFI does carry over to roof systems. However, there

is a very distinct lack of material information available, and the convective heat transfer coefficient is very rudimentary. These facts limit the widespread use of WUFI in the design market and necessitate this work.

The turn of the century brought a renewed sense of green building and energy efficiency in our built environment. Following this trend, the research papers on cool roofing and energy efficiency drastically increased in numbers.

In 2000, passive night cooling of roof surfaces in tropical zones was experimentally studied by Khedari [14]. He found night roof temperatures 1°C - 6°C below ambient temperature. Al-Sanea [15] produced a theoretical numerical model based on a finite-volume method for heat flow and temperature of various roof systems under time variable atmospheric inputs. The results of Al-Sanea's work were not surprising: the theoretical roof system with the most thermal insulation proved to be the most effective at lowering heat transfer to the building interior.

Tang [16] provided a theoretical treatment of the thermal behavior of curved roof surfaces. Essentially, the standard methods and models provide for incoming radiation incident to a flat surface. A surface such as a dome requires the use of the same principals as a flat roof surface, but a far more elaborate system of accounting for the radiation exchange.

In 2003 and in 2005 Akbari [16] [17] produced field studies of roof temperatures and building energy usage before and after the application of a cool roof coating on the existing roof. All of the buildings monitored were in California and Nevada. In this climate region the results of the studies are not surprising, finding lowered cooling costs with cool roof coatings. The reported results varied from \$0.67 - \$2.0 per m^2 of roof area per year. In 2008, Jo [18] produced a similar study of a 144,236ft^2 single story office building in Arizona. Through computer modeling, using a United States Department of Energy program called EnergyPlus and field

temperature data, Jo reported a net reduction of 2.8 - 3.4% of the building's total electricity consumption by covering the roof with a reflective surface.

According to Jain [19], in many developing countries the availability and reliability of electricity based cooling systems is low. Passive cooling techniques are attractive in these regions. Some methods Jain explored for cooling are evaporative roof cooling and roof ponds. Both of these concepts were tested in experiments conducted during the 1960s and 1970s [20] but were generally abandoned by developed countries as impractical and high risk in event of leakage. However, academic studies continue to explore these concepts because they do work [19] [21].

In 2007 Rose [22], examined moisture accumulation under cool roof membranes. In his study, he discusses the basic theoretical temperature model used. Rose focused on the night time radiative cooling aspect of membranes and the lower membrane service temperatures of highly reflective membranes. The results of this study found an inability for cooler operating membranes to move accumulated moisture away.

In Australia, Suehrcke [23] produced a theoretical paper in 2008 examining the effects of "roof colour" on heat gain for buildings. The theoretical exercise Suehrcke undertakes is of little academic value as it recreates work done by others such as Berdahl, Akrdige and Akbari years earlier. In fact, the paper arrives at the exact same conclusions that reflective roof surfaces are advantageous in hot climates by reducing cooling loads. The paper does have some value in that it briefly explores the effects of the total energy absorbed by a roof against the assumed sky temperature. With the sky temperature theoretically varied by 20°K, the net energy absorbed by the roof varied by approximately 50%. This finding does indicate the importance of accurate sky temperature readings for accurate heat transfer calculation.

Kaska [24] compared theoretical calculations to experimental data for differing wall constructions in Turkey. In addition to the walls, he instrumented and analyzed the roof of the test structure. Using his theoretical model, he was able to achieve 1°C - 2°C differences between the theoretical and experimental data during afternoon hours.

In developing an accurate roof membrane temperature model, one of the major difficulties lies in the convection coefficient of the heat transfer. In 2009 Jiantao showed that many of the analytical attempts to produce a coefficient model fall short as they each seem to utilize different parameters and have large errors accumulated during measurements [25]. In the heat transfer field many of the coefficient models are arrived at via small scale wind tunnel testing and do not carry over well to real buildings. Shao determined a wind speed based coefficient of $h_{conv} = 6.91V + 3.9$ (h_{conv} in W/m^2 K and V in m/s). This result correlated well with a more traditional heat balance method for the coefficient.

In 2011, the present author [26] presented a paper on night time radiative cooling of low slope roofing membranes at the International Roofing Symposium was held in Washington D.C. In this study, it was shown that low slope roof membranes cool 10°C below air temperature on typical nights.

The decay of roofing materials exposed to the environment is a constant factor in the life cycle of a roof. Berdahl [27] provides a summary of the major factors causing degradation of roofing materials. These factors included wind, precipitation, moisture, atmospheric gases, pollutants, biological growth, ultraviolet exposure, and elevated temperatures. The mechanism of the most interest here is elevated roof temperatures. The degradation of roof membranes typically involves chemical reactions. By the Arrhenius equation, increases in temperature can lead to exponential increases in reaction rates; therefore, roof membrane temperatures are of great concern to the roofing industry. The prediction of service temperatures could lead to better system selection and / or design methodology.

The component of temperature-based degradation of single-ply roofing membranes has been given a good deal of discussion in the last few years. As discussed and shown in Chapter 1, TPO membranes have become the most widely used low-slope roofing membrane in the United States. Several papers [28, 29], coauthored by multiple well known roofing groups, have focused on the premature aging of TPO membranes caused by heat aging. These papers conclude that the prominent cause was chemical Ultra-Violet and thermal stabilizers migrating within and out of the TPO matrix. The loss of these stabilizers was primarily caused by elevated membrane temperatures. This fact further reinforces the need for this research.

References

1. Houghten, F.C. and C. Gutberlet, *Absorption of solar radiation in its relation to the temperature, color, angle and other characteristics of the absorbing surface.* Heating, Piping and Air Conditioning, 1929. **1**(8): p. 677-682.

2. Goodman, W., *Figuring solar heat gains of buildings.* Heating, Piping and Air Conditioning, 1938. **10**(10): p. 657-659.

3. Hoglund, B.I., G.P. Mitalas, and D.G. Stephenson, *Surface temperatures and heat fluxes for flat roofs.* Building Science, 1967. **2**(1): p. 29-36.

4. Michell, D. and K.L. Biggs, *RADIATION COOLING OF BUILDINGS AT NIGHT.* Applied energy, 1979. **5**(Compendex): p. 263-275.

5. Abrantes, V. and N. Galanis. *PREDICTION AND MEASUREMENTS OF THE DYNAMIC THERMAL BEHAVIOR OF BUILDINGS*. in *CANCAM 81: Comptes Rendus 8th Congres Canadien de Mecanique Appliquee.* 1981. Moncton, NB, Can: Univ of Moncton, Faculty of Science & Engineering.

6. Nayak, J.K., et al., *RELATIVE PERFORMANCE OF DIFFERENT APPROACHES TO THE PASSIVE COOLING OF ROOFS.* Building and Environment, 1982. **17**(Compendex): p. 145-161.

7. Flynn, J. and H.M. Gueven. *SOLAR HEAT-REDUCING PROPERTIES OF REFLECTIVE ROOFING MATERIALS*. in *Strategic Planning for Cogeneration and Energy Management. Papers from the 8th World Energy Engineering Congress.* 1986.

8. Wilkes, K.E., *Model for Roof Thermal Performance*. 1989, U.S. Department of Energy: Oak Ridge National Labs. p. 98.

9. Berdahl, P. and S.E. Bretz, *Preliminary survey of the solar reflectance of cool roofing materials.* Energy and Buildings, 1997. **25**(Compendex): p. 149-158.

10. A.M. Al-Turki, H.N.G., G.M. Zaki, *Comparative study on reduction of cooling loads by roof gravel cover.* Energy and Buildings, 1997. **25**(1).

11. Akridge, J.M. *High-albedo roof coatings - impact on energy consumption*. in *Proceedings of the 1998 ASHRAE Winter Meeting. Part 1 (of 2), January 18, 1998 - January 21, 1998*. 1998. San Francisco, CA, USA: ASHRAE.

12. Yarbrough, D.W. and R.W. Anderson, *Use of radiation control coatings to reduce building air-conditioning loads.* Energy Sources, 1993. **15**(Compendex): p. 59-66.

13. Kunzel, H.M., *Simultaeous Heat and Moisture Transport in Building Components*, in *Fraunhofer Institute of Building Physics*. 1995, University of Suttgart: Suttgart, Germany. p. 65.

14. Khedari, J., et al., *Field investigation of night radiation cooling under tropical climate.* Renewable Energy, 2000. **20**(Compendex): p. 183-193.

15. Al-Sanea, S.A., *Thermal performance of building roof elements.* Building and Environment, 2002. **37**(Compendex): p. 665-675.

16. Akbari, H., *Measured energy savings from the application of reflective roofs in two small non-residential buildings.* Energy, 2003. **28**(953-967).

17. Akbari, H., R. Levinson, and L. Rainer, *Monitoring the energy-use effects of cool roofs on California commercial buildings.* Energy and Buildings, 2005. **37**(Compendex): p. 1007-1016.

18. Jo, J.H., et al., *An integrated empirical and modeling methodology for analyzing solar reflective roof technologies on commercial buildings.* Building and Environment, 2010. **45**(Compendex): p. 453-460.

19. Jain, D., *Modeling of solar passive techniques for roof cooling in arid regions.* Building and Environment, 2006. **41**(Compendex): p. 277-287.

20. Yannas, S., *Roof Cooling Techniques a Design Handbook*. 1st ed. 2006: Earthscan.

21. Keskinel, S. *A SUPERINSULATED MOBILE HOME THAT UTILIZES A ROOF POND IN HOT, ARID CLIMATES* 1995 11/11/10]; http://www.usc.edu/dept/architecture/mbs/papers/ecs/95_roofpond/roof_95.html].

22. Rose, W.B., *White Roofs and Moisture in the US Desert Southwest*, in *Buildings X*. 2007, Oak Ridge National Labs: Clearwater Beach, Florida.

23. Suehrcke, H., E.L. Peterson, and N. Selby, *Effect of roof solar reflectance on the building heat gain in a hot climate.* Energy and Buildings, 2008. **40**(Compendex): p. 2224-2235.

24. Kaska, O. and R. Yumrutas, *Comparison of experimental and theoretical results for the transient heat flow through multilayer walls and flat roofs.* Energy, 2008. **33**(GEOBASE): p. 1816-1823.

25. Jiantao, S., et al., *A novel method for full-scale measurement of the external convective heat transfer coefficient for building horizontal roof.* Energy and Buildings, 2009. **41**(Copyright 2009, The Institution of Engineering and Technology): p. 840-7.

26. Dupuis, M., *Nighttime Radiative Cooling of Low Slope Roofs*, in *International Roofing Symposium* 2011, National roofing Contractiors Assoctaion (NRCA): Washington D.C.

27. Berdahl, P., et al., *Weathering of roofing materials - an overview.* Construction and Building Materials, 2008. **22**(Copyright 2008, The Institution of Engineering and Technology): p. 423-33.

28. Delgado, A.H., et al. *Investigation of the effect of heat on specially formulated thermoplastic polyolefin (TPO) films by thermogravimetry, dynamic mechanical analysis, and fourier transform infrared spectroscopy*. in *6th International Symposium on Roofing Research and Standards Development, December 2, 2007 - December 2, 2007*. 2007. Tampa, FL, United states: American Society for Testing and Materials.

29. Delgado, A.H., et al. *Thermoplastic polyolefin roof membranes exposed in the western united states for seven years*. in *7th Symposium on Roofing Research and Standards Development, December 4, 2011 - December 5, 2011*. 2011. Tampa, FL, United states: American Society for Testing and Materials.

Chapter 4: Field Data Collection

4.1 Location

Phase 3 of the proposed study involved collection of field rooftop data. This phase of the work required the design, procurement, and installation of a data acquisition system, along with the collection of data.

As discussed in Section 2.3, a test site was made available for use in this study through the courtesy of the Midwest Roofing Contractors Association (MRCA). This test site was located in Manhattan, Kansas. The site is unique in that the building owner had installed eight (8) different roof systems to include (3) white thermoplastic polyolefin (TPO), a white ethylene propylene diene monomer (EPDM), a black EPDM, a grey polyvinyl chloride (PVC), a white polymer-modified bitumen (mod bit), and a standing seam metal roof system on one building and over a common interior air space.

Having the same building roofed with these multiple membranes, on the same slope, utilizing the same insulation system, and over a common interior space was very advantageous for the purposes of this study. Other studies involving actual field data typically utilize different roofs on different buildings [1, 2]. Other studies focus on field data from one building, but have only one roof membrane present [3, 4]. Examining a single building with multiple roof membranes provides this study with a control on numerous variables that other studies lack. Each of the variables that have been controlled in this study is given a full treatment in the chapters and sections to follow.

4.2 Basic System Components

Table 4-1 outlines the components of the field data acquisition system and their purpose.

Instrument	Measurement	Make / Model
Thermocouple	Surface Temperature (°F/°C)	Omega / SA-1
Pyranometer	Short wave (W/m^2)	Hukseflux / SR11
Pyrgeometer	Long wave (W/m^2)	Hukseflux / IR02
Data Acquisition (DAQ)	Data Sampling (S/s)	NI / Compaq RIO
Meteorological Station	Wind Speed (mph) Wind Direction (degrees) Air Temperature (°F/°C) Relative Humidity (%) Precipitation Rate (in/hr)	Davis Instruments / Vantage Pro2
Computer Program	Data Collection (S/s)	NI / LabVIEW 2010

Table 4-1 Overview of field data acquisition system.

4.3 Roof Membrane Temperature Sensors

For measuring the temperature of the roof membranes, Type T thermocouples (Copper/Constantan) were chosen. Type T thermocouples were chosen for two specific reasons. The first is their common commercial availability. Type K, K, T and E thermocouples are widely available from many commercial sources. The second and far more important reason for the

Type T selection is its accuracy rating under ASTM E230. Type T thermocouples are listed under this standard to have an accuracy of "The greater of ±0.5°C or ±0.4 %" for Special Tolerances. For comparison, Type K and J thermocouples are listed as "The greater of ±1.1°C or ±0.4 %" for Special Tolerances.

Omega Engineering SA-1 Type T thermocouples were selected. These units have a self-adhering capability. The self-adhering patch can be placed on the backside of the roof membranes so that it remains fixed in place. In addition, the SA-1 have the advantage of being only available as the increased accuracy "Special Tolerance" class of thermocouple.

Prior to deployment, all thermocouples used were subjected to a 4-point calibration check. In each case, none of the thermocouples varied more than ±0.1°C at any calibration point. During installation, the thermocouples were placed directly under the roof membrane. The leads were passed through a drilled hole approximately one foot away. "Special Tolerance" Type T thermocouple wire was used for the leads back to the data acquisition system.

4.4 Meteorological Station

To record roof top meteorological conditions such as air temperature, relative humidity, wind speed, wind direction, and precipitation rate, a meteorological station was needed. The Davis instruments Vantage Pro2 Plus was selected for this purpose.

Given the availability of the sophisticated data acquisition system in use for this study, it would have been preferable to assemble a custom meteorological station from various

manufacturers. However, the budget for this was not available. The meteorological station in use here provides an acceptable level of accuracy and falls in line with the roof membrane thermocouples in terms of tenths of a degree accuracy.

The Davis Vantage Pro2 Plus fit into the project budget. This unit has acceptable accuracy in the integrated instrument package. In addition, the Vantage Pro2 has software that allows it to data log to a computer against the computer's system clock. This feature allowed the data from the rest of the field data acquisition system, roof membrane temperature, and radiation sensors to be logged against the same clock as the meteorological data, which allowed the data to be merged in later phases of the study.

4.5 Short Wave Radiation

Radiation from the sun that reaches the Earth's surface is typically referred to as solar radiation or short wave radiation. These terms are generally interchangeable for building envelope thermal studies. The term short wave is relative to the longer wave lengths of infrared radiation in flux on a terrestrial surface.

Short wave radiation is in the electromagnetic spectrum in the range of approximately 280nm to 3000nm. Most of the Ultraviolet (UV) spectrum, visible spectrum, near-infrared (NIR), and short wave infrared spectrums are included in the electromagnetic spectrum. The short wave radiation incident to a building's surface is measured in watts per square meter (W/m^2)

The primary detector for determining the incident short wave radiation on a surface is a Pyranometer. There are several commercial manufacturers of research grade pyranometers in the world. For this study, a Hukseflux SR11 was utilized. The SR11 is a first class pyranometer by ISO classification. Its manufacturer reported response spectrum is 285nm to 3000nm. The SR11 measures 180 degree hemispherical incident radiation, within its response spectrum.

The roof slope on the Manhattan, Kansas building is 1:12 slope or 4.76°. Once the SR11 was leveled to gravity, then it was rotated, with an inclinometer to match the slope. This rotation ensured accuracy by accounting for the radiation incident on the plane of the roof, including any potential terrestrial radiation sources by reflection. Figure 4-1 demonstrates the hemispherical field of view as mounted on the building. Photo 4-2 shows the SR11 mounted on the roof.

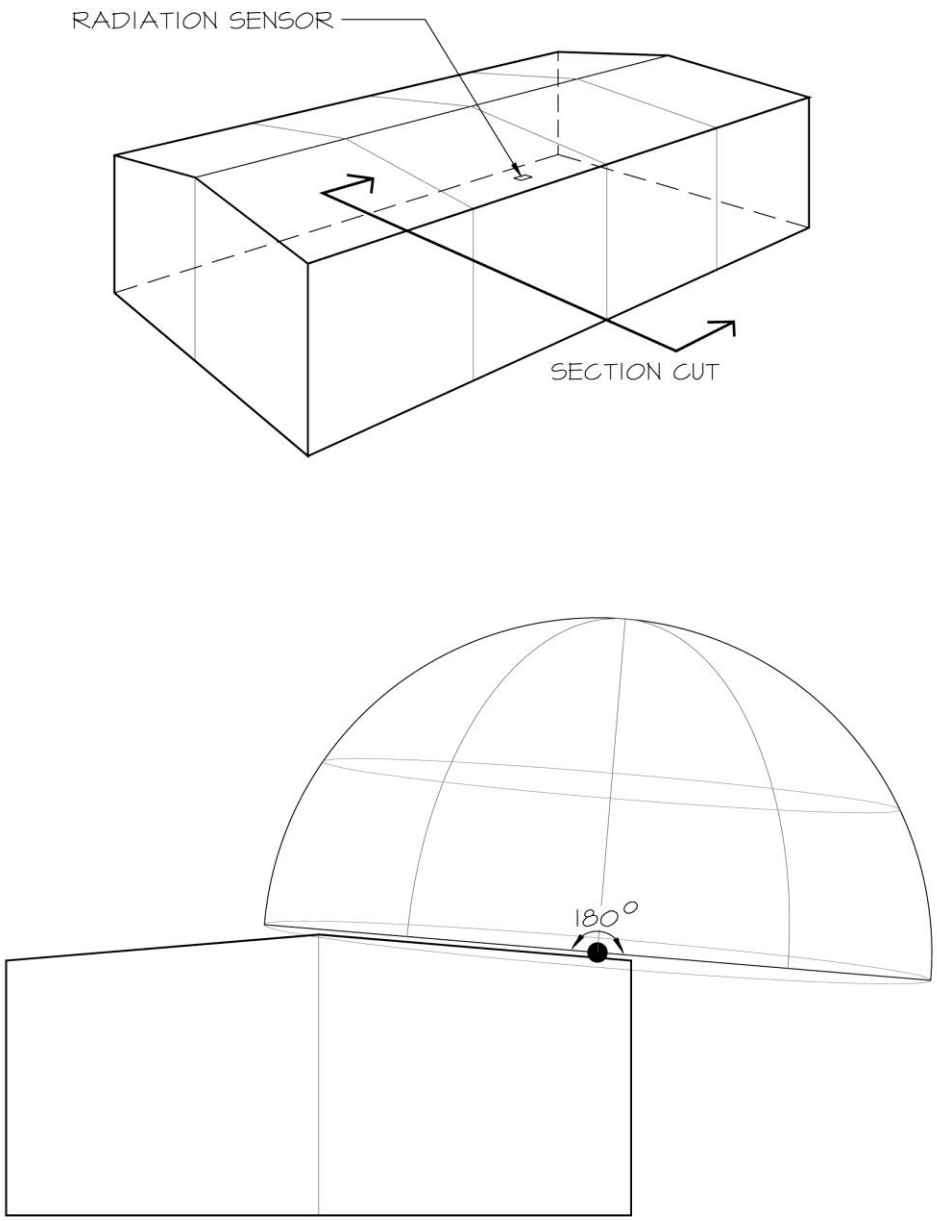

Figure 4-1 180 degree hemispherical field of view for the SR11.

Photo 4-2 Hukseflux SR11 and IR02

4.6 Long Wave Radiation

Long wave radiation refers to infrared radiation beyond the 3000nm cut off for the short wave. The long wave radiation spectrum is typically considered to run from 3000nm to 50,000nm. For a point of reference, a common infrared camera from a company such as FLIR is sensitive to the 8,000nm-12,000nm range.

All matter above absolute zero emits infrared energy. This includes the atmospheric gases and atmospheric water vapor, and the dust and clouds above the roof. The long wave radiation emitted by sources located above the roof will lead to an irradiance. In order to measure the incident long wave infrared radiation to the roof, an instrument called a pyrgeometer is utilized.

In most available building envelope studies, investigators make an approximation of the incoming long wave radiation. Typical studies will make approximations utilizing time of day, relative humidity, and air temperature by authors such as Berdahl and Martin[5]. However, these are only approximations. In order to maximize the accuracy of the roof membrane radiation exchange calculations a pyrgeometer is required.

For this study, a Hukseflux IR02 Pyrgeometer was utilized. The spectral sensitivity of the IR02 is reported as 4,500nm to 40,000nm. The IR02 has a field of view of 150°. As the IR02 is mounted on the same cross arm as the SR11, it too was mounted and leveled to gravity and then rotated to match the plane of the roof. Figure 4-2 shows the field of view for the IR02. The IR02 is shown installed with the SR11 Pyranometer in Photo 4-2.

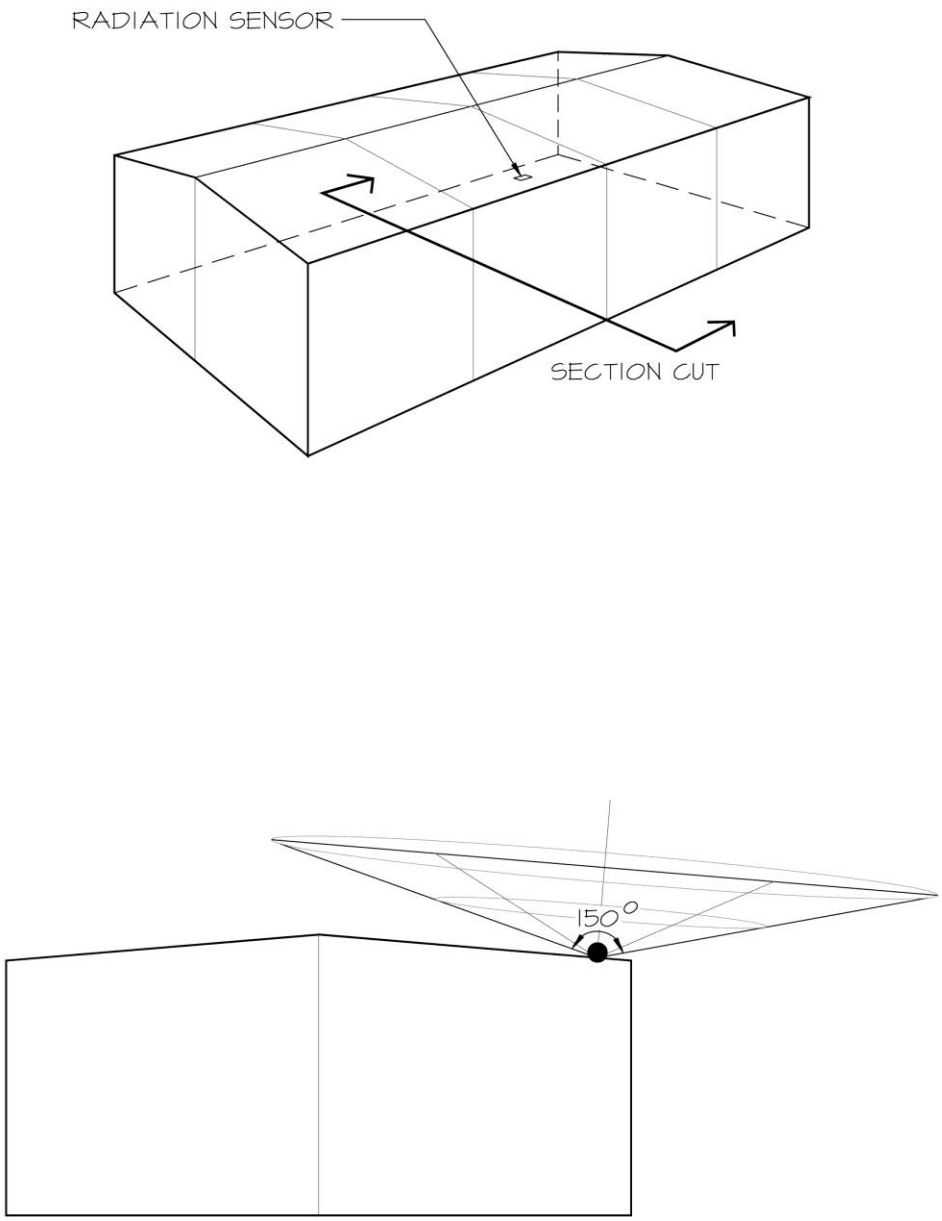

Figure 4-3 Combined field of view for the IR02 (150°) with the SR11 (180°)

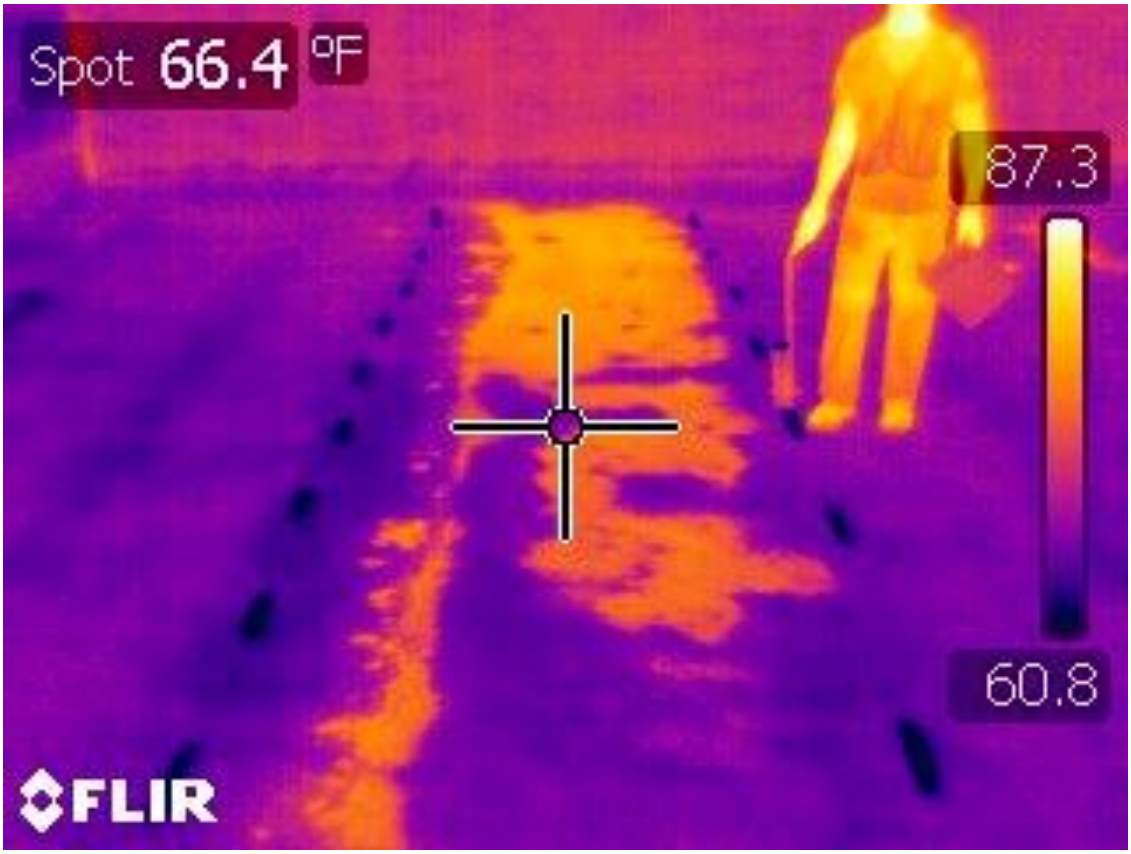

Photo 4-3 Infrared image of a moisture survey being conducted on a 500,000 ft^2 warehouse roof. The warm areas are areas of moisture-laden insulation that, with increased moisture mass, retain higher temperatures into the night.

4.7 Data Acquisition

The pyranometer, the pyrgeometer, and the leads for roof membrane thermocouples were routed to a data acquisition system (DAQ). The National Instruments Compact RIO (NI-cRIO 9073) real time data acquisition back plane was utilized for data acquisition.

The Compact RIO DAQ is a modular chassis system, allowing it to be configured with numerous variations of data collection modules. Compact RIO modules are available for accelerometers, strain gauges, microphones, voltage, current, Resistance Thermal Devices

(RTD), and thermocouples as examples of instruments these modules are able to measure. For this study, the DAQ was outfitted with a pair of National Instruments 16 channel thermocouple modules (NI 9213) for roof membrane thermocouple readings. This gave the DAQ a total of 32 channels for temperature readings.

In addition to the thermocouple modules, a 4-channel voltage module (NI 9211) and a 4-channel RTD module (NI 9217) were installed to record the voltage and RTD outputs from the pyranometer and pyrgeometer.

The Compact RIO DAQ chassis only acquires the signals. After acquisition, the DAQ consolidates the signals and transmits them over a wireless or wired TCP/IP network for analysis and / or collection by a computer. In this study, the DAQ was connected to an onsite desktop PC computer via standard TCP/IP over a 10/100 Ethernet network. Photo 4-4 shows the NI Compact RIO system installed.

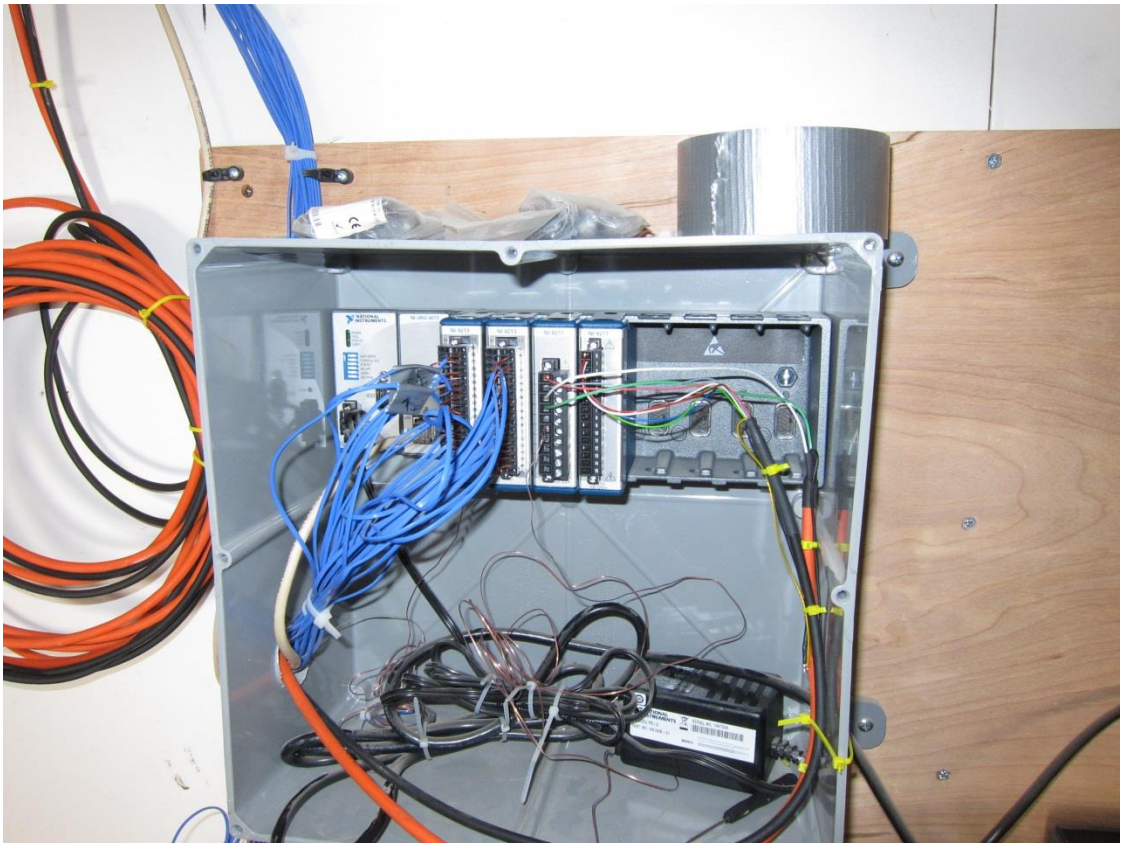

Photo 4-4 The National Instruments Compact RIO data acquisition system installed with all modules and instrument leads.

4.8 Software

The DAQ system discussed in 4.7 is comprised of hardware, not software. To analyze and record the data stream from the DAQ, software is required. Lab View 2010 Full Development System was installed on a desktop PC at the test site. Within the Lab View 2010 software, a Virtual Instrument (VI) was programmed to acquire data from each of the 35 data channels, wait for a user specified time and make the next set of readings. At the end of each 24 hour period, the VI created a .CSV data file that contained the readings. This file can be opened and manipulated in a spread sheet program such as Microsoft Excel.

As described in 4.4, the meteorological station data stream was also simultaneously routed to the desktop PC. To collect and store the meteorological data, a software package called Virtual Weather Station from Ambient Weather was selected. This software is able to collect readings from the weather station and package them into a tab delimitated text file every 24 hours. Both the LabVIEW and Virtual Weather Station software log the data stream with a time and date stamp from the computer's system clock. As such, the readings recorded in the two separate files are synchronized and easily merged during analysis.

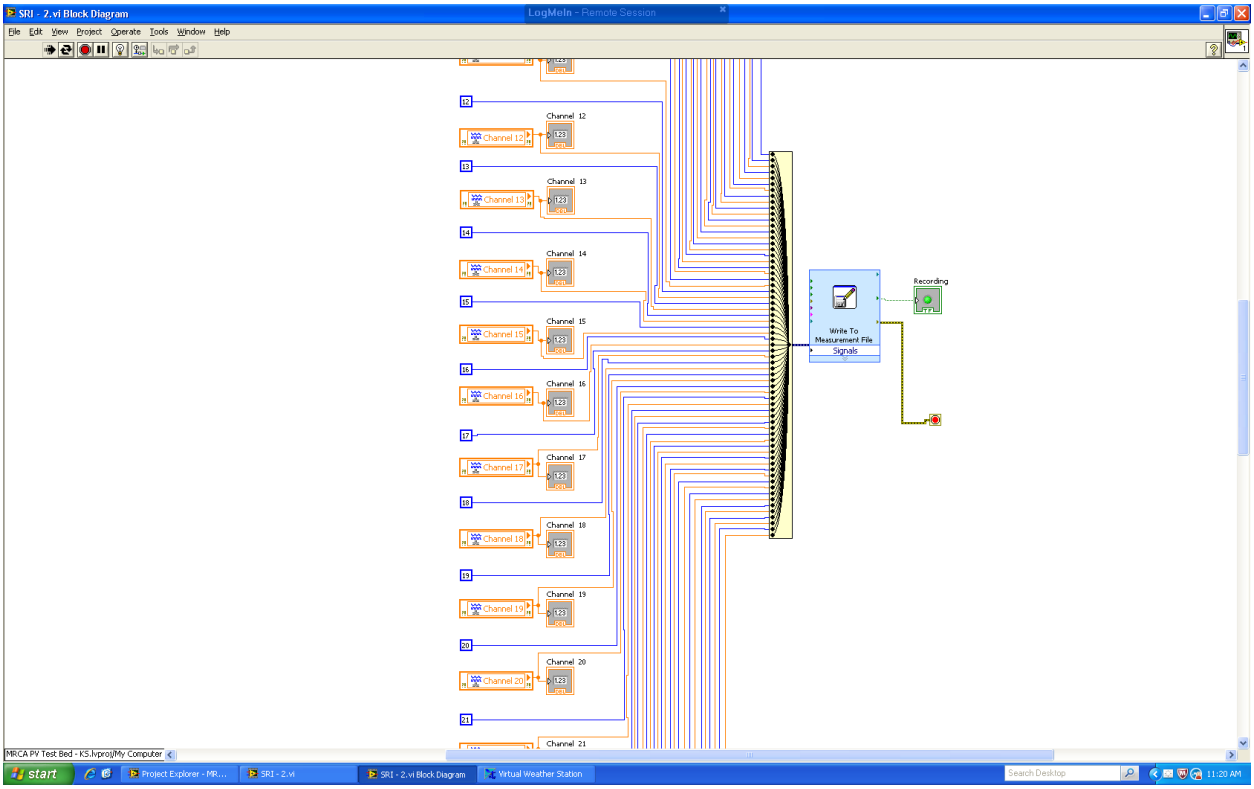

Photo 4-5 Shows a screen shot of the LabVIEW Virtual Instrument backend of the data collection.

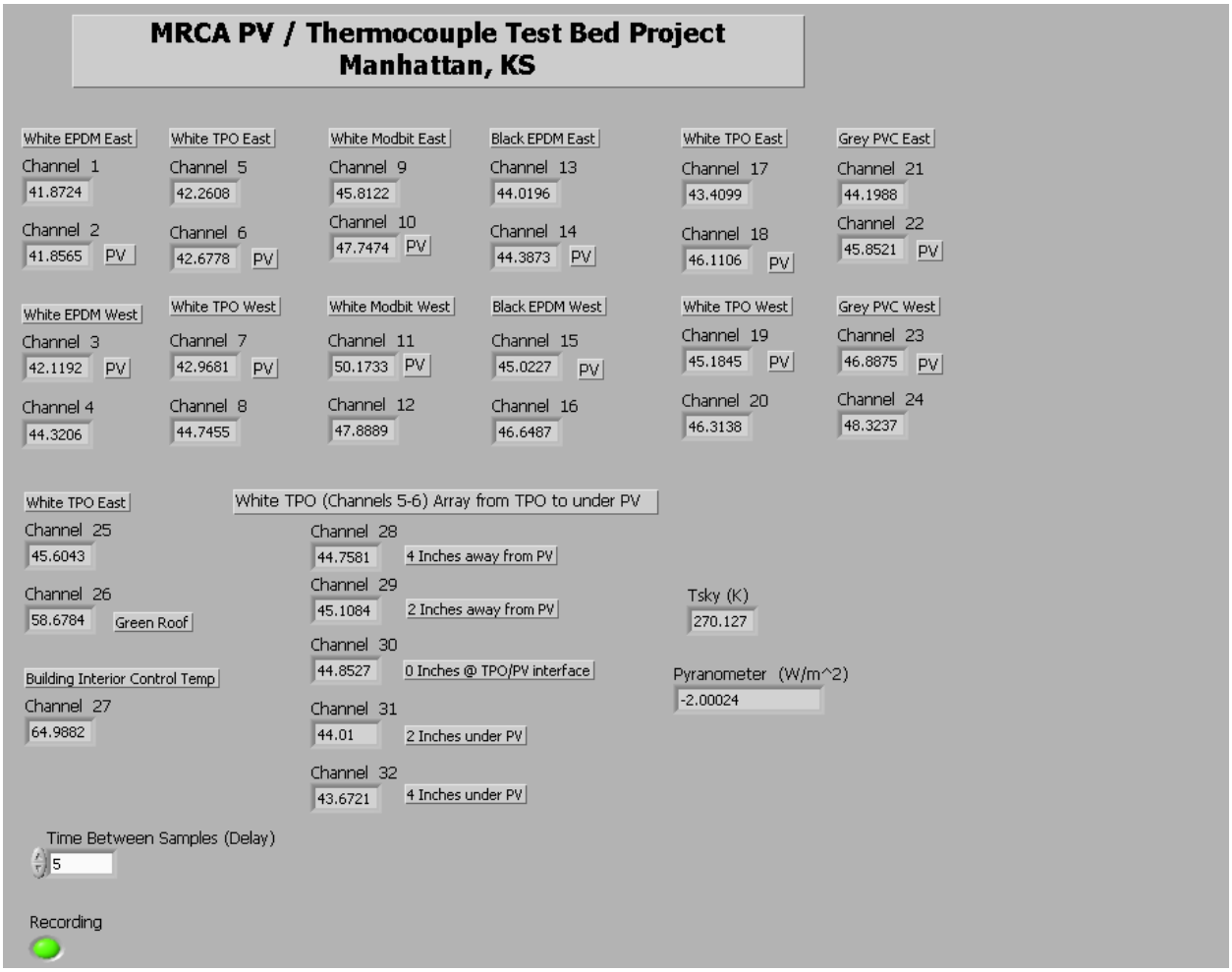

Photo 4-6 Shows a screen shot of the LabVIEW front end during development

4.9 Installation

In July of 2010, instruments described above were brought online at the Manhattan, Kansas site. For this project, the system ran for the full month of August 2010. During this time, the system captured readings at a sample rate of 1 Sample every 10 seconds. Each day of the study the system acquired approximately 1,200,000 points of raw data. This data set represents the actual data for use in Phase 3.

References

1. Akbari, H., *Measured energy savings from the application of reflective roofs in two small non-residential buildings.* Energy, 2003. 28(953-967).

2. Akbari, H., R. Levinson, and L. Rainer, *Monitoring the energy-use effects of cool roofs on California commercial buildings.* Energy and Buildings, 2005. 37(Compendex): p. 1007-1016.

3. Akridge, J.M. *High-albedo roof coatings - impact on energy consumption*. in *Proceedings of the 1998 ASHRAE Winter Meeting. Part 1 (of 2), January 18, 1998 - January 21, 1998*. 1998. San Francisco, CA, USA: ASHRAE.

4. J., D.A.a.K., *MODELING OF ROOF HEAT TRANSFER UNDER SOLAR PHOTOVOLTAIC PANELS*. 2010, University of California, San Diego. p. 1-7.

5. Berdahl, P. and M. Martin, *EMISSIVITY OF CLEAR SKIES.* Solar energy, 1984. 32(5): p. 663-664.

Chapter 5: Roof System Physical Properties

In order to accurately model the heat flux in the roof membrane it is necessary to characterize the physical properties of the roof membranes and the roof system. Some of the properties can be readily obtained from manufacturer data sheets, such as unit weight. However, some of the properties are not even known by the manufacturer, such as Specific heat capacity; these properties are best obtained by the individual researcher.

5.1 Unit Weight

The unit weight for a membrane is simply obtained by utilizing a material sample of the subject membrane. In this experiment, samples were trimmed to exactly 4 inches square so they would fit within the confines of a calibrated laboratory balance accurate to thousands of a gram. Four samples of each membrane were prepared, massed, and then averaged. The results are reported in Table 5-1.

$$U = \frac{M}{A}$$

Equation 5-1 Roof Membrane Unit Mass

Where:

A = Unit Area (m^2)
M = Mass (g)
U = Unit Membrane Mass (g/m^2)

Membrane Study Label	Manufacturer	Membrane	Unit Weight (g/m^2)
White EPDM	Firestone	Eco White – 60 Mil	2096.117
White TPO A	Firestone	Ultra-Ply 60 Mil	1501.961
White Modbit	Derbigum	Derbibrite	3559.033
Black EPDM	Carlisle Syntec	Sure-Seal - 60 Mil	1848.507
White TPO B	Carlisle Syntec	Sure-Weld 60 Mil	1501.961
Grey PVC	Sarnafil	G-410 60 Mil	1730.937

Table 5-1 Unit weights of the roof membranes.

5.2 Reflectivity

One of the radiative properties needed for temperature modeling is the insolation reflectivity or, more simply, the solar reflectivity. The solar reflectivity is expressed as a decimal percentage of the total incoming solar energy that is reflected away from a surface.

The measurement of solar reflectivity of roof membranes is typically conducted with a Solar Spectrum Reflectometer such as the Devices and Services Company model SSR. Manufacturers will almost exclusively list the aged reflectivity values for their membranes as tested under the Cool Roof Rating Council standard CRRC-1. This standard is a prescriptive aging process under ASTM G7, before conducting solar reflectivity testing under ASTM C1549. It has been shown that while the CRRC-1 methodology for aged values gives a reasonable aged reflectivity number, the local roof conditions have a large influence on measured field values[1].

Therefore, for this study, a recently calibrated SSR reflectometer was utilized to measure the in situ reflectivity. Each of the eight membranes on the Manhattan, Kansas roof were measured on July 21, 2010. The field data was collected in August of 2010. The reflectivity for the membranes modeled in this study are reported in Table 5-2.

Membrane	Solar Reflectivity
White EPDM	0.690
White TPO A	0.699
White Modbit	0.759
Black EPDM	0.067
White TPO B	0.724
Grey PVC	0.455

Table 5-2 Solar reflectivity of the roof membranes.

Photo 5-1 A SSR reflectometer in use during a 2012 study of field reflectivity in Texas.

5.3 Emissivity

Emissivity refers to Plankian type radiative emission from a real body. All matter above absolute zero emits infrared radiation. With the exception of a theoretical black body, which is a perfect emitter of radiation, almost all bodies are grey bodies that emit energy less efficiently than a black body. Grey bodies emit infrared energy according to the Stefan-Boltzmann law, which is shown as Equation 5-2. The term we are interested in here is the emissivity (ε) term. This term is the expression of efficiency by which the grey body (also referred to as real body) emits energy compared to a black body radiator at the same temperature.

An examination of relevant literature finds that no measurements of in-situ roof membrane emissivity according to ASTM C1371 or ASTM E408 have been published. In addition, a field portable emissometer was not available for this study so in situ emissivity measurements of the roof membranes in Manhattan, Kansas were not possible.

However, the Cool Roof Rating Council (CRRC) publishes data for aged values for reflectivity and emissivity. The values published in the CRRC data assume roof membranes to be Lambertian emitters; meaning they emit energy in all directions equally. This assumption is currently in dispute in the roofing industry. This author has research underway to begin quantifying some of these non-Lambertian emissivity values. However, for this study the published emissivity values from the CRRC are assumed correct. The emissivity values for the appropriate membranes were located in the CRRC directory and are reported in Table 5-3.

$$\frac{P}{A} = \varepsilon\sigma T^4$$

Equation 5-2 The Stefan-Boltzmann law

Where:

P = Radiated power (W/m^2)

A = Unit area (m^2)

ε = Emissivity (%)

σ = Stefan-Boltzmann constant (5.670373×10^{-8} $W / m^2 \cdot K^4$)

T = Temperature (K)

Membrane	Emissivity
White EPDM	0.86
White TPO A	0.83
White Modbit	0.83
Black EPDM	0.84
White TPO B	0.86
Grey PVC	0.85

Table 5-3 Thermal emissivity for the roof membranes.

5.4 Specific Heat Capacity

Specific heat, also known as specific heat capacity, is the amount of heat energy required to change the temperature of a unit mass by a degree. This property is possibly the most fundamental one for modeling temperature change in roof membranes. Unfortunately, this property is never published by manufacturers. The only literature found to report this material property was Clear [2]. Clear's study reports a heat capacity of a granulated polymer-modified bitumen cap sheet to be 1.51 J/g·K.

In addition to a lack of published values, there is a compounding factor that each manufacturer uses a proprietary blend for their membranes. For example, a polymer-modified bitumen sheet will contain varying amounts of asphalt, Atactic Polypropylene (APP), polyester reinforcement sheets, fillers (clay), and some form of surfacing, such as granules and other proprietary ingredients. It may be possible to extract the heat capacity for one or more of the generic components in this sheet from a chemistry reference handbook or other source. However,

we wouldn't know the proportions to make a weighted value for the sheet as a whole. Therefore, the most expedient way to access this property was to measure it for the roof membranes under study here.

Utilizing a TA Instruments Q100 Differential Scanning Calorimeter (DSC) in the Soft Materials Laboratory in the University of Wisconsin – Madison, College of Engineering, specific heat capacities for the roof membranes being modeled were measured. The membranes were characterized with isothermals at 110°C and -10°C to produce a smooth reading between 0°C and 100°C. The membranes were tested under a nitrogen atmosphere. The heating and cooling rates for the testing were 10°C/min.

All membranes exhibited thermal hysteresis. That is, each membrane demonstrated a different specific heat capacity during endothermic measurements versus exothermic measurement. An example of the graphical readout of the DSC data is shown in Figure 5-1. For this work the endothermic and exothermic values were arithmetically averaged.

Samples were obtained for all the roof membranes except TPO A. Therefore, TPO B served as the representative sample for the TPO class of membranes in this study. The samples tested were full cross sections of the membranes – outside surface to outside surface. This means any constituent part of the membrane was tested as well, including any reinforcement. Each membrane tested had a replicate. The results of replicates were included in an arithmetic average for each membrane or membrane class. The results of the DSC work is summarized in Table 5-4. The DSC outputs for each membrane or membrane class and its replicates are presented in Appendix A.

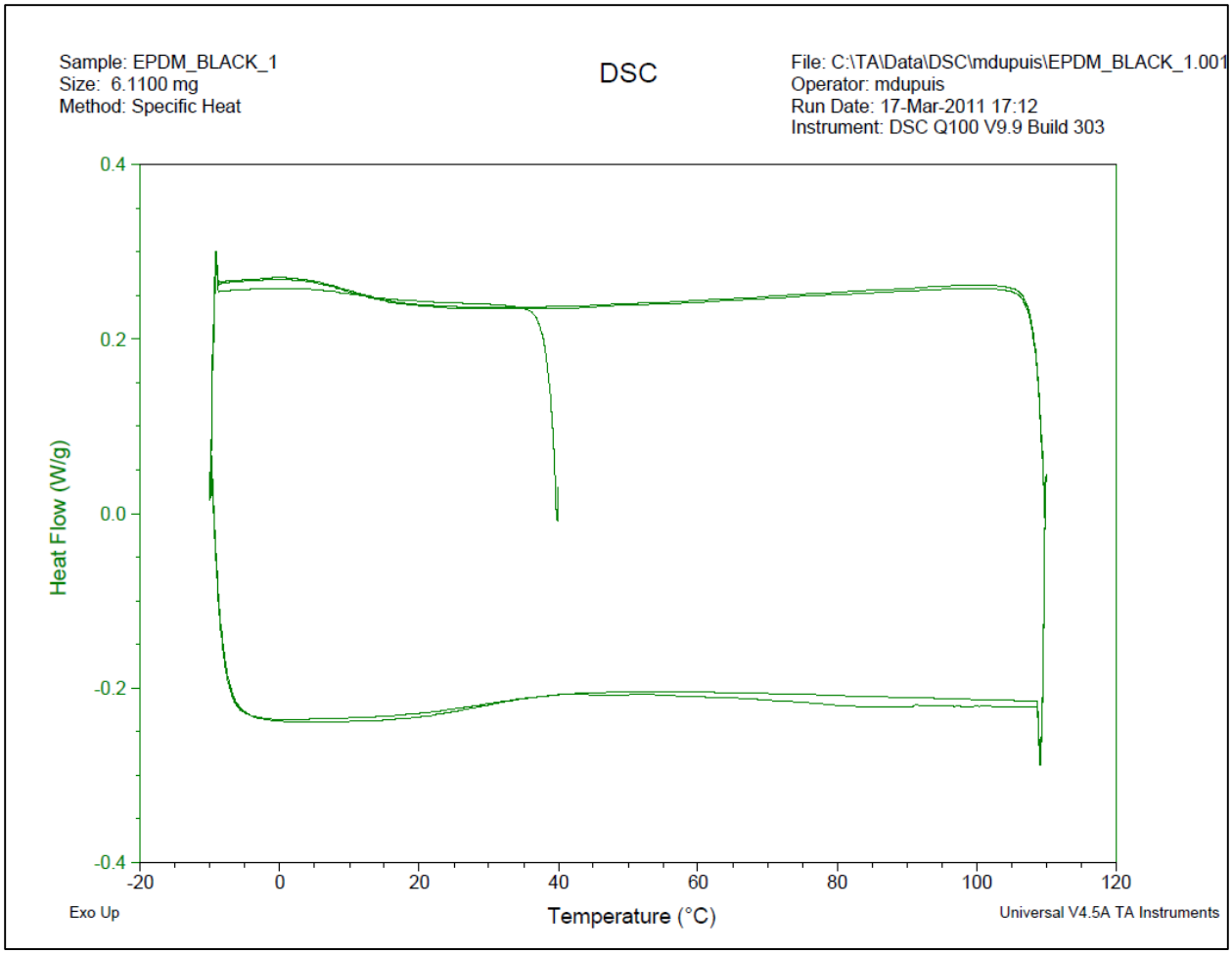

Figure 5-1 Sample graphical output from the Q100 DSC

	Specific Heat Capacity (J/g·K)		
Membrane	**Combined**	**Endothermic**	**Exothermic**
White EPDM	1.24	1.16	1.32
Modified Bitumen	1.23	1.12	1.34
Black EPDM	1.40	1.32	1.48
PVC	1.13	1.05	1.21
TPO	1.78	1.63	1.92

Table 5-4 Specific Heat Capacity of the roof membranes

5.5 Roof System Thermal Resistance

In order to calculate the heat flux through the roof into the building interior the thermal resistance of the roof system needs to be calculated. This value is the inverse of the thermal conductivity.

The laboratory measurement of thermal resistance has been a controversial topic within the building envelope community since at least the 1980's. Of particular concern is how to prepare and measure insulation and at what temperature to measure thermal resistance. As of this writing, this issue has yet to be resolved with any finality.

For the purposes of this study, a definitive source of accepted knowledge and data is used to determine the roof system thermal resistance. In The American Society of Heating, Refrigerating, and Air Conditioning Engineers (ASHRAE) publishes the ASHRAE Handbook – Fundamentals [3]. This book contains commonly accepted values for thermal conductivity for building components.

The transmission of heat energy from exterior surface to the interior surface, and vice versa, is a series circuit. Therefore, the one-dimensional resistance to the movement of heat energy is additive. For this study, only one thermal conductivity is necessary, as all of the roof membranes are over the same underlying insulation system. The different membranes present negligible differences in thermal conductivity to the roof system as a whole.

Figure 5-1 shows a cross section view of the roof system. Table 5-5 gives the roof system conductivity, by layers.

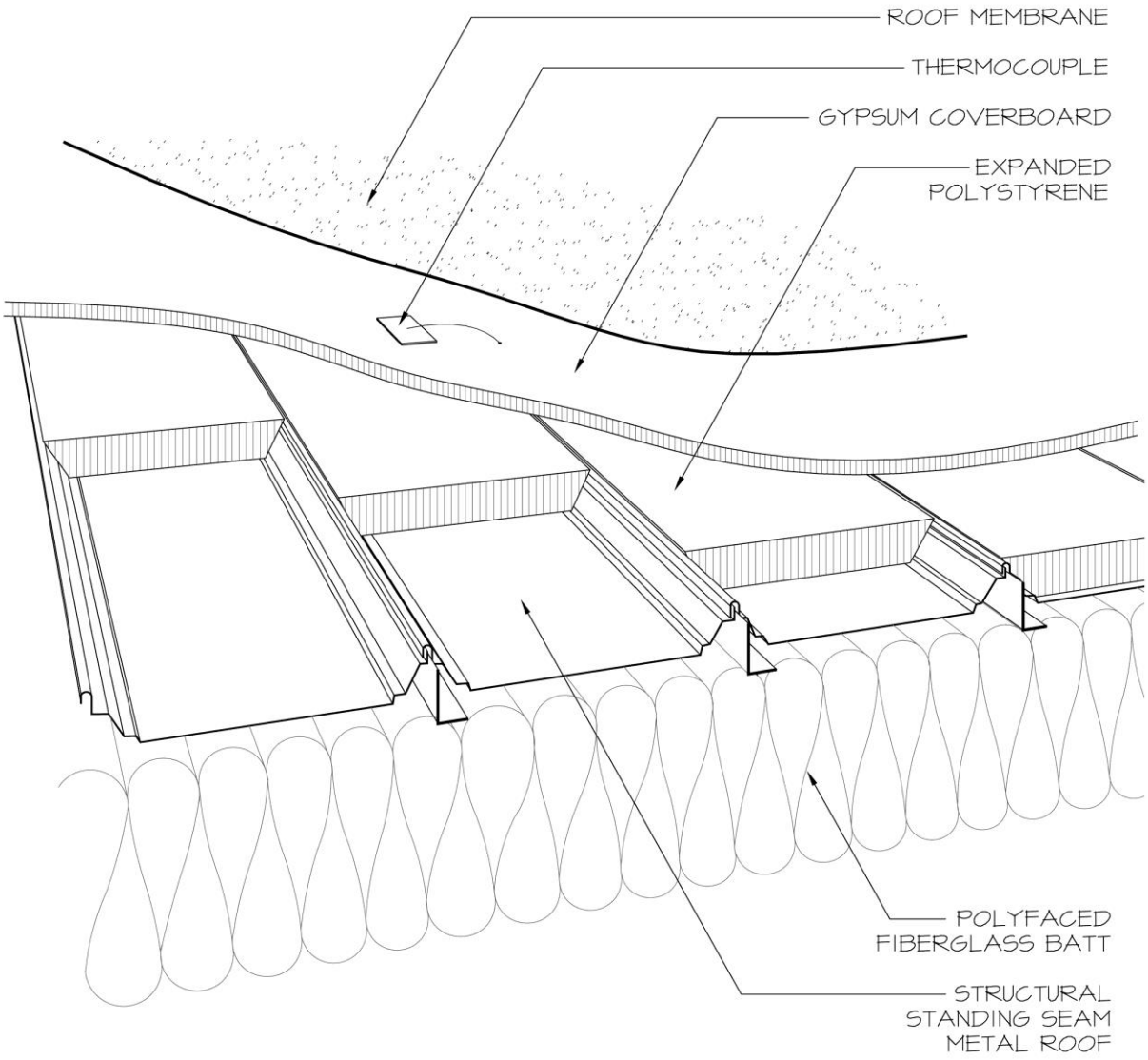

Figure 5-1 Roof system cross section.

System Component	Thermal Resistance ($m^2 \cdot K/W$)
0.25 inch DensDeck	0.05
1.5 inch EPS @15PSI	1.24
22 ga. Steel deck	0.01
12 inch Poly-faced HD Fiberglass Batt	3.35
Interior Air Film	0.14
Total	4.79

Table 5-5 Roof system thermal conductivity by layer

References

1. Dupuis, M., *Highly Reflective*, in *Professional Roofing*. May 2013, National Roofing Contractors Association: Rosemont, IL.

2. Clear, R.D., L. Gartland, and F.C. Winkelmann, *An empirical correlation for the outside convective air-film coefficient for horizontal roofs.* Energy and Buildings, 2003. **35**(8): p. 797-811.

3. ASHRAE, *2013 ASHRAE Handbook - Fundamentals (I-P Edition)*. 2013: American Society of Heating, Refrigerating and Air-Conditioning Engineers, Inc.

Chapter 6: Roof Membrane Thermal Model

The construction of a closed form analytical temperature model for the roof membranes is an important step in this research. The basic components of this model are terms for heat transfer via conduction, convection and radiation. These terms and the subsequent model can generally be assembled from the treatments within a traditional heat transfer text [1]. As was discussed in the literature review, several efforts have been made to do this in previous studies [2-4]. These efforts varied from basic programs to a complex finite element approach. Whether the simple or complex methods were used, the heat transfer portions all contain the same elements, conduction, radiation, and convection.

The end goal of this model is to predict the roof membrane temperature. To calculate the change in temperature for the roof membrane we require an initial temperature and then track all energy entering or leaving the membrane over time. This idea follows from the law of conservation of energy; any net change in energy will result in a temperature change.

For the purposes of this study we treat the roof membrane, typically only 0.060 inches thick, as a continuous surface that has a uniform temperature throughout. This assumption simplifies the heat transfer model to a one-dimensional lumped capacitance model. In such a model, we are not concerned with how heat energy flows within or is distributed within the roof membrane. We only are concerned with quantities of energy that come and go from the surface (roof membrane) over time. This reduces the problem to a summation of the three sources of heat

flux, as shown in Equation 6-1. This equation forms the basis of the model development that follows.

$$\boldsymbol{q''_{Net} = q''_{Conduction} + q''_{Radiation} + q''_{Convection}}$$

Equation 6-1 Basic form Roof Membrane Thermal Model

Where:

$q'' = \text{Heat flux in } W/m^2$

6.1 Conduction

The movement of heat energy via conduction is typically defined as the movement of heat energy from a region of matter with higher energy to a region of lower energy, in accord with the second law of thermodynamics. For the purposes of this research, we are interested solely in calculating the rate at which the energy moves through the roof system. More specifically we are interested in the rate (energy / time) at which heat energy moves from the roof membrane to the building's opposing interior surface, or vice versa.

To calculate the rate of heat energy conduction through the roof system, we utilize a general form equation shown in Equation 6-2. In this study, we know the constituent materials and thicknesses of the roof system. Therefore, we can simplify Equation 6-2 by replacing the thermal conductivity (k) and roof system thickness (L) with the thermal resistance calculated in Section 5.5. This simplification leads to Equation 6-3 used in the model.

$$q"_{Conduction} = \frac{\mathrm{k}\,(T_I - T_S)}{\mathrm{L}}$$

Equation 6-2 Basic form for conduction rate

Where:

k = Thermal conductivity (W/m·K)

T_I = Interior temperature (K)

T_S = Roof surface temperature (K)

L = Roof system thickness (m)

$$q"_{Conduction} = \frac{T_I - T_S}{\mathrm{R}}$$

Equation 6-3 Model form of conduction rate

Where:

R = Thermal resistance in m^2·K/W

6.2 Radiation

The radiation term refers to the electromagnetic energy exchanged at the exterior surface of the roof membrane with its surroundings. This energy exchange results from incident radiation absorbed and emitted by the roof membrane. Calculation of the net radiation exchange requires

accounting for all sources of irradiance. The sources of radiation that must be accounted for include incident solar radiation, incident long wave radiation, and emitted long wave radiation.

The global solar irradiance on the roof membrane was measured by the pyranometer, as discussed in Section 4.5. A percentage of the incident solar radiation was reflected away by the roof membrane. This reflectivity value was determined in Section 5.2. The net solar radiation absorbed was the solar irradiance less the reflected portion.

The global long wave irradiance on the roof membrane was measured by the pyrgeometer, as discussed in Section 4.6. A percentage of the incident long wave radiation was reflected away by the roof membrane. The long wave reflectivity of roof membranes has not been published to the author's knowledge. However, an assumption is made in the literature [3] that the long wave reflectivity is related to the grey body emissivity discussed in Section 5.3. Rose suggests that the long wave infrared wave-lengths that the material readily emits it is also sensitive to in absorbance. In effect, the long wave reflectivity is taken as the difference of one and the roof membrane's emissivity in Section 5.3.The net long wave radiation absorbed is the long wave irradiance subtracted from the reflected portion.

All matter above absolute zero emits long wave radiation, as is described by the Stefan-Boltzmann Law. The roof membranes under study are not black bodies – i.e., perfect radiators of

energy. Therefore, they are grey bodies that have an emissivity defined in Section 5.3. The rate of energy radiated by the roof membranes in the long wave infrared is shown in Equation 6-4

$$\boldsymbol{E_{Roof} = \varepsilon \sigma T^4}$$

Equation 6-4 the Stefan-Boltzmann equation for real bodies.

Where:

E_{Roof} = Emitted energy from the roof membrane in W/m^2

ε = Roof membrane emissivity (%)

σ = Stefan-Boltzmann Constant (5.6704×10^{-8} $W/m^{2 \cdot}K^4$)

Collecting the three sources of radiative energy exchange on the roof membrane, we arrive at Equation 6-5 and then with substitutions in Equation 6-6 and simplification in Equation 6-7

$$\boldsymbol{q"_{Radiation} = (1 - \propto_{Solar}) G_{Solar} + (1 - \propto_{Roof}) G_{Long} - E_{Roof}}$$

Equation 6-5 Net radiative exchange for the roof membrane

Where:

$\propto_{Solar}$ = Solar reflectance of roof membrane (%)

G_{Solar} = Global incident solar irradiation (W/m^2)

$\propto_{Roof}$ = Long Wave reflectance of roof membrane (%)

G_{Long} = Global atmospheric irradiation (W/m^2)

$$q''_{Radiation} = (1-\alpha_{Solar})G_{Solar} + (1-(1-\epsilon)G_{Long} - \varepsilon\sigma {T_S}^4$$

Equation 6-6 Net radiative exchange for the roof membrane

$$q''_{Radiation} = (1-\alpha_{Solar})G_{Solar} + \epsilon G_{Long} - \varepsilon\sigma T_S^4$$

Equation 6-7 Net radiative exchange for the roof membrane

6.3 Convection

The convection term describes the heat transfer rate of energy brought into or taken away from the roof membrane by exterior fluid movement. For building science purposes, we generally are concerned only with the exterior air as the fluid. The air movement comes in two forms. The first air movement type is wind, or forced convection. Wind forces air over the roof surface bringing with it air of ambient temperature to exchange energy with the roof membrane.

The second form of air movement, involving air buoyancy, is more complex. It is commonly referred to as natural convection.

Equation 6-8 shows the basic form of the convective energy transfer rate. This form of the equation is typically referred to as Newtonian Cooling [1]. The temperature components of this equation are self-explanatory. The convection heat transfer coefficient term is not so.

$$q''_{Convection} = h_{Convection}(T_S - T_A)$$

Equation 6-8 Basic form of convective heat transfer

Where:

$h_{Convection}$ = Convection heat transfer coefficient ($W/m^2 \cdot K$)

T_S = Roof surface temperature in degrees (K)

T_A = Ambient air temperature in degrees (K)

The convective coefficient is one that accounts for the effects of both the forced and the natural convection. In previous roof membrane temperature studies, the convection term was typically simplified [2-4] to only a constant or utilized the closed form text book solution for a flat plate. The exact reason for this is not known. However, these assumptions made in other studies may result from the wide variations in reported convective heat transfer coefficients from multiple studies [5-7]. It appears every building may have its own unique coefficient.

Determining how much error is induced in the temperature model by errors in the assumption of this coefficient is a goal of this research.

6.4 Compiled Roof Temperature Model

Combining the conduction, convection and radiation terms, will produce a theoretical heat transfer model for the roof surface in W/m^2. The compiled roof temperature model is shown in Equation 6-9:

$$\boldsymbol{q''_{Net} = \frac{T_I - T_S}{R} + (1 - \propto_{Solar}) G_{Solar} + \epsilon G_{Long} - \varepsilon \sigma T_S^4 + h_{Convection}(T_S - T_A)}$$

Equation 6-9 Compiled heat flux model

Equation 6-9 is the heat flux equation, quantifying an energy exchange rate in J/s·m^2. This is not yet a temperature model. In order to get a result in the temperature domain we must convert using the specific heat capacity (J/g· K), the mass per square meter of each specific roof membrane (g/m^2) and a time period(s). This will give a predicted temperature change, positive or negative. Equation 6-10 shows the roof temperature mode. This model contains all the variables collected from chapters 4 and 5. The only remaining unknown in Equation 6-10 is the convective

coefficient for the building studied. The value of the convective coefficient ($h_{convective}$) is discussed in Section 6.5.

$$\Delta \mathbf{T} = \frac{\frac{\boldsymbol{T_I - T_S}}{\mathbf{R}} + (\mathbf{1} - \propto_{\boldsymbol{Solar}})\boldsymbol{G_{Solar}} + \boldsymbol{\epsilon G_{Long}} - \boldsymbol{\varepsilon \sigma T_S^4} + \boldsymbol{h_{Convection}(T_S - T_A)}}{\boldsymbol{\Delta t C U}}$$

Equation 6-10 Roof temperature model

Where:

$\Delta T =$ Change in Temperature during time period (K)

$\Delta t =$ Time period (s)

C = Specific Heat Capacity (J/g·K)

6.5 Determination of Convective Coefficient

Using the assumption that each building's coefficient is unique, it is necessary for accuracy to determine the convective coefficient for the building under study. The determination of the convective coefficient is not a trivial matter. There are four common methods for determining the convective heat transfer coefficient for a real building:

1. Utilize a published value by others
2. Conduct a Computerized Fluid Dynamics (CFD) model of the building
3. Conduct a field experiment to measure the heat transfer
4. Utilize field data from the building in question to interpolate one

Given the necessity for accuracy and the wide variations in the numbers reported in the literature [7], the utilization of a published number was considered a last choice. The use of CFD for

determination of the convective coefficient was considered. However, if an error were made in the simulation, even a small one, it would lead to errors in the final model that may not be evident or even traceable. Therefore, the use of CFD was rejected. The conduction of a field experiment to determine the coefficient was considered the most accurate way to measure the convective coefficient. However, the monetary funds required to travel and instrument the building for this measurement were not available. Therefore, field data was utilized to interpolate a convective coefficient for the model.

Equation 6-10 was solved for the convective coefficient. The measured temperature change for each membrane was known for each time period. The solved equation for the convective coefficient is shown in Equation 6-11:

$$\boldsymbol{h_{Convection}} = \frac{\Delta \mathbf{T} \Delta \boldsymbol{tCU} - \frac{\boldsymbol{T_I} - \boldsymbol{T_S}}{\mathbf{R}} - (\mathbf{1} - \propto_{\boldsymbol{Solar}}) \boldsymbol{G_{Solar}} - \boldsymbol{\epsilon G_{Long}} + \boldsymbol{\varepsilon \sigma T_S^4}}{(\boldsymbol{T_S} - \boldsymbol{T_A})}$$

Equation 6-11 Roof temperature model solved for the convective coefficient

In the population of collected data for August 2010, there were 29 viable days of data. From these days, a random number generator was used to select three days of data to enter into Equation 6-11, combine the results for all membranes, and calculate a convective coefficient for

use in the predictive model of Equation 6-10. The data from August 3, 6, and 8 where utilized for the calculation of the convective coefficient.

From the literature [5-7] it was known that the convective coefficient is dependent on the wind speed. At zero wind speed the roof experiences natural convection. When the wind speed is greater than zero, the roof is subject to combined natural and forced convection. Therefore, it is

necessary to plot the results from the convective coefficient calculation against the wind speed that produced that value. The results of over 150,000 samples are plotted in Figure 6-1 below.

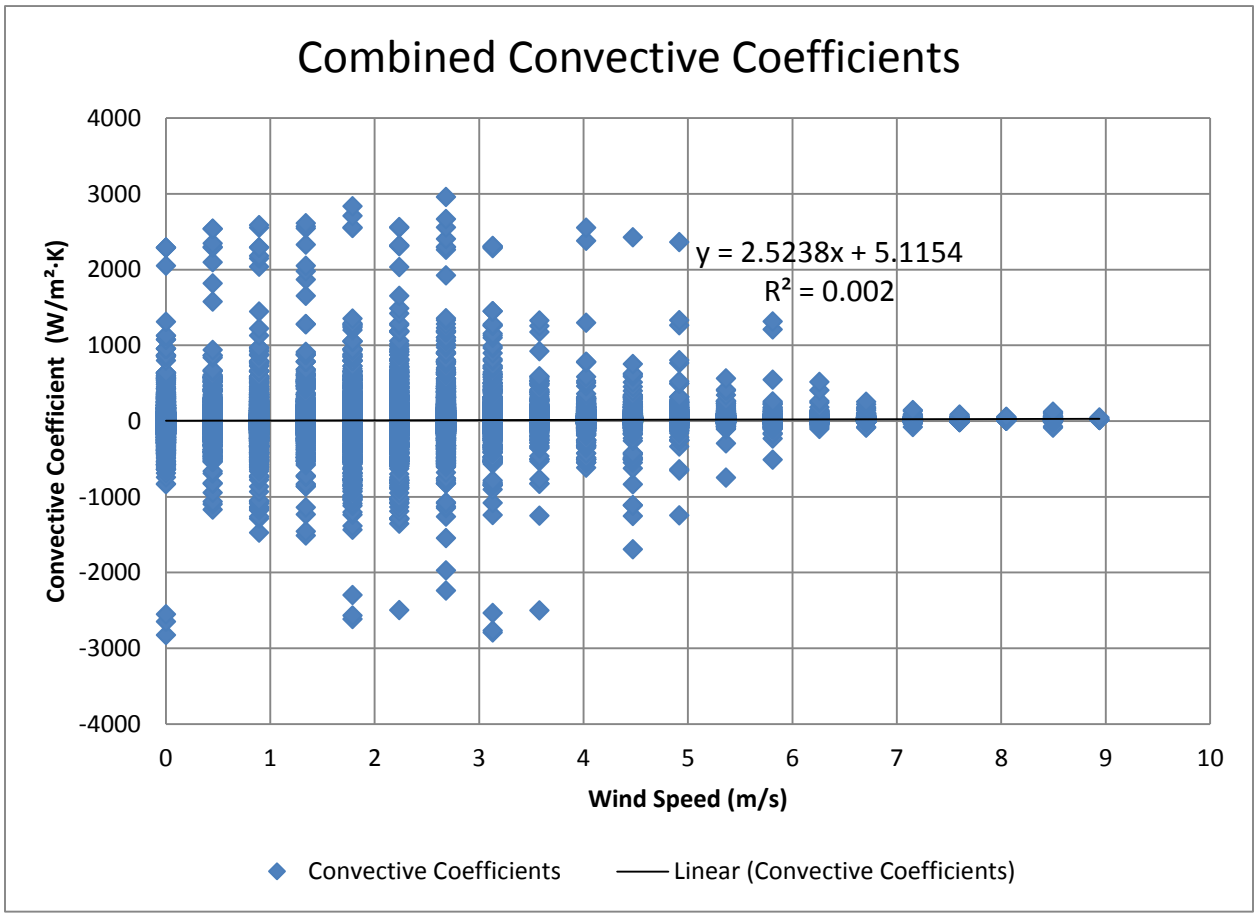

Figure 6-1 Combined plotting of calculated convective coefficients for over 150,000 data points.

The results for Figure 6-1 were concerning. The coefficient of determination is very poor. The sheer number of data points appears to be causing the appearance of poor data. A data transform was conducted in an effort to produce a more satisfactory result. Each of the wind speed values was binned with their value of the convective coefficient arithmetically averaged. The arithmetic

average of the calculated convective coefficients for each wind speed bin was calculated and again plotted against its wind speed. The result of this data transform is shown in Figure 6-2.

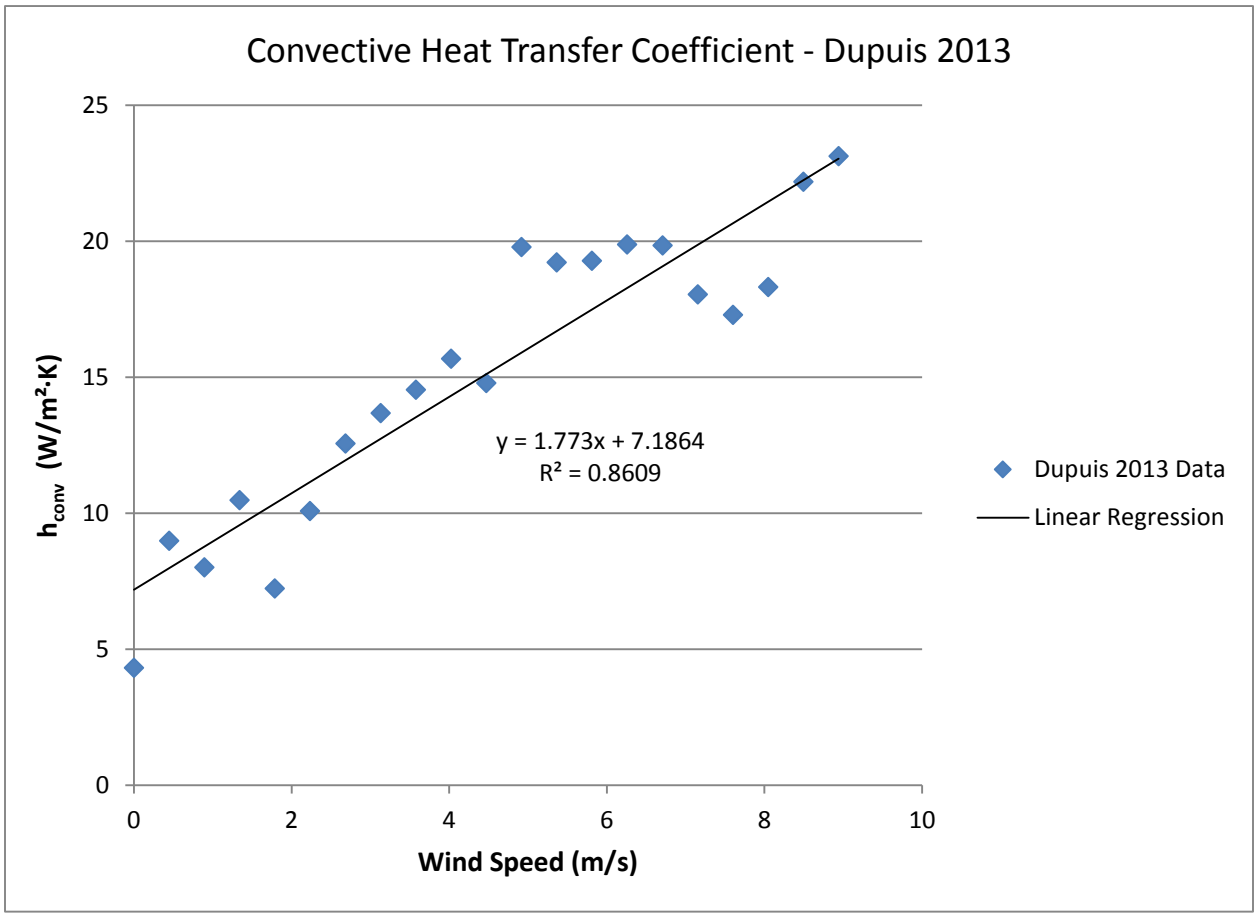

Figure 6-2 Transformed data for the calculated convective coefficient.

The coefficient of determination returned from the data shown in Figure 6-2 was far superior to that of Figure 6-1, while producing a similar convective coefficient.

In order to confirm the reasonableness of the convective coefficient arrived at in Figure 6-2, that coefficient was plotted with other convective coefficients from other published studies [5, 8]. The result of this plot are shown in Figure 6-3. As previously stated, it is assumed that

every roof will have a convective coefficient unique to factors such as but not limited to slope, orientation to the wind, surface roughness, height above ground, and upwind distance from ground level obstructions. Given this assumption, the result in Figure 6-3 demonstrates that the convective coefficient arrived at for this model appears reasonable and valid.

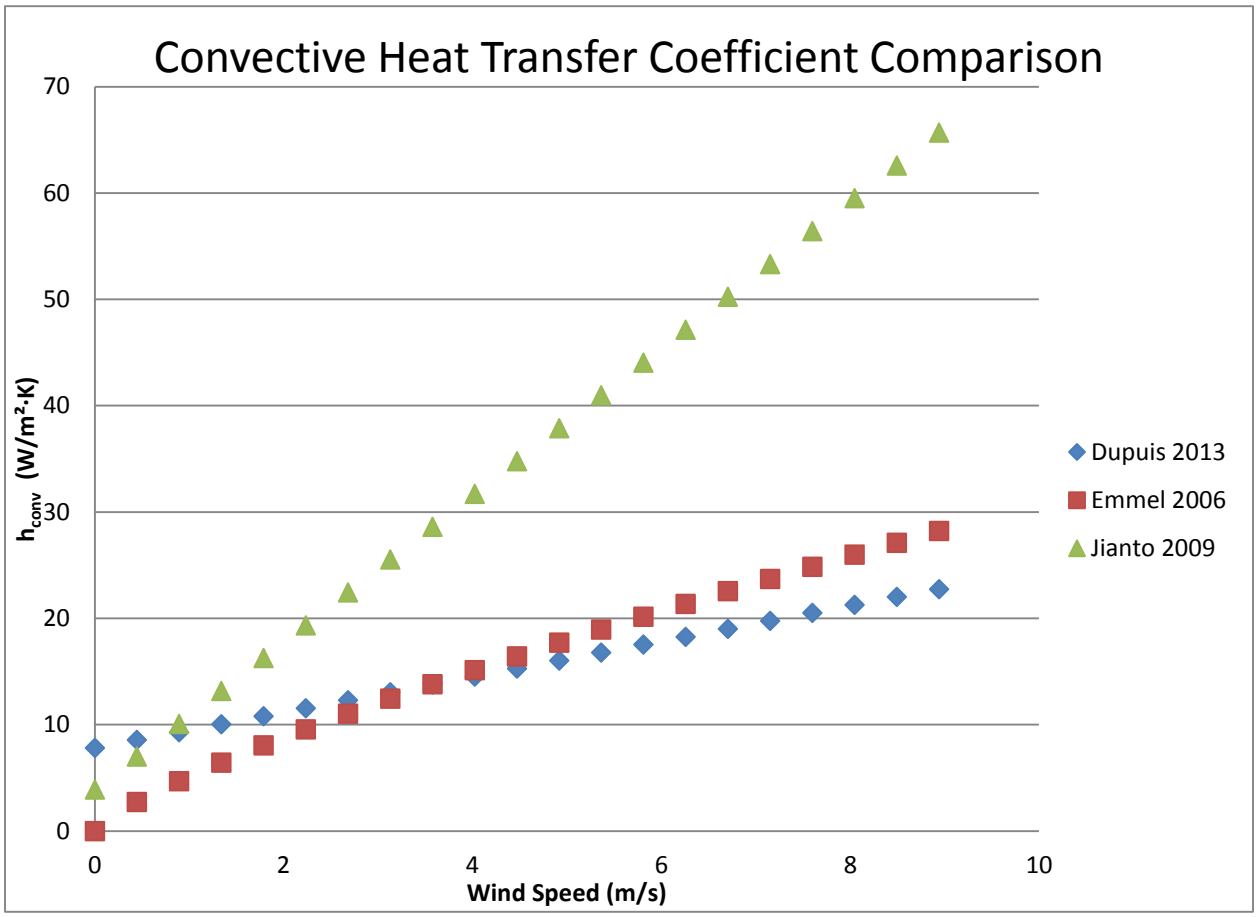

Figure 6-3 Comparison of different convective coefficients for low slope roofs.

6.6 Final Form of Roof Temperature Model

Using the convective coefficient determined in Section 6.5, the final form of the roof temperature model is presented in Equation 6-11. In Equation 6-10, the temperature differential caused by the addition or removal of energy during the time step (Δt) was solved for. In Equation

6-11, the additional step of solving for the final temperature (T) at the end of the time step is made. The roof membrane temperature at the beginning of the time step (T_S) is changed by the result of equation 6-10 to arrive at the final temperature in equation 6-11.

$$\mathbf{T} = \boldsymbol{T_s} + \frac{\frac{\boldsymbol{T_I - T_S}}{\mathbf{R}} + (\mathbf{1} - \propto_{\boldsymbol{Solar}})\boldsymbol{G_{Solar}} + \boldsymbol{\epsilon G_{Long}} - \boldsymbol{\varepsilon \sigma T_S^4} + (\mathbf{1.1773W + 7.1864})(\boldsymbol{T_S - T_A})}{\boldsymbol{\Delta t C U}}$$

Equation 6-11 Roof Temperature Model

Where:

T= Roof membrane temperature at the end of time step (K)

W = Wind speed (m/s)

References

1. Incropera, et al., *Fundamentals of Heat and Mass Transfer*. 6th Edition ed. 2007: Wiley. 995.

2. Wilkes, K.E., *Model for Roof Thermal Performance*. 1989, U.S. Department of Energy: Oak Ridge National Labs. p. 98.

3. Rose, W.B., *White Roofs and Moisture in the US Desert Southwest*, in *Buildings X*. 2007, Oak Ridge National Labs: Clearwater Beach, Florida.

4. Kunzel, H.M., *Simultaeous Heat and Moisture Transport in Building Components*, in *Fraunhofer Institute of Building Physics*. 1995, University of Suttgart: Suttgart, Germany. p. 65.

5. Jiantao, S., et al., *A novel method for full-scale measurement of the external convective heat transfer coefficient for building horizontal roof.* Energy and Buildings, 2009. 41(Copyright 2009, The Institution of Engineering and Technology): p. 840-7.

6. Clear, R.D., L. Gartland, and F.C. Winkelmann, *An empirical correlation for the outside convective air-film coefficient for horizontal roofs.* Energy and Buildings, 2003. 35(8): p. 797-811.
7. Palyvos, J.A., *A survey of wind convection coefficient correlations for building envelope energy systems' modeling.* Applied Thermal Engineering, 2008. 28(8-9): p. 801-808.

8. Emmel, M.G., M.O. Abadie, and N. Mendes, *New external convective heat transfer coefficient correlations for isolated low-rise buildings.* Energy and Buildings, 2007. 39(3): p. 335-342.

Chapter 7: Model Validation

Assembling the model in Equation 6-11 is a theoretical exercise. In order to proceed with a sensitivity analysis of this model, it needs to be validated against the field roof membrane temperatures that were recorded. In order to perform this validation and all subsequent calculations, the model must be programed into a computer.

7.1 Excel Workbook Assembly

In past attempts to model roof temperatures, custom computer programs were needed and written for this purpose[1, 2]. Common computer spreadsheet programs are capable of making these calculations. However, versions of spreadsheet programs, such as Microsoft Excel 95 (v.7) and earlier, were limited within the program to 4 million cells for each worksheet. This limitation would narrowly allow the raw daily data set from this study to be opened in a spreadsheet. Therefore, the custom programing used in earlier studies appears to have been necessary.

In the current release of Microsoft Excel 2013(v.15), the cell limitation per worksheet was raised to over seventeen billion cells. The limitation on workbook size, the collection of active worksheets, was removed and is currently limited only by the memory available on the computer. This allowed Microsoft Excel to be used for all necessary calculations and to store data, calculate heat fluxes, calculate errors, and display results.

As noted earlier, there are 29 viable data sets in the population. To facilitate expedience in the validation calculations, a master spreadsheet was created. The use of a master spreadsheet allowed for quickly linking the next raw data set into a master spreadsheet and for saving that

day as the appropriate day for that raw data set. There are three basic steps in the master spreadsheet.

The first step is importation of the raw data files. The LabVIEW program saves a .CSV file (Comma Separated Values). The Virtual Weather Station Pro software from Ambient Weather outputs a tab delimited text (.TXT) file. Both of these formats are readily imported into Excel as separate worksheets.

Once the raw data is imported into worksheets, the next step is to select the appropriate data and convert it to the appropriate units. The raw data sets contain numerous cells and columns of data that are not needed for these calculations. The data from some sensors were recorded in Imperial units and needed to be converted to metric units. Separate worksheets were created for both the LabVIEW data and the meteorological data to filter and convert the desired data.

With the desired data collected in the appropriate units, these cells and columns can be targeted by a worksheet seeking to utilize Equation 6-11 for calculation of the roof membrane temperature. An example of the worksheet calculation is shown in Figure 7-1.

white EPD	white TPO	white modb	Black epdr	White TPC	Grey PVC						white EPD	white TPO	white mod
2096.117	1501.961	3559.03277	1848.507	1501.961	1730.937			Specific heat		J / K g	1.24	1.78	1.23
								Averaged					
white EPDM							white TPO A						
Cond	Rad	Conv	q_{net}	Δt	T_2	Error	Cond	Rad	Conv	q_{net}	Δt	T_2	Error
W/m2	W/m2	W/m2	W/m2	s	K°	%	W/m2	W/m2	W/m2	W/m2	s	K°	%
2.2	-18.3	47.4	31.4	10.0	294.2	0.00	2.3	-16.5	50.0	35.8	10.0	294.1	0.05
2.2	-18.6	51.1	34.6	10.0	294.4	0.04	2.2	-17.5	52.3	37.1	10.0	294.3	0.09
2.2	-19.2	49.6	32.5	10.0	294.5	0.08	2.2	-18.0	50.7	34.9	10.0	294.4	0.13
2.1	-19.6	51.6	34.2	10.0	294.6	0.13	2.2	-18.4	52.8	36.5	10.0	294.5	0.18
2.1	-20.4	40.1	21.8	10.0	294.7	0.16	2.1	-19.2	41.0	23.9	10.0	294.6	0.21
2.1	-20.5	32.8	14.4	10.0	294.8	0.17	2.1	-19.4	33.5	16.2	10.0	294.7	0.22
2.1	-20.9	29.1	10.2	10.0	294.8	0.18	2.1	-19.8	29.7	12.0	10.0	294.7	0.22
2.1	-21.2	38.4	19.2	10.0	294.9	0.20	2.1	-20.1	39.1	21.1	10.0	294.8	0.25
2.0	-21.7	40.8	21.1	10.0	295.0	0.22	2.1	-20.6	41.5	23.0	10.0	294.9	0.28
2.0	-22.0	33.8	13.9	10.0	295.0	0.24	2.0	-20.9	34.4	15.6	10.0	295.0	0.29
2.0	-21.9	27.3	7.5	10.0	295.0	0.24	2.0	-20.8	27.8	9.0	10.0	295.0	0.29
2.0	-21.9	27.1	7.2	10.0	295.1	0.25	2.0	-20.9	27.5	8.7	10.0	295.0	0.30
2.0	-22.0	26.9	6.9	10.0	295.1	0.25	2.0	-21.0	27.3	8.3	10.0	295.0	0.31
2.0	-22.1	26.7	6.6	10.0	295.1	0.26	2.0	-21.1	27.1	8.0	10.0	295.1	0.31
2.0	-22.7	31.9	11.2	10.0	295.2	0.26	2.0	-21.7	32.3	12.6	10.0	295.1	0.32
2.0	-22.8	32.0	11.1	10.0	295.2	0.29	2.0	-21.9	32.4	12.5	10.0	295.2	0.34
2.0	-22.4	40.2	19.9	10.0	295.3	0.31	2.0	-21.4	40.6	21.2	10.0	295.3	0.37
2.0	-22.9	36.6	15.6	10.0	295.3	0.33	2.0	-22.0	36.9	16.9	10.0	295.3	0.40
2.0	-23.2	27.7	6.4	10.0	295.4	0.34	2.0	-22.3	27.9	7.6	10.0	295.3	0.41
2.0	-23.0	35.7	14.7	10.0	295.4	0.36	2.0	-22.1	36.0	15.8	10.0	295.4	0.43
1.9	-23.5	27.1	5.5	10.0	295.4	0.36	1.9	-22.6	27.2	6.6	10.0	295.4	0.44
1.9	-23.2	29.6	8.3	10.0	295.5	0.38	2.0	-22.3	29.7	9.3	10.0	295.5	0.45
1.9	-23.4	29.3	7.8	10.0	295.5	0.37	1.9	-22.5	29.4	8.9	10.0	295.5	0.46
1.9	-23.7	23.8	2.0	10.0	295.5	0.38	1.9	-22.8	23.9	3.0	10.0	295.5	0.46
1.9	-24.1	23.7	1.6	10.0	295.5	0.38	1.9	-23.2	23.8	2.5	10.0	295.5	0.46
1.9	-23.7	23.7	1.8	10.0	295.5	0.38	1.9	-22.9	23.7	2.7	10.0	295.5	0.46
1.9	-23.8	23.6	1.7	10.0	295.5	0.38	1.9	-23.0	23.6	2.6	10.0	295.5	0.46

Figure 7-1 Example of a worksheet calculation for roof membrane temperature modeling.

The original concept of using Equation 6-11 in one cell to accomplish the entire calculation in a single step proved cumbersome, due to complicated tracking of references and the length of the expression entered in Excel. The components of Equation 6-11 are calculated in separate columns as Equations 6-2, 6-7, and 6-8 respectively, as shown in Figure 7-1. The net heat exchange in watts per square meter of roof membrane is calculated. A watt equals a joule per second. Therefore, we multiply by the time differential between readings to determine the net energy gained or lost during that time step. Using the specific heat capacity and membrane mass, as previously measured, we can then compute the membrane temperature at the end of the time step, as shown in Equation 7-1

$$T_n = T_{n-1} + \Delta T$$

Equation 7-1 Calculation of Temperature at the end of time step.

Where

T_n = Temperature and the end of current time step

T_{n-1} = Temperature at the end of the previous time step

ΔT = Change in temperature during current time step

The process of computing each time step of 10 seconds is repeated for the entire 24-hour data set. Each time step is dependent on the previous step's calculation of membrane temperature. The only exception is the very first step, where the previous time temperature, T_{n-1} in Equation 7-1, is obviously not available. Therefore, the measured temperature for that membrane at the beginning of the data set was used. After this first calculation, the model is run with no external corrections: only the input variables are used.

7.2 Discussion of Significance

A treatment of validating the roof membrane temperature model would be lacking without a discussion of significant figures in the predicted temperature. Equation 6-11 contains ten (10) independent variables. In addition to the large number of variables, these variables are mathematically linked with addition, subtraction, multiplication, division, and exponential operators. This condition leads to a very complicated propagation of error in the independent variables and in the dependent variable (the predicted roof temperature).

It may be possible for the instruments to determine a theoretical error interval and / or accuracy for the model by using advanced statistical methods and manufacturer specified error. However, this outside the scope of this study.

The relevant question remaining is how many significant figures can be reasonably reported from the roof temperature model. In this case, there is a very complicated condition of error propagation and numerous variables in the model, each with its own number of significant figures. For this reason, the most conservative approach is to utilize the most basic method taught in the sciences for significant figures: one cannot report more significant figures in their answer than is contained in their least accurate measurement. In this case, the least accurate instrument used, and therefore the measurement that should be used in the model, is the measurement of thermocouples. The accuracy in the thermocouples, as discussed in Section 4.3, is limited to the tenths of a degree. Therefore, the temperatures recorded in the spreadsheet calculations are rounded half up to the tenths place. The final temperature calculation, as shown in the t2 column of Figure 7-1, is nested within a round function.

7.3 Discussion of Statistical Methods Available

The use of statistical methods for the analysis of the model results was considered at great length. However, these methods are not appropriate here for three major reasons.

1. *Independence of data points*. As discussed in Section 7.1, the time-step temperature model requires the temperature from the previous time step to complete the calculation in

the current time-step. Therefore, the model output is not independent, and it precludes the use of statistics.

2. *Random sample*. The use of statistical methods typically requires the population sample be random and not biased in any way. In this case, the month of August 2010 was selected based upon scheduling convenience and expected high roof membrane temperatures. In short, if one considers the population under study every day of the year, or if taken to the extreme every day for the life of the roof, the sample of one month, selected by the researcher, is not a random sample. Therefore, randomness in the data sample could not be assumed.
3. *Population being studied*. Considering the lack of random data sampling, it seems reasonable to treat the data set of August 2010 as a closed data set, or more simply as a population onto itself. Statistics allows us to make mathematically founded statements about population metrics from random samples taken from that population. In this case, the August 2010 is a population onto itself. Therefore, utilizing the computational brute force of the computer, we do not need to utilize statistics. Here we are directly measuring the population values, not just a sample of. The difference is akin to a comparison of a sample mean (S) versus a population mean (μ). In this study we are looking directly at the population mean and not a sample mean.

For the reasons discussed in points 1 – 3, the use of statistical methods are generally precluded in this study. Brute force calculations of the population values will be used.

7.4 Error Level Requirement

The author is not aware of any United States standard, such as ASTM, that prescribes a fitment or allowed numerical deviation of predicted values from actual values. In published works authors have used subjective measures such as "very good agreement between calculated and measured values." [1]

The commercial WUFI program, as discussed in Chapter 3, states that it adheres to DIN EN 15026. According to this standard, the only temperature specification is that the model must report a temperature within ±2.5% of the analytical solution for an extremely large thermal mass in a prescribed problem.

As discussed in Section 2.5, the metric used for this model's performance will be percent error. Therefore, the model presented here will be considered valid if the combined average for all membranes and days is less than 2.5% percent error.

7.5 Initial Error Results

With the model entered into an Excel worksheet and the raw metrological and sensor data imported for each day, the model performance and accuracy could be examined. Each of the 29 days were entered into its own workbook and saved. The results of the model predicted temperature against the measured temperatures were plotted. The entire collection of these plots are made available in Appendix B. Figures 7-2, 7-3, and 7-4 are selected plots from the group. These plots visually demonstrate the ability of the model to closely track with the recorded

membrane temperatures without any user corrections or input. The model, after the first time step, appears to make 8,639 successive accurate calculations.

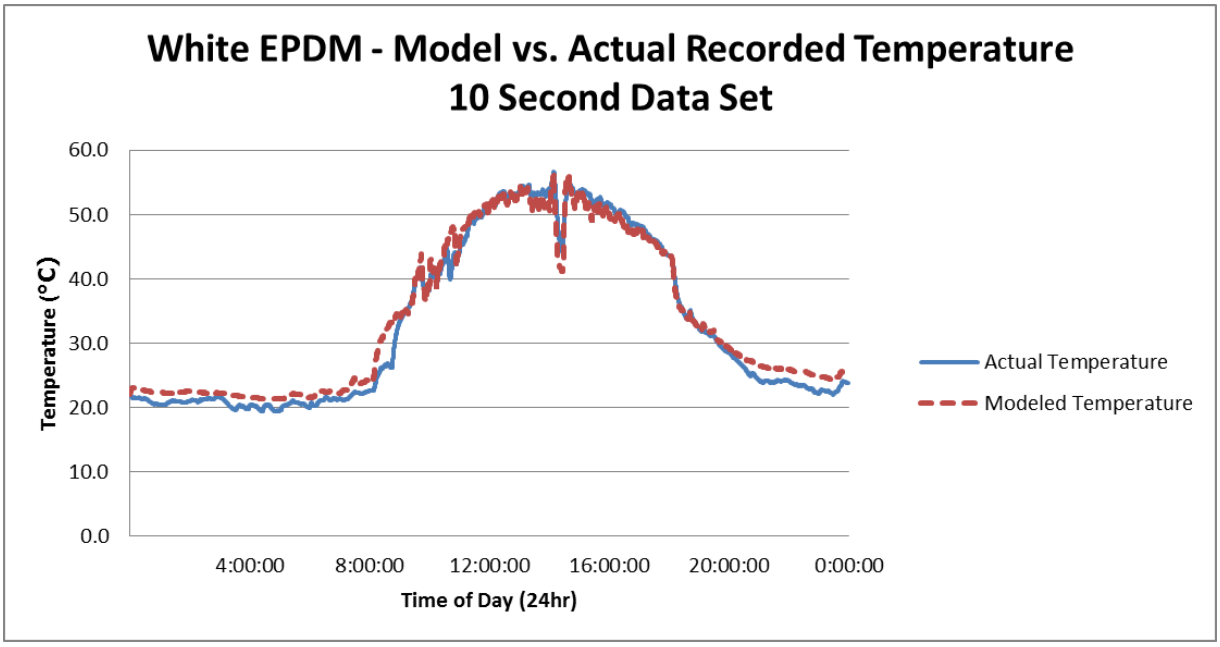

Figure 7-2 Plot of predicted temperature against modeled temperature for White EPDM on August 11, 2010

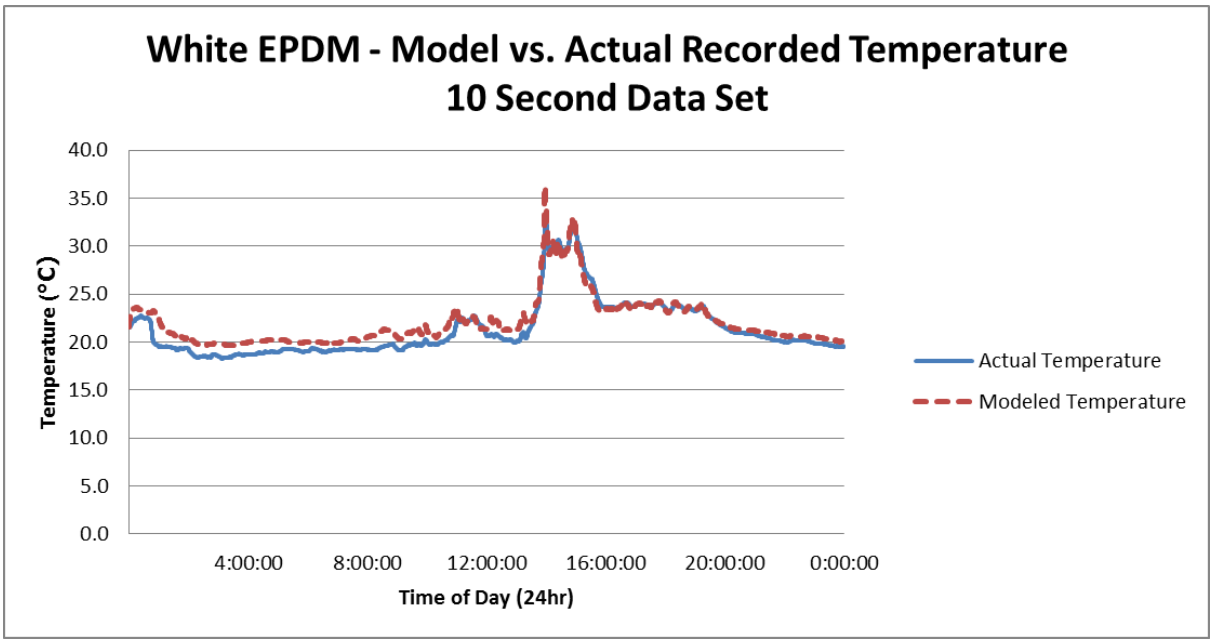

Figure 7-3: Plot of predicted temperature against modeled temperature for White EPDM on August 17, 2010. Intermittent precipitation was recorded on this day. The model was still able to track very respectably with the measured membrane temperature.

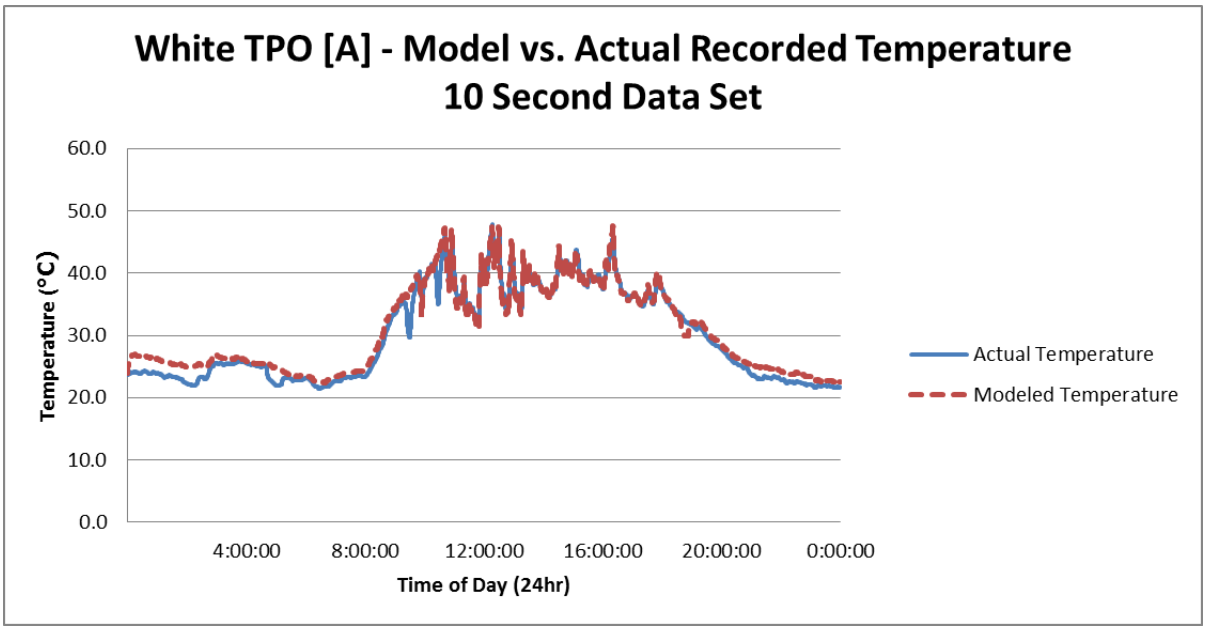

Figure 7-4: Plot of predicted temperature against modeled temperature for White TPO [A] on August 4, 2010. The insolation on this day was highly varied. It was possibly a day with high broken clouds. The model still appears to track very well.

Figure 7-3 demonstrates an interesting issue, that of precipitation and nighttime surface condensation. For the purpose of this study the effects of precipitation and latent heat inherent with roof membrane surface condensation and evaporation, are ignored. A more thorough discussion of these effects and their impact on the model are discussed in Appendix C.

While the model visually appears to perform well, the question of quantitative performance remains. Within each workbook, the error for each time step was calculated for each membrane. This calculation was done in accordance with Equation 2-1 and can be seen in its own column in Figure 7-1. The results for each membrane were calculated and tabulated within each workbook. These error results were then combined and plotted. Figures 7-5 and 7-6

show boxplots for the average daily error for each membrane and all membranes combined respectively.

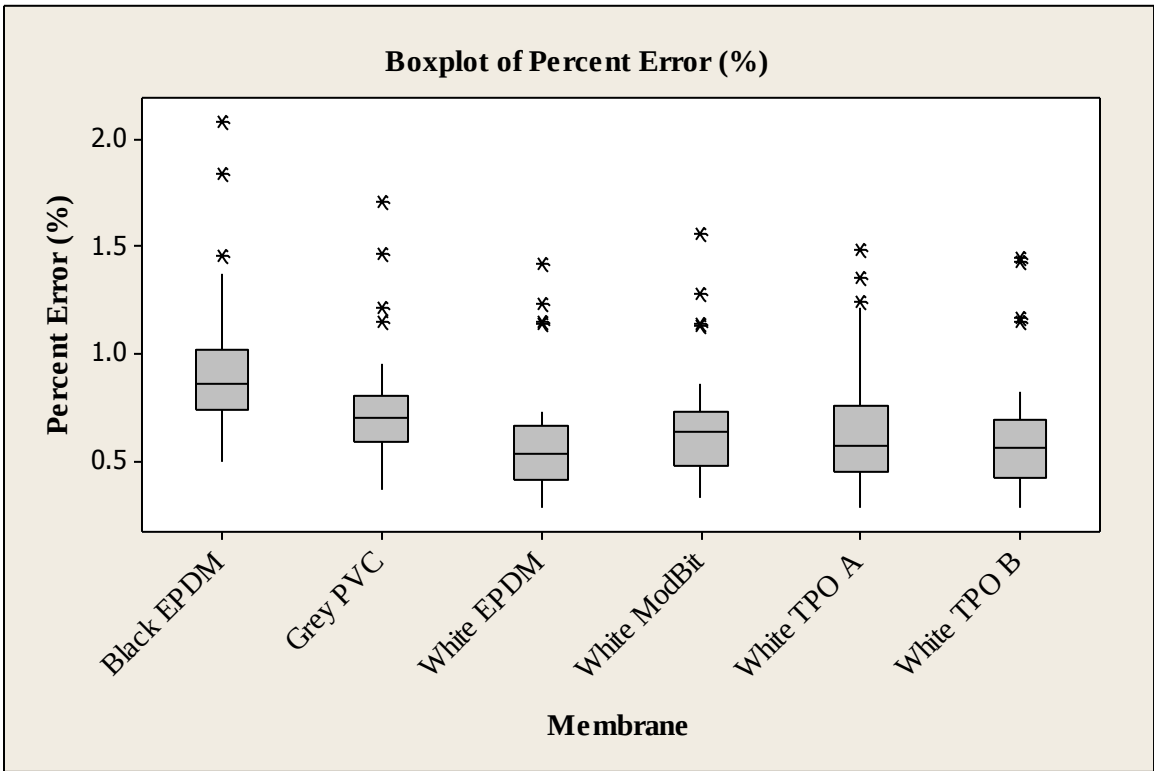

Figure 7-5 A boxplot of the average percent error for each day of August, 2010. In this Boxplot each membrane is shown separately.

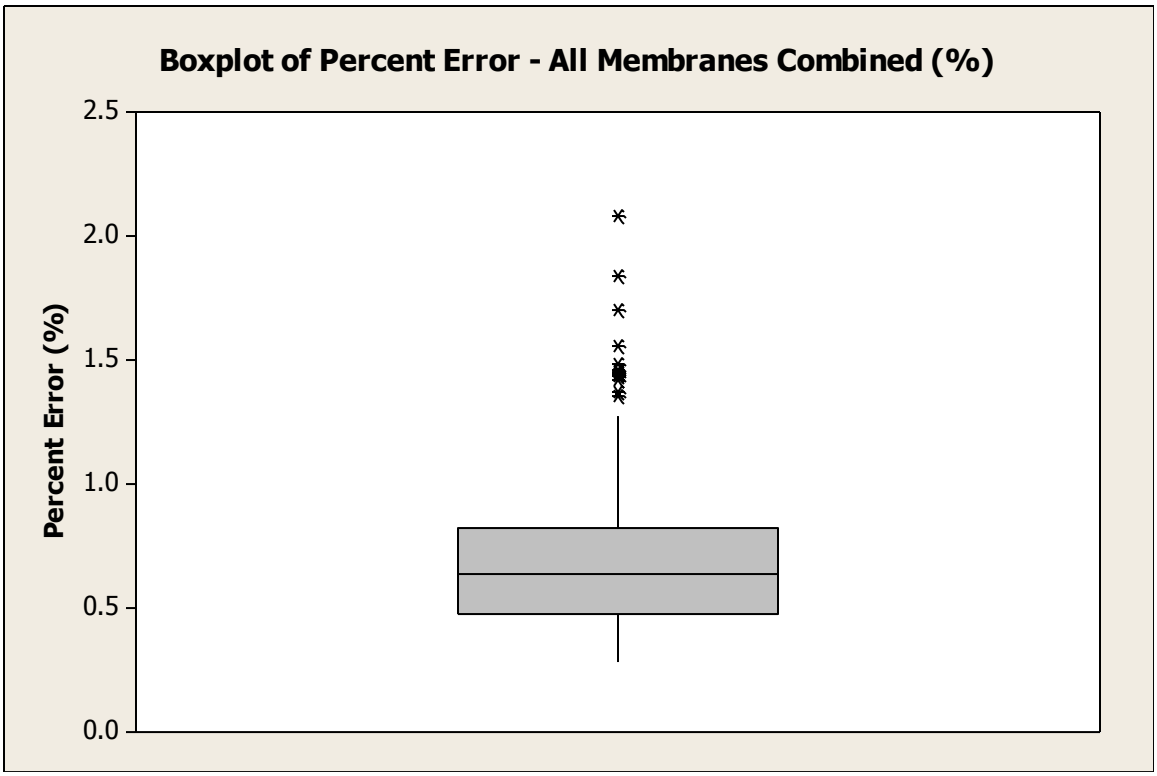

Figure 7-6 A boxplot of the average percent error for each day of August, 2010. In this boxplot, each day has all the membranes combined into a single error number for that day.

The membrane to membrane average error numbers vary slightly, suggesting some membranes performed better than others under the model. However, the goal was a combined average for all membranes and for all days. The combined average percent error for all membranes and all days was 0.71%. This number is well below the goal of 2.5% set out. Therefore, based on a qualitative visual analysis of the plots in Figures 7-2, 7-3, 7-4, and Appendix B, combined with the quantitative result of the cumulative average percent error, the model is validated.

References

1. Wilkes, K.E., *Model for Roof Thermal Performance*. 1989, U.S. Department of Energy: Oak Ridge National Labs. p. 98.

2. Kunzel, H.M., *Simultaeous Heat and Moisture Transport in Building Components*, in *Fraunhofer Institute of Building Physics*. 1995, University of Suttgart: Suttgart, Germany. p. 65.

Chapter 8: Model Sensitivity Analysis

8.1 Introduction

With a validated model from Chapter 7, the focus of this study turned to conducting a sensitivity analysis on the following independent variables in the model:

1. Interior Temperature (T_I)
2. Thermal Resistance (R)
3. Solar Reflectivity ($\propto_{Solar}$)
4. Insolation (G_{Solar})
5. Emissivity (ε)
6. Long Wave Irradiance (G_{Long})
7. Convective Coefficient ($h_{Convection}$)
8. Air Temperature (T_A)
9. Specific Heat (C)
10. Membrane Mass (U)

The purpose of this sensitivity analysis of a model is to ascertain how uncertainty or measurement errors in the input variables affect the accuracy of the model output. As a model becomes more and more complex, the ability of the researcher to assess sensitivity merely by inspection diminishes quickly with additional variables and mathematical operators. In a case such as this one, with ten variables and numerous mathematical operators, the ability to determine sensitivity by inspection is not reasonable.

While sensitivity information is not easily obtained, this information is of great importance in contemporary and future roof temperature work, as researchers have to make decisions about instrumentation types, instrument placement, and costs. At the same time, architecture and engineering practitioners are beginning to use energy studies and, to lesser degrees, hygrothermal modeling to make design decisions for buildings ranging from single family homes to capital projects. In these cases, practitioners are required to select meteorological and material data sets to enter into these programs with little or no knowledge of the impacts on results. The assumptions and decisions made about the experiment carried out to evaluate the independent variable sensitivity is discussed in the next section.

8.2 Design of Experiment for Sensitivity Analysis

With the inability to assess sensitivity by inspection for this model, a technique or method must be employed. There were multiple methods available, including inspection of scatter plots or factorial experimental design. In this case, the 2^k factorial design would probably have been the preferred method for sensitivity investigation. However, with ten variables to investigate, the sheer number of experimental runs approaches 30,000 without any replicates. Resources were not available to complete this. A fractional factorial was also considered. However, this too would lead to an unacceptable number of required runs.

Another available method was the One Factor At a Time (OFAT) method. When model complexity in number of variables or available computational resources precludes the use of a factorial design, the OFAT method becomes more attractive. This experimental design has been

used by other researchers with complex models[1]. For these reasons, the OFAT method was selected for this study.

The OFAT experimental design artificially manipulates one of the input variables at a time and observes the result. This method treats the model more like a black box in which we cannot know what is going on inside and in which we can only observe and measure inputs and outputs. We must draw our conclusions from what we change going in and what we observe coming out.

The OFAT method is not without a disadvantage. The weakness of the OFAT method is that it is it cannot test for interactions between input variables. While this is not ideal, it is a reasonable tradeoff for an initial research effort in this area.

With the experimental method identified, the methodology must be established and followed. The Microsoft Excel spreadsheet format in which the roof temperature model was constructed and validated is very suitable to using the OFAT method of sensitivity analysis. This format allows a process to be followed in this order, the file to be opened, the desired variable to be manipulated, the result to be recorded, and then the file closed. This process can then be repeated for all 29 days of data collection and for each variable.

While the method of carrying out the OFAT experiment, by its name, is somewhat self-explanatory, the amount of manipulation for each factor or variable is a critical decision in the experiment. Initial consideration was given to selecting a manipulation level for each variable based on what reasonable ranges of their properties might be. For example, if a practitioner did not have the material data for a roof membrane they wished to study, but a competitor's product data was available, would that hypothetical scenario be a good metric for input variable

manipulation? This methodology is poor and unacceptable as it introduces an artifact of subjective variable manipulation. This subjective and non-uniform manipulation would preclude the comparison of variable-to-variable results from the sensitivity analysis.

The most conservative approach is to manipulate objectively each variable by a uniform amount. From other studies this author has conducted [2], field measured reflectivity values were found to be significantly lower than manufacturer reported values – as much as 20% or more below the number reported in the manufacturer's literature. Based on this experience, the 20% variation appeared to be a reasonable and realistic variable manipulation.

The 20% manipulation could easily be applied to each of the input data. The question remained whether to use 120% or 80% of the actual input numbers. After careful consideration 80% was chosen because increasing several of the input variables, or variable data streams, would create out of domain situations. To be more specific, the increase of solar irradiance and emissivity by 20% is not physically possible and therefore not reasonable.

Consider, the power of solar radiation reaching the exterior of the earth's atmosphere is approximately 1,362 W/m^2. This value is referred to as the solar constant. Therefore, the solar irradiance on a roof, below miles of atmosphere, cannot exceed the solar constant. However, readings in excess of 1200 W/m^2 were recorded in the August 2010 data. If we were to increase even the 1200 W/m^2 by 20%, we would arrive at 1440 W/m^2, which cannot be, as it is greater than the solar constant.

The concept of emissivity is derived from that of a Plankian black body, or a perfect absorber and radiator of infrared radiation. The measure of emissivity is based on a percentage of the energy emitted by a real body versus what a theoretical black would emit. In this study, we

examined roof membranes with a manufacturer reported aged emissivity of 0.86. Increasing this 0.86 by 20% makes it greater than a black body with an emissivity of 1.03, which is physically impossible. Because increasing the input data by 20% would create out of domain values, the decision was made to use a decrease of 20% as the standard value for the OFAT experiment.

The methodology for conducting the OFAT experiment is as follows:

1. Open spreadsheet for specific day
2. Manipulate input variable by multiplying value or data column by 0.8
3. Record the resultant predicted temperature error against the measured value using Equation 2-1
4. Close the file
5. Repeat steps 1-4 separately for each of the 29 days and for each of the 10 variables
6. Consolidate the OFAT results and analyze

The primary metric for analyzing the OFAT results is the difference between the baseline percent error values established during the validation portion of this study and the resultant percent error change measured from the OFAT input manipulation. This comparison of percent error is calculated within days and compared as a population.

8.3 Sensitivity Results

The effect of the input variable manipulation is shown between Figures 8-1 and 8-2. Figure 8-1 shows the original model predicted roof membrane temperature against the measured roof membrane temperature. Figure 8-2 shows the model predicted roof temperature, after the 20% reduction of the incoming long wave radiation, against the measured roof membrane

temperature. The reduction in incoming energy leads to an obvious underprediction of roof membrane temperature.

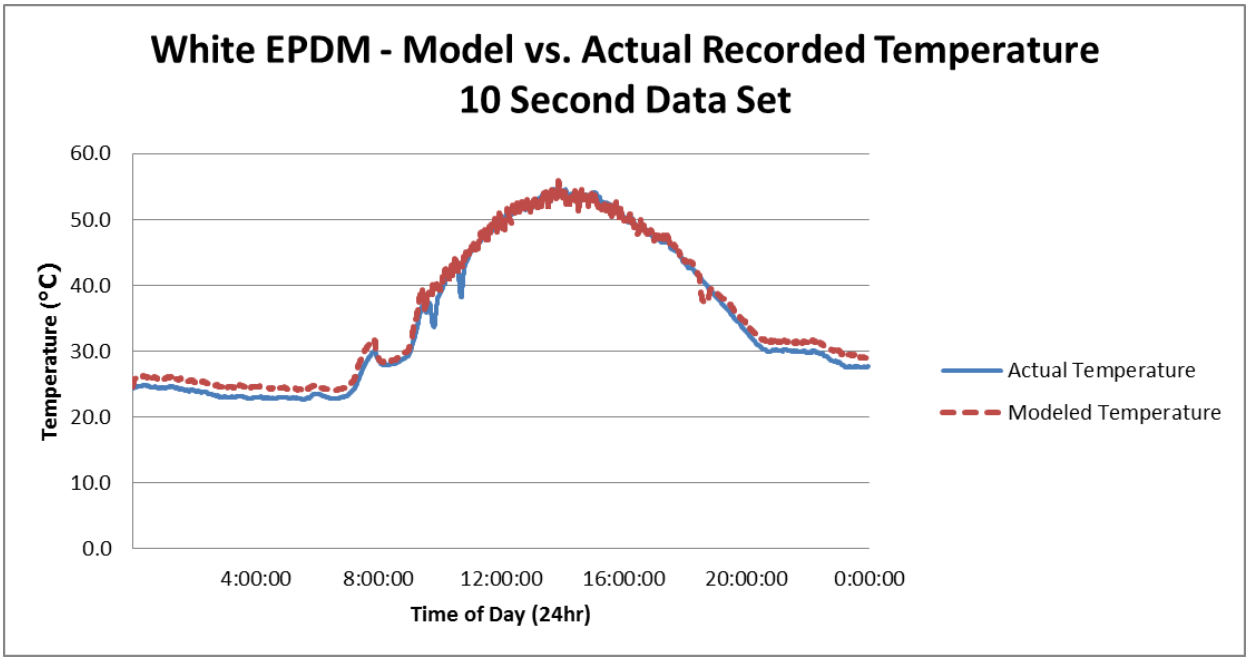

Figure 8-1 Model predicted roof membrane temperature against the measured value for 8/8/2010.

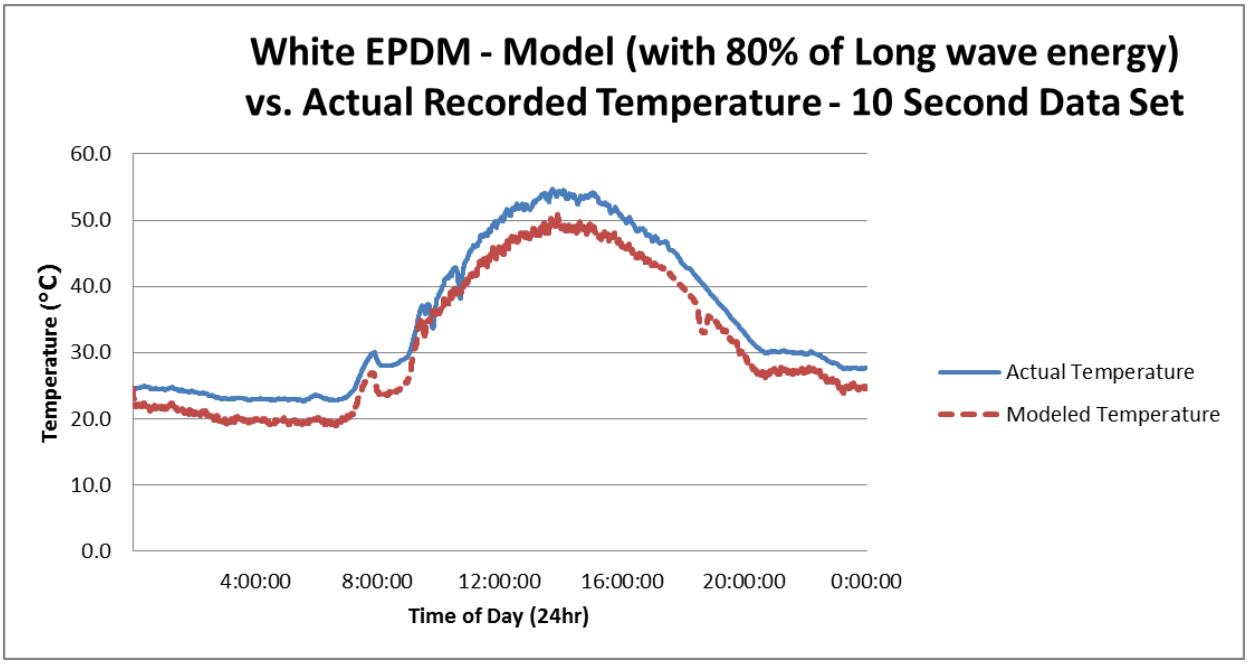

Figure 8-2 Model predicted roof membrane temperature, with a 20% deduction in incoming long wave radiation, against measured temperature for 8/8/2010.

Figure 8-3 presents a box plot for the within day change for the entire OFAT analysis. The metric used is shown in Equation 8-1. The percent error was averaged for each membrane during the day being modeled, as was done in validation. This daily average percent error for each membrane was subjected to Equation 8-1. The resultant six membranes were averaged and recorded as the resultant change in percent error during the OFAT analysis ($\Delta_{\%Accuracy}$) for that day.

$$\Delta_{\%Accuracy} = Percent\ Error_{OFAT} - Percent\ Error_{Validated}$$

Equation 8-1 Metric used to measure impact of OFAT analysis

Where:

$\Delta_{\%Accuracy}$ = Change in Accuracy (%)

$Percent\ Error_{OFAT}$ = Percent Error from OFAT Analysis (%)

$Percent\ Error_{Validated}$ = Percent Error from Validation Phase (%)

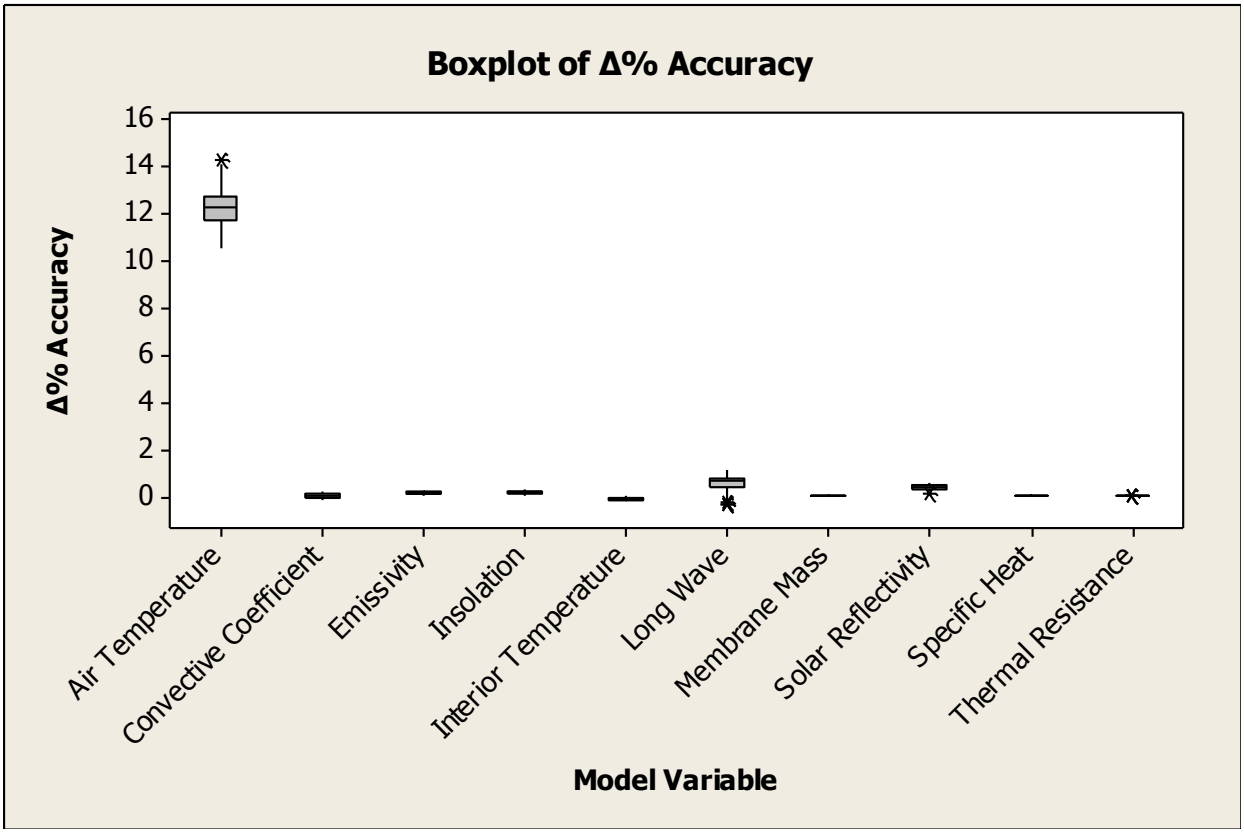

Figure 8-3 A box plot for the resultant within days percent error change for the OFAT analysis.

The obvious observation from Figure 8-3 is the scale impact of the air temperature (T_A) variable. This fact makes inspection of the other variables difficult. Therefore, air temperature (T_A) is

presented as its own boxplot in Figure 8-4. The remaining variables are presented in an additional boxplot in Figure 8-5.

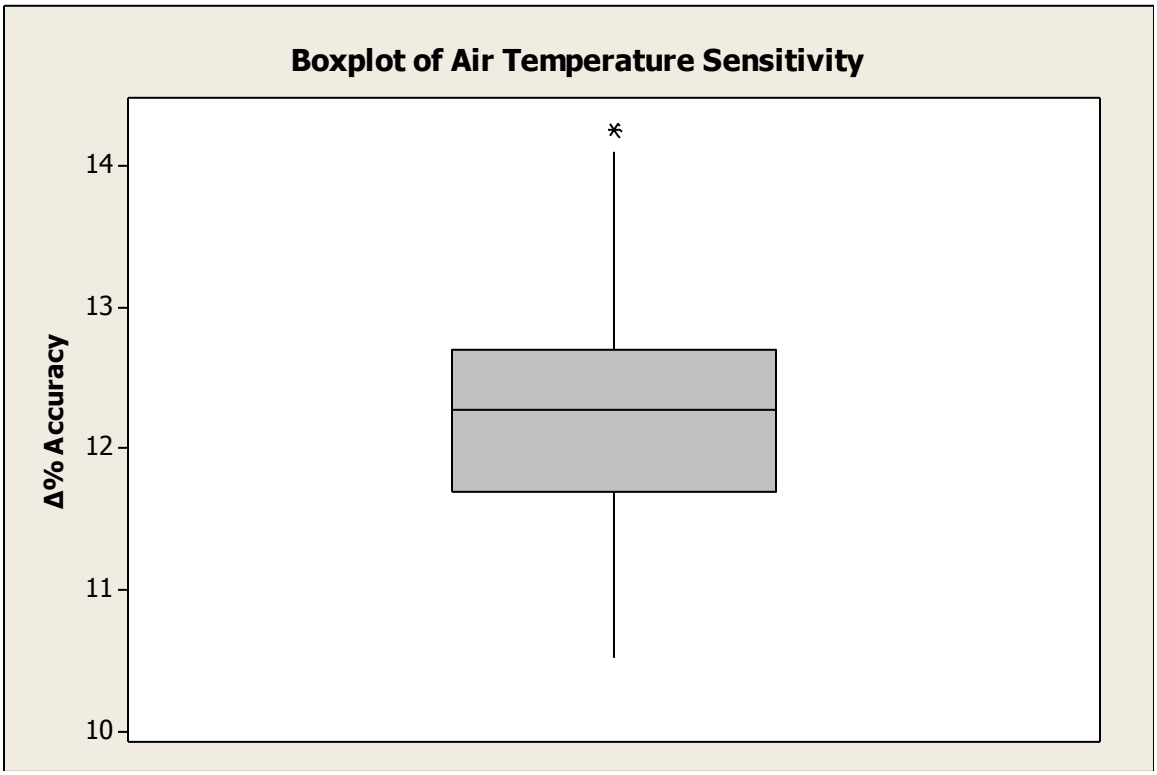

Figure 8-4 A boxplot showing the within day impact of the OFAT analysis for air temperature (T_A)

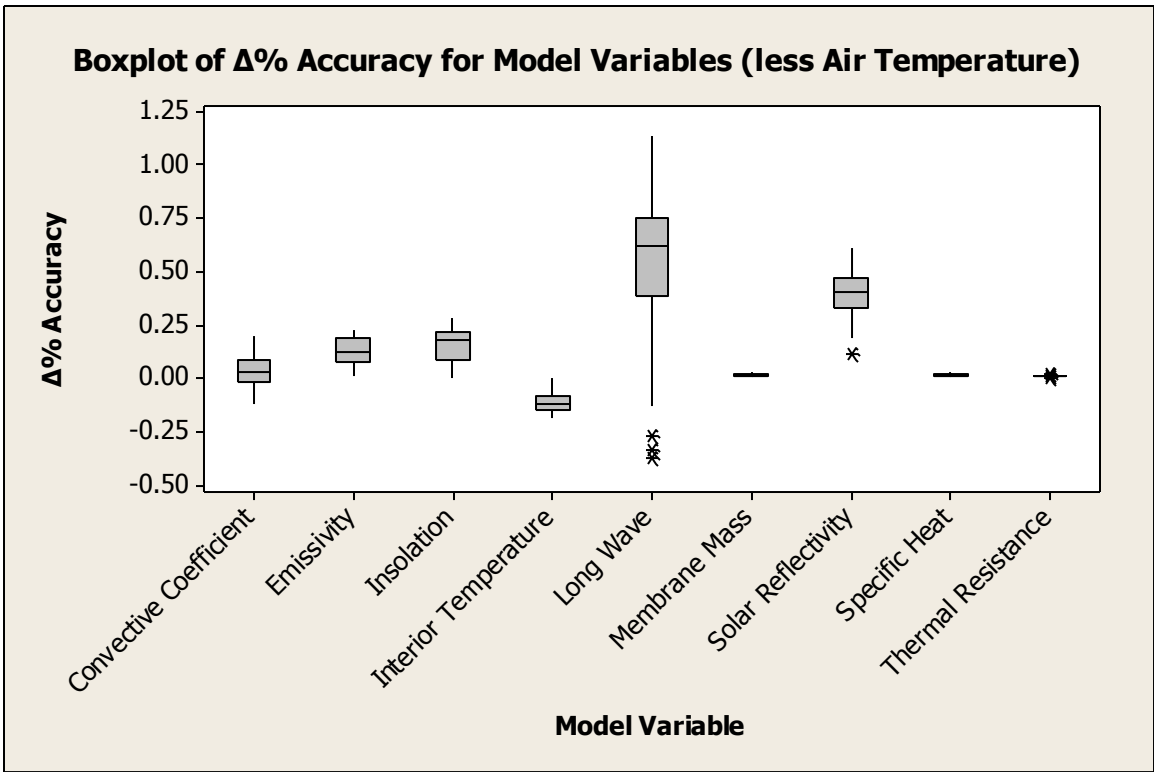

Figure 8-5 A boxplot of the remaining input variables, studied under the OFAT analysis, once air temperature (T_A) was removed.

With the within day analysis completed, a more comprehensive look at the cumulative effect of the OFAT experiment on the population month was done. Each variable studied was averaged, over the population, from its effect on the respective day. This method allows the best overall display of the OFAT result. Figure 8-6 presents a bar chart of the sensitivity of the roof temperature model to its input variables. As with the boxplots, the strength of the Air Temperature (T_A) signal tends to mask the other variables. Figure 8-7 presents a bar chart of the cumulative effect on the accuracy of the roof temperature model by the nine (9) remaining variables.

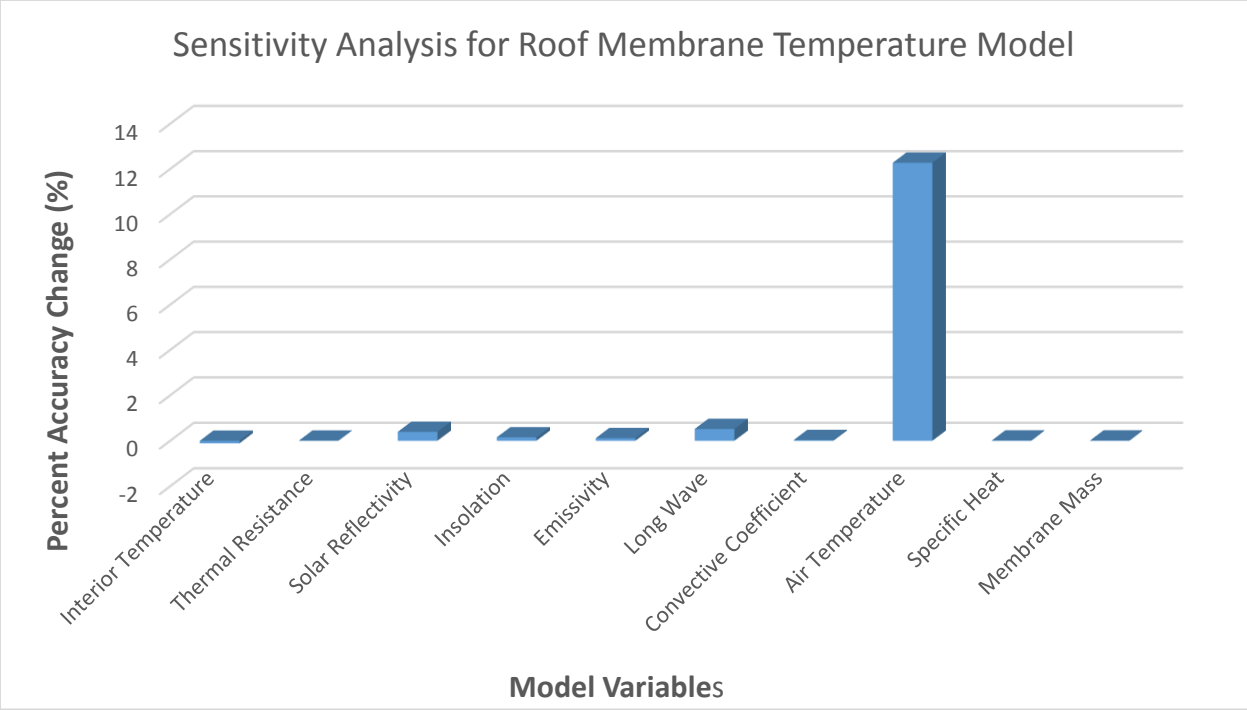

Figure 8-6 Cumulative bar chart of OFAT analysis on 29 day population of data.

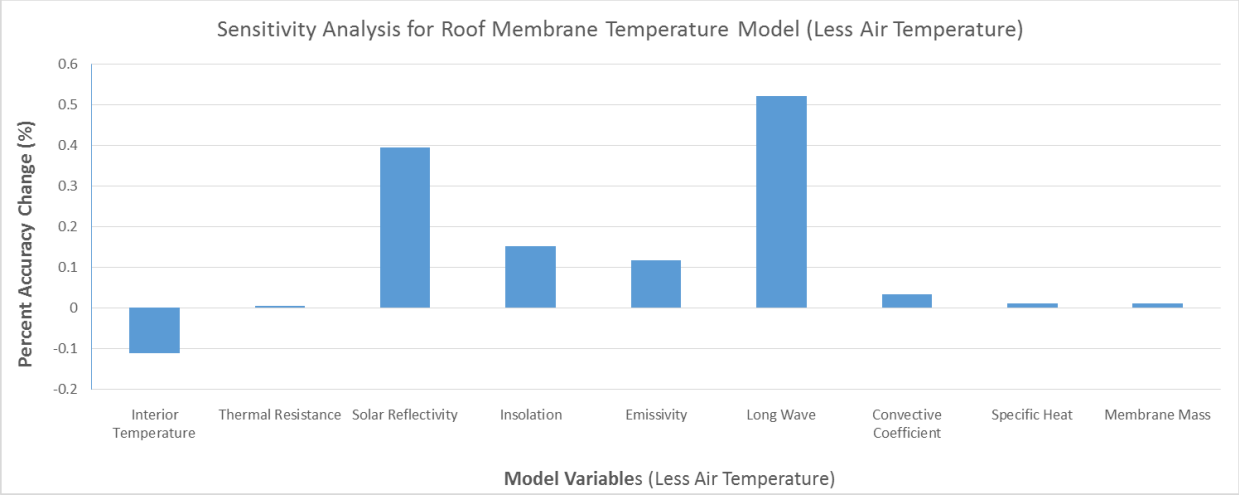

Figure 8-7 Cumulative bar chart of OFAT analysis on 29 day population of data, with air temperature (T_A) removed to improve the resolution of the remaining variables.

Table 8-1 presents the numeric results of the OFAT analysis on the roof temperature model.

Model Variable	Percent Change in Accuracy (%)
Interior Temperature (T_I)	-0.11
Thermal Resistance (R)	0.01
Solar Reflectivity ($\propto_{Solar}$)	0.39
Insolation (G_{Solar})	0.15
Emissivity (ε)	0.12
Long Wave (G_{Long})	0.52
Convective Coefficient ($h_{Convection}$)	0.03
Air Temperature (T_A)	12.28
Specific Heat (C)	0.01
Membrane Mass (U)	0.01

Table 8-1 Numeric results of the OFAT analysis on the roof membrane temperature model.

8.4 Discussion of Sensitivity Results

By observing the results presented in Table 8-1 we can rank the input variables in terms of their absolute influence on the accuracy of the roof membrane temperature model:

1. Air Temperature (T_A)
2. Long Wave (G_{Long})
3. Solar Reflectivity ($\propto_{Solar}$)
4. Insolation (G_{Solar})
5. Emissivity (ε)
6. Interior Temperature (T_I)
7. Convective Coefficient ($h_{Convection}$)
8. Thermal Resistance (R)
8. Specific Heat (C)
8. Membrane Mass (U)

Clearly, the air temperature term is the dominant variable in terms of model accuracy. In fact, air temperature is two orders of magnitude more dominant than the next term, long wave radiation.

We must interpret these results carefully. The goal of the OFAT analysis was to determine how uncertainty or, more commonly, error in estimation or measurement of the input variables can affect the accuracy of the roof membrane temperature model, not how these variables affect the temperature of the roof membrane. The exercise to determine sensitivity

impact on roof membrane temperature could easily be accomplished with this model, but is not the focus here.

Because air temperature (T_A) was so dominant in the OFAT study, it generated additional interest. Unlike some of the other variables, where a 20% increase in value would place them in an out of bounds domain, the air temperature can be increased. In order to avoid large calculation loads, a simple scanning exercise was performed on a single day of the data population. In this exercise, the same metric was used from Equation 8-1. However, in this exercise the temperature was varied from -20% to +20% in one percent increments. This was done to see the effect on both sides of the domain and verify the result of the initial OFAT experiment. The results are shown in Figure 8-8. At low percentages, there appears to be almost parity. However, as the percentage of artificially induced air temperature errors are increased, there is a small divergence. This is most likely due to the membrane temperature and interaction with long wave energy emission, where the calculation involves membrane temperature as a power function. This exercise reinforced the finding of the magnitude of influence air temperature (T_A) has on the model accuracy.

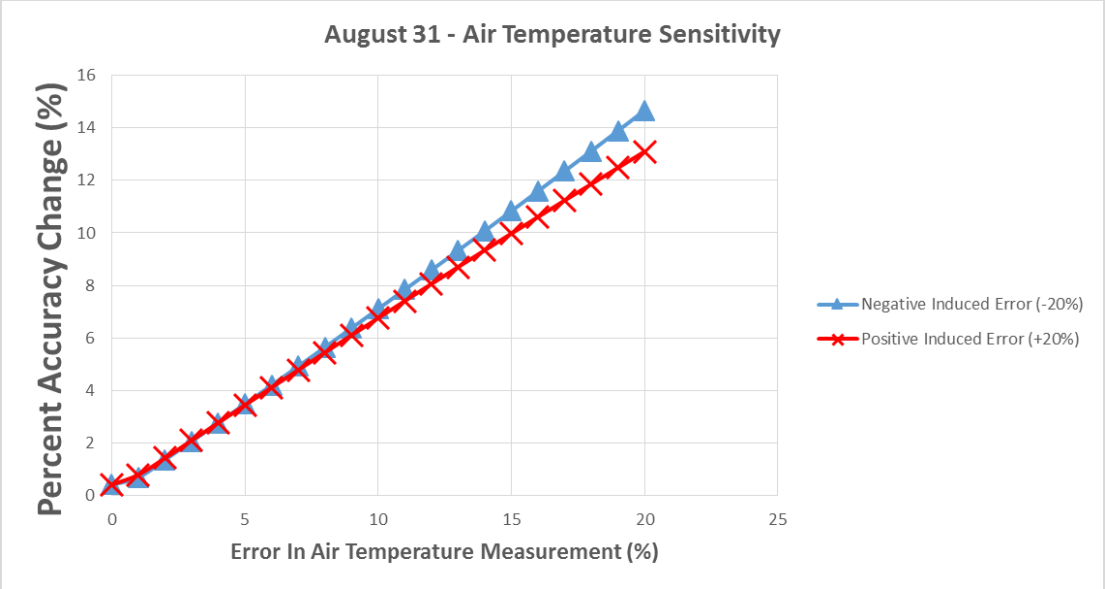

Figure 8-8 Analysis for white EPDM membrane

The interior temperature (T_I) stands out in Table 8-1 because it is negative, while all others are positive. This difference implies that by lowering the interior temperature, the model was made more accurate. This implication is counterintuitive. Careful review of the data and instrumenting suggests that this number may be an artifact of incorrect instrumentation. The data collected for the interior temperature (T_I) variable was in fact air temperature under the roof. When examining the theory for conduction through a solid mass, the calculation is made from one surface to the opposing surface. In this case, it should be calculated as the interior surface temperature to exterior surface temperature not interior air temperature to exterior surface temperature, as was done. During night time hours, the roof membrane is radiatively cooling below air temperatures by 10° K or more [3]. This cooling would lead to the interior surface losing heat energy to the exterior, and it would lead to cooling of this interior surface, which may or may not be detected by the interior air temperature data.

Exterior air temperature is one of the more accessible metrological variables to measure. Even the most basic weather station has this capability. The exact location where we measure the air temperature should be carefully considered. Do we measure on the roof top? If so, how far above the roof provides the most accurate measure of air temperature (T_A) that the roof will see? In the summer of 2013, this author conducted a separate study in which air temperatures above multiple roofs in the Chicago area were studied. Shielded air temperature measurements were made between 1 and 8 feet above the roof membrane. The study concluded that regardless of the roof membrane instrumented less than 1°F difference, on average, existed between any of the levels measured above the roof membrane. Therefore, the author concludes that instrumenting height above the roof membrane between 1 and 8 feet minimally impacts rooftop air temperature measurements.

However, given the fact that winds will move air in from outside the area of influence of the roof, it is reasonable to ask if it is better to measure air temperature at the ground level instead. One study has shown up to a 3°C difference in air temperatures measured at ground level versus at roof top levels in London [4]. This aspect may warrant more investigation.

To further complicate the issue of meteorological data and air temperatures, predictive models used for forensic and design situations rely on meteorological data from sources such as the National Oceanic and Atmospheric Administration. These data sets, collected from weather stations around the United States, provide historical meteorological data at one hour intervals. NOAA's sampling rate is one sample per hour. However, the data was collected for this study at a rate of one sample every 10 seconds. The sampling rate is a confounding variable. Fortunately,

the validated model and spreadsheet format is suitable to answer this confounding issue and is looked at in the following chapter.

References:

1. Murphy, J.M., et al., *Quantification of modelling uncertainties in a large ensemble of climate change simulations.* Nature, 2004. **430**(7001): p. 768-772.

2. Dupuis, M., *Highly Reflective*, in *Professional Roofing*. May 2013, National Roofing Contractors Association: Rosemont, IL.

3. Dupuis, M., *Nighttime Radiative Cooling of Low Slope Roofs,* in *International Roofing Symposium* 2011, National roofing Contractiors Assoctaion (NRCA): Washington D.C.

4. Grillini, B., *A comparison of air temperatures at street and roof level in London.* Weather, 1981. **36**(4): p. 104-108.

Chapter 9: Error Introduced by Data Sampling Rate

In Chapter 8 the One Factor At a Time (OFAT) method was utilized to study the sensitivity of each independent variable in the roof membrane temperature model. There remains a confounding variable that was not explored in the OFAT analysis. The variable that remains to be explored is the data sample rate. The sample rate refers to the data acquisition and how many measurements are recorded in a given time period. For this study, the raw data acquisition was made every 10 seconds. This means that every instrument on the roof to include roof membrane temperature, radiation, and meteorological readings were recorded every 10 seconds.

The data sample rate should not be confused with the time period (Δt) variable in the roof membrane temperature model. This variable refers to the time difference between calculations of membrane temperature. Out of convenience this variable was set to the 10-second data sampling rate for this study. In past studies, researchers did do sensitivity analysis on the time period variable[1]. However, this effort seemed oriented towards reducing computational time, as a smaller time period leads to more computations. With current computer processing power, this is not as much of a concern. Therefore, the 10-second time period (Δt), sometimes referred to as a time step, was left at a constant throughout this study.

The data sampling rate utilized in past studies was averaged hourly data [1]. If commercial energy analysis software or hygrothermal modeling software is used, the program must be provided with input meteorological data for the location being studied. Historical meteorological data is available from sources such as the National Oceanic and Atmospheric

Administration's National Climatic Data Center. However, this data is only available in an hourly format.

As discussed in Chapter 1, the author of this study in not aware of any prior studies in which data was collected at the high data sampling rate used in this study. Nor is the author aware of a study in which the data sampling rate's effect on accuracy was examined. Utilizing the validated model for this study and the ability to quickly resample the raw data in the spreadsheets, the roof temperature model's sensitivity to the data sampling rate variable can be explored.

9.1 Data Sample Rate Sensitivity Experiment Methodology

As with the OFAT analysis in Chapter 8, the principle methodology here to modify the data sampling rate and observe the resulting change in accuracy of the roof membrane temperature model. Then a level of manipulation for the data sampling rate was selected. The native or base line data sampling rate used in this study has been 1S/10s (one sample every ten seconds). The logical choice for the top end of the manipulation, based on discussion earlier in this chapter, was 1S/1hr (one sample per hour).

However, one of the advantages of using a spread sheet for these calculations is the ability to compose the master spread sheet, which allows multiple data sampling rates to be calculated simultaneously. To perform this these calculations, the raw data for one day is inserted into one worksheet, and by referring to common cells and using data sorting functions, the spreadsheet can calculate multiple data sampling rates and their associated percent error in one step. Setting up a master spread sheet to simultaneously calculate these iterations saved time

overall, and only 29 runs were technically needed to cover the entire population. Thus within each run multiple data sampling rates were calculated.

Given the ability to streamline the calculation process, six (6) data sampling rates were simultaneously calculated. These data sampling rates were one sample every 10 seconds, 30 seconds, 1 minute, 5 minute, 10 minute, and 1 hour.

The altering the data sampling rate was accomplished with a count column and a simple conditional command. A selection of cells from a “1 Hour” worksheet are shown in Figure 9-1. In order to convert the 1S/10s data into the desired data sampling rate, each input data cell used the condition “IF” command that was conditional on the count. An example of a cell entry is as follows: “=IF(P11/360-INT(P11/360)=0,'10 sec'!M11,M10)”. It should be noted that this method produces a true sampling of data at the specified time interval. This is in contrast with a method in which one would record an average of the readings within the time interval. Taking this true sample best mimics the situation of using historical weather data that is termed “hourly readings” by the National Climatic Data Center.

Pyran (V)	Pyran	Interior 2		time	Count	Air Temp	Vind Spee	Dew Point	Rain
V	w/m2	K°		hh:mm:ss		K°	m / s	K°	cm / hr
0.00	-1.09	306.83		0:00:00	0	303.48	1.79	294.17	0.00
0.00	-1.09	306.83		0:00:10	1	303.48	1.79	294.17	0.00
0.00	-1.09	306.83		0:00:20	2	303.48	1.79	294.17	0.00
0.00	-1.09	306.83		0:00:30	3	303.48	1.79	294.17	0.00
0.00	-1.09	306.83		0:00:40	4	303.48	1.79	294.17	0.00
0.00	-1.09	306.83		0:00:50	5	303.48	1.79	294.17	0.00
0.00	-1.09	306.83		0:01:00	6	303.48	1.79	294.17	0.00
0.00	-1.09	306.83		0:01:10	7	303.48	1.79	294.17	0.00
0.00	-1.09	306.83		0:01:20	8	303.48	1.79	294.17	0.00

Figure 9-1 An example of cells from a 1S/1hr spreadsheet

The master workbook was assembled to calculate the percent error in the roof membrane temperature model for one sample every 10 seconds, 30 seconds, 1 minute, 5 minutes, 10 minutes, and 1 hour. The master workbook was then utilized to calculate the percent error for these sampling rates and averaged for the 29 days in the population. The results are reported in the following section.

9.2 Results of Data Sample Rate Sensitivity

The graphical results of decreasing the data sampling rate from the native 1S/10s are shown in Figures 9-2 through 9-7. These figures demonstrate that the model predicted temperature slowly becomes less and less accurate. When we arrive at the 1S/1hr sample rate in Figure 9-7, we can see that the predicted model appears to be more of a step-wise graph.

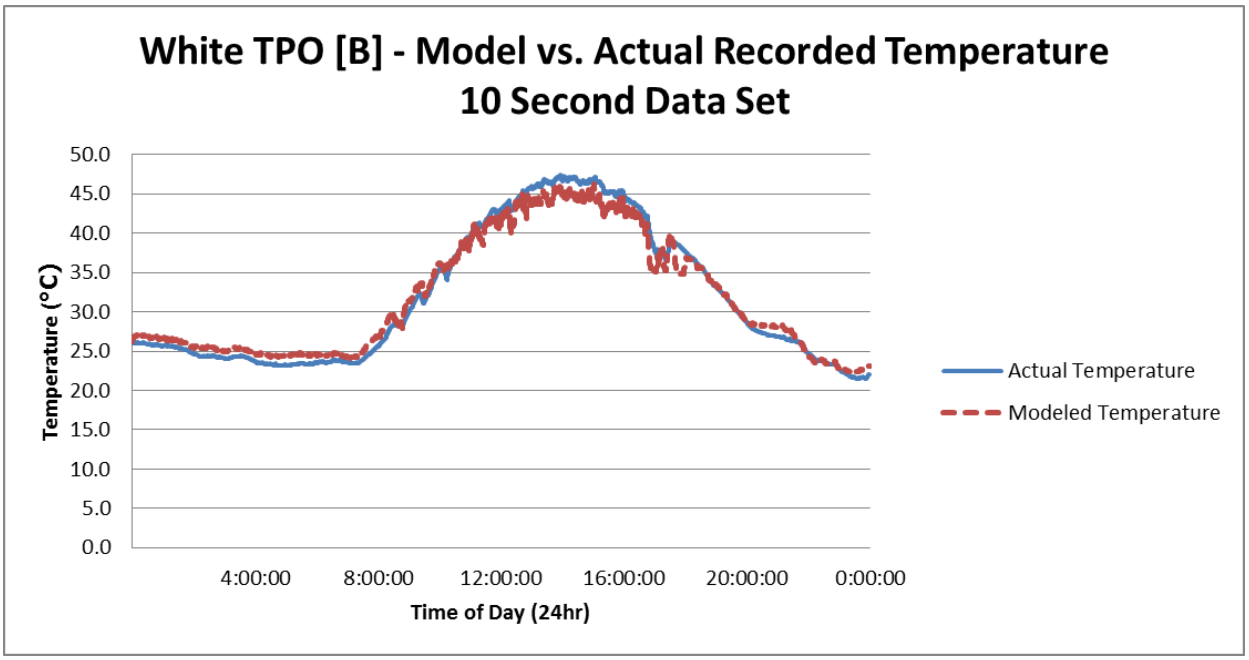

Figure 9-2 1S/10s for 8/31/2010

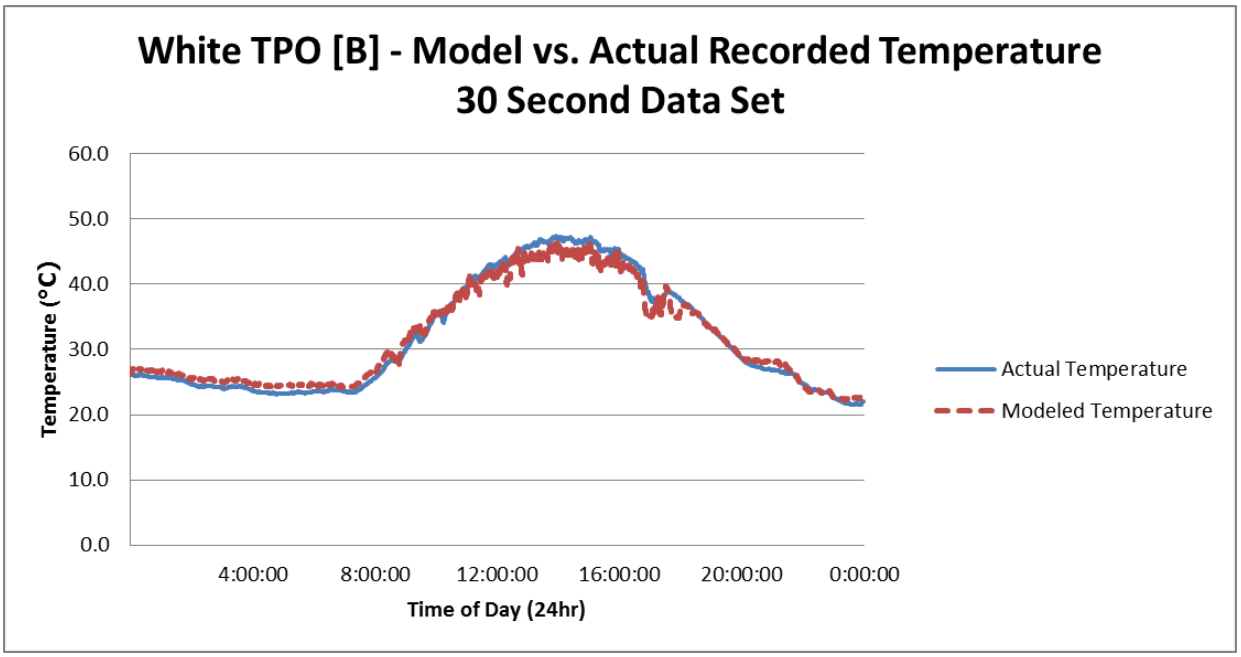

Figure 9-3 1S/30s for 8/31/2010

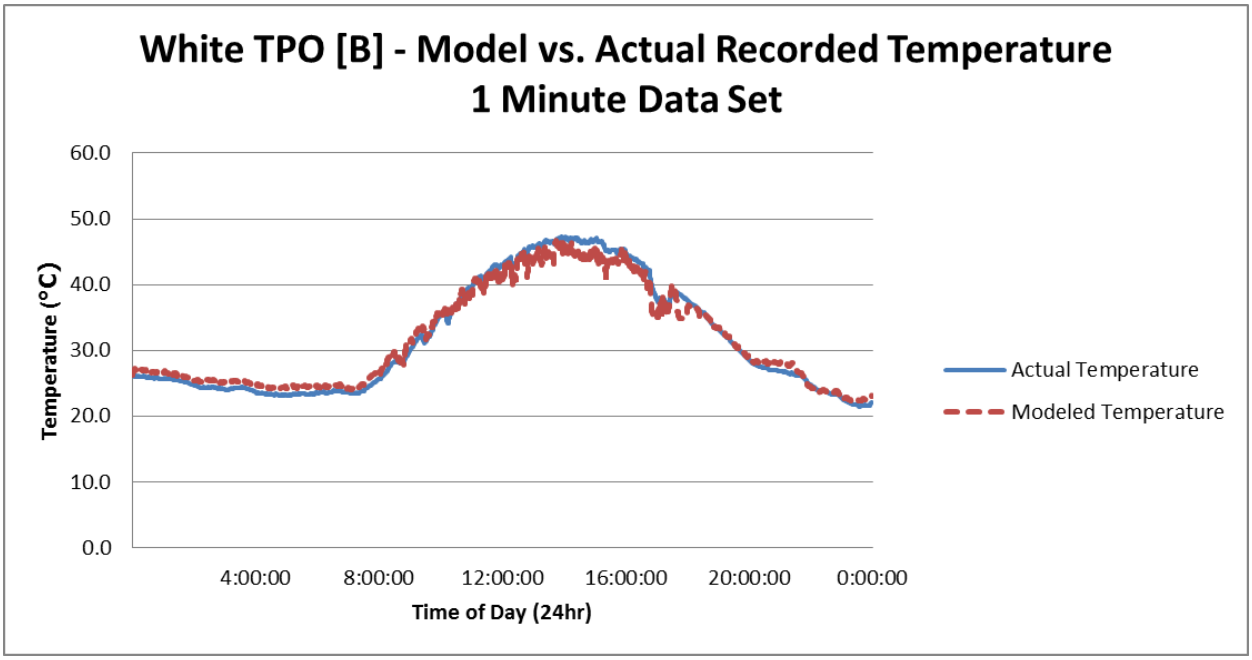

Figure 9-4 1S/1min for 8/31/2010

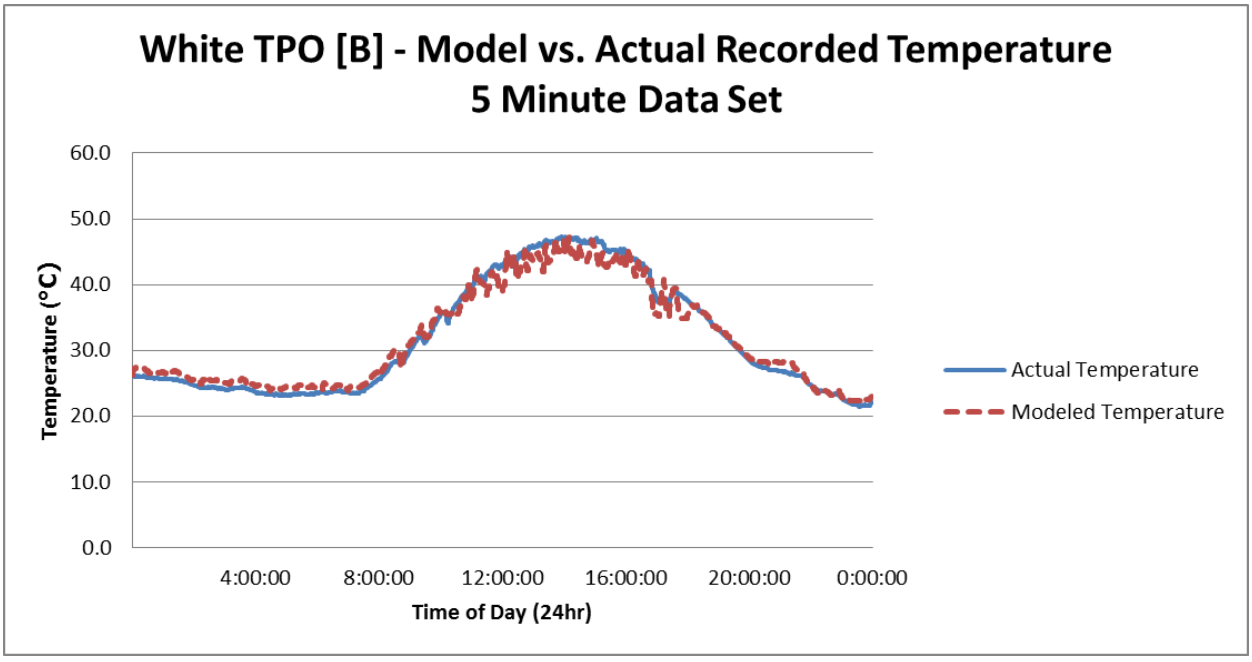

Figure 9-5 1S/5min for 8/31/2010

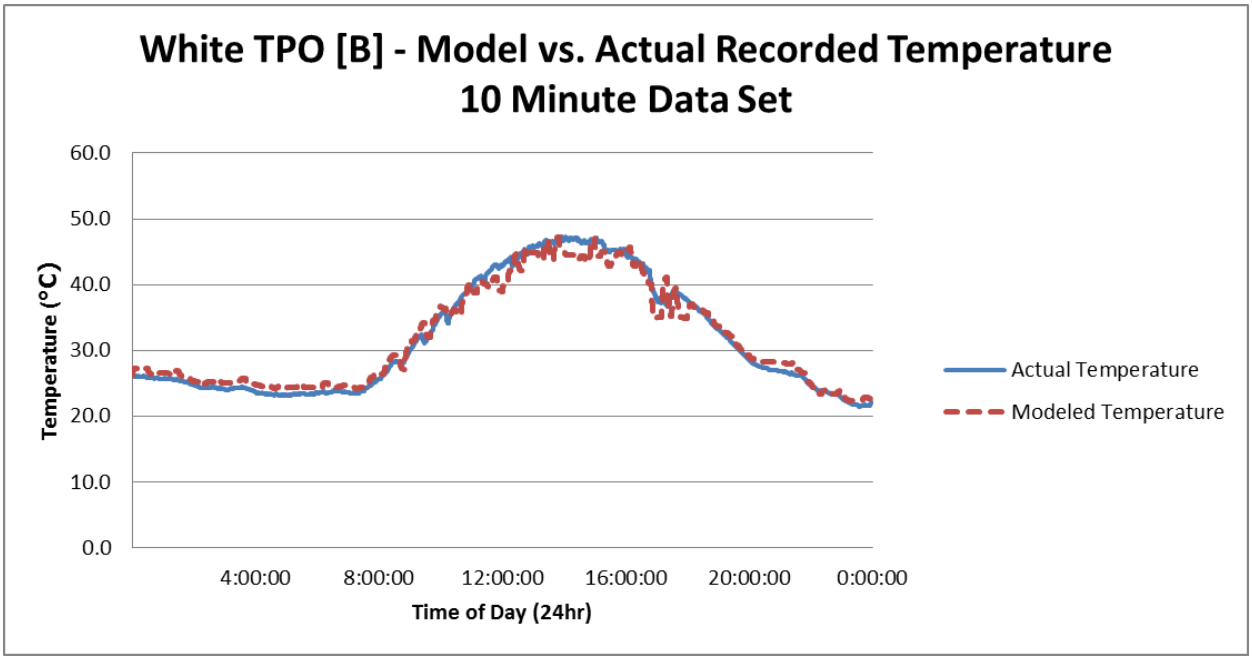

Figure 9-6 1S/10min for 8/31/2010

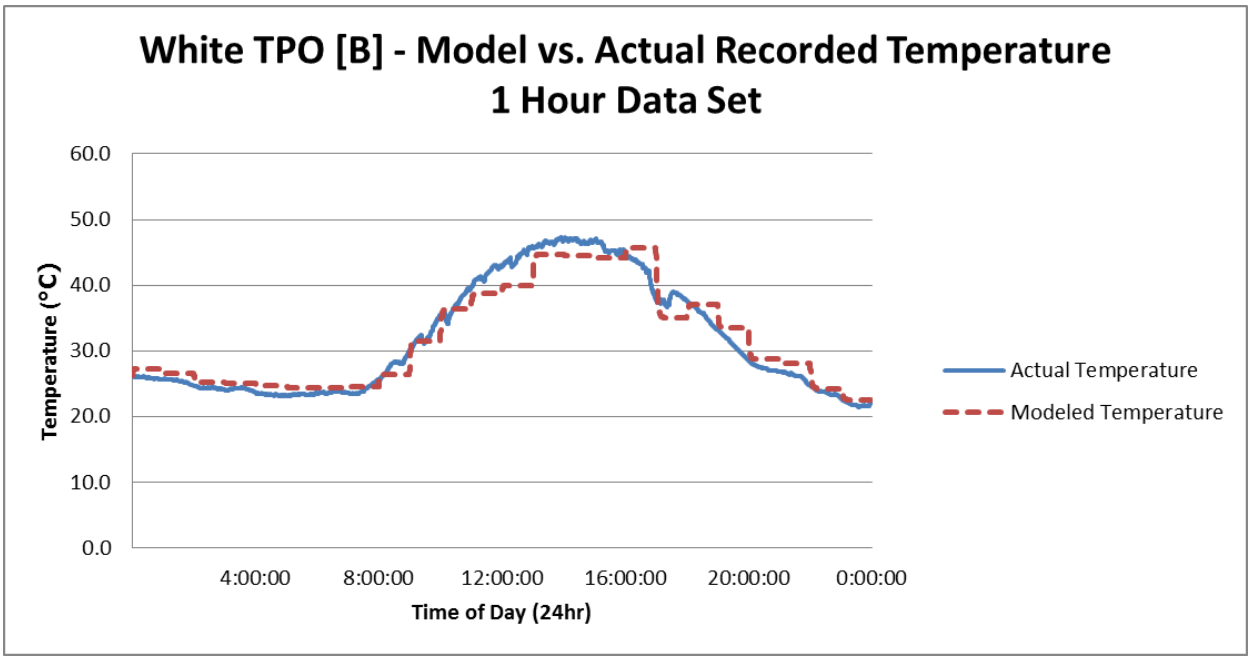

Figure 9-7 1S/1hr for 8/31/2010

In figure 9-8 the resultant population mean of the percent error for model predicted versus actual temperature for each data sample rate is presented in a bar chart

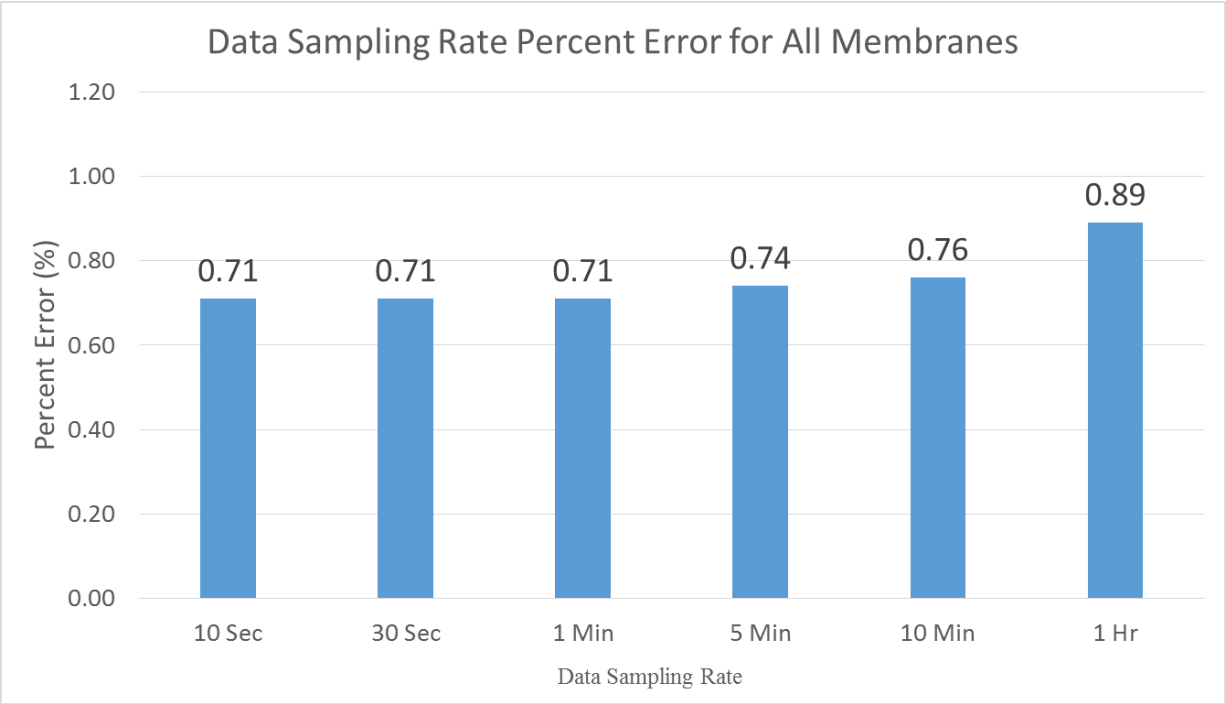

Figure 9-8 Population mean for each data sampling rate

Figure 9-9 shows the population means for each membrane by data sampling rate. Of note in figure 9-9 is the common shape for each membrane, except for the polymer modified bitumen membrane.

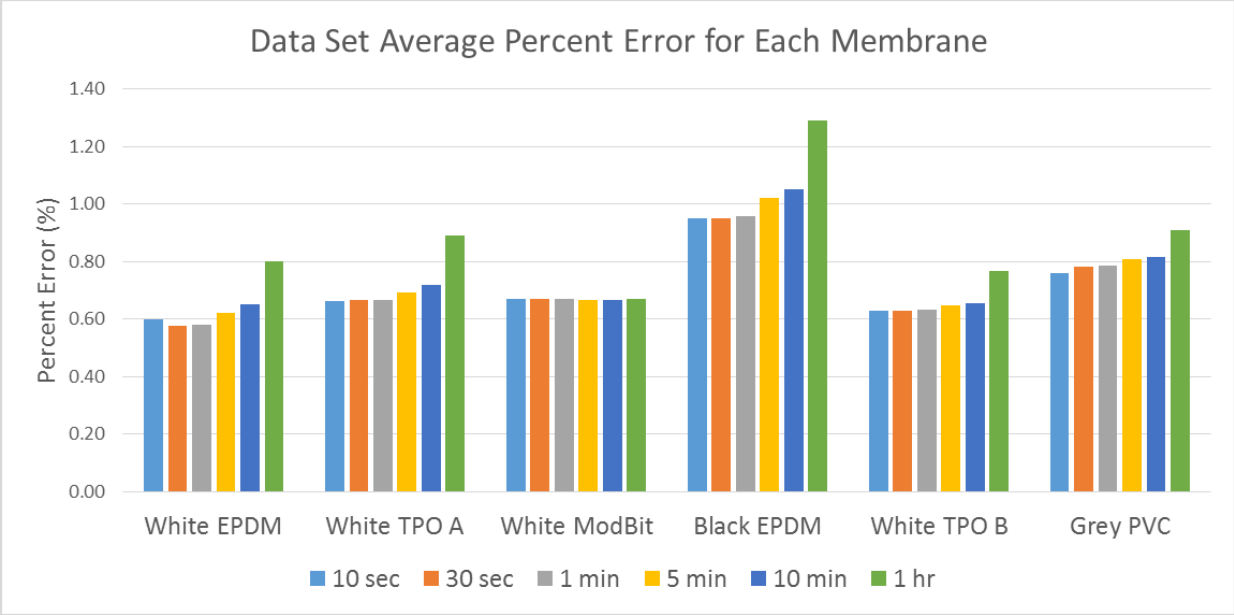

Figure 9-9 Population mean for each membrane by data sampling rate.

Table 9-1 displays the numeric results of the percent error of the model predicted temperature versus the actual temperature for the sampling rate variable analysis.

	Time Step					
Membrane	**10 sec**	**30 sec**	**1 min**	**5 min**	**10 min**	**1 hr**
White EPDM	0.60	0.58	0.58	0.62	0.65	0.80
White TPO A	0.66	0.66	0.66	0.69	0.72	0.89
White ModBit	0.67	0.67	0.67	0.67	0.67	0.67
Black EPDM	0.95	0.95	0.96	1.02	1.05	1.29
White TPO B	0.63	0.63	0.63	0.65	0.66	0.77
Grey PVC	0.76	0.78	0.78	0.81	0.82	0.91

Table 9-1 Numerical results for population means of percent error by data sample rate and membrane

Utilizing the same metric as was used in Chapter 8 and defined in Equation 8-1, the results of the data sampling rate variable were transformed and presented as the variable sensitivity in Figure 9-10

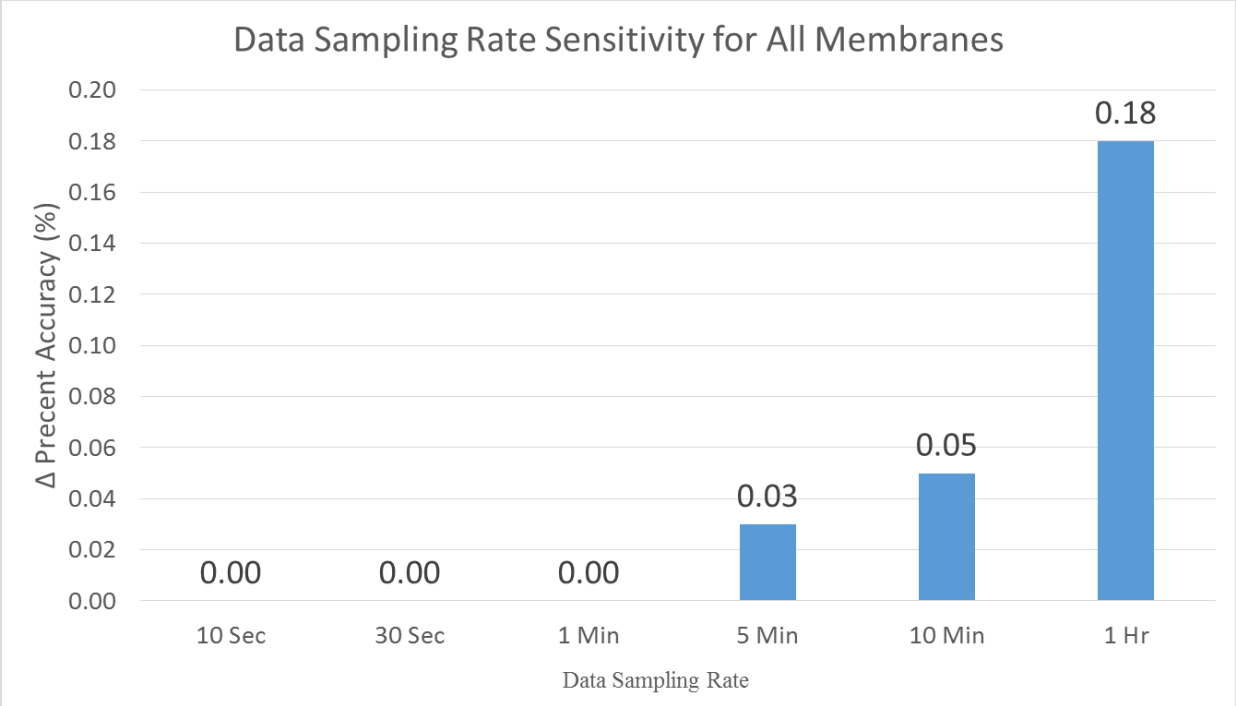

Figure 9-10 Sensitivity results for data sampling rate variable.

9.3 Discussion of Results

The overall result of the data sampling rate sensitivity analysis was predictable. Consider the Fundamental Theory of Calculus that states that the error goes to zero as the area of the sections goes to zero under a continuous function. By analogy, in this study we started with a small sliver of area under our temperature curve at the 1S/10s sample rate. As the data sample rate went to the slower and slower sample rates, and figuratively to the larger sliver area, we

expected the difference between the temperature we calculate and the actual temperature to get bigger.

With the level of computing power available today the determining factor for researchers is not so much the calculation load on the computer as the quality of data. When researchers design experiments such as this one, they can select their own data-sampling rate. However, if they were to use historical data or a preexisting source of data for making a roof membrane temperature model, they would be at the mercy of the individuals who collected that data for the sampling rate. In that case, they would have no ability to assess the impact of the sampling rate on the accuracy.

If we look at the two extremes of the data sampling rates, 1S/10s versus 1S/1hr, the first and obvious conclusion is that the longer sample rate does make a 0.18% decrease in accuracy of the model. However, it can also be said that this is not as large as was expected prior to this experiment being conducted. When comparing the order of magnitude of this result to the sensitivities calculated in Chapter 8, the resampling to the 1S/1hr data sampling rate has a marginal impact on the model accuracy. Being limited to an available or historical data set that utilized a 1S/1hr sample rate should not be reason alone to reject the data as unsuitable for a roof membrane temperature experiment.

Reference:

1. Wilkes, K.E., *Model for Roof Thermal Performance*. 1989, U.S. Department of Energy: Oak Ridge National Labs. p. 98.

Chapter 10: Summary and Conclusions

Our society continues to demand energy efficient buildings. These buildings cannot be designed without research into materials and building methods that lower their energy use while maintaining material performance. One of the many tools available to researchers is energy modeling and hygrothermal modeling. Both of these tools need temperature models for the building envelope.

This project was designed in response to a lack of information in the field of building science about the accuracy of temperature models and the input variables used in them. A problem statement for this research was formed from this issue and states:

Quantify the amount of error in predicted temperature that errors in the input variables will cause in a roof membrane temperature model.

In order to solve the problem statement an experiment with a roof membrane temperature model was required. In order to conduct this experiment, a roof membrane temperature model needed to be developed. In order to utilize this roof membrane temperature model as a reference for error measurements, it needed to be validated against actual roof membrane temperature measurements. To collect actual roof top measurements, a data acquisition system needed to be designed and installed. These steps together were all required to solve the problem statement. These steps combined form a research methodology that is summarized in the following section.

10.1 Summary of Work and Results

Field data collection was an important aspect of this study. The unusual qualities of the building selected for instrumentation in Manhattan, Kansas made it of great use to the purposes of this study. The building has six (6) unique, low slope roof membranes with identical installation and identical insulation. In addition, each has the same roof slope and each covers a common air space below, making it one of the best in-service buildings ever instrumented for a roof temperature study, to date. The roof membranes instrumented during this study include:

1. White EPDM
2. Black EPDM
3. Grey PVC
4. White Polymer Modified Bitumen
5. White TPO [Manufacturer A]
6. White TPO [Manufacturer B]

The test building was instrumented with Type T thermocouples under the field of each roof membrane. In addition to the temperature data, long and short wave radiation was monitored with a pyrgeometer and pyranometer, respectively. Meteorological data was collected on the roof top as well. These three major sources of roof data were acquired and recorded using an onsite computer system. The native data sampling rate for this study was one sample every ten seconds (1S/10s). At times this data rate produced over one million aggregate data points from the roof every 24 hours. This data sampling rate was facilitated by current storage and processing capabilities of contemporary computer systems. This data sampling rate, to the author's

knowledge, has never been accomplished in previous studies, and it allowed for more analysis than would otherwise have been possible to be performed in this study.

The data acquisition system was installed and programmed prior to the August 2010 start date of data collection. Roof membrane reflectivity readings were taken days prior to beginning full time data collection. During the month of August 2010, the data acquisition system collected a population of 29 days of data. This data was stored and then analyzed during later portions of the study.

With field data collected for simulation and analysis the focus of the study turned to assembling a lumped capacitance temperature model for the roof membranes in the study. The basic theoretical treatments for the model in terms of heat transfer from conduction, convection, and radiation are drawn from classical heat transfer principals [1].Forms of this model have been assembled in previous works[2-4]. However, each of these models differs in intended application; some are general models and some are site or building specific. The goal for the model in this study was accuracy. Therefore, a roof membrane temperature model was assembled from the basic components, while building specific components, such as the convective heat transfer coefficient, were developed specifically for the building under study. Each of these previous modeling works was used only as a guide in constructing the model used in this study. The resultant closed form equation for the roof membrane temperature model, which was shown in Equation 6-11, is as follows:

$$\mathbf{T} = \boldsymbol{T_s} + \frac{\frac{\boldsymbol{T_I - T_S}}{\mathbf{R}} + (\mathbf{1} - \propto_{\boldsymbol{Solar}})\boldsymbol{G_{Solar}} + \boldsymbol{\epsilon G_{Long}} - \boldsymbol{\varepsilon \sigma T_S^4} + (\mathbf{1.1773W + 7.1864})(\boldsymbol{T_S - T_A})}{\boldsymbol{\Delta t C U}}$$

Equation 6-11 Roof Temperature Model

The model was validated against the field data collected from the Manhattan, Kansas roof membranes. The validation utilized an average percent error approach as a metric of performance. The threshold for a valid model was set utilizing available standards at 2.5% average percent error. The model was considered validated after returning a 0.71% average percent error for all membranes and days in the population.

With the model validated, focus was placed on solving the problem statement. This required a sensitivity study of the ten (10) input variables in Equation 6-11. These variables are listed below:

1. Interior Temperature (T_I)
2. Thermal Resistance (R)
3. Solar Reflectivity ($\propto_{Solar}$)
4. Insolation (G_{Solar})
5. Emissivity (ε)
6. Long Wave Irradiance (G_{Long})
7. Convective Coefficient ($h_{Convection}$)
8. Air Temperature (T_A)
9. Specific Heat (C)
10. Membrane Mass (U)

The method used to analyze the variable sensitivity was the One Factor At a Time (OFAT) method. This method has the advantage of being useful on models with high numbers of variables that would otherwise be computationally prohibitive for a more traditional factorial analysis. The disadvantage of the OFAT method is that it does not allow us to detect or assess the impact of variable interactions, where the factorial method excels.

The result of the OFAT sensitivity analysis was the ability to quantitatively assess and then rank the input variables in terms of their influence on the average percent error accuracy of the model against the measured roof membrane temperatures. The quantitative results of the sensitivity analysis are restated in Table 8-1 below.

Model Variable	Percent Change in Accuracy (%)
Interior Temperature (T_I)	-0.11
Thermal Resistance (R)	0.01
Solar Reflectivity ($\propto_{Solar}$)	0.39
Insolation (G_{Solar})	0.15
Emissivity (ε)	0.12
Long Wave (G_{Long})	0.52
Convective Coefficient ($h_{Convection}$)	0.03
Air Temperature (T_A)	12.28
Specific Heat (C)	0.01
Membrane Mass (U)	0.01

Table 8-1 Numeric results of the OFAT analysis on the roof membrane temperature model.

Utilizing the numerical results of Table 8-1 allowed the input variables to be ranked by their influence on the model accuracy. The ranking of the variables is as follows.

1. Air Temperature (T_A)
2. Long Wave (G_{Long})
3. Solar Reflectivity ($\propto_{Solar}$)
4. Insolation (G_{Solar})
5. Emissivity (ε)
6. Interior Temperature (T_I)
7. Convective Coefficient ($h_{Convection}$)
8. Thermal Resistance (R)
8. Specific Heat (C)
8. Membrane Mass (U)

Additionally, this study provided the opportunity to examine one of the confounded variables in the roof membrane temperature model that, to date, appears to have been neglected by other researchers. This variable was the data sampling rate. The state of data acquisition and computer storage allowed for a 1S/10s sample rate in this study. This data sampling rate is far faster than was available when previous studies were conducted [3, 5]. The high native sampling rate allowed for it to be resampled, allowing for progressively lower sampling rates to be utilized and then for records of the resulting average percent error in the predicted temperature to be made.

The resulting loss in accuracy as the sample rate was decreased, up to 1S/1hr, was not unexpected. However, the accuracy penalty incurred from a lower data sampling rate was previously unknown. The results of the data sampling rate sensitivity are reshown in Figure 9-10.

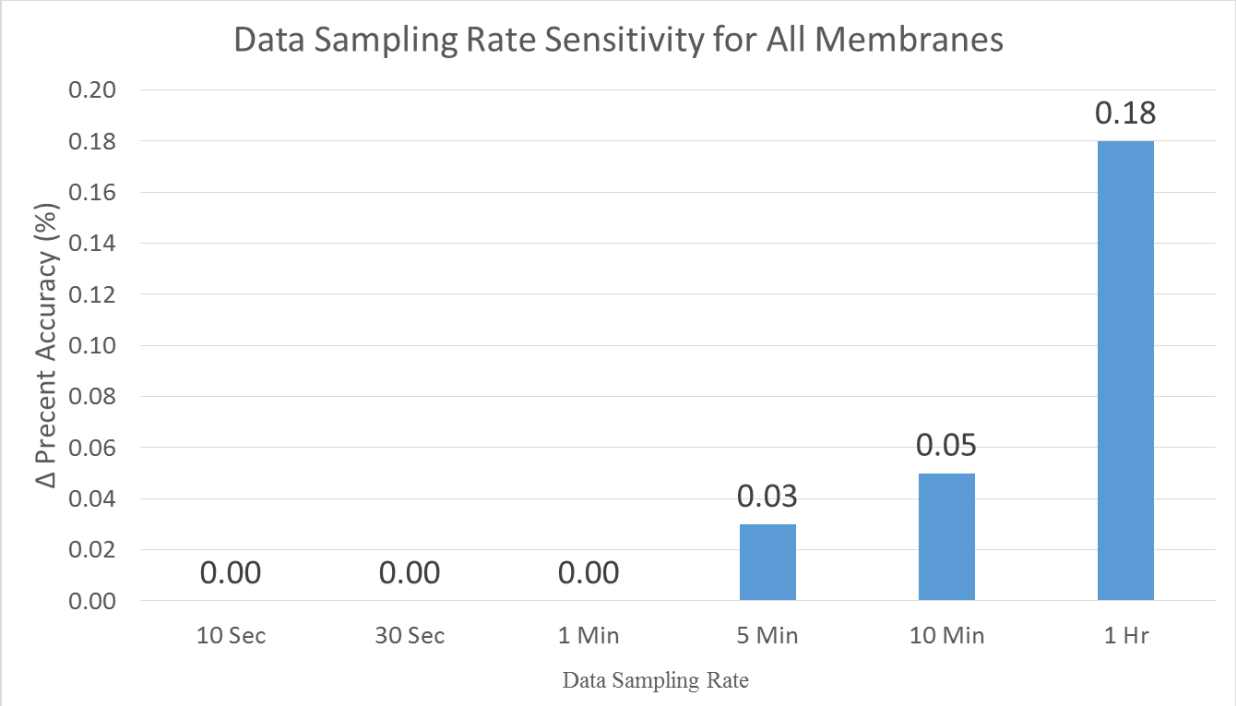

Figure 9-10 Sensitivity results for data sampling rate variable.

10.2 Conclusions

The first and most prominent conclusion to be drawn from this work is the ability to answer the original problem statement. This problem statement was as follows: “Quantify the amount of error in predicted temperature that errors in the input variables will cause in a roof membrane temperature model.” This was successfully accomplished, as the discussion above shows.

The results of the sensitivity analysis were unexpected. Specifically the strength of influence the air temperature has on accuracy was not anticipated. Based on the results, Air temperature (T_A) is 24x more important to accurate predictions, from the model, than the next most important variable, Long Wave Radiation (G_{Long}), in achieving accurate predicted roof membrane temperature. The results of this study allow researchers to make educated decisions about instrumentation, data sampling rates, and needed assumptions in future roof temperature work. Additionally, inferences can be made about past work relating to these same issues.

Using the result of the sensitivity analysis, it is apparent that air temperature needs to be measured as accurately as possible. The typical air temperature reading is taken with a shielded air temperature probe. An example of an air temperature probe utilizing a naturally aspirated solar radiation shield is shown in Photo 10-1. The naturally aspirated solar radiation shield uses louvered baffles to block and / or reflect insolation from reaching the temperature sensor and irradiating it. This radiation subsequently warms the sensor and leads to erroneously high temperature readings. The shape of the baffles allows for air to move in and out of the shield. An air temperature probe with a naturally aspirated solar radiation shield was utilized for this study.

Photo 10-1 A close up view of a naturally aspirated solar radiation shield in place over an air temperature probe.

While the naturally aspirated solar radiation shield produces acceptable accuracy at a very low instrument cost point and can thus be considered a good value proposition, the fan aspirated solar radiation shield utilizes a blower to continuously pass ambient air over the sensor, which results in a more accurate reading of the ambient air temperature. However, the fan aspirated radiation shield is more complicated to implement and much more costly to procure and install. Given the results of the sensitivity analysis, it is recommended that a researcher with the proper funding utilize the fan aspirated air temperature probe.

Looking at the evolution of roof membrane market, which is discussed in Chapter 1, the current prominence of TPO low slope roof membranes must be acknowledged. As is also discussed in Chapter 1, the TPO membrane and its manufacturers have had catastrophic

membrane failures in the recent past, which have been associated with chemical formulation. These formulation errors lead to premature heat and ultraviolet degradation of the membranes.

The TPO manufacturers have taken steps to improve the TPO membranes. *ASTM D6878 - Standard Specification for Thermoplastic Polyolefin Based Sheet Roofing* is the consensus standard that describes, among other issues, how TPO membranes must pass physical testing after laboratory oven heat aging. This laboratory heat aging was originally specified in D6878-03 at 240°F for 670 hours in D6878-13 it is now 5376 hours. The current time requirement has become prohibitive to product development cycles and product conformance testing by independent labs, as this represents 32 weeks of oven time before physical testing can even begin. The current discussion in committee is to move this standard to a higher heat aging temperature – closer to 280°F. This higher ageing temperature will allow for a shorter oven time.

While no roof should ever see temperatures as high as 280°F, at service conditions, the concept is to artificially accelerate the roof membrane ageing process and to reproduce decades of service in days. However, one of the most fundamental concepts in engineering is to determine, through calculation and science, the minimum material required to perform at a given load. It is possible that the ASTM standards are over aging these TPO membranes in a reactive response to the catastrophic TPO membrane failures seen earlier in this century. Quite simply, roof membrane temperature modeling is necessary to calculate and engineer in a situation such as this. The body of work in this study advances the state of knowledge on this topic and therefore benefits our society as a whole.

10.3 Future work

This work offers many useful tools for future research to expand upon. In order to produce a validated roof membrane temperature model, this author was required to study numerous pieces of literature, searching for pieces of information that when combined led to a validated model. This work can provide a starting point for future researchers looking to produce a roof membrane temperature model to investigate their own roof related problems and questions. While it does not eliminate the need to review the existing literature reviewed by this author, this work provides a consolidated guide to the essential components needed to produce a roof membrane temperature mode.

This research does not only serve as a reference for future work, additional avenues for research as an extension of this work exist. The validated model developed for the roof membranes in Manhattan, Kansas can be utilized for additional sensitivity analyses. The OFAT analysis conducted for this dissertation used percent error as a metric for assessing the input variable influence. However, for an energy analysis, understanding which of the input variables affect roof membrane temperature is just as important as accuracy. By utilizing the resultant temperature shift from the OFAT method to repeat the exercise in Chapter 8 of this dissertation, insight can be gained into what factors are most important in controlling roof membrane temperatures. This information may be invaluable in shaping the next generation of building energy design criteria and public energy policy in regards to roofing.

In addition to OFAT analyses, the limitation to preforming the factorial experimental design was based on the number of runs required. The current method of model runs is

essentially a manual process that requires the operator to make one run at a time. However, with professional programming assistance, it should be possible to automate this process. In effect, the power of personal computers can be utilized to accomplish the 30,000 plus runs needed to perform a factorial analysis in a matter of hours. If this can be accomplished, both the percent error metric and temperature differential can be explored using the factorial method with variable interactions studied. The factorial analysis for accuracy combined with a factorial analysis of roof membrane temperature sensitivity would improve the concepts required for building energy design and public energy policy. Both of these factorial experiments would benefit from this current research on roof temperature models as a foundation piece.

There remains an additional aspect of this research that may prove even more fruitful than others. Previous studies in this area have focused on roof temperature and the total heat flux through the roof system as metrics. In this study, these two metrics were outputs as well. However, in this study each source of heat flux (radiation, convection, and conduction) was calculated separately and then aggregated for a net heat flux. Upon initial consideration these separate calculations seem like an obvious and unassuming step. However, if one inspects and studies a plot of the heat flux sources, it opens a new avenue of study previously unutilized.

Consider the plots in Figure 10-1 and 10-2, where the heat flux sources for White EPDM and Black EPDM on a selected day are plotted respectively. In these plots, we can see that the radiation and convection heat fluxes generally counter each other. The conduction through the roof system, positive or negative, is dwarfed by the magnitudes of the other two. If we focus on the magnitudes of the convection at the peak of the day, we find the Black EPDM moving three

times (3X) more heat energy into the atmosphere by convection than is moved by the White EPDM. This issue is a debated topic in the building sciences community. One study [6] has presented a questionable experiment that suggests non-reflective roofs, such as black EPDM, actually produce lower air temperatures above the roof. Simply by inspecting Figures 10-1 and 10-2 we can see that the convective portion of the heat flux is transferring heat energy into the surrounding by three times (3X) as much on this particular day.

The benefit of the roof membrane temperature model was latent and unexpected. Much like a data transform allows us to visually recognize a pattern or aspect of data that was not evident before the transform, this method of visualizing the heat flux sources may be invaluable in answering questions in the building sciences field. Of the roof temperature research that has come before this study, including those that this study is based on, none explored the heat flux sources. It is even possible that none of the models were capable of separating them into the individual components, as was done here. In either case the concept of examining the heat fluxes separately, in addition to combined heat flux and temperature, represents a very fertile area for future research.

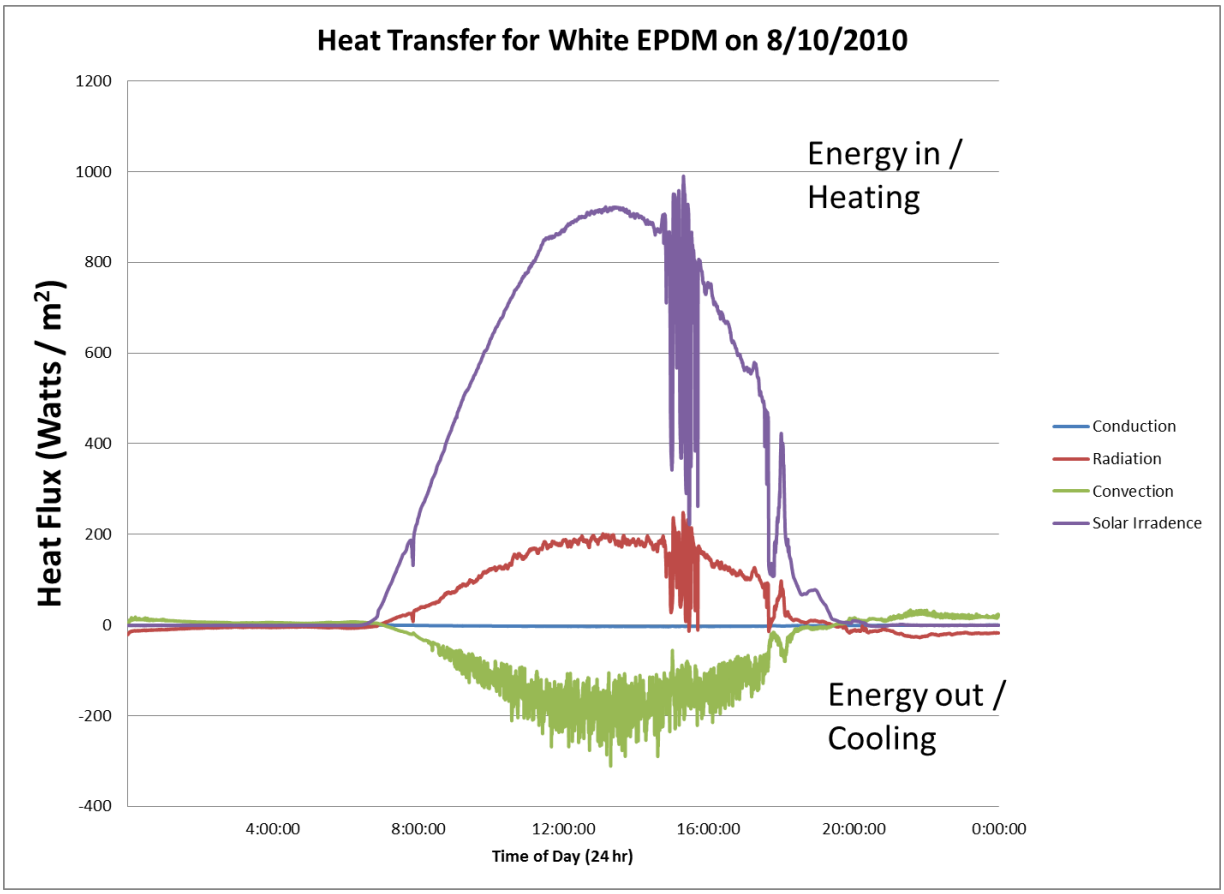

Figure 10-1 Heat flux sources for White EPDM. The conduction varies throughout the day with a maximum value of 8 W/m^2, a tiny portion of the convective and radiative portions. The Solar iradiance is plotted as a reference betweeen Figures 10-1 and 10-2.

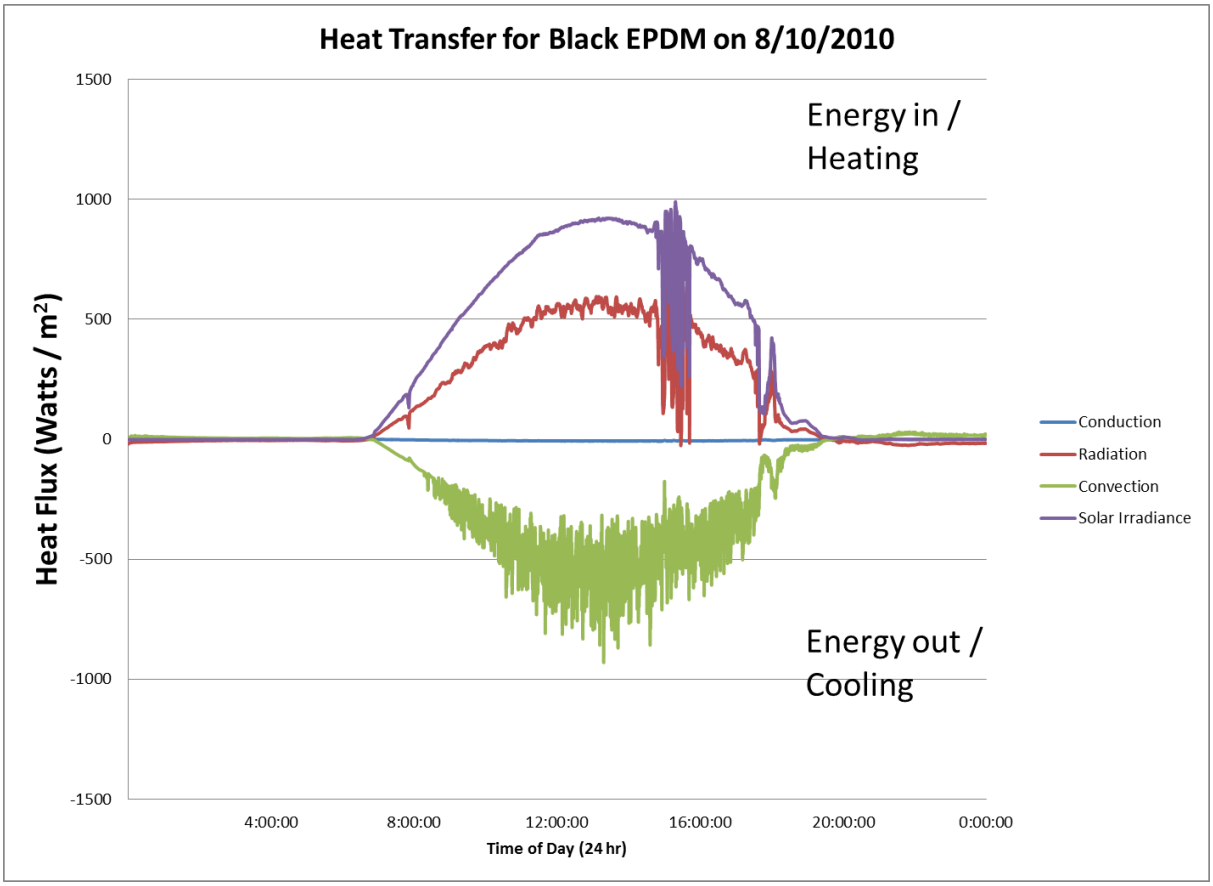

Figure 10-2 Heat flux sources for Black EPDM. The Solar iradiance is plotted as a reference betweeen Figures 10-1 and 10-2. Here the magnitudes of convection and conduction are much higher, as the black EPDM is obtaining a higher temperture than the white EPDM under exactly the same conditions.

References

1. Incropera, F.P., *Fundementals of Heat and Mass Transfer*. 6th ed. 2007: John F. Wiley and Sons, Inc.

2. Rose, W.B., *White Roofs and Moisture in the US Desert Southwest*, in *Buildings X*. 2007, Oak Ridge National Labs: Clearwater Beach, Florida.

3. Wilkes, K.E., *Model for Roof Thermal Performance*. 1989, U.S. Department of Energy: Oak Ridge National Labs. p. 98.

4. Kunzel, H.M., *Simultaeous Heat and Moisture Transport in Building Components*, in *Fraunhofer Institute of Building Physics*. 1995, University of Suttgart: Suttgart, Germany. p. 65.
5. Clear, R.D., L. Gartland, and F.C. Winkelmann, *An empirical correlation for the outside convective air-film coefficient for horizontal roofs.* Energy and Buildings, 2003. **35**(8): p. 797-811.

6. IBRAHIM, S.K., *SUSTAINABLE ROOF DESIGN: MORE THAN A BLACK-AND-WHITE ISSUE*, in *Symposium on Building Envelope Technology*. 2009, RCI Inc. p. 111-120.

Appendix A

Specific Heat Capacity Graphs for Low Slope Roof Membranes

Sample: EPDM_WHITE_1
Size: 6.7900 mg
Method: Specific Heat

DSC

File: C:\TA\Data\DSC\mdupuis\EPDM_WHITE_1.001
Operator: mdupuis
Run Date: 17-Mar-2011 21:45
Instrument: DSC Q100 V9.9 Build 303

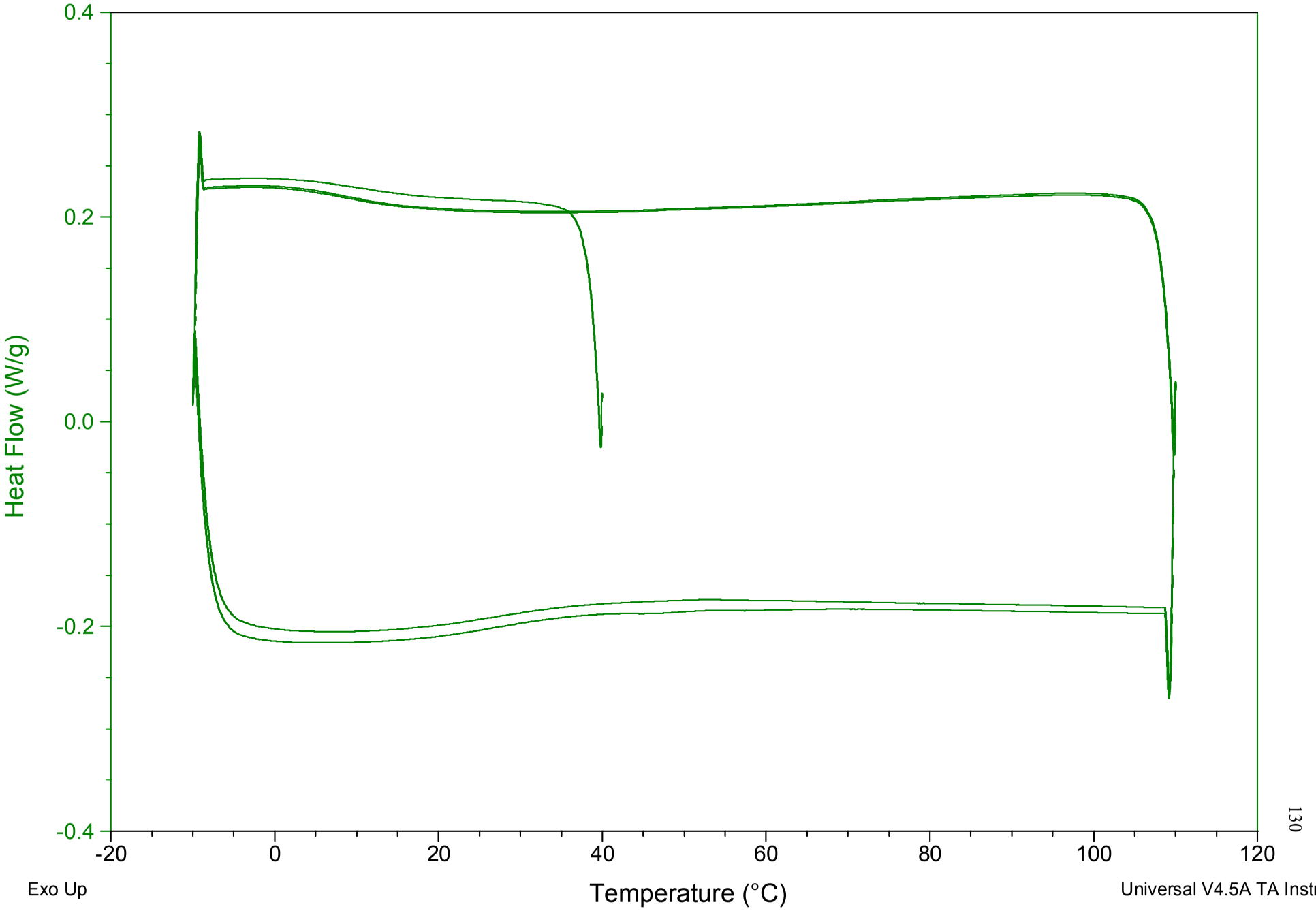

Sample: EPDM_WHITE_2
Size: 7.1200 mg
Method: Specific Heat

DSC

File: C:\TA\Data\DSC\mdupuis\EPDM_WHITE_2.001
Operator: mdupuis
Run Date: 17-Mar-2011 22:53
Instrument: DSC Q100 V9.9 Build 303

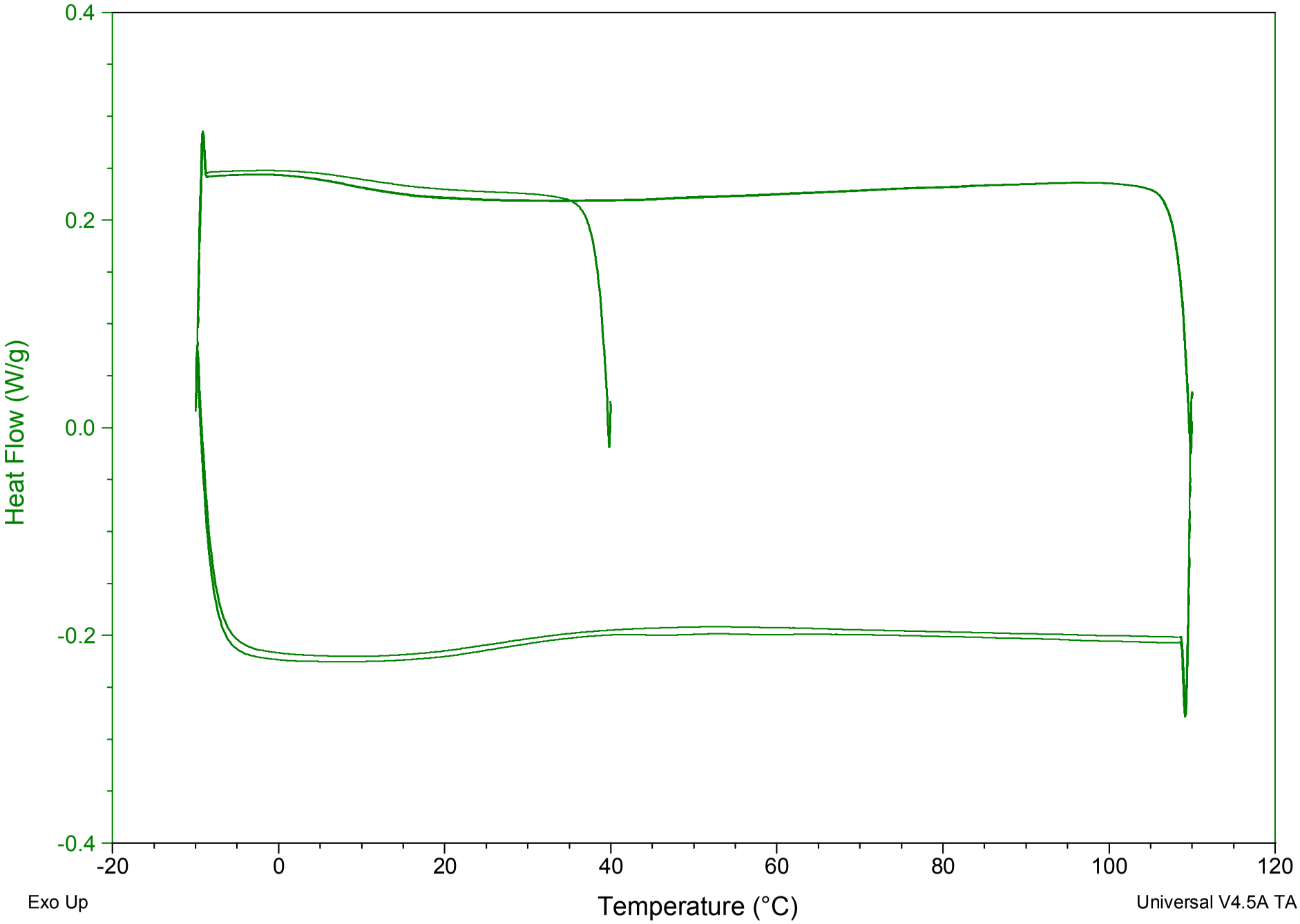

Sample: TPO_1
Size: 4.0400 mg
Method: Specific Heat

DSC

File: C:\TA\Data\DSC\mdupuis\TPO_1.001
Operator: mdupuis
Run Date: 18-Mar-2011 00:01
Instrument: DSC Q100 V9.9 Build 303

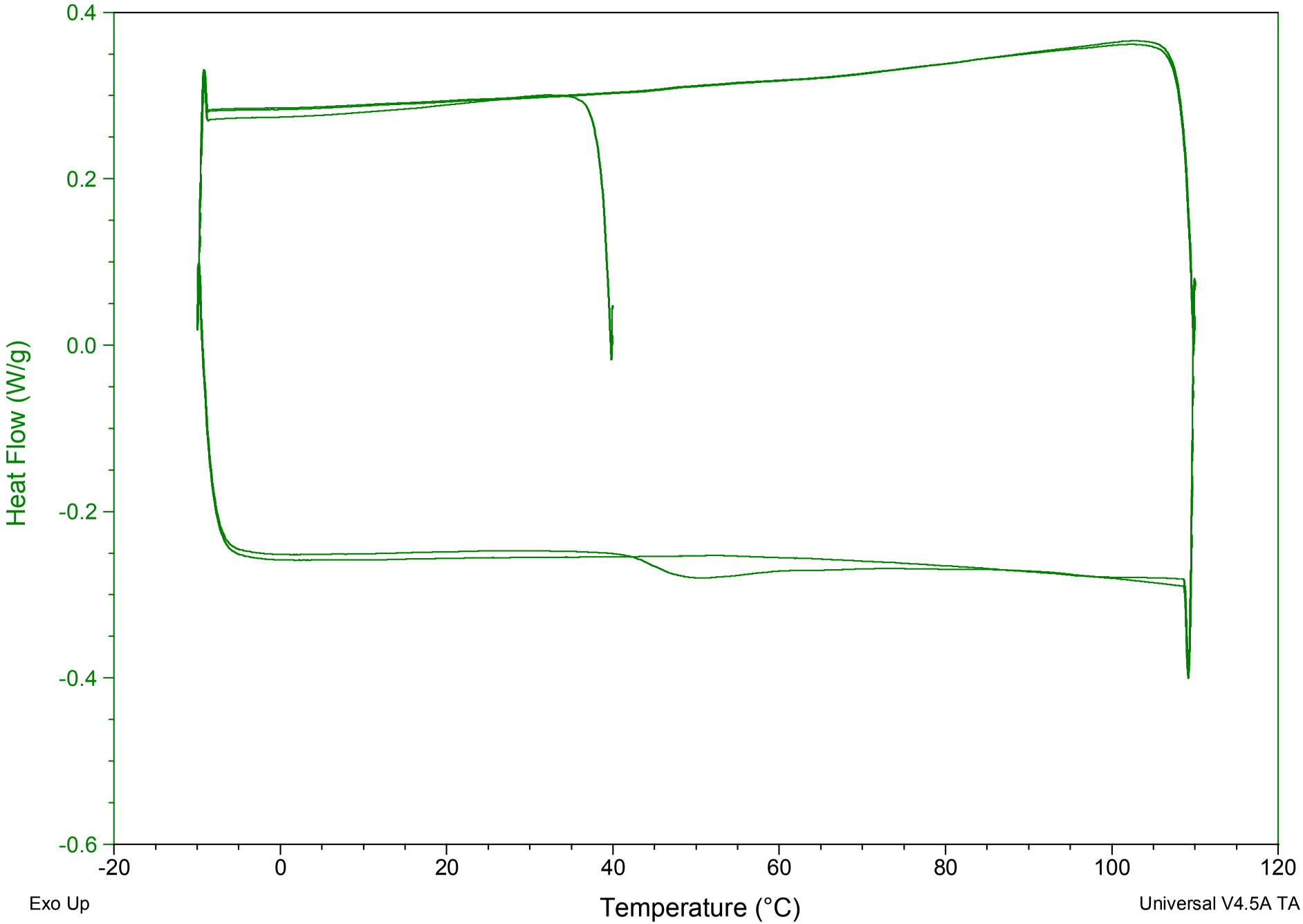

Sample: TPO_2
Size: 5.3600 mg
Method: Specific Heat

DSC

File: C:\TA\Data\DSC\mdupuis\TPO_2.001
Operator: mdupuis
Run Date: 18-Mar-2011 01:09
Instrument: DSC Q100 V9.9 Build 303

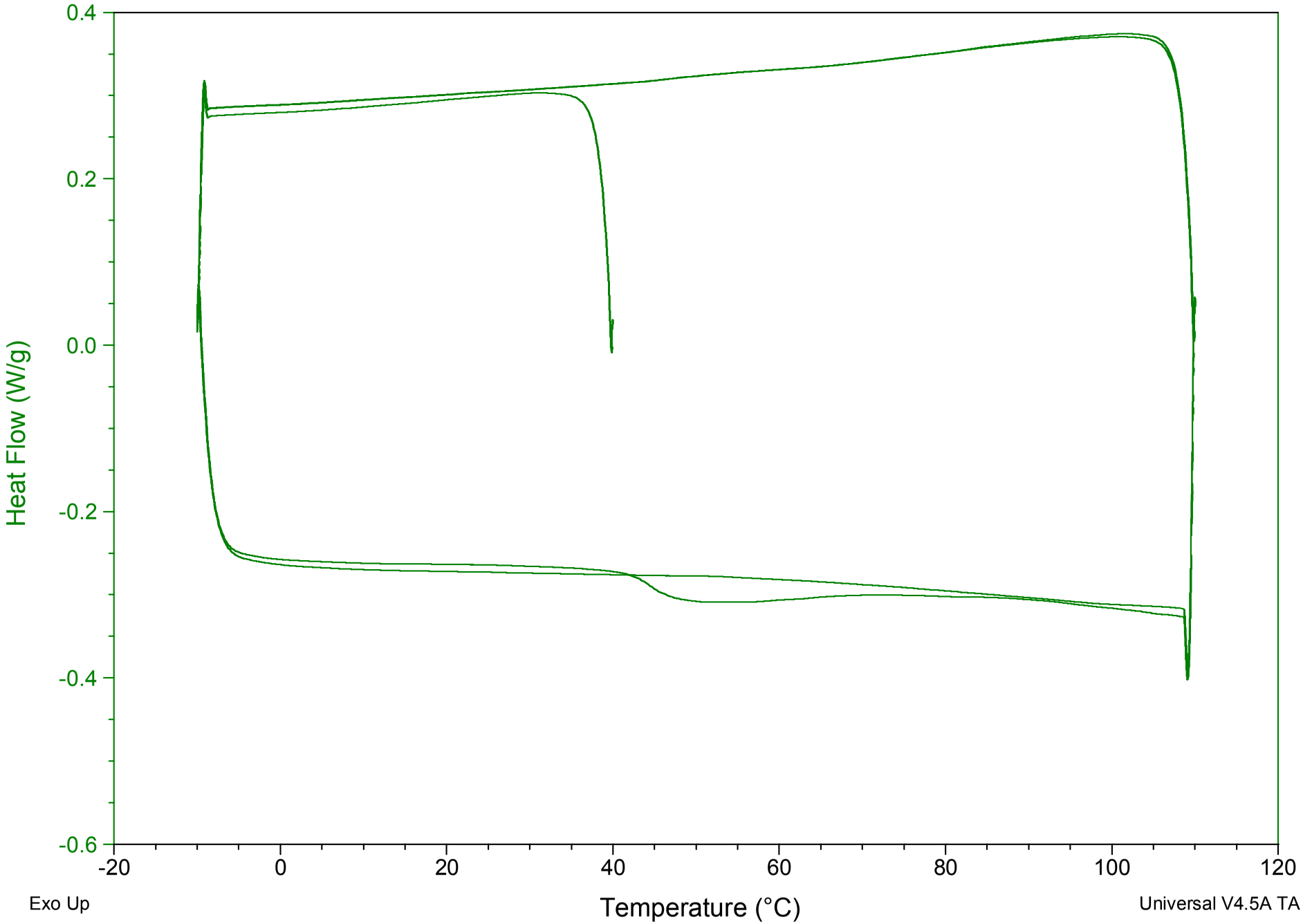

Universal V4.5A TA Instruments

Sample: CAPSHEET_1
Size: 3.7600 mg
Method: Specific Heat

DSC

File: C:\TA\Data\DSC\mdupuis\CAPSHEET_1.001
Operator: mdupuis
Run Date: 18-Mar-2011 02:18
Instrument: DSC Q100 V9.9 Build 303

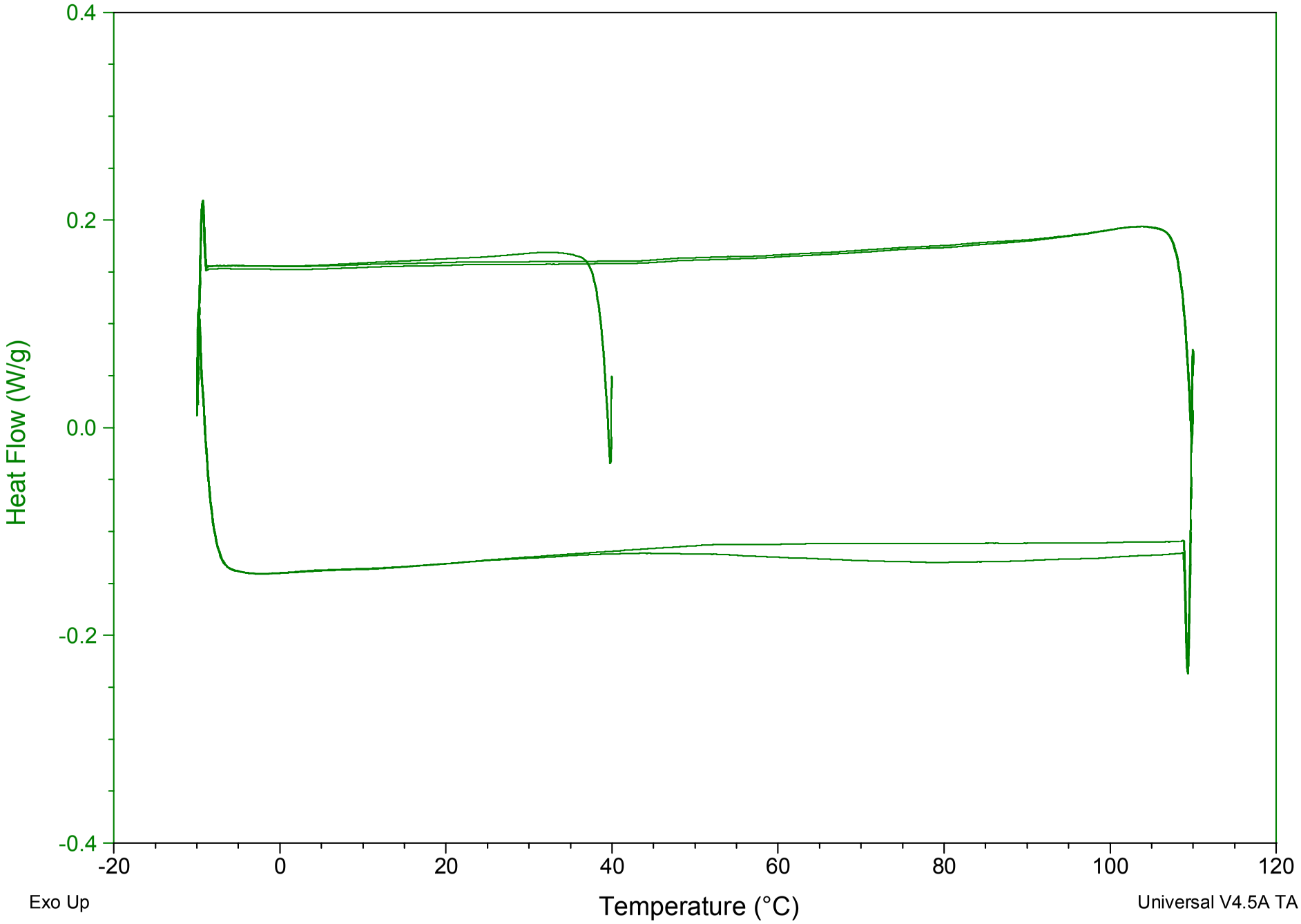

Sample: CAPSHEET_2
Size: 4.9900 mg
Method: Specific Heat

DSC

File: C:\TA\Data\DSC\mdupuis\CAPSHEET_2.001
Operator: mdupuis
Run Date: 18-Mar-2011 03:26
Instrument: DSC Q100 V9.9 Build 303

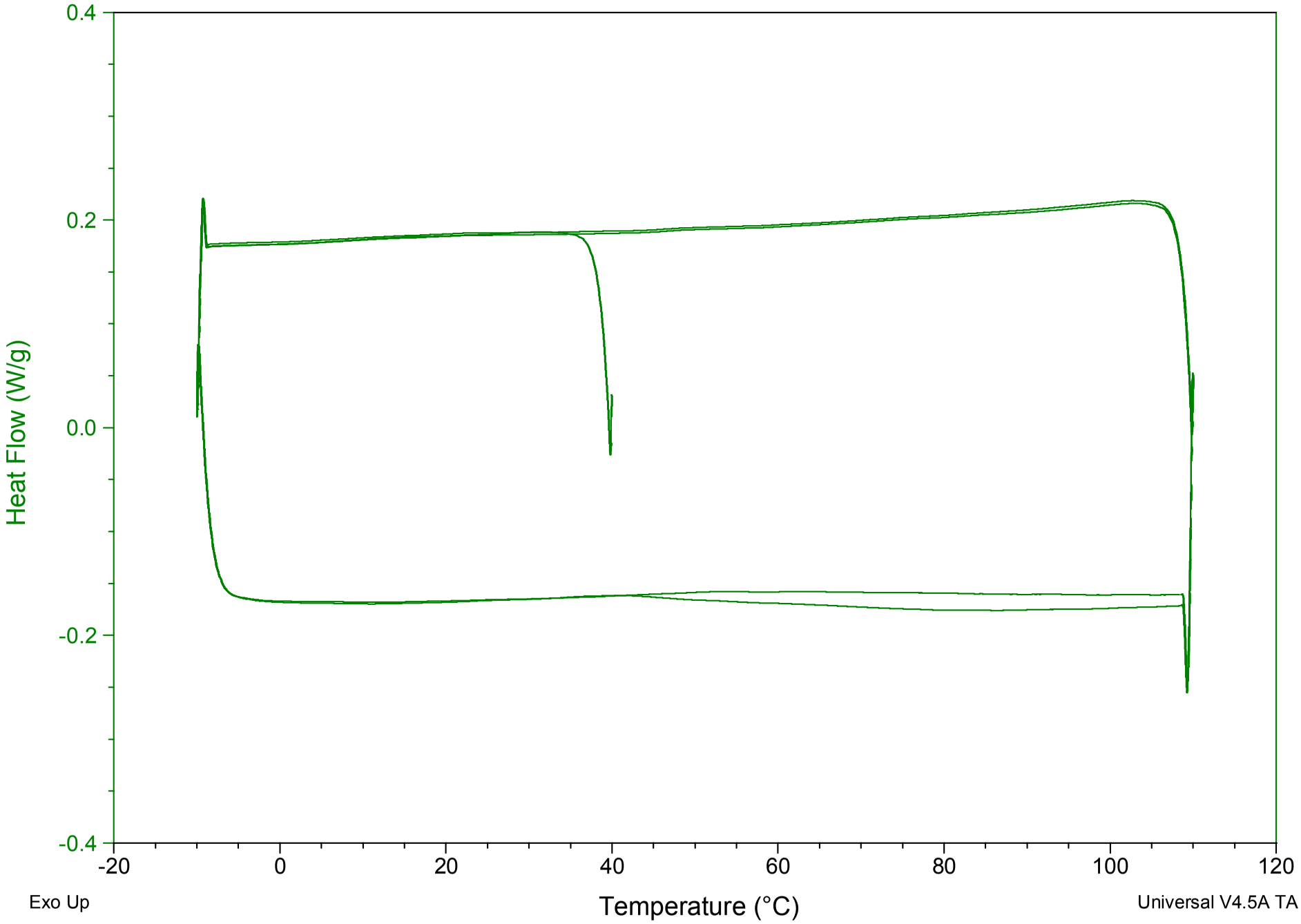

Sample: MODBIT_1
Size: 3.6300 mg
Method: Specific Heat

DSC

File: C:\TA\Data\DSC\mdupuis\MODBIT_1.001
Operator: mdupuis
Run Date: 18-Mar-2011 04:34
Instrument: DSC Q100 V9.9 Build 303

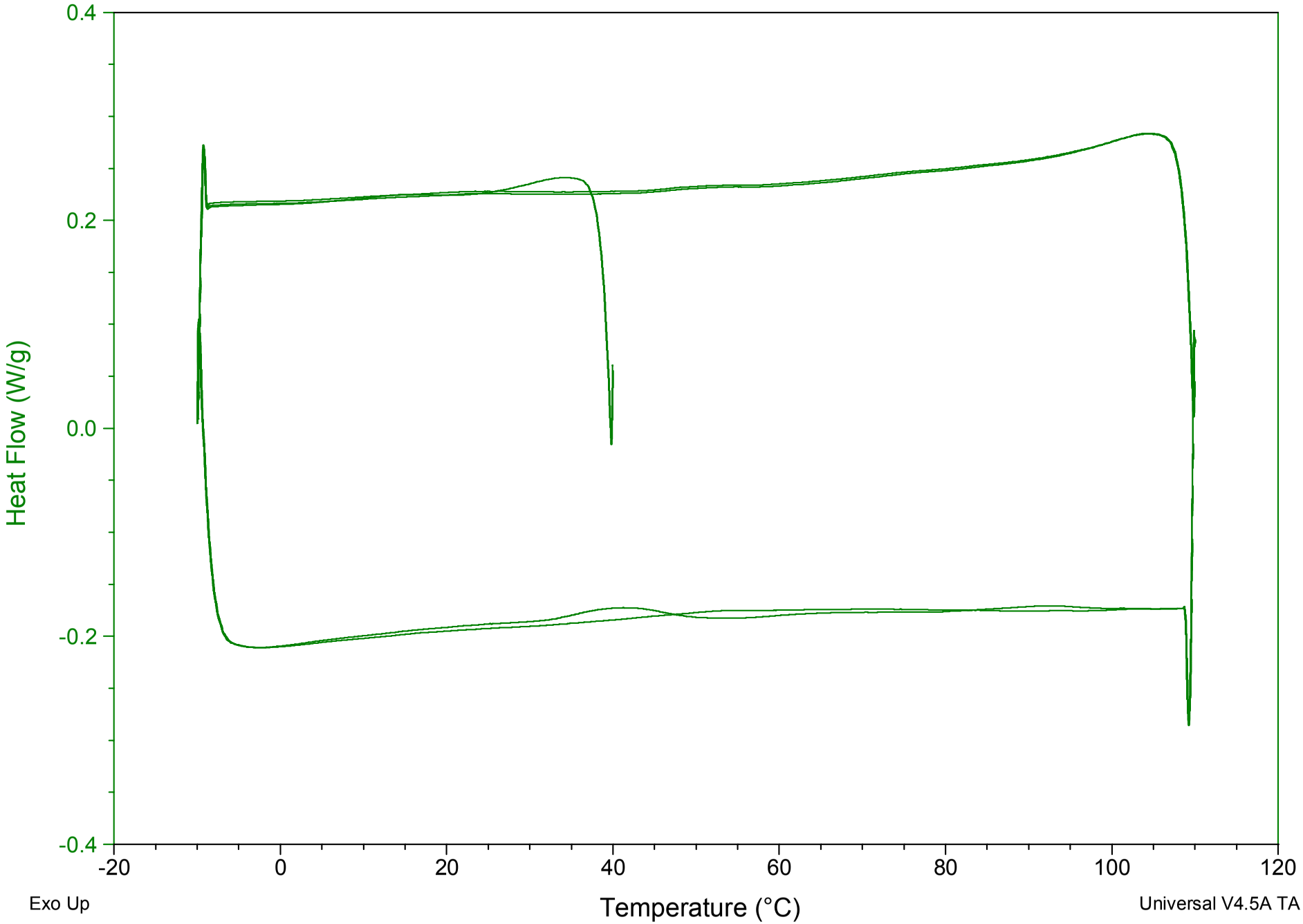

Sample: MODBIT_2
Size: 10.5600 mg
Method: Specific Heat

DSC

File: C:\TA\Data\DSC\mdupuis\MODBIT_2.001
Operator: mdupuis
Run Date: 18-Mar-2011 05:42
Instrument: DSC Q100 V9.9 Build 303

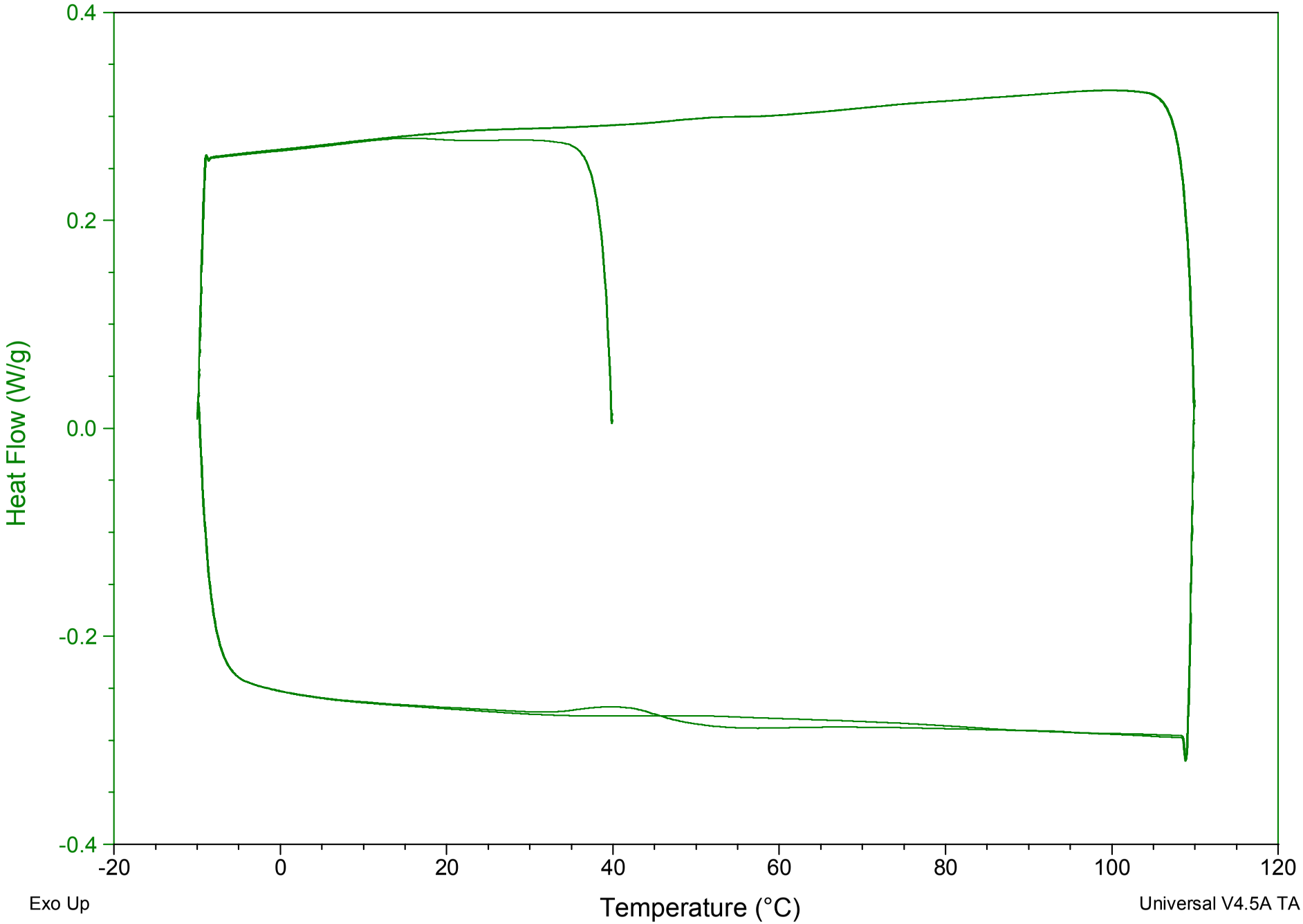

Universal V4.5A TA Instruments

Sample: EPDM_BLACK_1
Size: 6.1100 mg
Method: Specific Heat

DSC

File: C:\TA\Data\DSC\mdupuis\EPDM_BLACK_1.001
Operator: mdupuis
Run Date: 17-Mar-2011 17:12
Instrument: DSC Q100 V9.9 Build 303

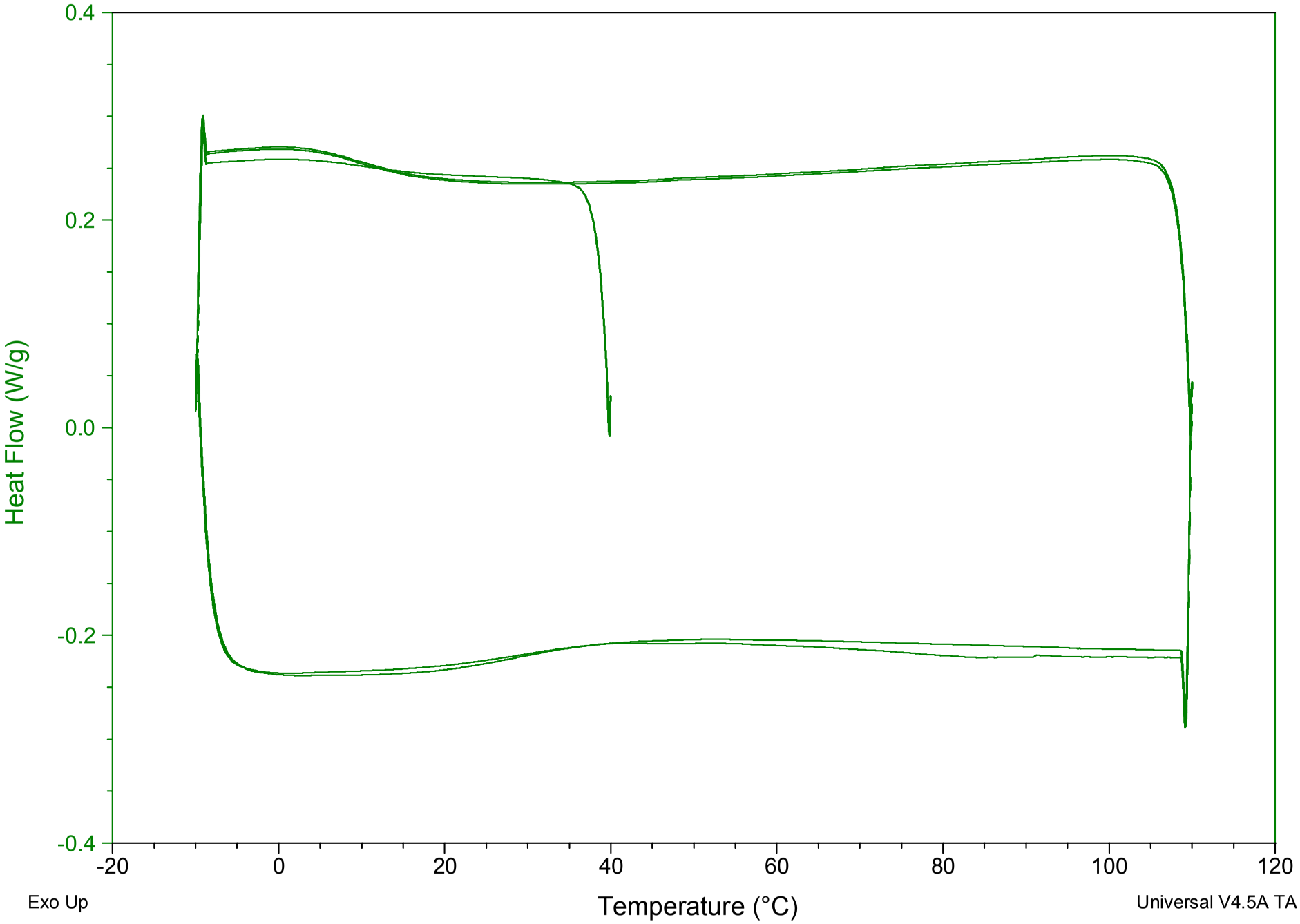

Sample: EPDM_BLACK_2
Size: 8.1000 mg
Method: Specific Heat

DSC

File: C:\TA\Data\DSC\mdupuis\EPDM_BLACK_2.002
Operator: mdupuis
Run Date: 17-Mar-2011 18:21
Instrument: DSC Q100 V9.9 Build 303

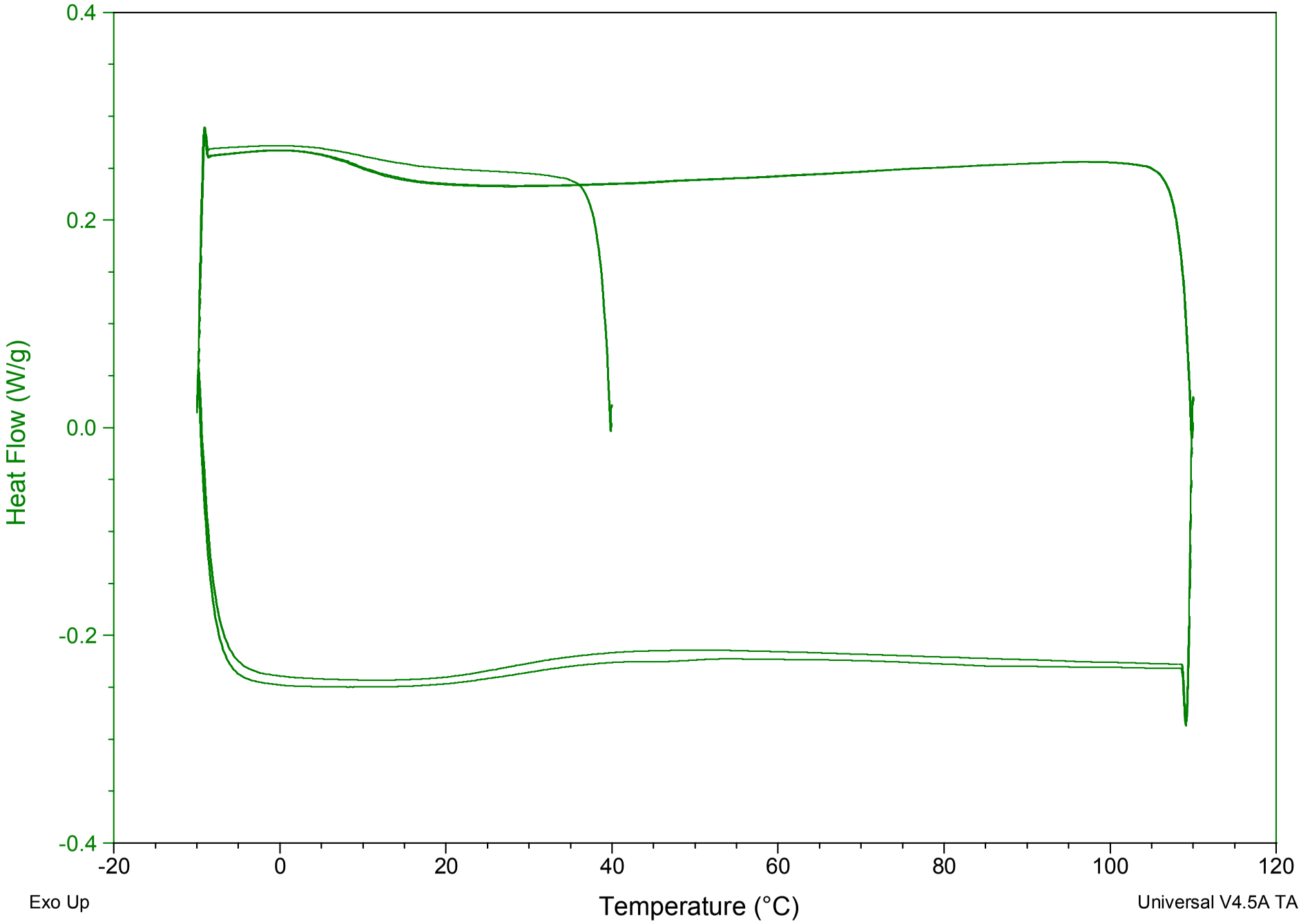

Sample: PVC_1
Size: 9.7800 mg
Method: Specific Heat

DSC

File: C:\TA\Data\DSC\mdupuis\PVC_1.001
Operator: mdupuis
Run Date: 17-Mar-2011 19:29
Instrument: DSC Q100 V9.9 Build 303

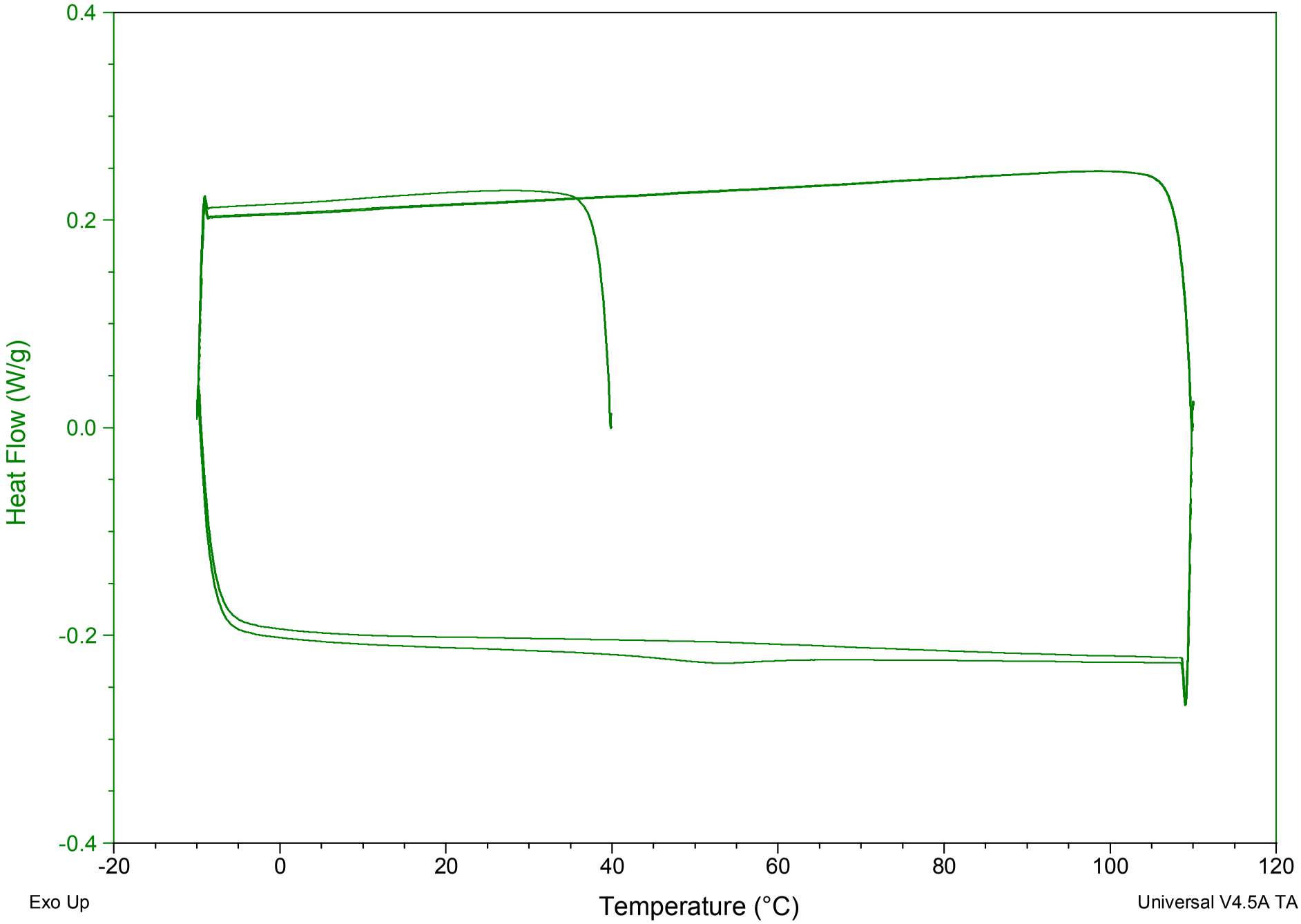

Sample: PVC_2
Size: 6.4000 mg
Method: Specific Heat

DSC

File: C:\TA\Data\DSC\mdupuis\PVC_2.002
Operator: mdupuis
Run Date: 17-Mar-2011 20:37
Instrument: DSC Q100 V9.9 Build 303

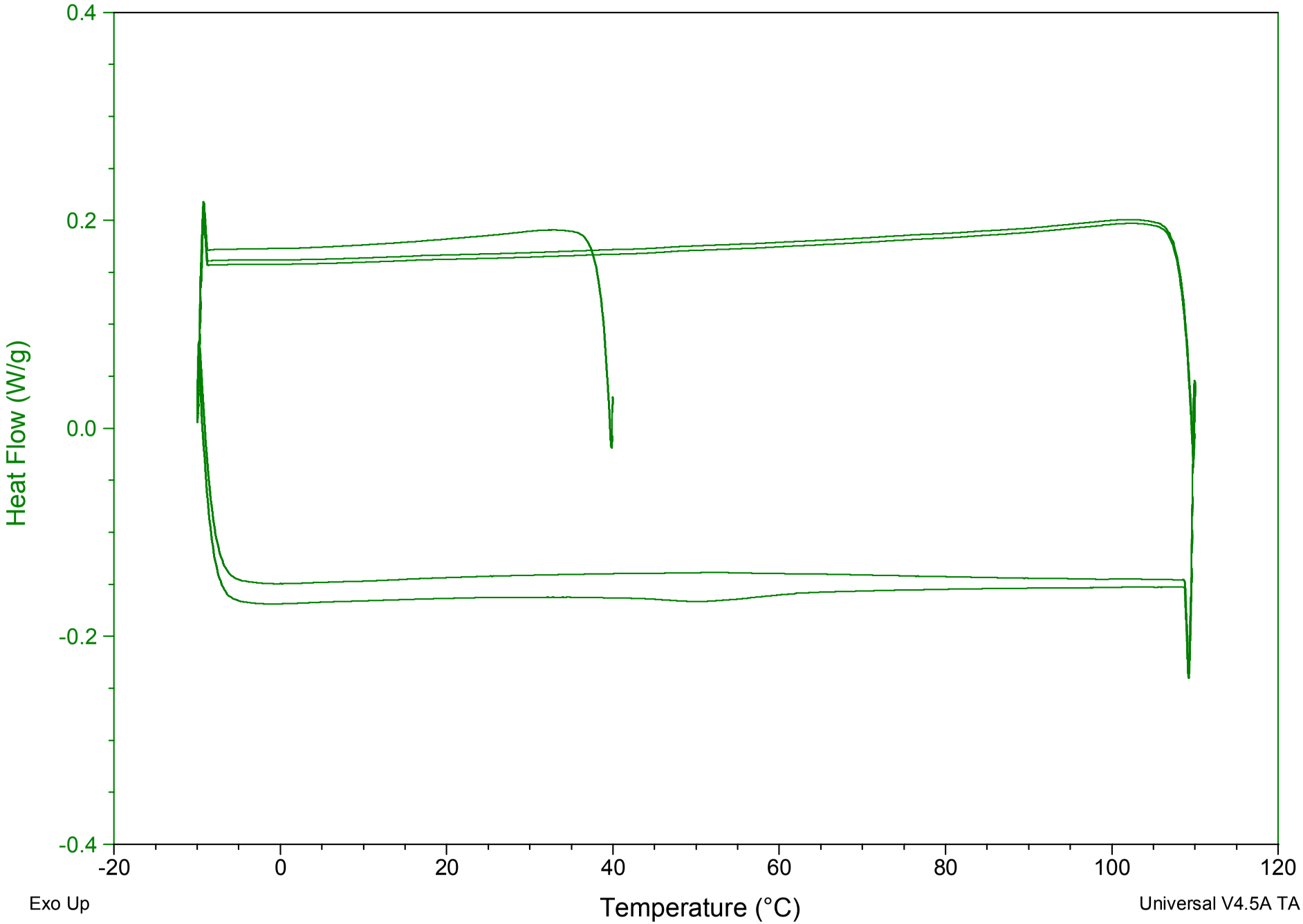

Appendix B

Measured results versus model predicted temperature for all days in population

August 2, 2010

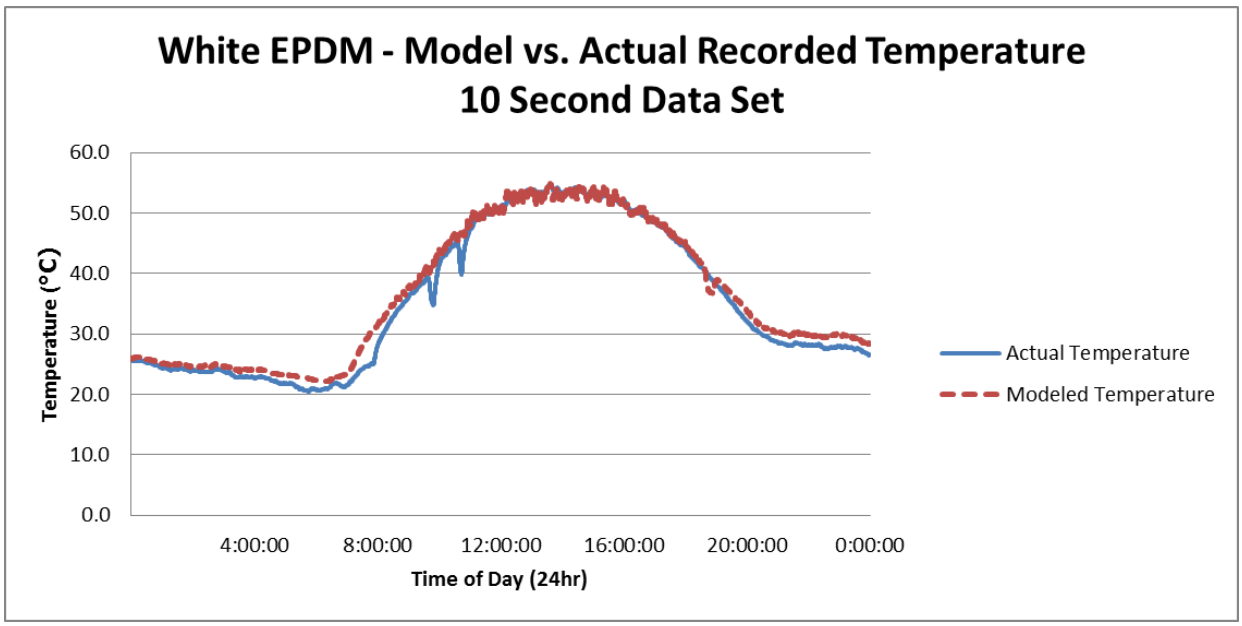
White EPDM - Model vs. Actual Recorded Temperature
10 Second Data Set
60.0
50.0
40.0
30.0
20.0
10.0
0.0
Temperature (°C)
4:00:00
8:00:00
12:00:00
16:00:00
20:00:00
0:00:00
Time of Day (24hr)
Actual Temperature
Modeled Temperature

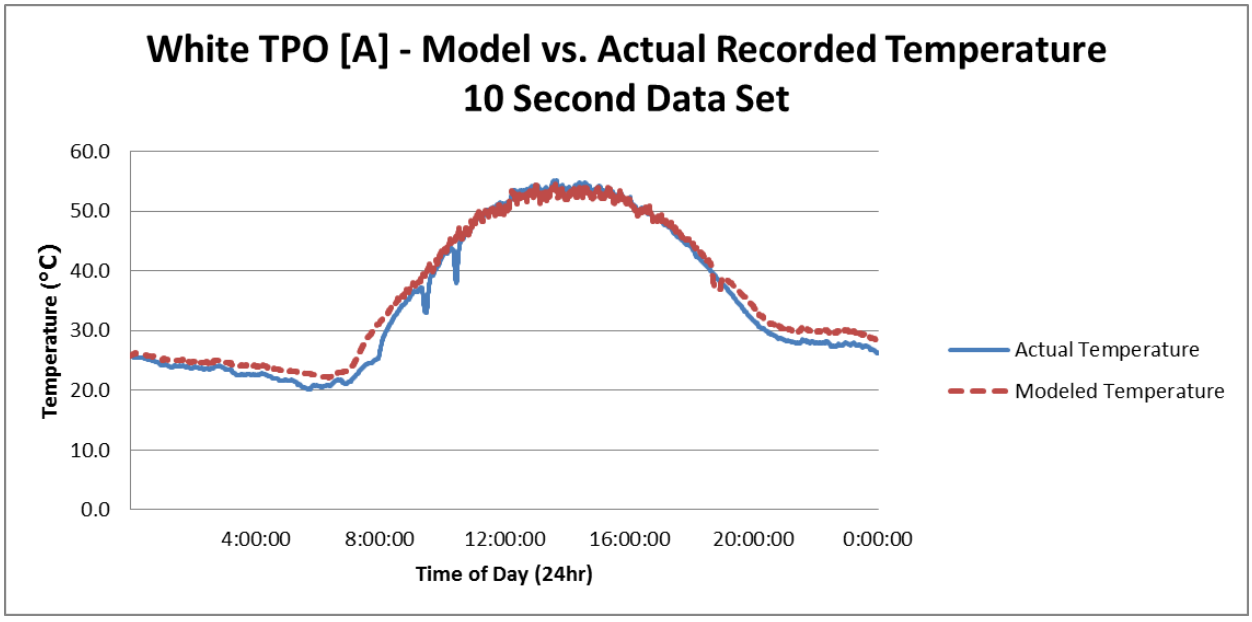
White TPO [A] - Model vs. Actual Recorded Temperature
10 Second Data Set
60.0
50.0
40.0
30.0
20.0
10.0
0.0
Temperature (°C)
4:00:00
8:00:00
12:00:00
16:00:00
20:00:00
0:00:00
Time of Day (24hr)
Actual Temperature
Modeled Temperature

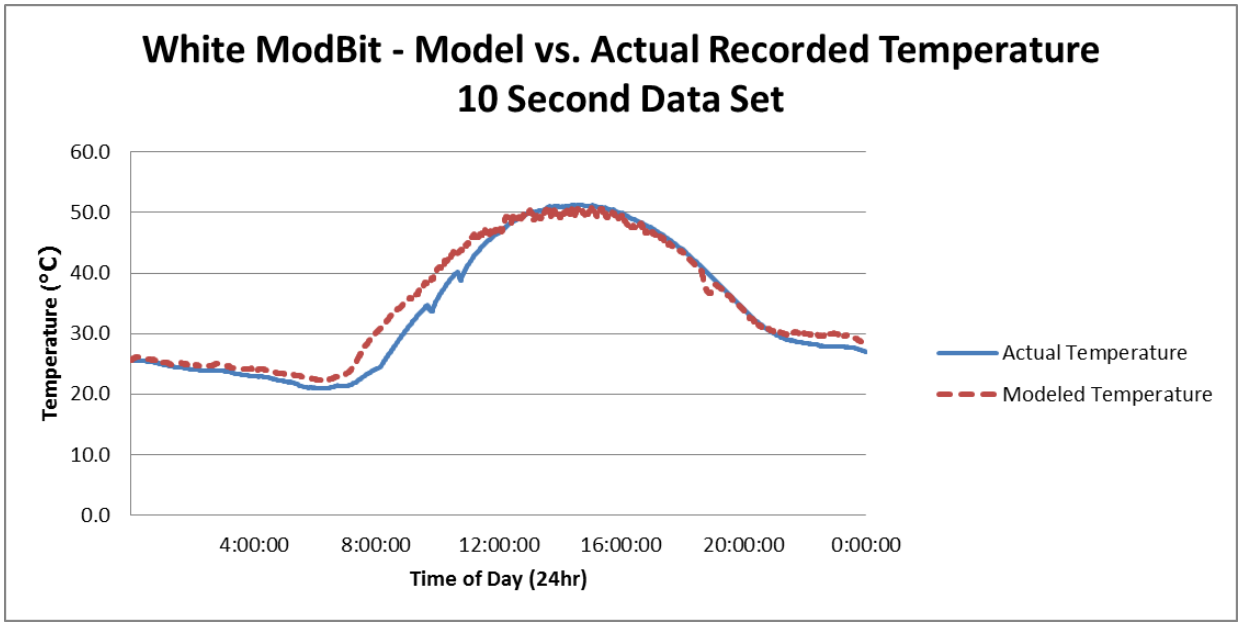
White ModBit - Model vs. Actual Recorded Temperature
10 Second Data Set
60.0
50.0
40.0
30.0
20.0
10.0
0.0
Temperature (°C)
4:00:00
8:00:00
12:00:00
16:00:00
20:00:00
0:00:00
Time of Day (24hr)
Actual Temperature
Modeled Temperature

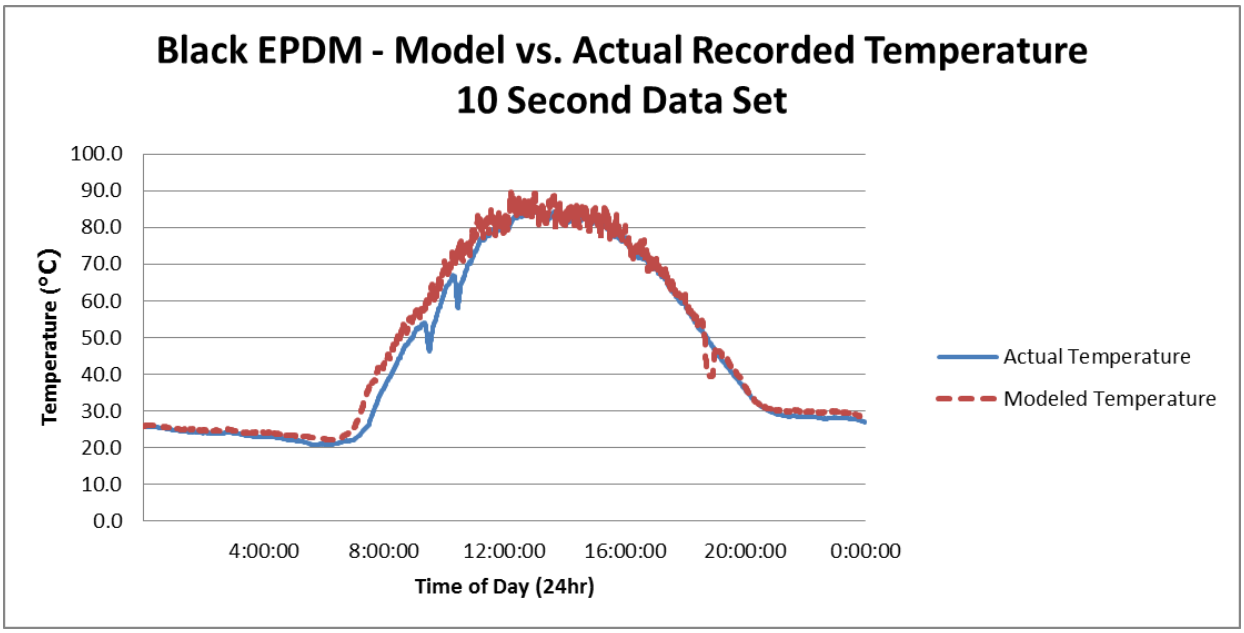
Black EPDM - Model vs. Actual Recorded Temperature
10 Second Data Set
100.0
90.0
80.0
70.0
60.0
50.0
40.0
30.0
20.0
10.0
0.0
Temperature (°C)
4:00:00
8:00:00
12:00:00
16:00:00
20:00:00
0:00:00
Time of Day (24hr)
Actual Temperature
Modeled Temperature

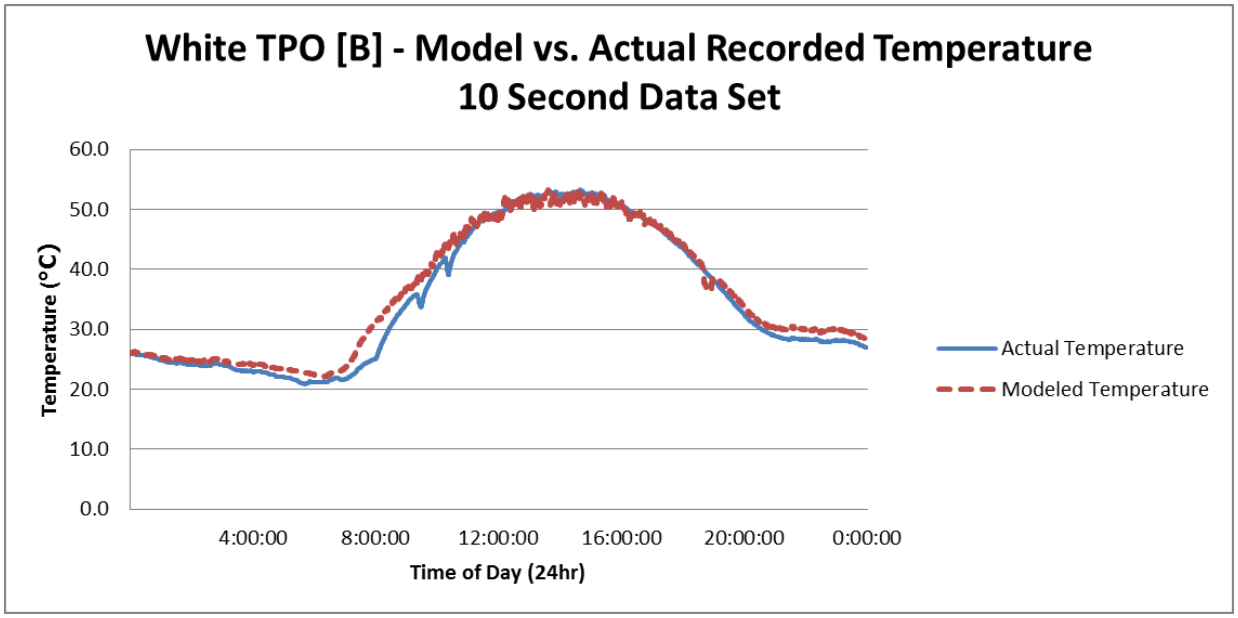
White TPO [B] - Model vs. Actual Recorded Temperature
10 Second Data Set
Temperature (°C)
60.0
50.0
40.0
30.0
20.0
10.0
0.0
4:00:00
8:00:00
12:00:00
16:00:00
20:00:00
0:00:00
Time of Day (24hr)
Actual Temperature
Modeled Temperature

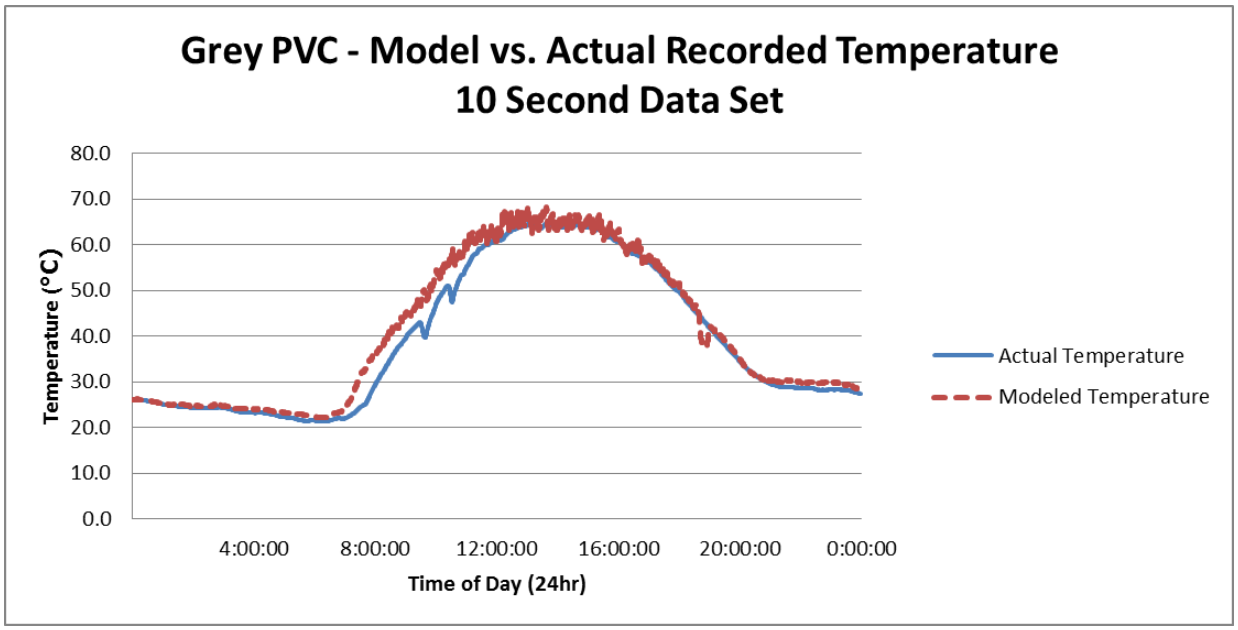
Grey PVC - Model vs. Actual Recorded Temperature
10 Second Data Set
Temperature (°C)
80.0
70.0
60.0
50.0
40.0
30.0
20.0
10.0
0.0
4:00:00
8:00:00
12:00:00
16:00:00
20:00:00
0:00:00
Time of Day (24hr)
Actual Temperature
Modeled Temperature

August 3, 2010

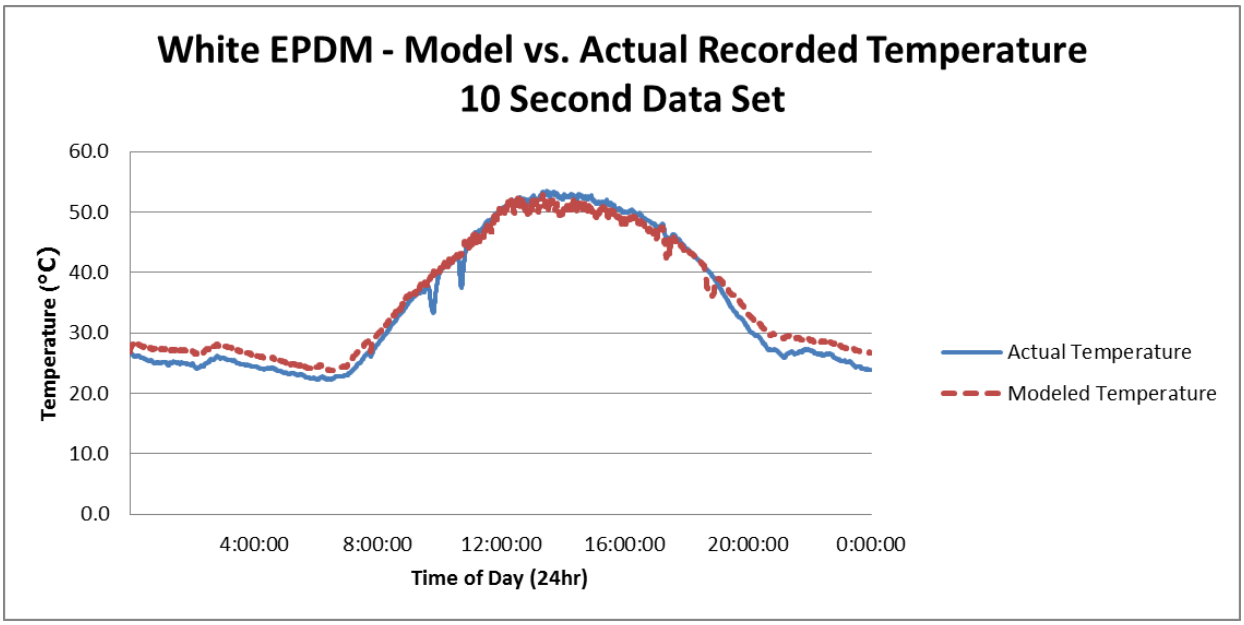
White EPDM - Model vs. Actual Recorded Temperature
10 Second Data Set
Temperature (°C)
60.0
50.0
40.0
30.0
20.0
10.0
0.0
4:00:00
8:00:00
12:00:00
16:00:00
20:00:00
0:00:00
Time of Day (24hr)
Actual Temperature
Modeled Temperature

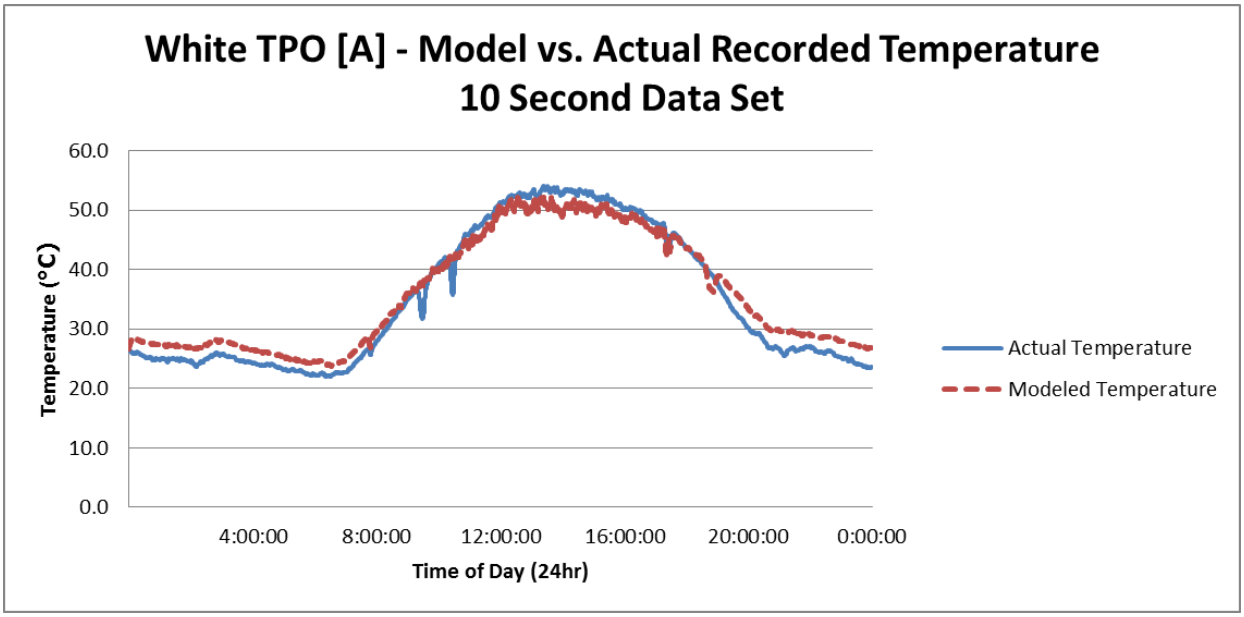
White TPO [A] - Model vs. Actual Recorded Temperature
10 Second Data Set
Temperature (°C)
60.0
50.0
40.0
30.0
20.0
10.0
0.0
4:00:00
8:00:00
12:00:00
16:00:00
20:00:00
0:00:00
Time of Day (24hr)
Actual Temperature
Modeled Temperature

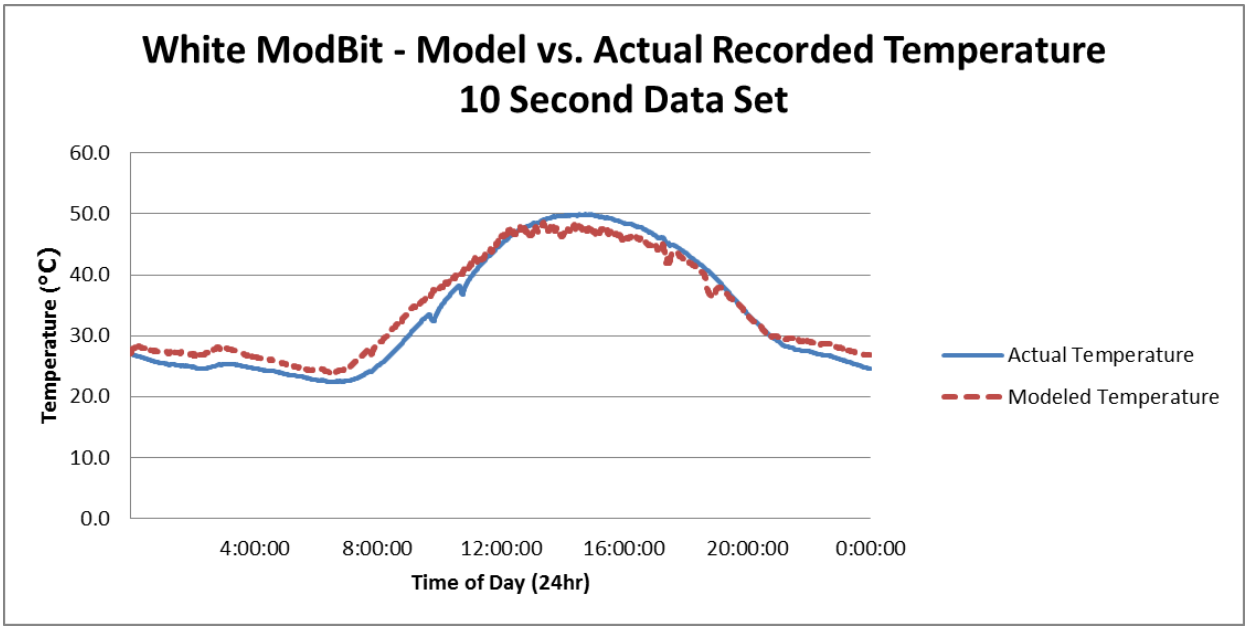
White ModBit - Model vs. Actual Recorded Temperature
10 Second Data Set
60.0
50.0
40.0
30.0
20.0
10.0
0.0
Temperature (°C)
4:00:00
8:00:00
12:00:00
16:00:00
20:00:00
0:00:00
Time of Day (24hr)
Actual Temperature
Modeled Temperature

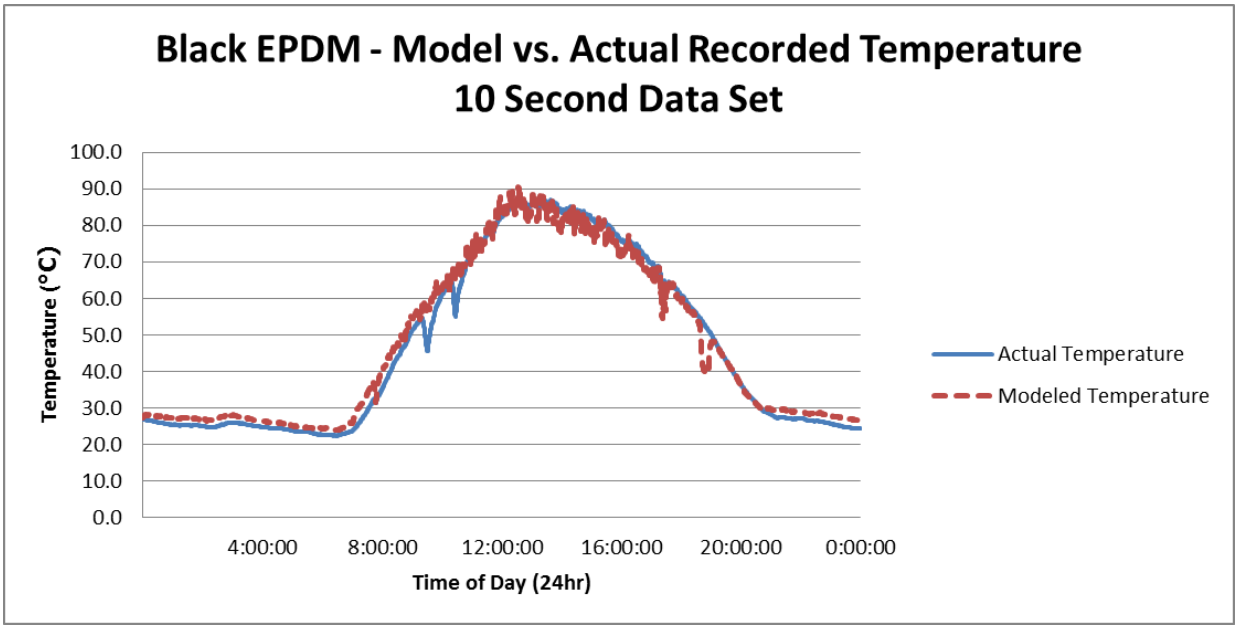
Black EPDM - Model vs. Actual Recorded Temperature
10 Second Data Set
100.0
90.0
80.0
70.0
60.0
50.0
40.0
30.0
20.0
10.0
0.0
Temperature (°C)
4:00:00
8:00:00
12:00:00
16:00:00
20:00:00
0:00:00
Time of Day (24hr)
Actual Temperature
Modeled Temperature

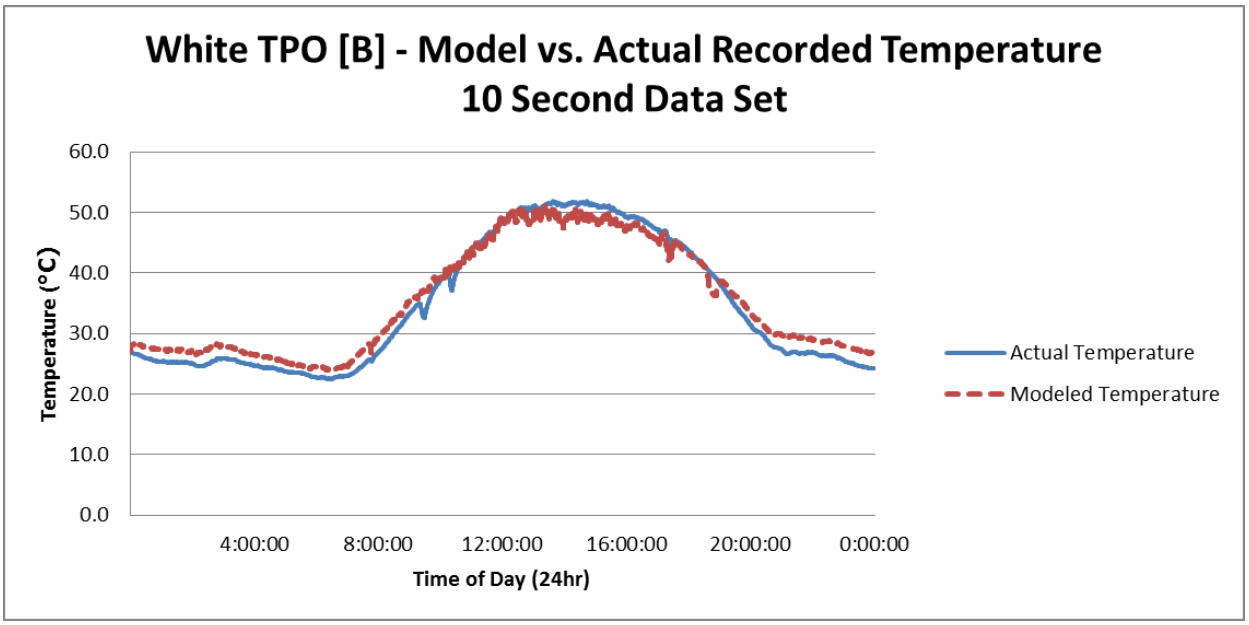
White TPO [B] - Model vs. Actual Recorded Temperature
10 Second Data Set
Temperature (°C)
60.0
50.0
40.0
30.0
20.0
10.0
0.0
4:00:00
8:00:00
12:00:00
16:00:00
20:00:00
0:00:00
Time of Day (24hr)
Actual Temperature
Modeled Temperature

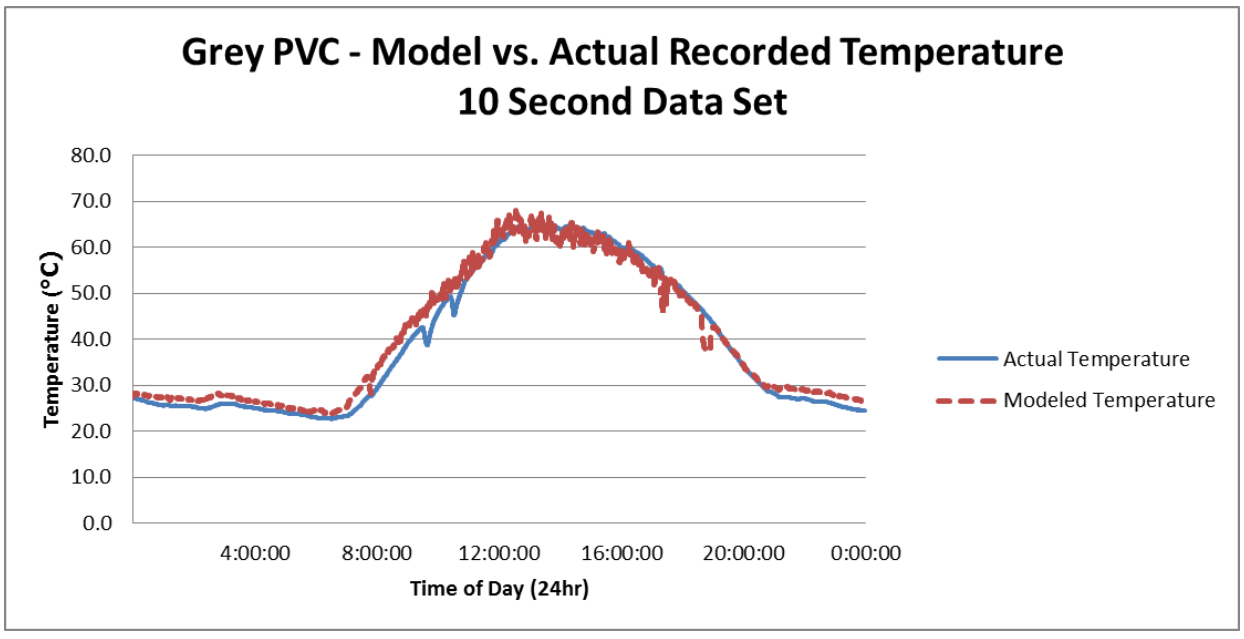
Grey PVC - Model vs. Actual Recorded Temperature
10 Second Data Set
Temperature (°C)
80.0
70.0
60.0
50.0
40.0
30.0
20.0
10.0
0.0
4:00:00
8:00:00
12:00:00
16:00:00
20:00:00
0:00:00
Time of Day (24hr)
Actual Temperature
Modeled Temperature

August 4, 2010

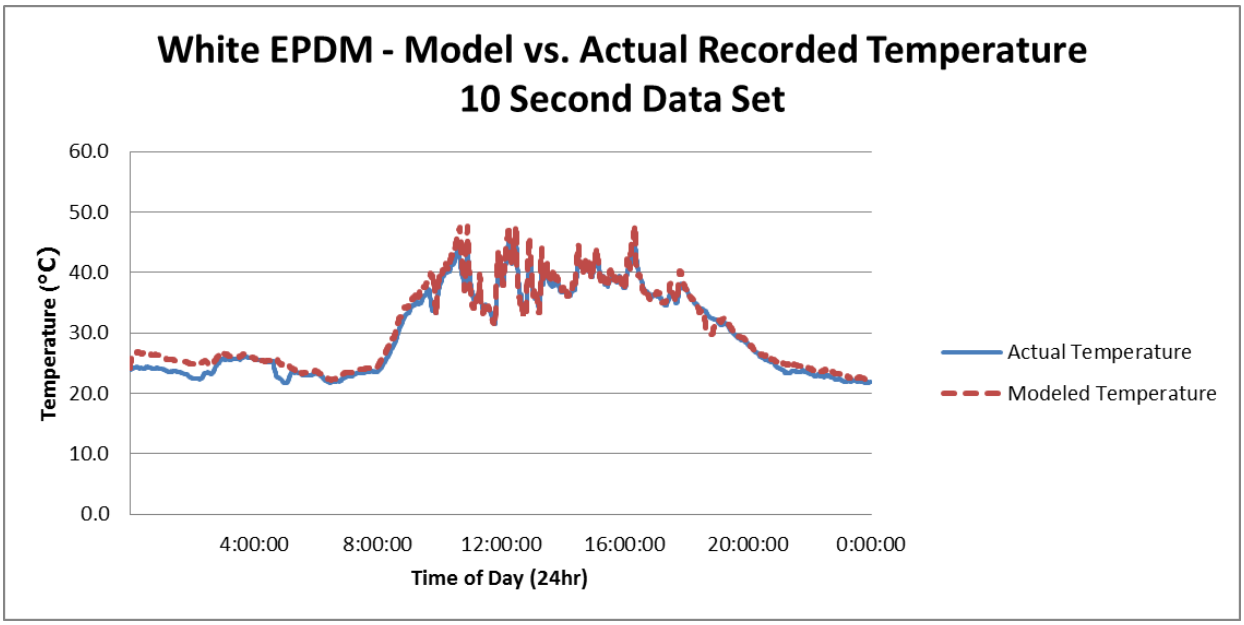
White EPDM - Model vs. Actual Recorded Temperature
10 Second Data Set
60.0
50.0
40.0
30.0
20.0
10.0
0.0
Temperature (°C)
4:00:00
8:00:00
12:00:00
16:00:00
20:00:00
0:00:00
Time of Day (24hr)
Actual Temperature
Modeled Temperature

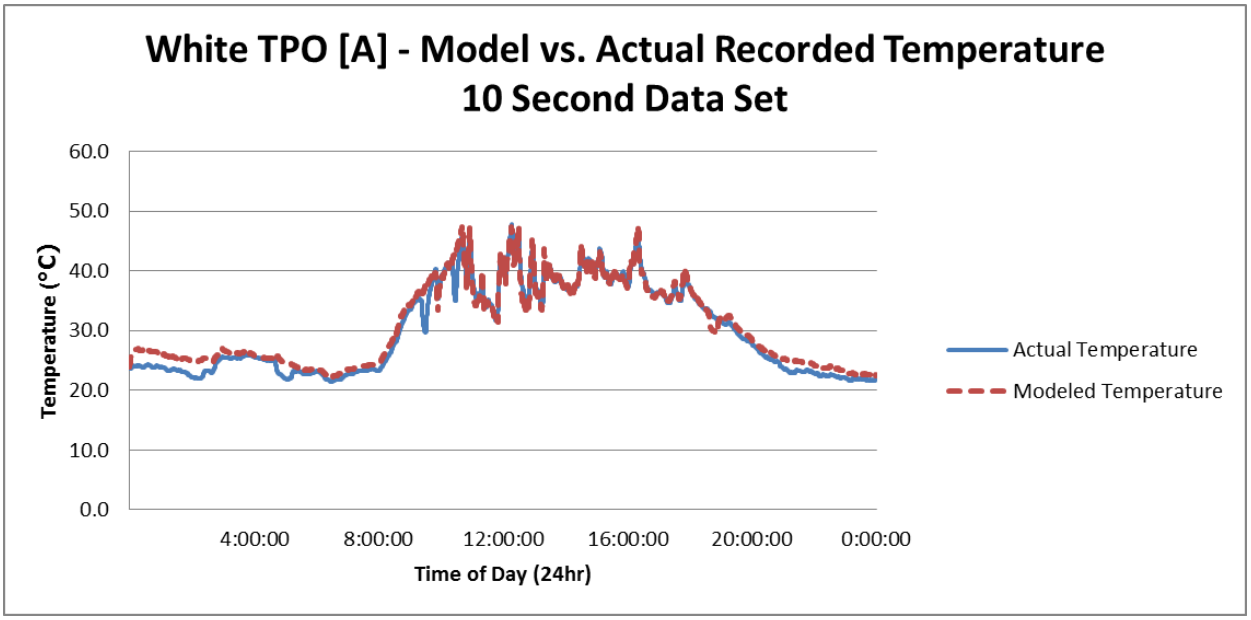
White TPO [A] - Model vs. Actual Recorded Temperature
10 Second Data Set
60.0
50.0
40.0
30.0
20.0
10.0
0.0
Temperature (°C)
4:00:00
8:00:00
12:00:00
16:00:00
20:00:00
0:00:00
Time of Day (24hr)
Actual Temperature
Modeled Temperature

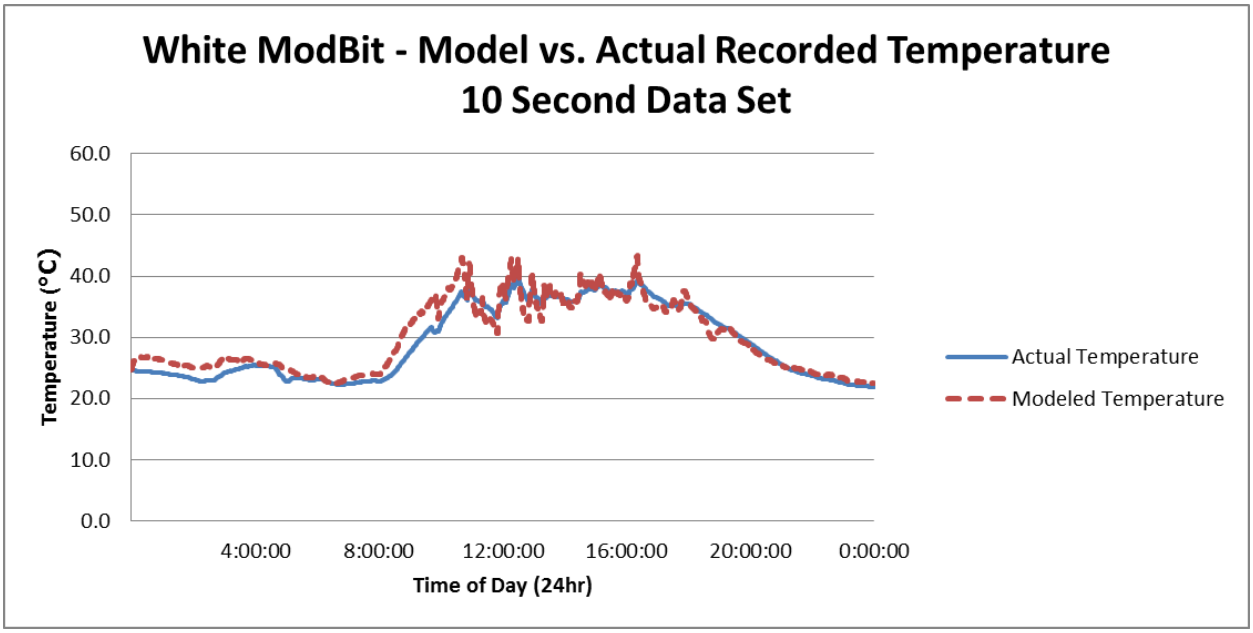
White ModBit - Model vs. Actual Recorded Temperature
10 Second Data Set
Temperature (°C)
60.0
50.0
40.0
30.0
20.0
10.0
0.0
4:00:00
8:00:00
12:00:00
16:00:00
20:00:00
0:00:00
Time of Day (24hr)
Actual Temperature
Modeled Temperature

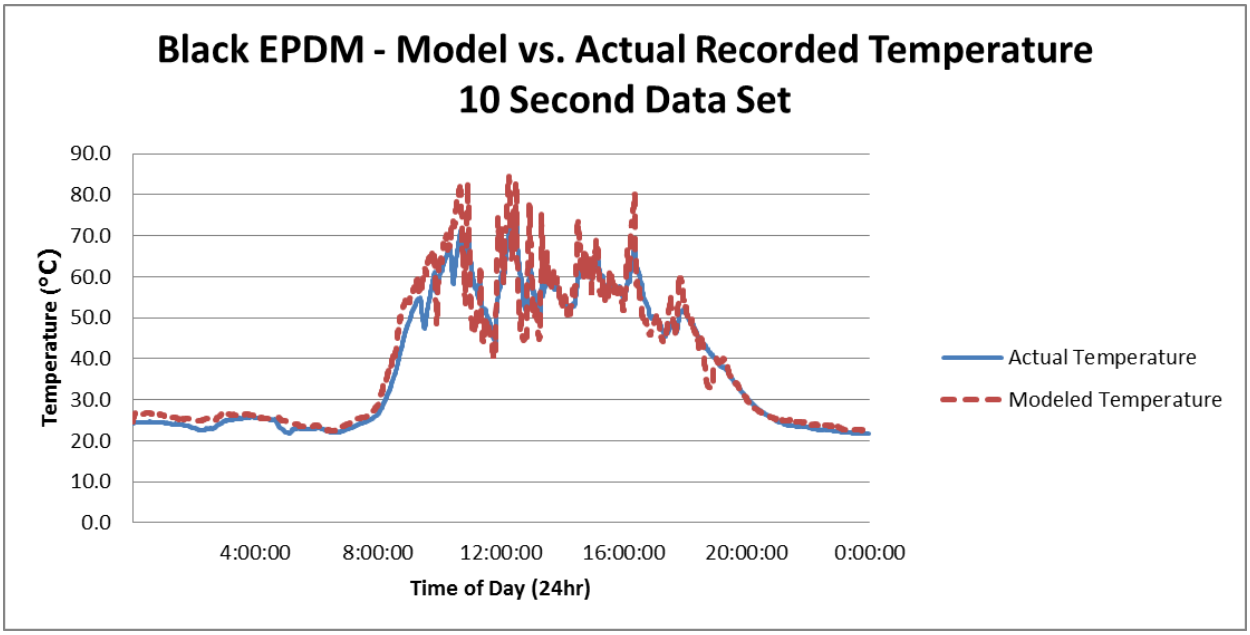
Black EPDM - Model vs. Actual Recorded Temperature
10 Second Data Set
Temperature (°C)
90.0
80.0
70.0
60.0
50.0
40.0
30.0
20.0
10.0
0.0
4:00:00
8:00:00
12:00:00
16:00:00
20:00:00
0:00:00
Time of Day (24hr)
Actual Temperature
Modeled Temperature

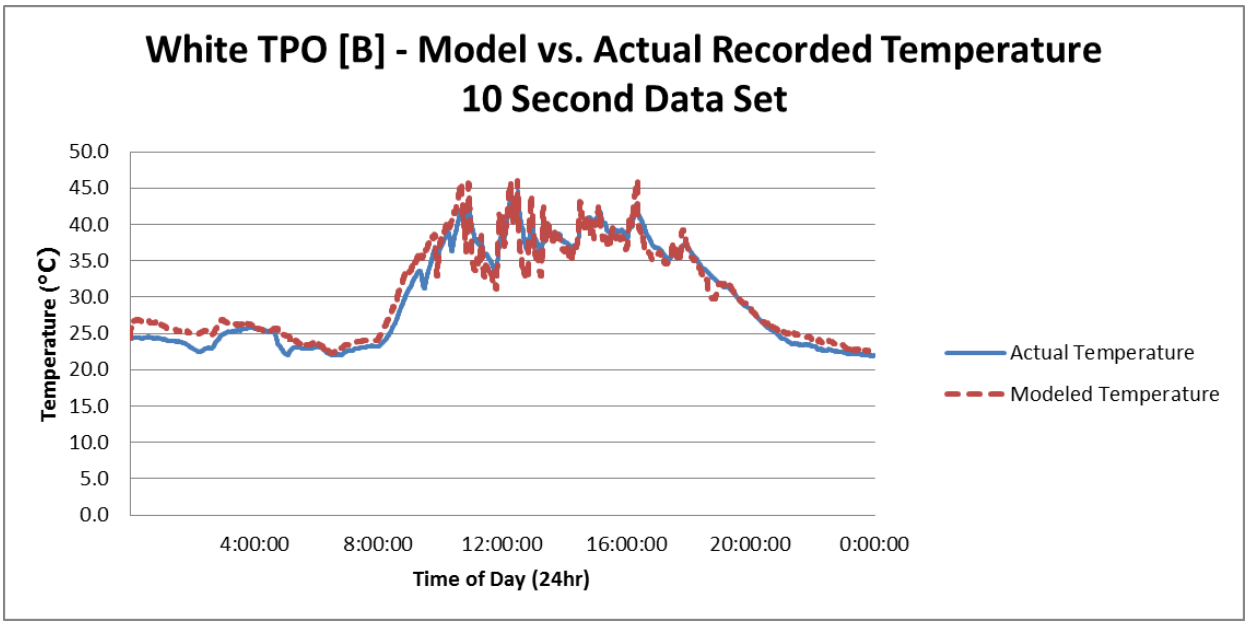
White TPO [B] - Model vs. Actual Recorded Temperature
10 Second Data Set
Temperature (°C)
50.0
45.0
40.0
35.0
30.0
25.0
20.0
15.0
10.0
5.0
0.0
4:00:00
8:00:00
12:00:00
16:00:00
20:00:00
0:00:00
Time of Day (24hr)
Actual Temperature
Modeled Temperature

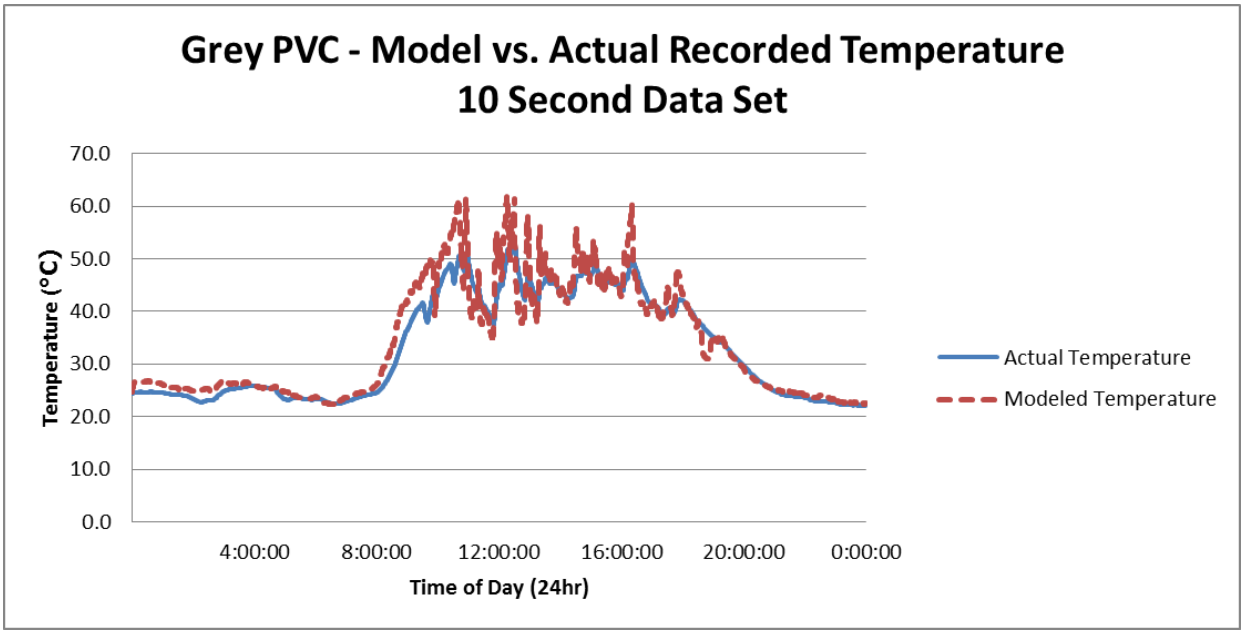
Grey PVC - Model vs. Actual Recorded Temperature
10 Second Data Set
Temperature (°C)
70.0
60.0
50.0
40.0
30.0
20.0
10.0
0.0
4:00:00
8:00:00
12:00:00
16:00:00
20:00:00
0:00:00
Time of Day (24hr)
Actual Temperature
Modeled Temperature

August 5, 2010

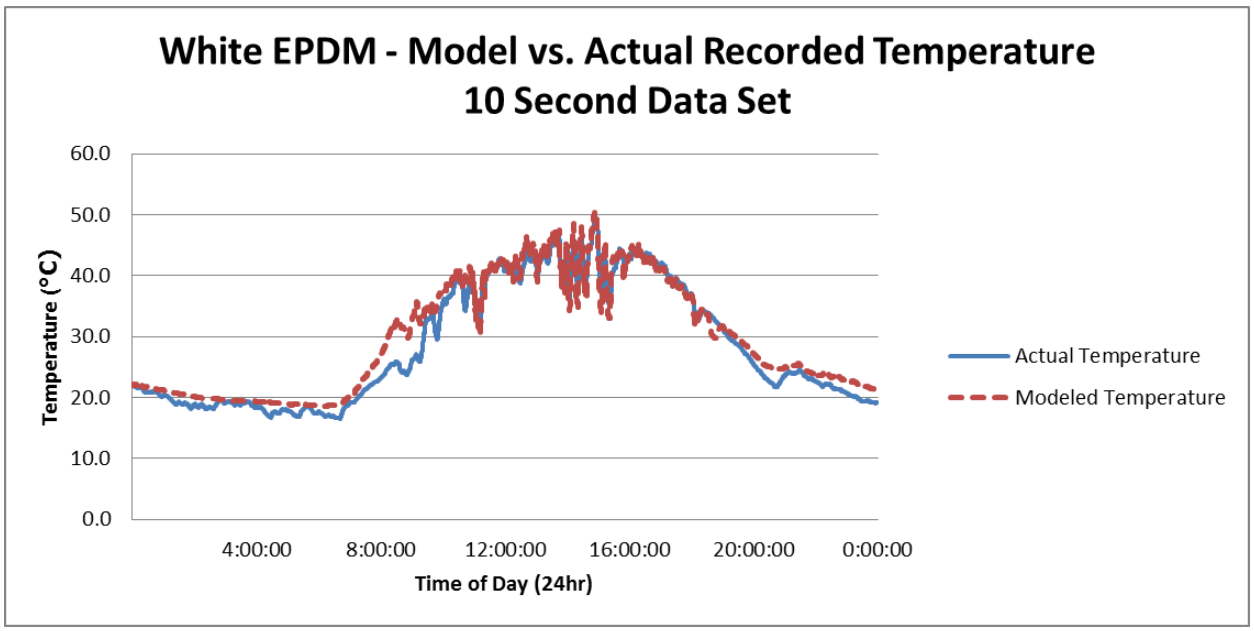
White EPDM - Model vs. Actual Recorded Temperature
10 Second Data Set
60.0
50.0
40.0
30.0
20.0
10.0
0.0
Temperature (°C)
4:00:00
8:00:00
12:00:00
16:00:00
20:00:00
0:00:00
Time of Day (24hr)
Actual Temperature
Modeled Temperature

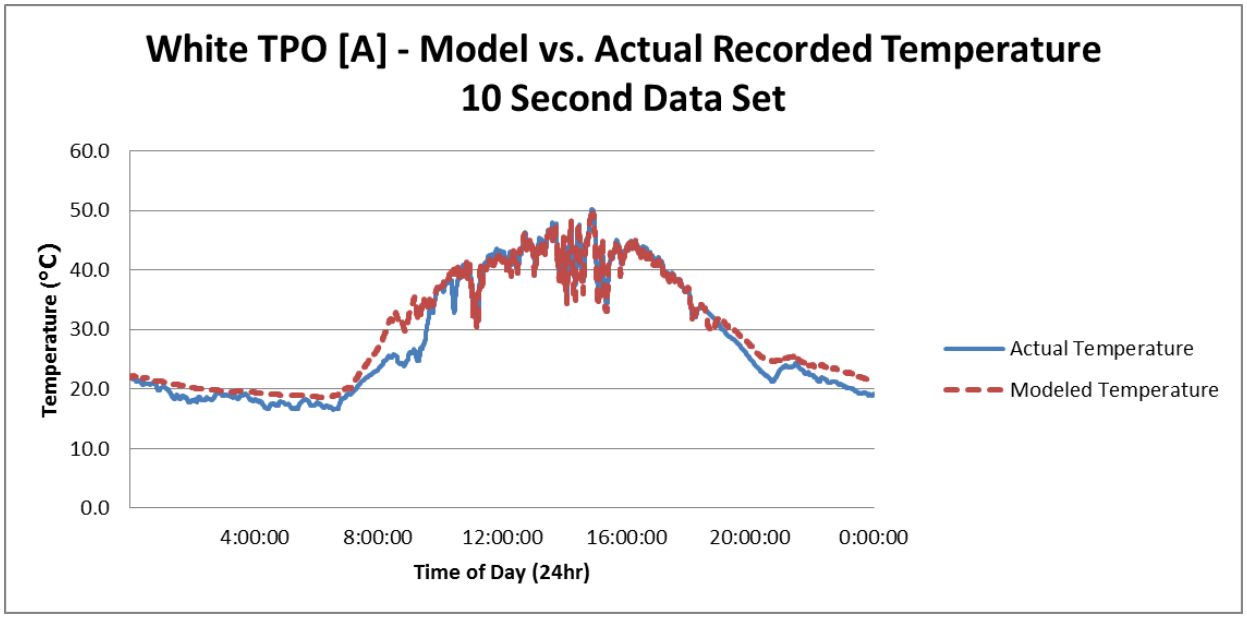
White TPO [A] - Model vs. Actual Recorded Temperature
10 Second Data Set
60.0
50.0
40.0
30.0
20.0
10.0
0.0
Temperature (°C)
4:00:00
8:00:00
12:00:00
16:00:00
20:00:00
0:00:00
Time of Day (24hr)
Actual Temperature
Modeled Temperature

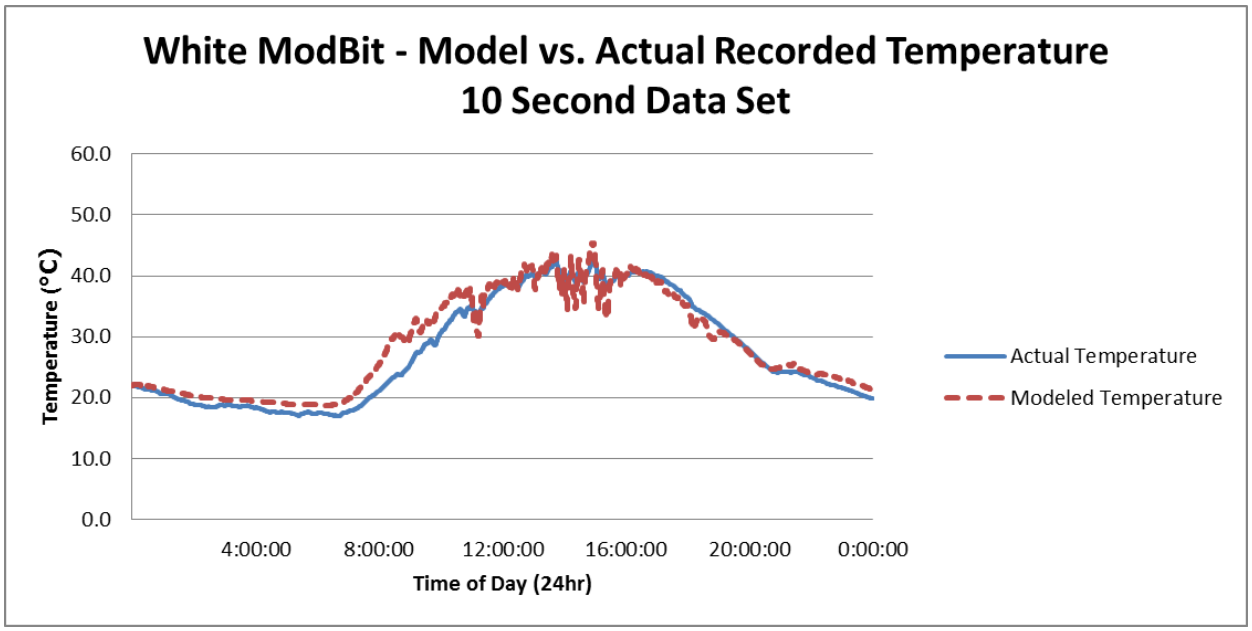
White ModBit - Model vs. Actual Recorded Temperature
10 Second Data Set
Temperature (°C)
60.0
50.0
40.0
30.0
20.0
10.0
0.0
4:00:00
8:00:00
12:00:00
16:00:00
20:00:00
0:00:00
Time of Day (24hr)
Actual Temperature
Modeled Temperature

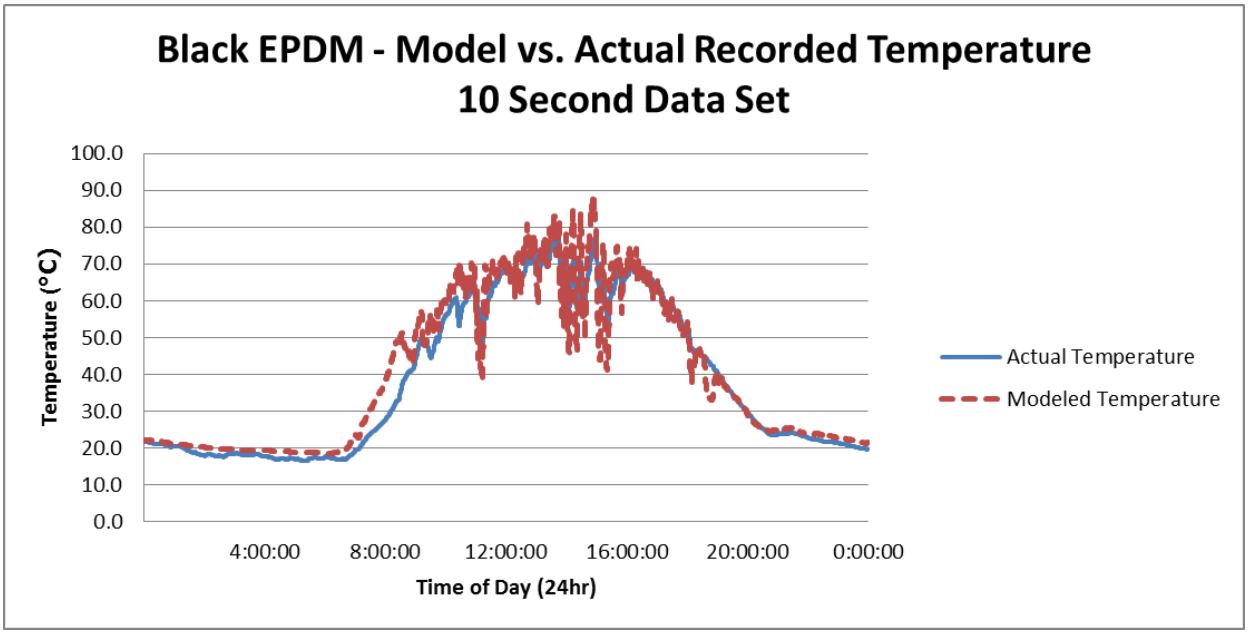
Black EPDM - Model vs. Actual Recorded Temperature
10 Second Data Set
Temperature (°C)
100.0
90.0
80.0
70.0
60.0
50.0
40.0
30.0
20.0
10.0
0.0
4:00:00
8:00:00
12:00:00
16:00:00
20:00:00
0:00:00
Time of Day (24hr)
Actual Temperature
Modeled Temperature

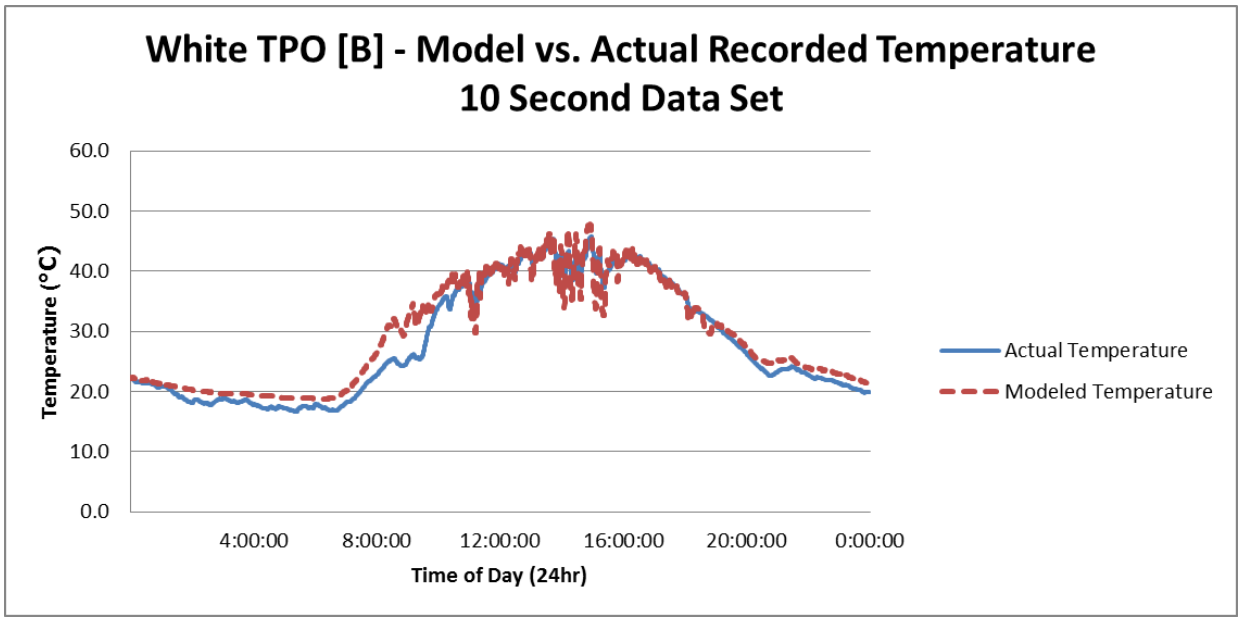
White TPO [B] - Model vs. Actual Recorded Temperature
10 Second Data Set
Temperature (°C)
60.0
50.0
40.0
30.0
20.0
10.0
0.0
4:00:00
8:00:00
12:00:00
16:00:00
20:00:00
0:00:00
Time of Day (24hr)
Actual Temperature
Modeled Temperature

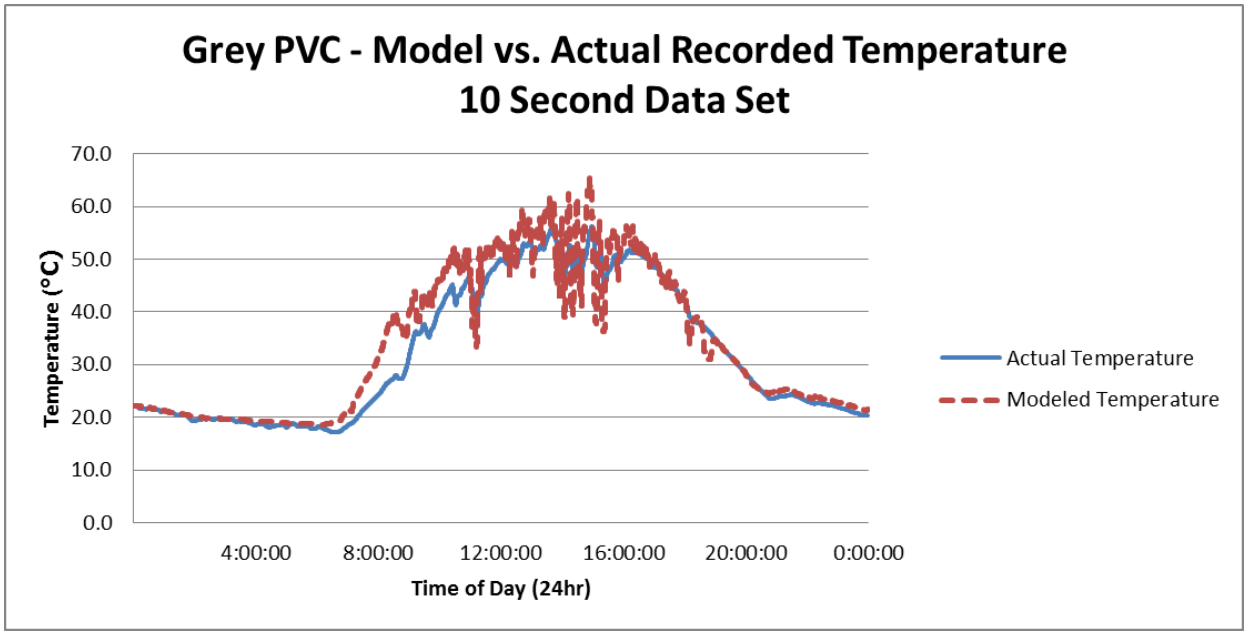
Grey PVC - Model vs. Actual Recorded Temperature
10 Second Data Set
Temperature (°C)
70.0
60.0
50.0
40.0
30.0
20.0
10.0
0.0
4:00:00
8:00:00
12:00:00
16:00:00
20:00:00
0:00:00
Time of Day (24hr)
Actual Temperature
Modeled Temperature

August 6, 2010

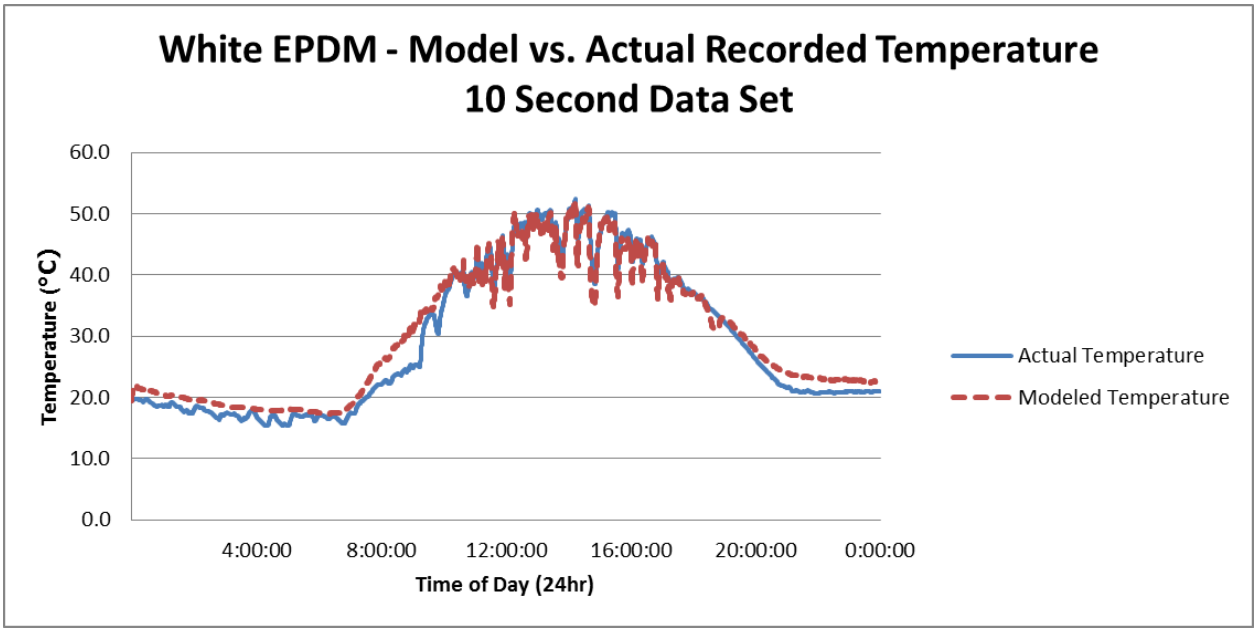
White EPDM - Model vs. Actual Recorded Temperature
10 Second Data Set
Temperature (°C)
60.0
50.0
40.0
30.0
20.0
10.0
0.0
4:00:00
8:00:00
12:00:00
16:00:00
20:00:00
0:00:00
Time of Day (24hr)
Actual Temperature
Modeled Temperature

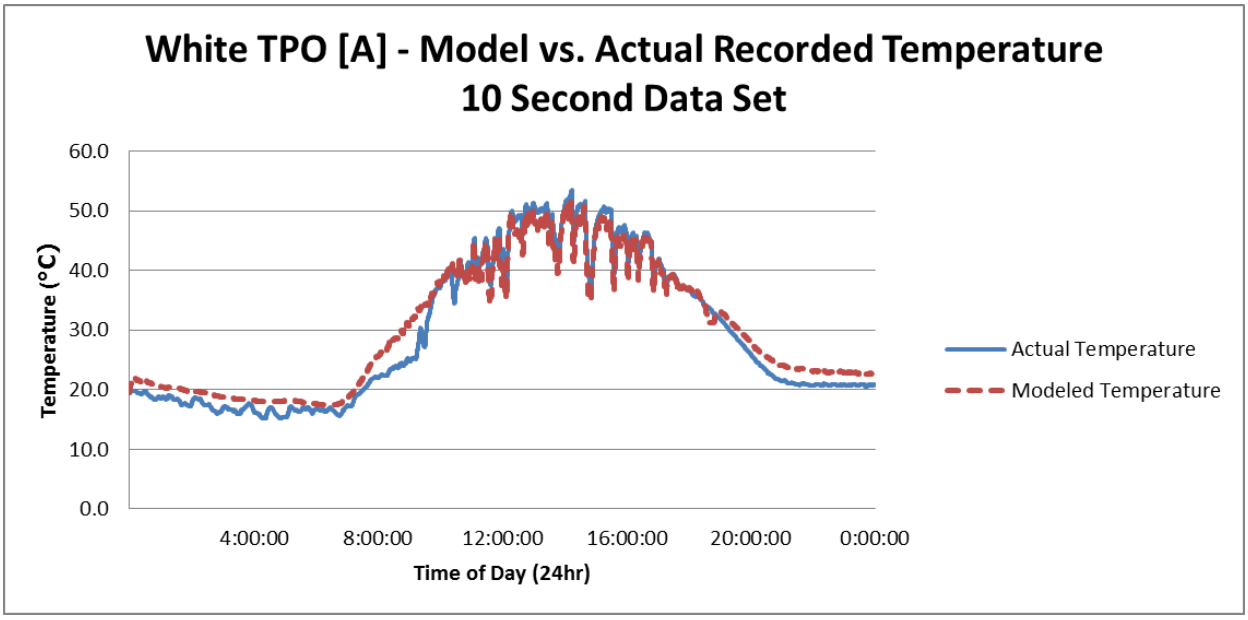
White TPO [A] - Model vs. Actual Recorded Temperature
10 Second Data Set
Temperature (°C)
60.0
50.0
40.0
30.0
20.0
10.0
0.0
4:00:00
8:00:00
12:00:00
16:00:00
20:00:00
0:00:00
Time of Day (24hr)
Actual Temperature
Modeled Temperature

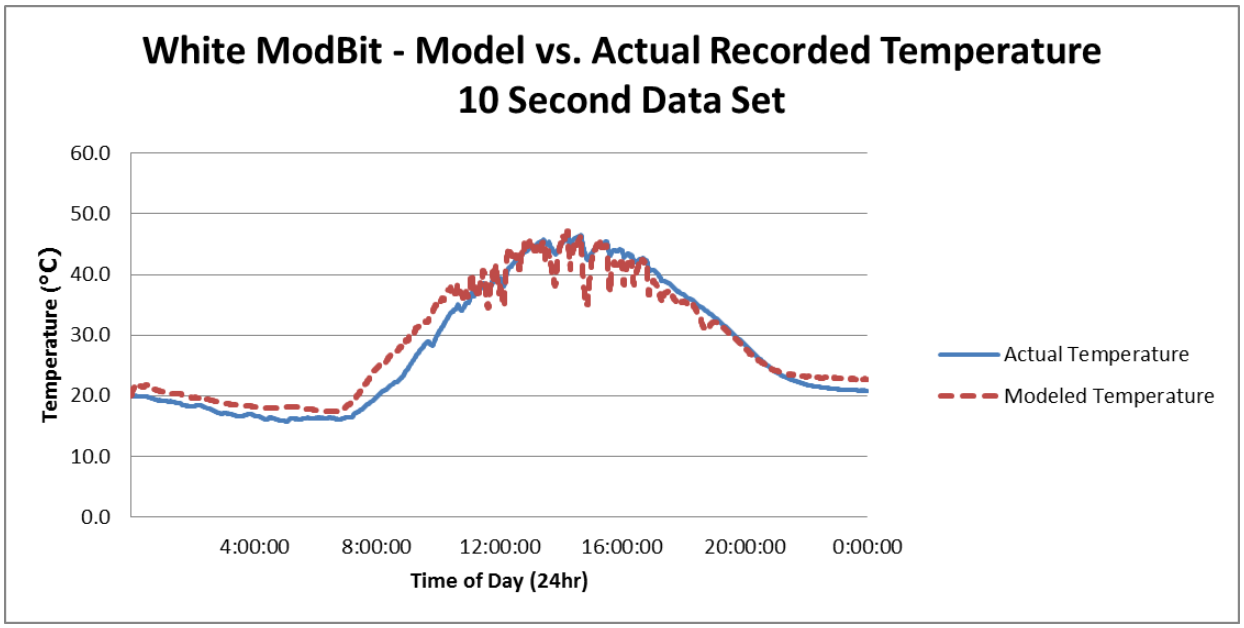
White ModBit - Model vs. Actual Recorded Temperature
10 Second Data Set
60.0
50.0
40.0
30.0
20.0
10.0
0.0
Temperature (°C)
4:00:00
8:00:00
12:00:00
16:00:00
20:00:00
0:00:00
Time of Day (24hr)
Actual Temperature
Modeled Temperature

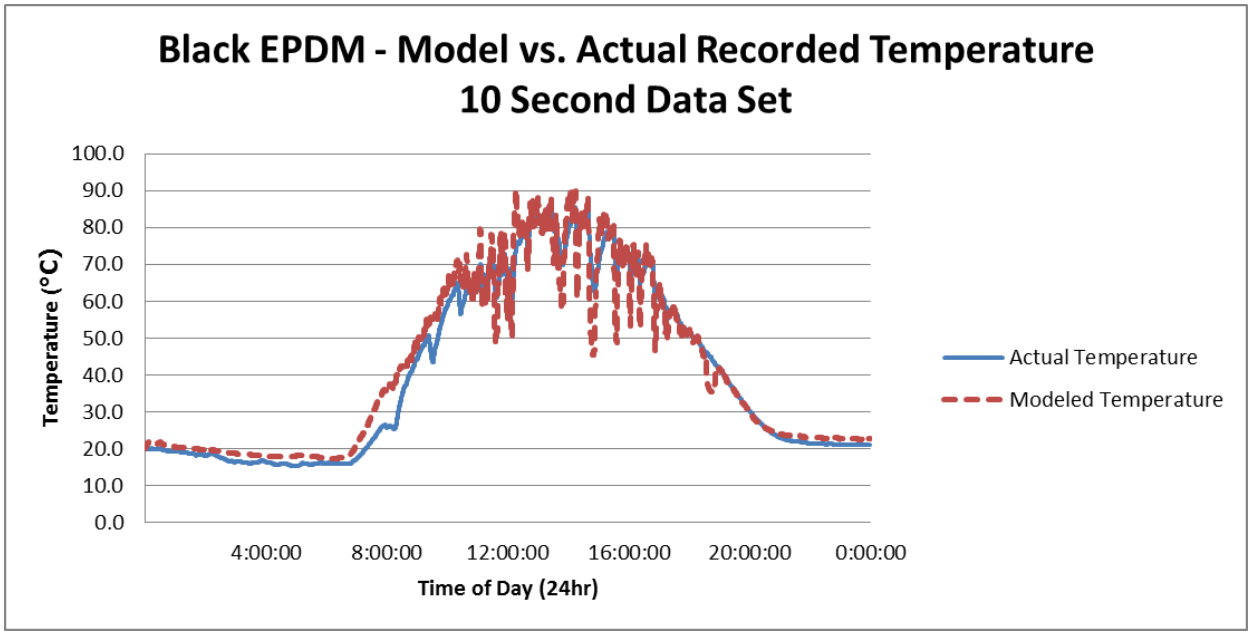
Black EPDM - Model vs. Actual Recorded Temperature
10 Second Data Set
100.0
90.0
80.0
70.0
60.0
50.0
40.0
30.0
20.0
10.0
0.0
Temperature (°C)
4:00:00
8:00:00
12:00:00
16:00:00
20:00:00
0:00:00
Time of Day (24hr)
Actual Temperature
Modeled Temperature

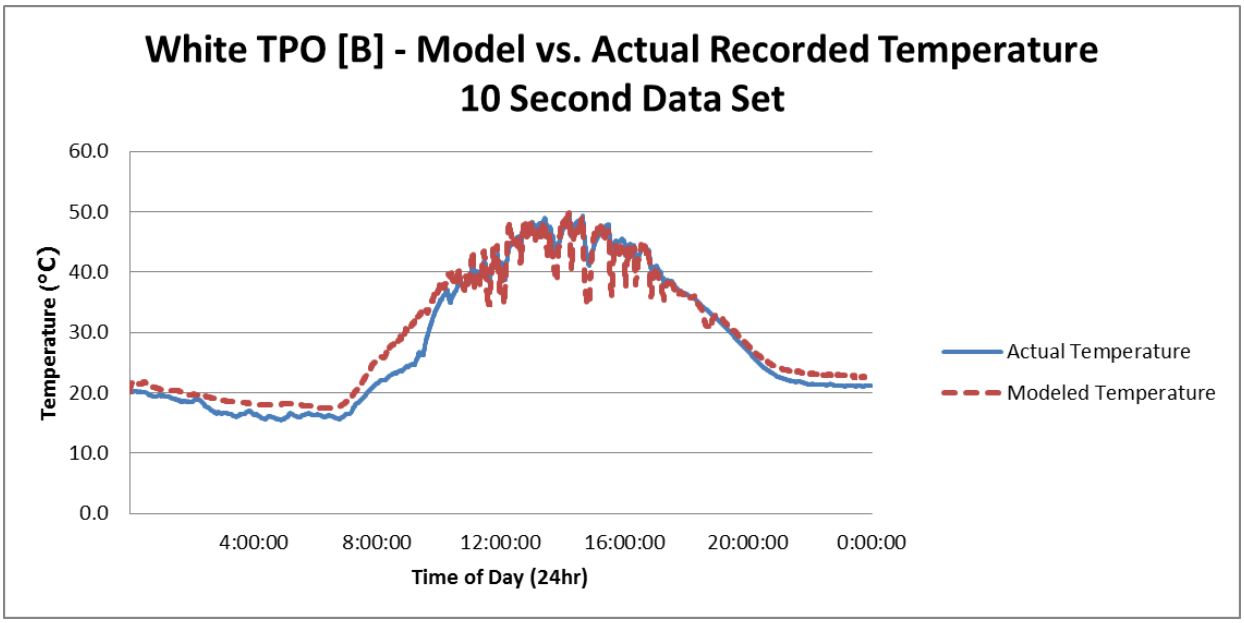
White TPO [B] - Model vs. Actual Recorded Temperature
10 Second Data Set
Temperature (°C)
60.0
50.0
40.0
30.0
20.0
10.0
0.0
4:00:00
8:00:00
12:00:00
16:00:00
20:00:00
0:00:00
Time of Day (24hr)
Actual Temperature
Modeled Temperature

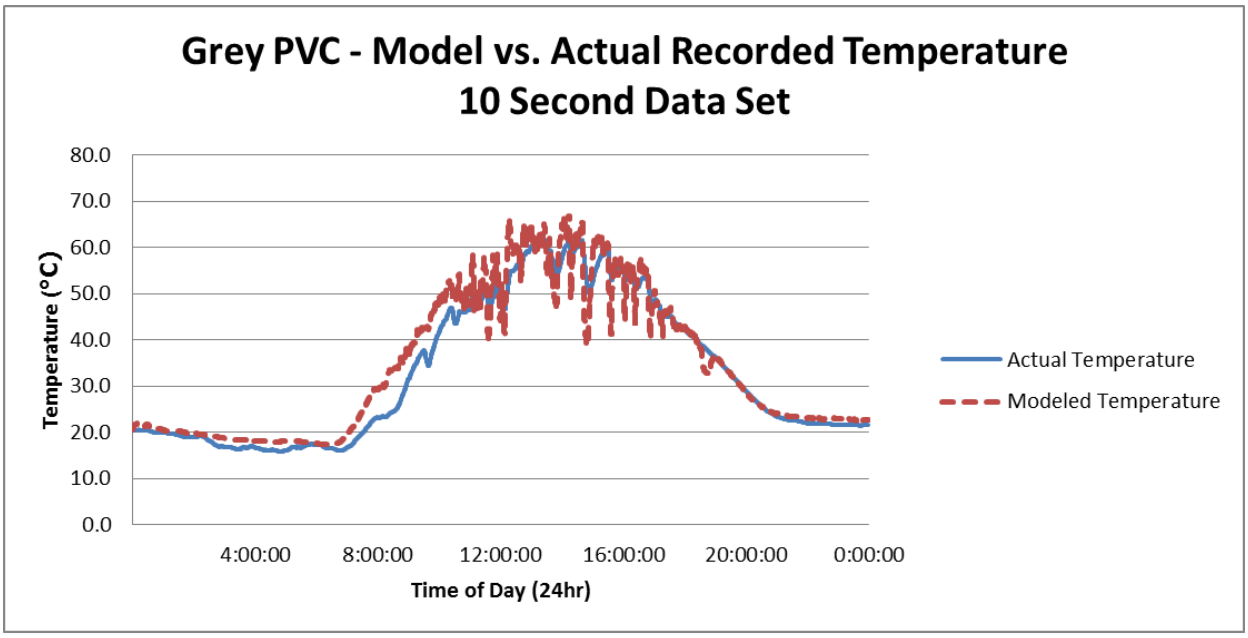
Grey PVC - Model vs. Actual Recorded Temperature
10 Second Data Set
Temperature (°C)
80.0
70.0
60.0
50.0
40.0
30.0
20.0
10.0
0.0
4:00:00
8:00:00
12:00:00
16:00:00
20:00:00
0:00:00
Time of Day (24hr)
Actual Temperature
Modeled Temperature

August 7, 2010

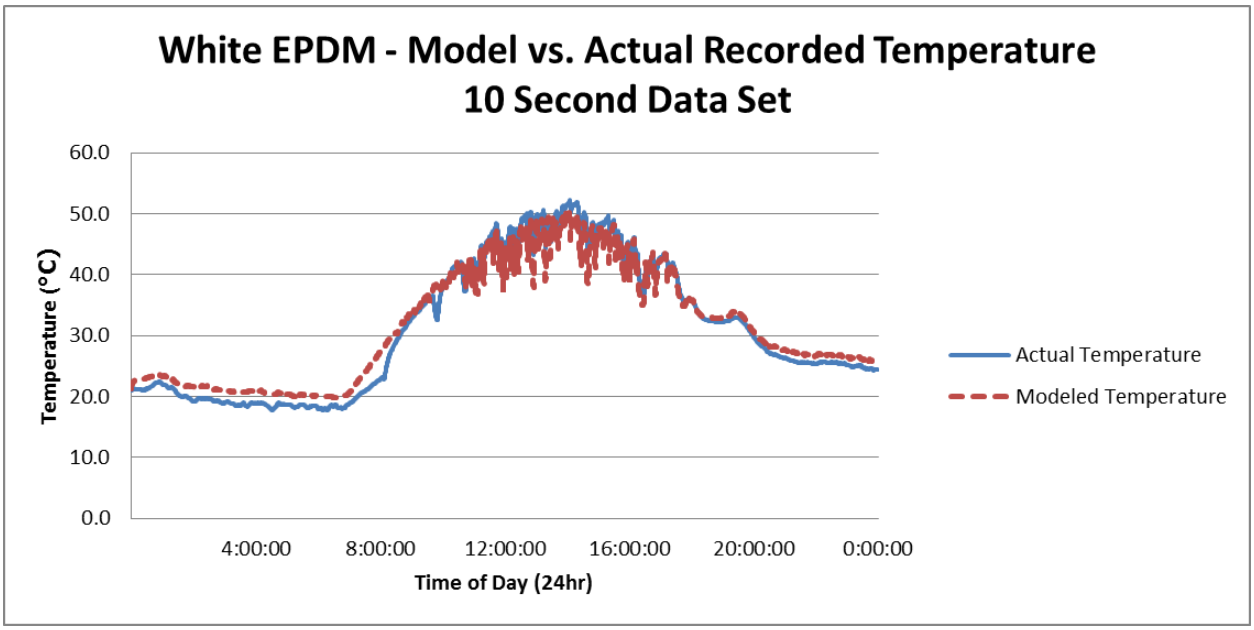
White EPDM - Model vs. Actual Recorded Temperature
10 Second Data Set
Temperature (°C)
60.0
50.0
40.0
30.0
20.0
10.0
0.0
4:00:00
8:00:00
12:00:00
16:00:00
20:00:00
0:00:00
Time of Day (24hr)
Actual Temperature
Modeled Temperature

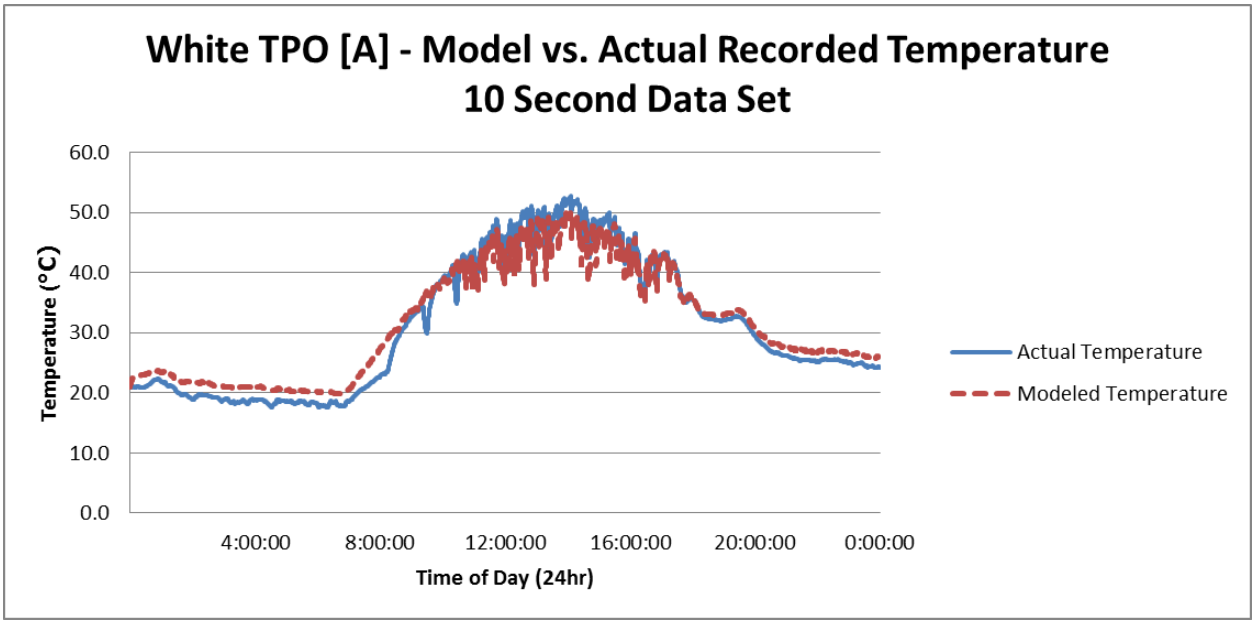
White TPO [A] - Model vs. Actual Recorded Temperature
10 Second Data Set
Temperature (°C)
60.0
50.0
40.0
30.0
20.0
10.0
0.0
4:00:00
8:00:00
12:00:00
16:00:00
20:00:00
0:00:00
Time of Day (24hr)
Actual Temperature
Modeled Temperature

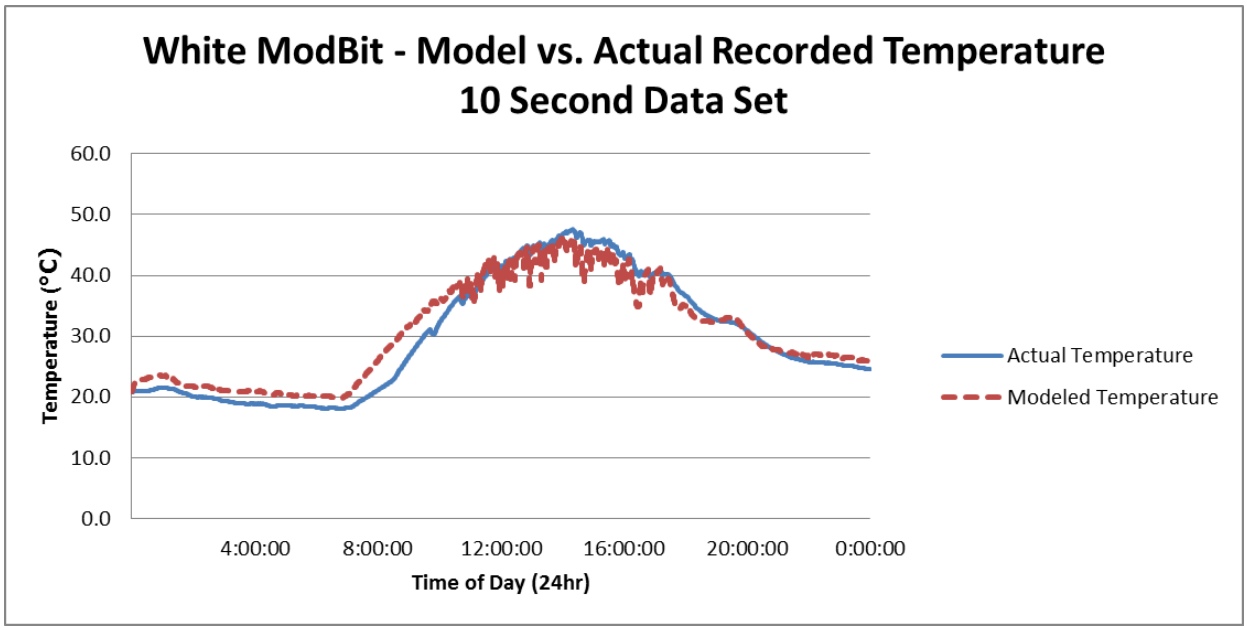
White ModBit - Model vs. Actual Recorded Temperature
10 Second Data Set
60.0
50.0
40.0
30.0
20.0
10.0
0.0
Temperature (°C)
4:00:00
8:00:00
12:00:00
16:00:00
20:00:00
0:00:00
Time of Day (24hr)
Actual Temperature
Modeled Temperature

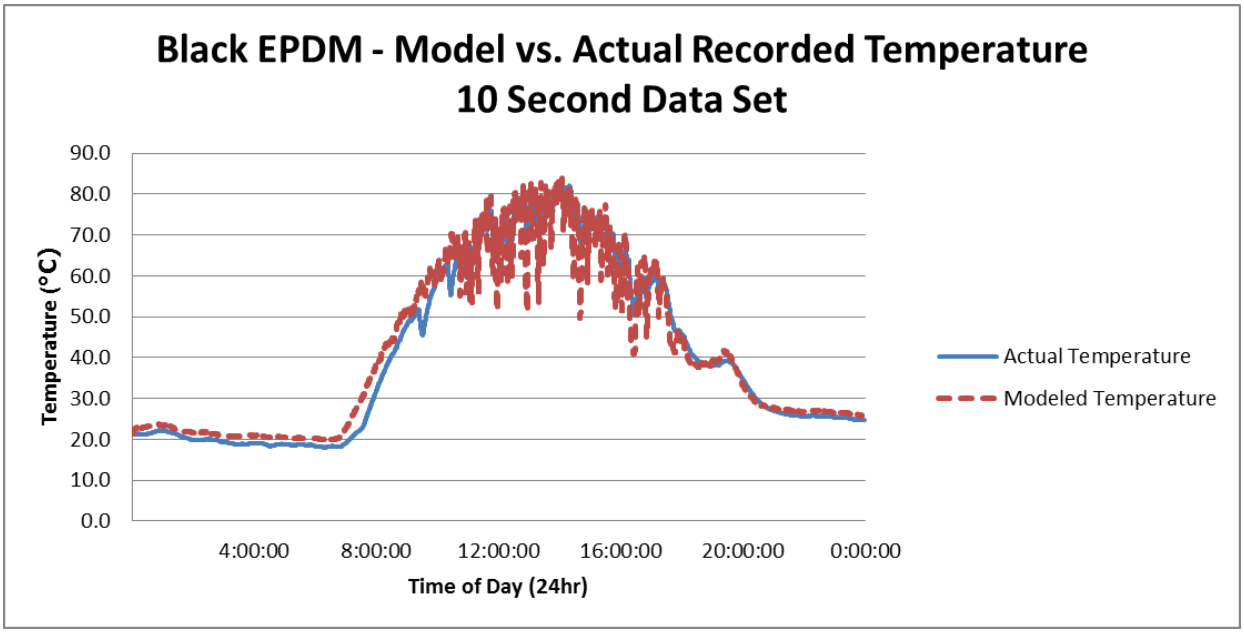
Black EPDM - Model vs. Actual Recorded Temperature
10 Second Data Set
90.0
80.0
70.0
60.0
50.0
40.0
30.0
20.0
10.0
0.0
Temperature (°C)
4:00:00
8:00:00
12:00:00
16:00:00
20:00:00
0:00:00
Time of Day (24hr)
Actual Temperature
Modeled Temperature

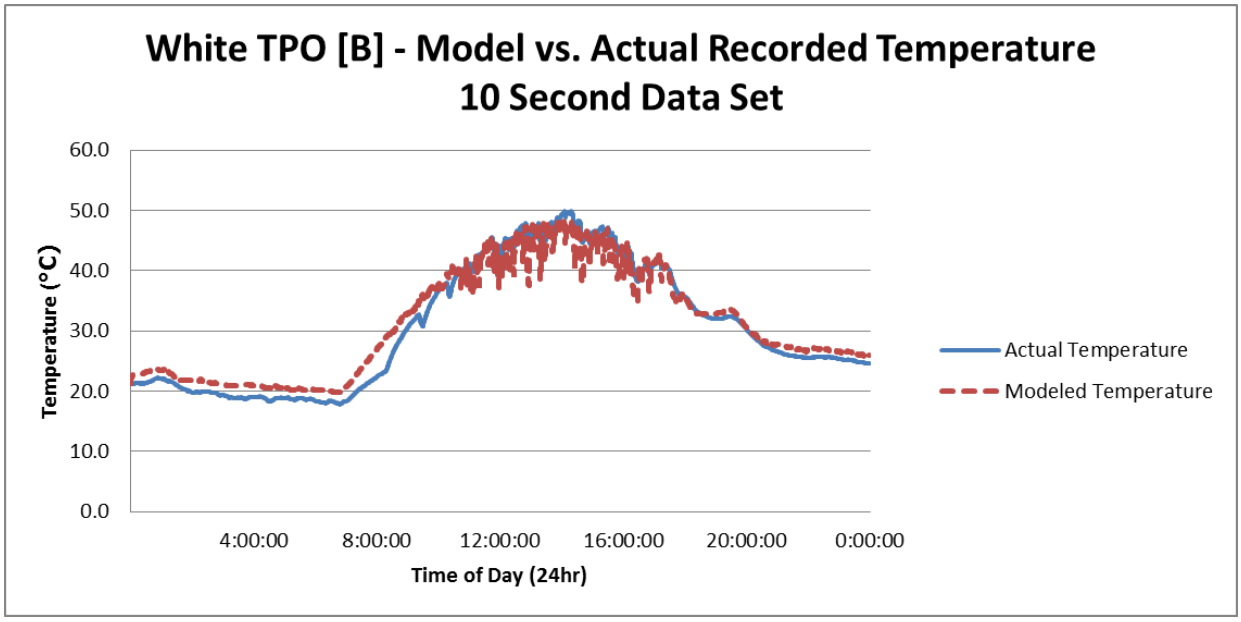
White TPO [B] - Model vs. Actual Recorded Temperature
10 Second Data Set
Temperature (°C)
60.0
50.0
40.0
30.0
20.0
10.0
0.0
4:00:00
8:00:00
12:00:00
16:00:00
20:00:00
0:00:00
Time of Day (24hr)
Actual Temperature
Modeled Temperature

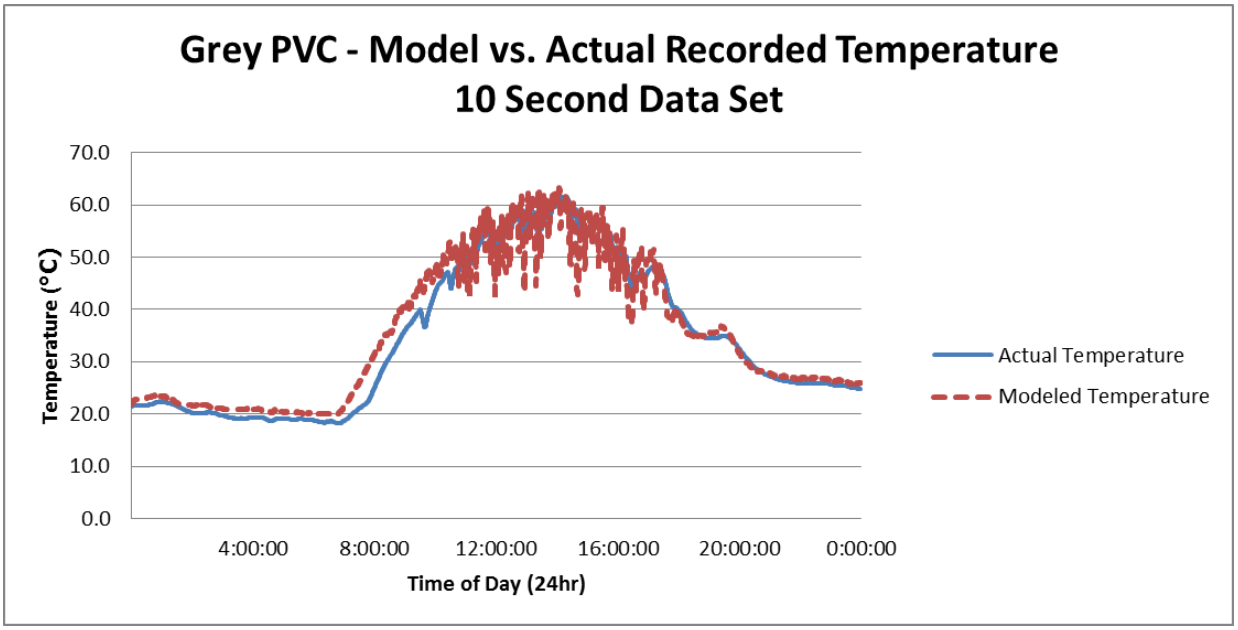
Grey PVC - Model vs. Actual Recorded Temperature
10 Second Data Set
Temperature (°C)
70.0
60.0
50.0
40.0
30.0
20.0
10.0
0.0
4:00:00
8:00:00
12:00:00
16:00:00
20:00:00
0:00:00
Time of Day (24hr)
Actual Temperature
Modeled Temperature

August 8, 2010

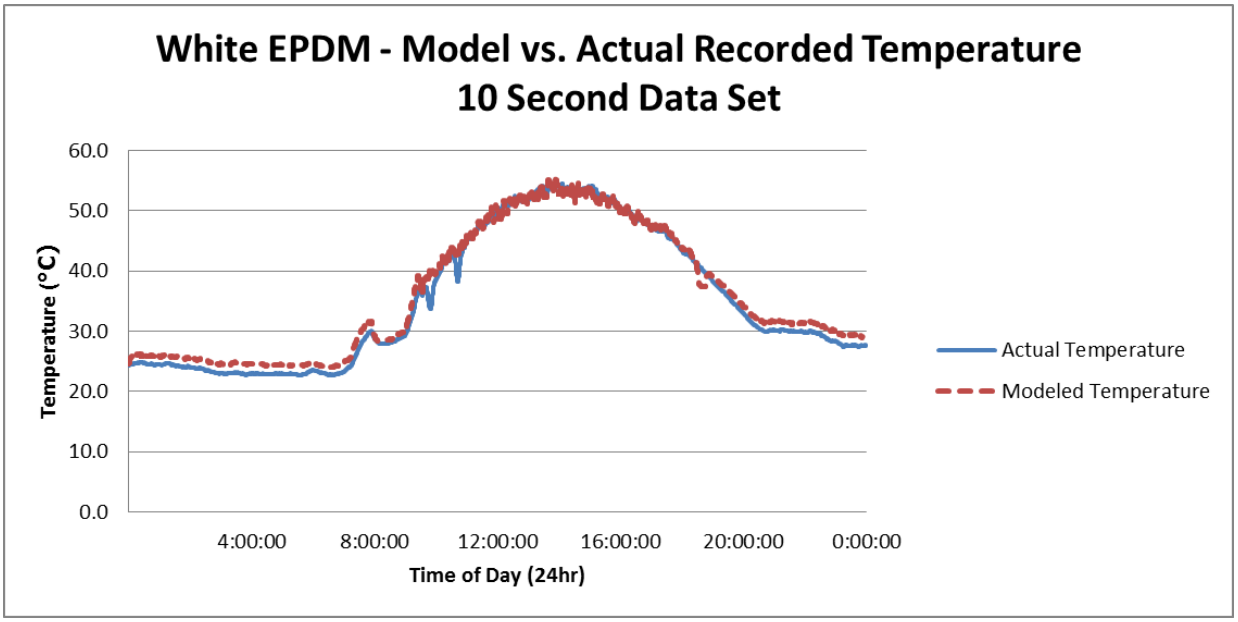
White EPDM - Model vs. Actual Recorded Temperature
10 Second Data Set
60.0
50.0
40.0
30.0
20.0
10.0
0.0
Temperature (°C)
4:00:00
8:00:00
12:00:00
16:00:00
20:00:00
0:00:00
Time of Day (24hr)
Actual Temperature
Modeled Temperature

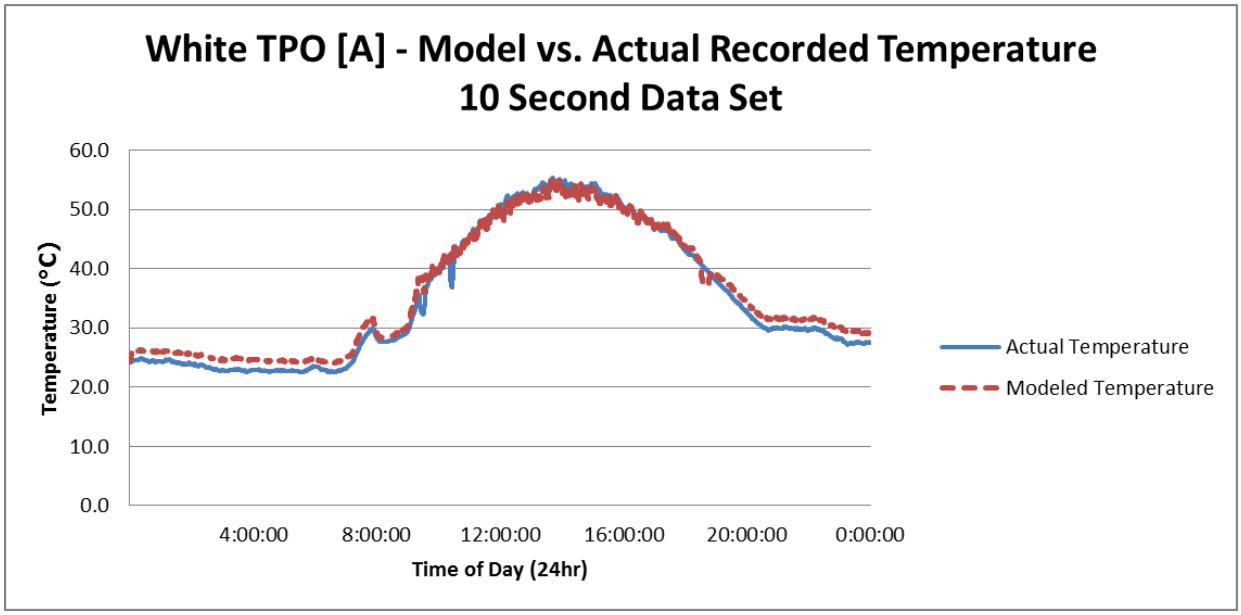
White TPO [A] - Model vs. Actual Recorded Temperature
10 Second Data Set
60.0
50.0
40.0
30.0
20.0
10.0
0.0
Temperature (°C)
4:00:00
8:00:00
12:00:00
16:00:00
20:00:00
0:00:00
Time of Day (24hr)
Actual Temperature
Modeled Temperature

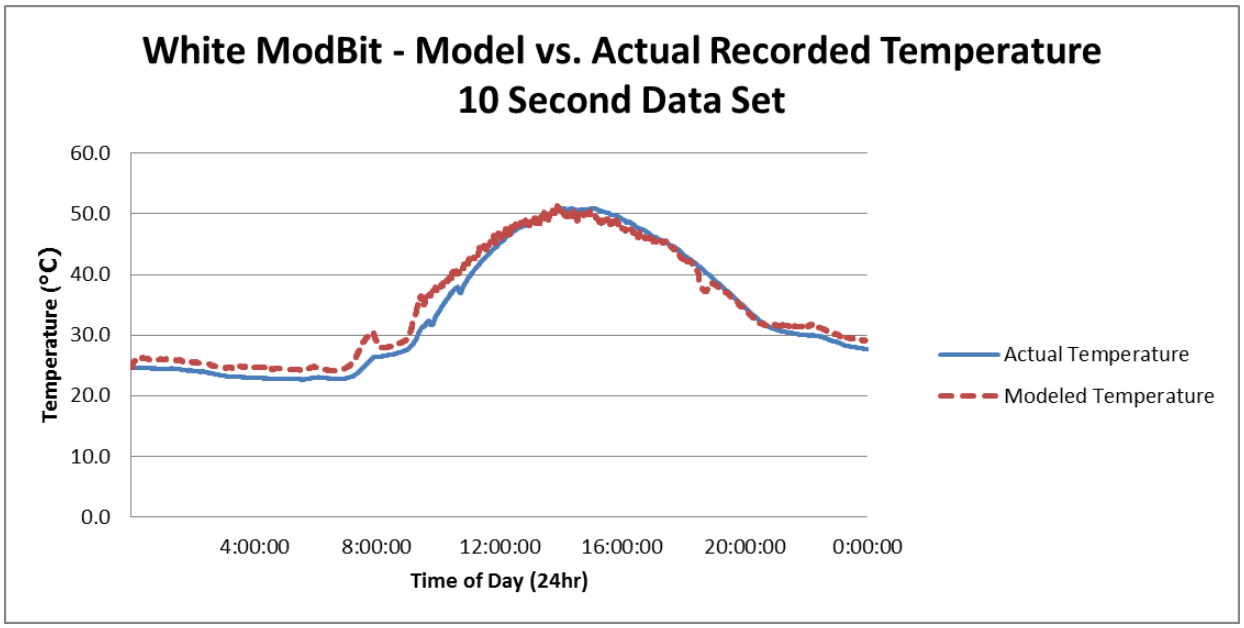
White ModBit - Model vs. Actual Recorded Temperature
10 Second Data Set
60.0
50.0
40.0
30.0
20.0
10.0
0.0
Temperature (°C)
4:00:00
8:00:00
12:00:00
16:00:00
20:00:00
0:00:00
Time of Day (24hr)
Actual Temperature
Modeled Temperature

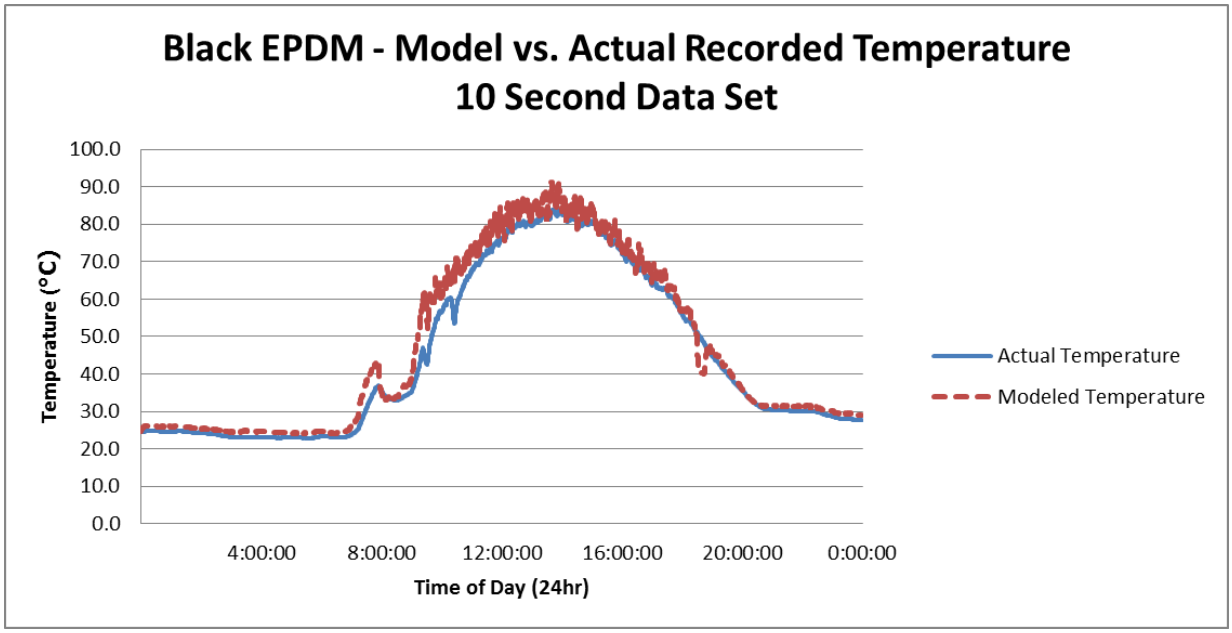
Black EPDM - Model vs. Actual Recorded Temperature
10 Second Data Set
100.0
90.0
80.0
70.0
60.0
50.0
40.0
30.0
20.0
10.0
0.0
Temperature (°C)
4:00:00
8:00:00
12:00:00
16:00:00
20:00:00
0:00:00
Time of Day (24hr)
Actual Temperature
Modeled Temperature

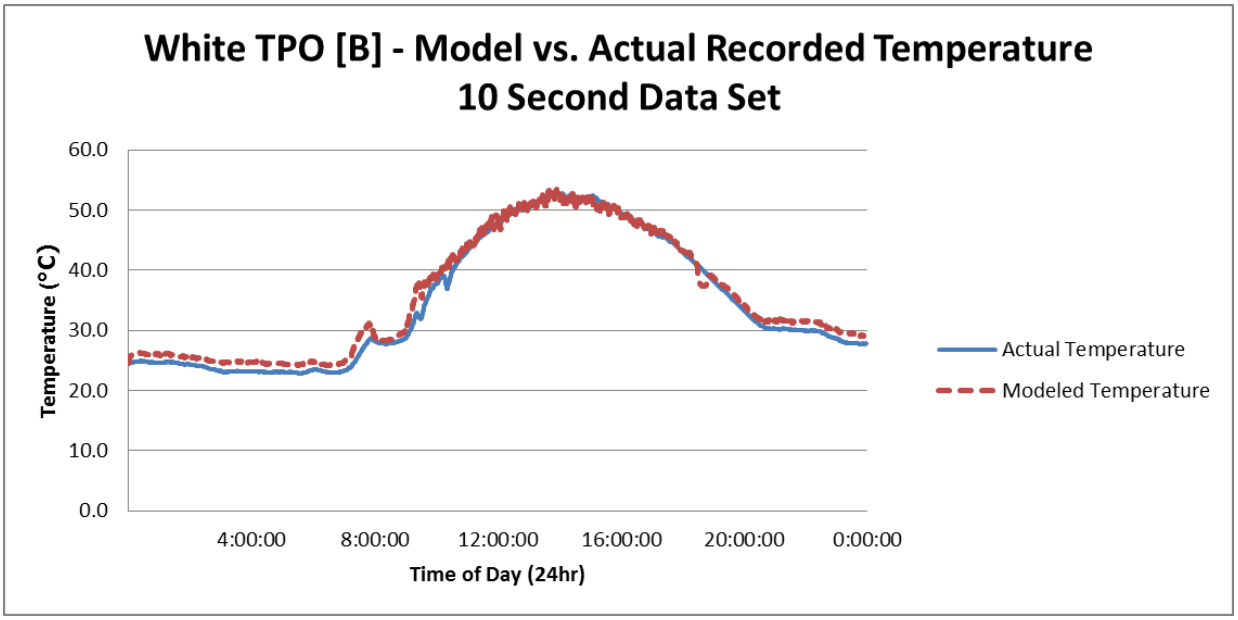
White TPO [B] - Model vs. Actual Recorded Temperature
10 Second Data Set
Temperature (°C)
60.0
50.0
40.0
30.0
20.0
10.0
0.0
4:00:00
8:00:00
12:00:00
16:00:00
20:00:00
0:00:00
Time of Day (24hr)
Actual Temperature
Modeled Temperature

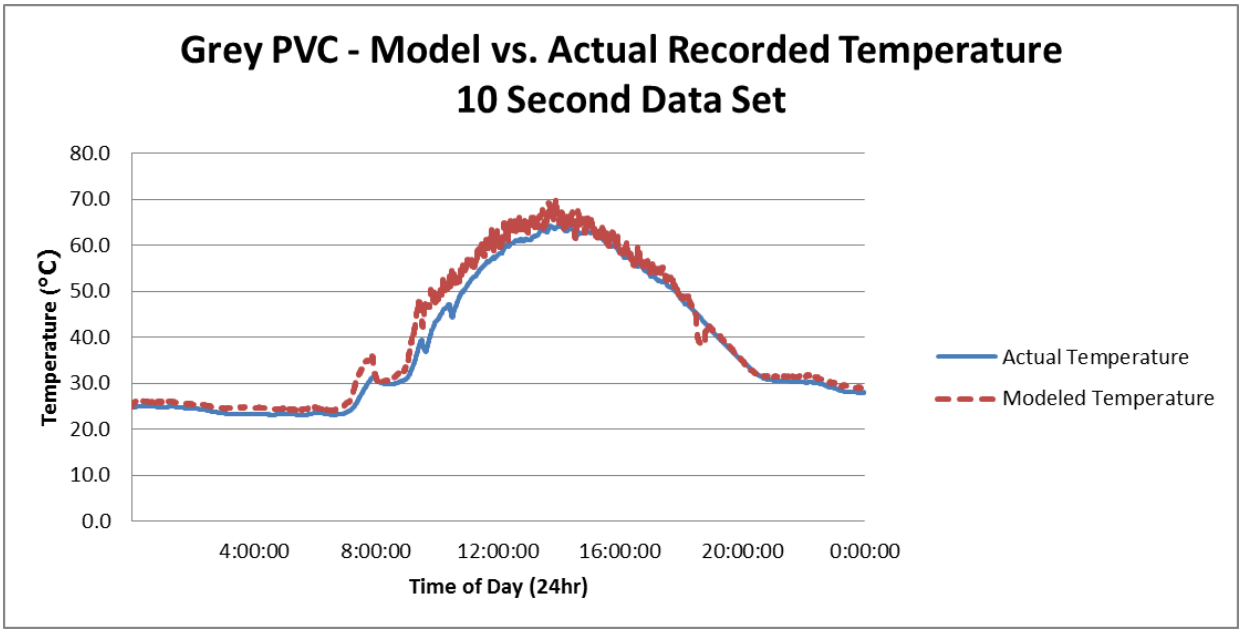
Grey PVC - Model vs. Actual Recorded Temperature
10 Second Data Set
Temperature (°C)
80.0
70.0
60.0
50.0
40.0
30.0
20.0
10.0
0.0
4:00:00
8:00:00
12:00:00
16:00:00
20:00:00
0:00:00
Time of Day (24hr)
Actual Temperature
Modeled Temperature

August 9, 2010

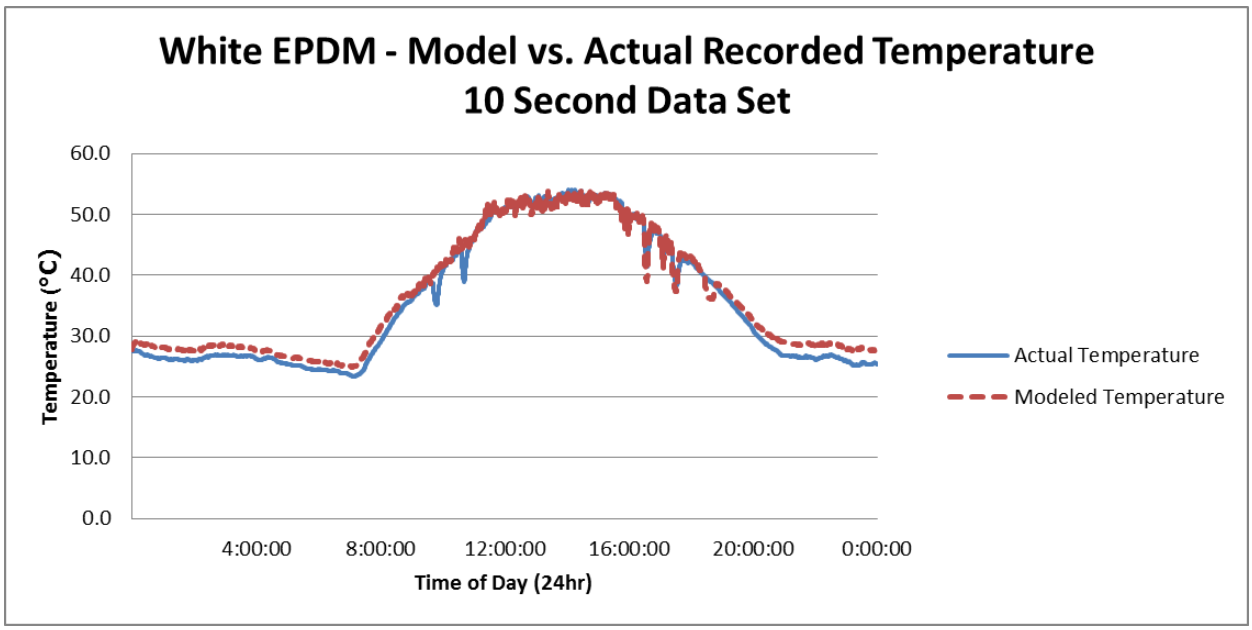
White EPDM - Model vs. Actual Recorded Temperature
10 Second Data Set
Temperature (°C)
60.0
50.0
40.0
30.0
20.0
10.0
0.0
4:00:00
8:00:00
12:00:00
16:00:00
20:00:00
0:00:00
Time of Day (24hr)
Actual Temperature
Modeled Temperature

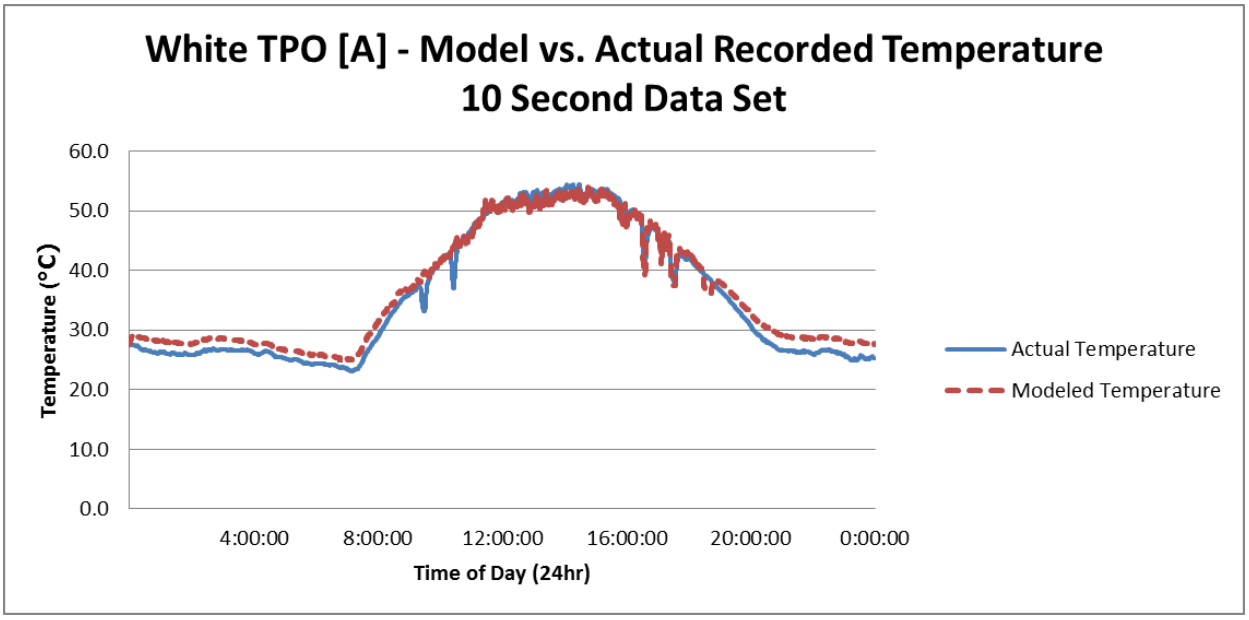
White TPO [A] - Model vs. Actual Recorded Temperature
10 Second Data Set
Temperature (°C)
60.0
50.0
40.0
30.0
20.0
10.0
0.0
4:00:00
8:00:00
12:00:00
16:00:00
20:00:00
0:00:00
Time of Day (24hr)
Actual Temperature
Modeled Temperature

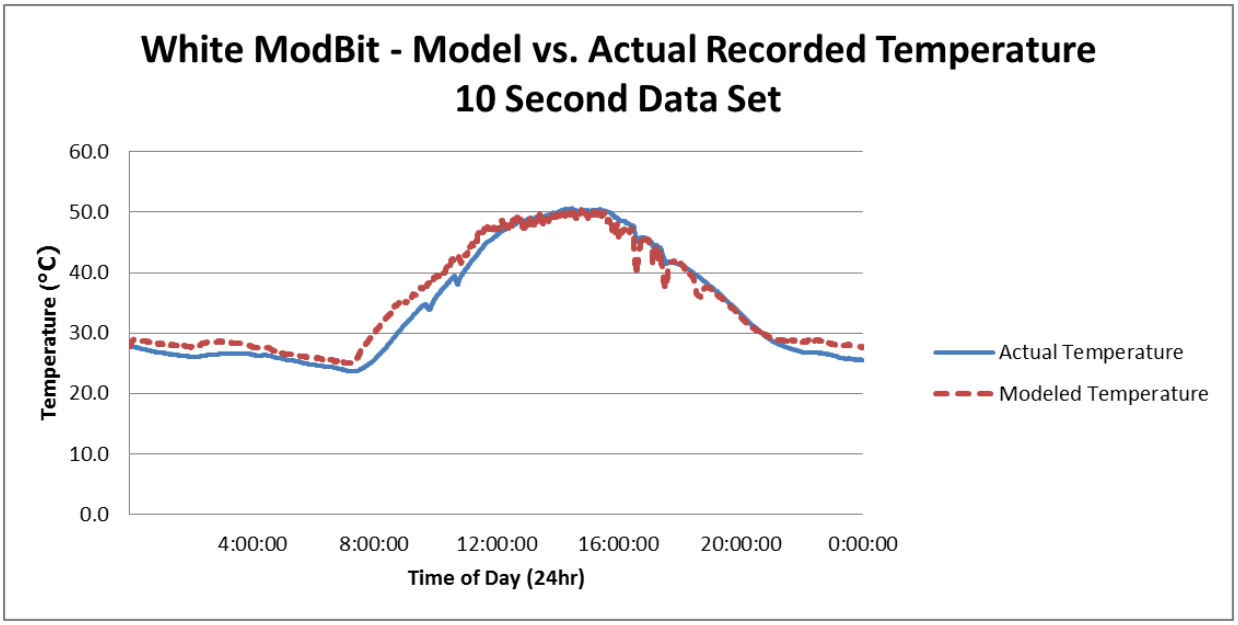
White ModBit - Model vs. Actual Recorded Temperature
10 Second Data Set
Temperature (°C)
60.0
50.0
40.0
30.0
20.0
10.0
0.0
4:00:00
8:00:00
12:00:00
16:00:00
20:00:00
0:00:00
Time of Day (24hr)
Actual Temperature
Modeled Temperature

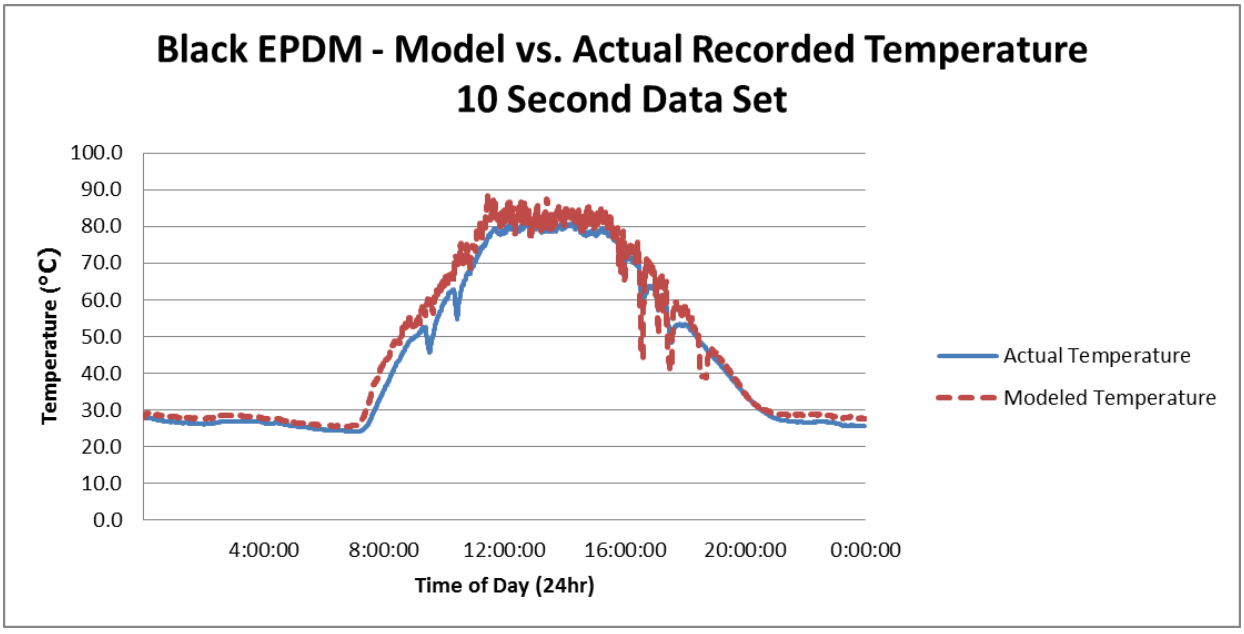
Black EPDM - Model vs. Actual Recorded Temperature
10 Second Data Set
Temperature (°C)
100.0
90.0
80.0
70.0
60.0
50.0
40.0
30.0
20.0
10.0
0.0
4:00:00
8:00:00
12:00:00
16:00:00
20:00:00
0:00:00
Time of Day (24hr)
Actual Temperature
Modeled Temperature

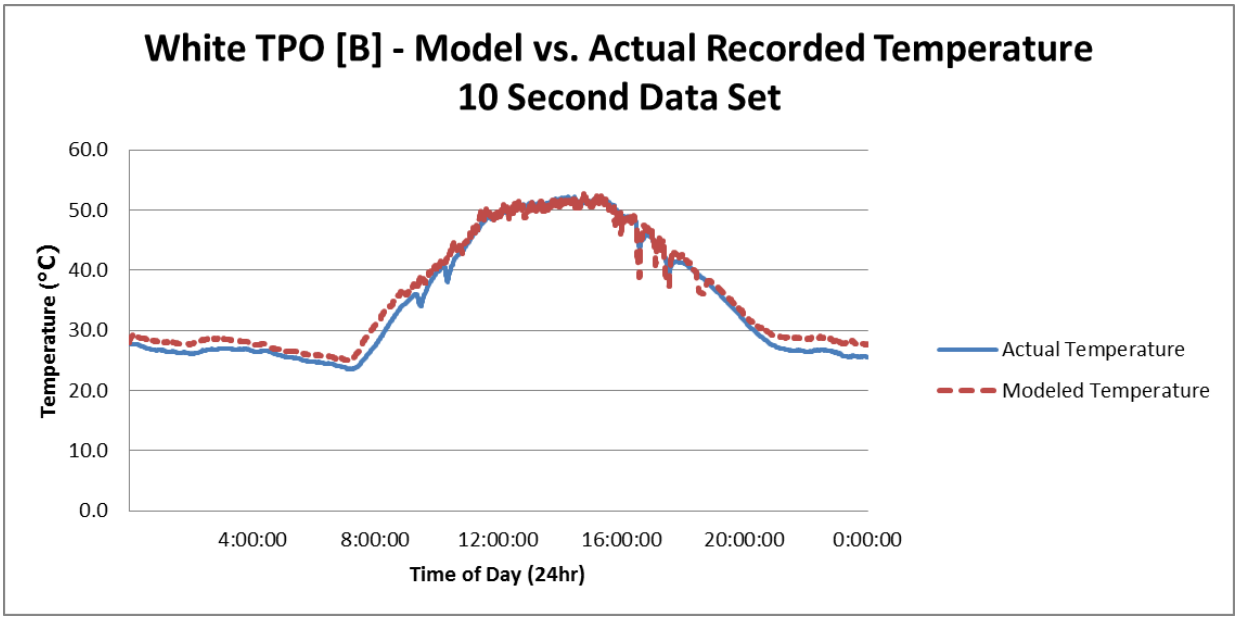
White TPO [B] - Model vs. Actual Recorded Temperature
10 Second Data Set
Temperature (°C)
60.0
50.0
40.0
30.0
20.0
10.0
0.0
4:00:00
8:00:00
12:00:00
16:00:00
20:00:00
0:00:00
Time of Day (24hr)
Actual Temperature
Modeled Temperature

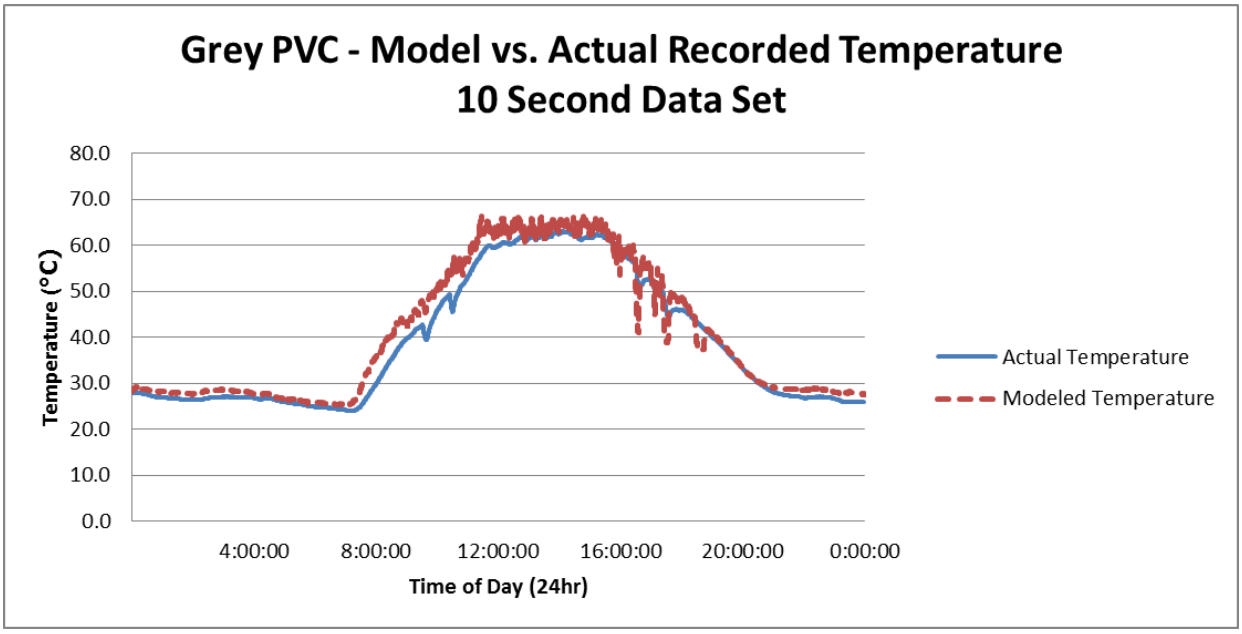
Grey PVC - Model vs. Actual Recorded Temperature
10 Second Data Set
Temperature (°C)
80.0
70.0
60.0
50.0
40.0
30.0
20.0
10.0
0.0
4:00:00
8:00:00
12:00:00
16:00:00
20:00:00
0:00:00
Time of Day (24hr)
Actual Temperature
Modeled Temperature

August 10, 2010

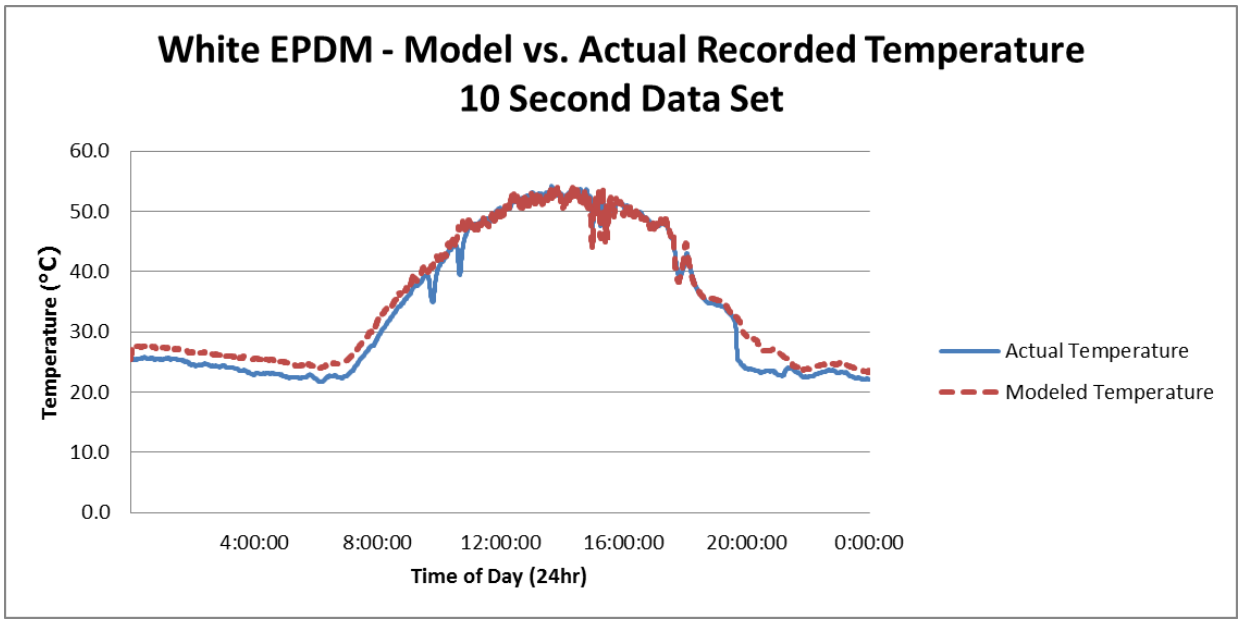
White EPDM - Model vs. Actual Recorded Temperature
10 Second Data Set
60.0
50.0
40.0
30.0
20.0
10.0
0.0
Temperature (°C)
4:00:00
8:00:00
12:00:00
16:00:00
20:00:00
0:00:00
Time of Day (24hr)
Actual Temperature
Modeled Temperature

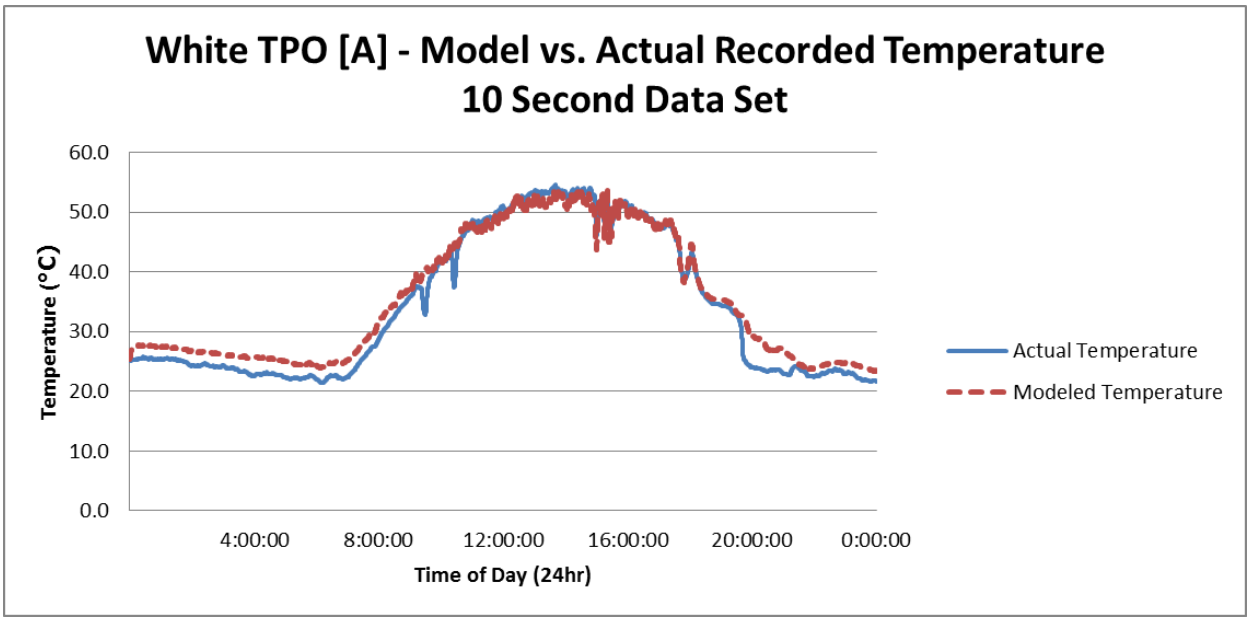
White TPO [A] - Model vs. Actual Recorded Temperature
10 Second Data Set
60.0
50.0
40.0
30.0
20.0
10.0
0.0
Temperature (°C)
4:00:00
8:00:00
12:00:00
16:00:00
20:00:00
0:00:00
Time of Day (24hr)
Actual Temperature
Modeled Temperature

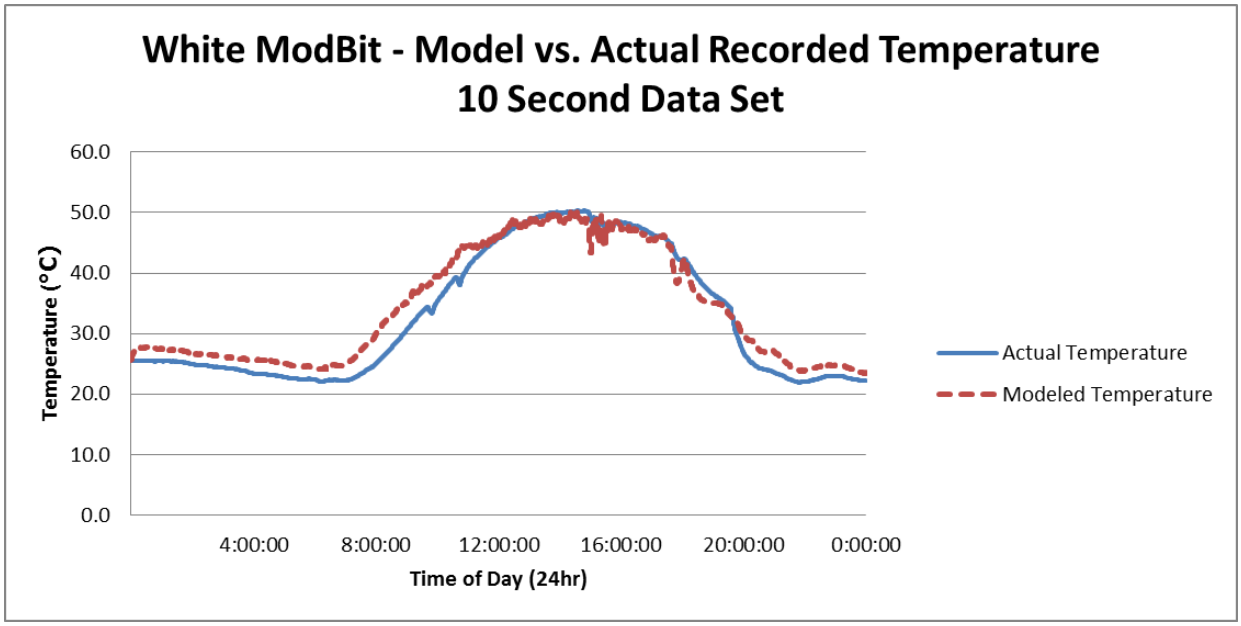
White ModBit - Model vs. Actual Recorded Temperature
10 Second Data Set
Temperature (°C)
60.0
50.0
40.0
30.0
20.0
10.0
0.0
4:00:00
8:00:00
12:00:00
16:00:00
20:00:00
0:00:00
Time of Day (24hr)
Actual Temperature
Modeled Temperature

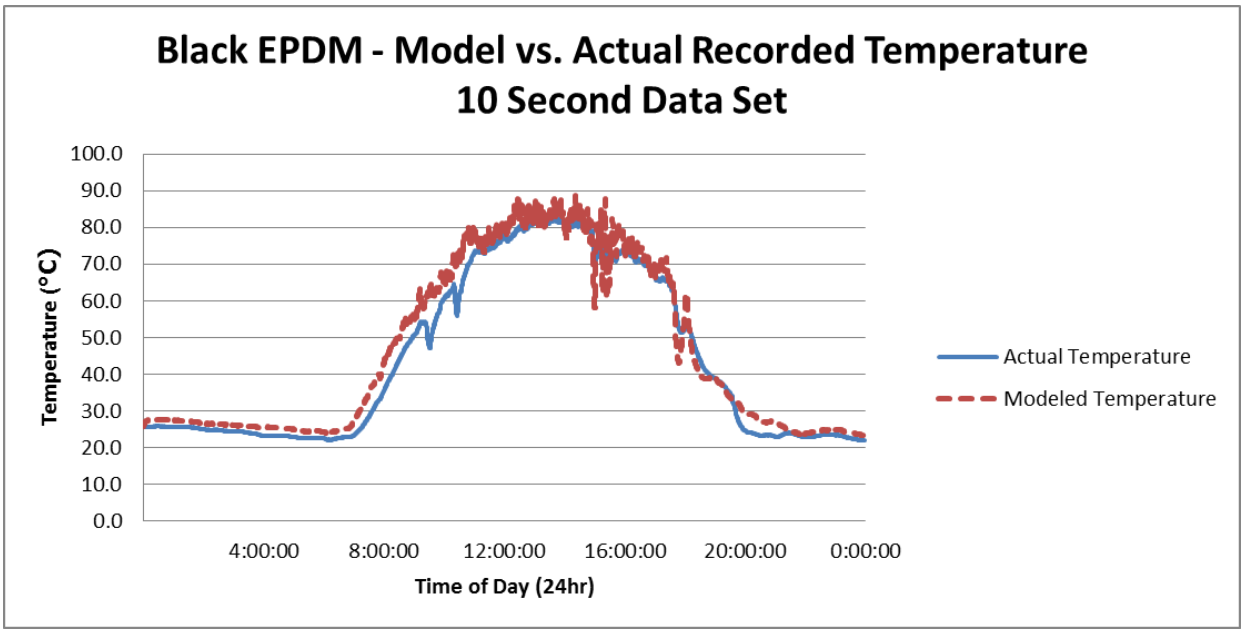
Black EPDM - Model vs. Actual Recorded Temperature
10 Second Data Set
Temperature (°C)
100.0
90.0
80.0
70.0
60.0
50.0
40.0
30.0
20.0
10.0
0.0
4:00:00
8:00:00
12:00:00
16:00:00
20:00:00
0:00:00
Time of Day (24hr)
Actual Temperature
Modeled Temperature

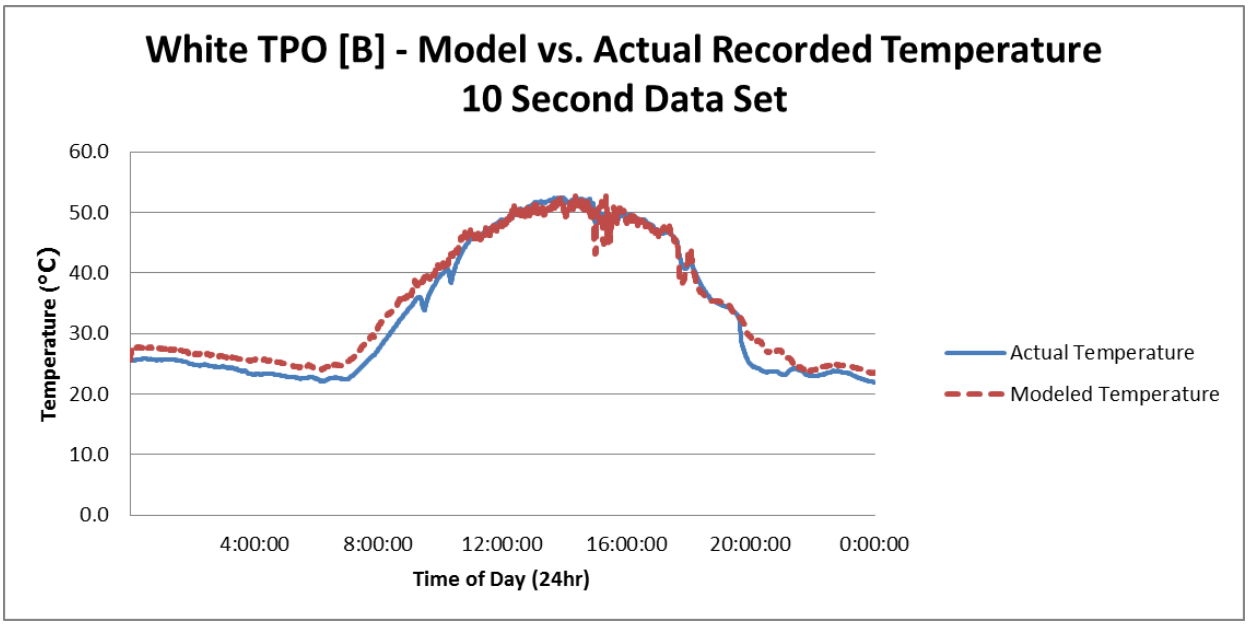
White TPO [B] - Model vs. Actual Recorded Temperature
10 Second Data Set
Temperature (°C)
60.0
50.0
40.0
30.0
20.0
10.0
0.0
4:00:00
8:00:00
12:00:00
16:00:00
20:00:00
0:00:00
Time of Day (24hr)
Actual Temperature
Modeled Temperature

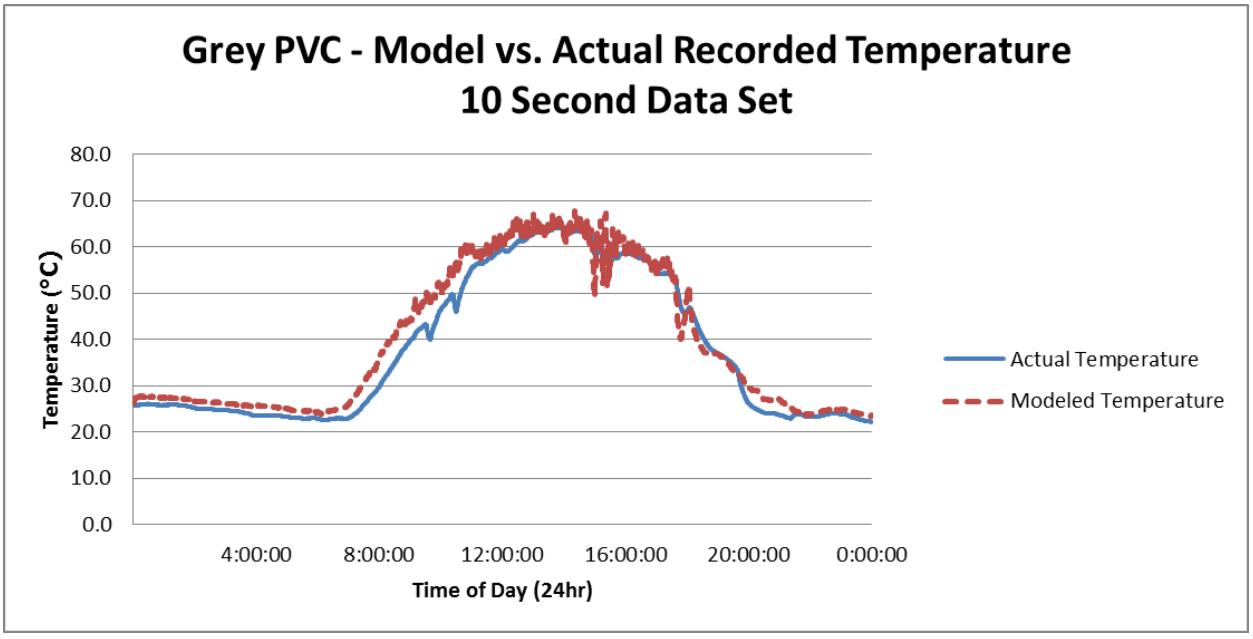
Grey PVC - Model vs. Actual Recorded Temperature
10 Second Data Set
Temperature (°C)
80.0
70.0
60.0
50.0
40.0
30.0
20.0
10.0
0.0
4:00:00
8:00:00
12:00:00
16:00:00
20:00:00
0:00:00
Time of Day (24hr)
Actual Temperature
Modeled Temperature

August 11, 2010

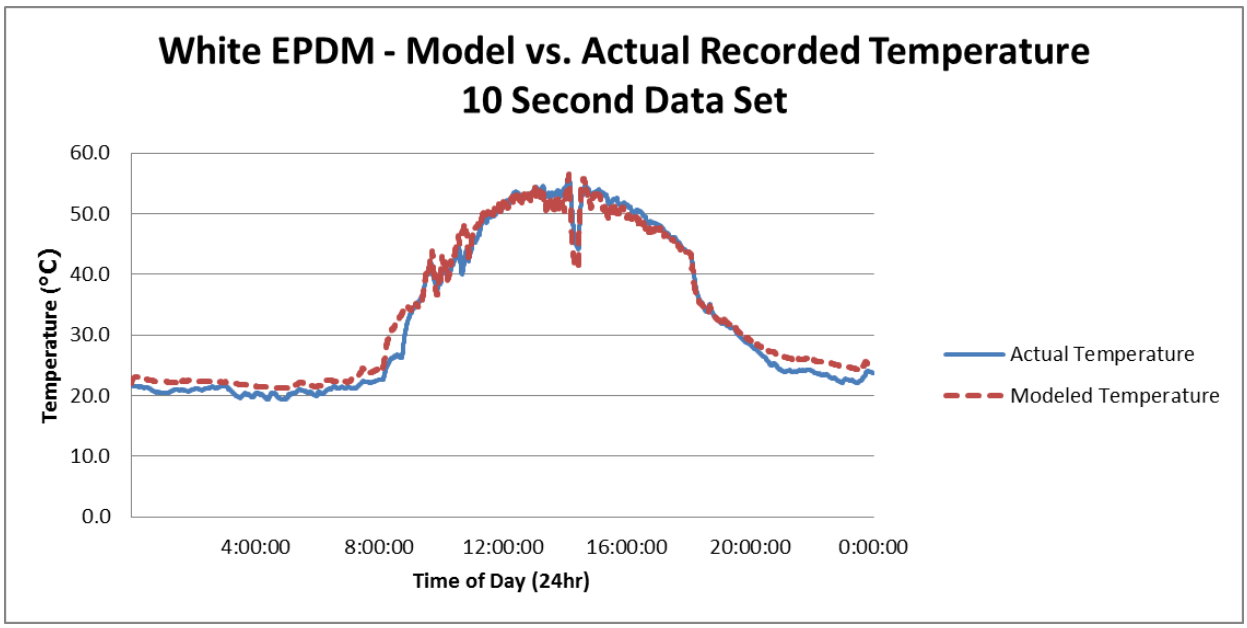
White EPDM - Model vs. Actual Recorded Temperature
10 Second Data Set
60.0
50.0
40.0
30.0
20.0
10.0
0.0
Temperature (°C)
4:00:00
8:00:00
12:00:00
16:00:00
20:00:00
0:00:00
Time of Day (24hr)
Actual Temperature
Modeled Temperature

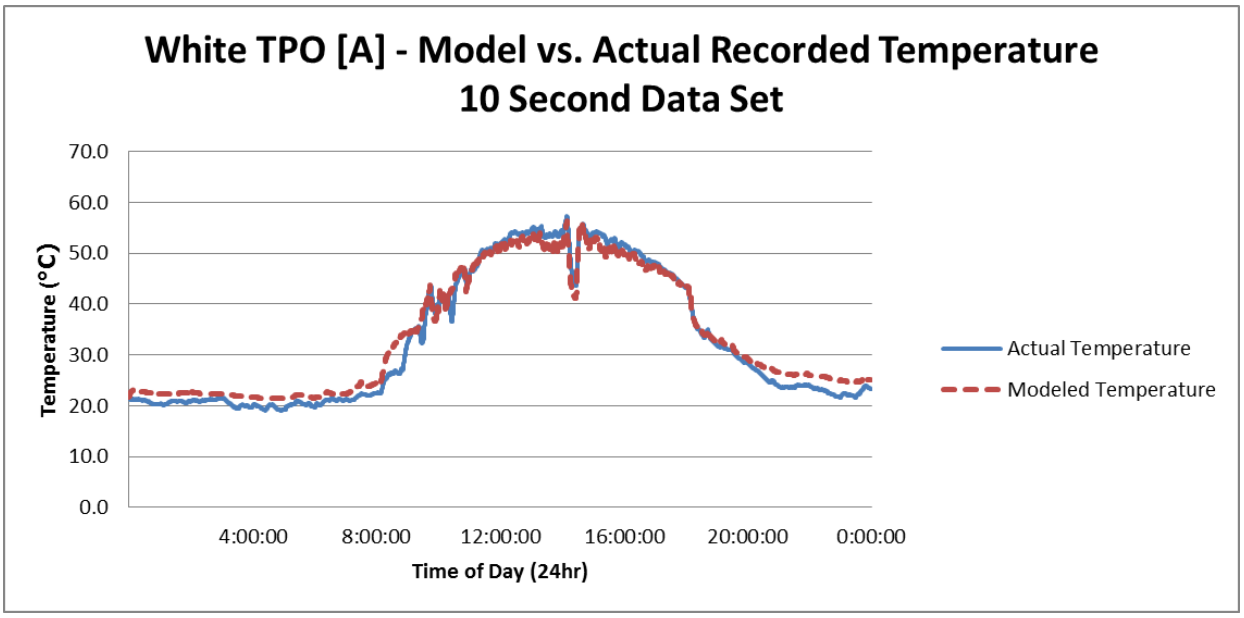
White TPO [A] - Model vs. Actual Recorded Temperature
10 Second Data Set
70.0
60.0
50.0
40.0
30.0
20.0
10.0
0.0
Temperature (°C)
4:00:00
8:00:00
12:00:00
16:00:00
20:00:00
0:00:00
Time of Day (24hr)
Actual Temperature
Modeled Temperature

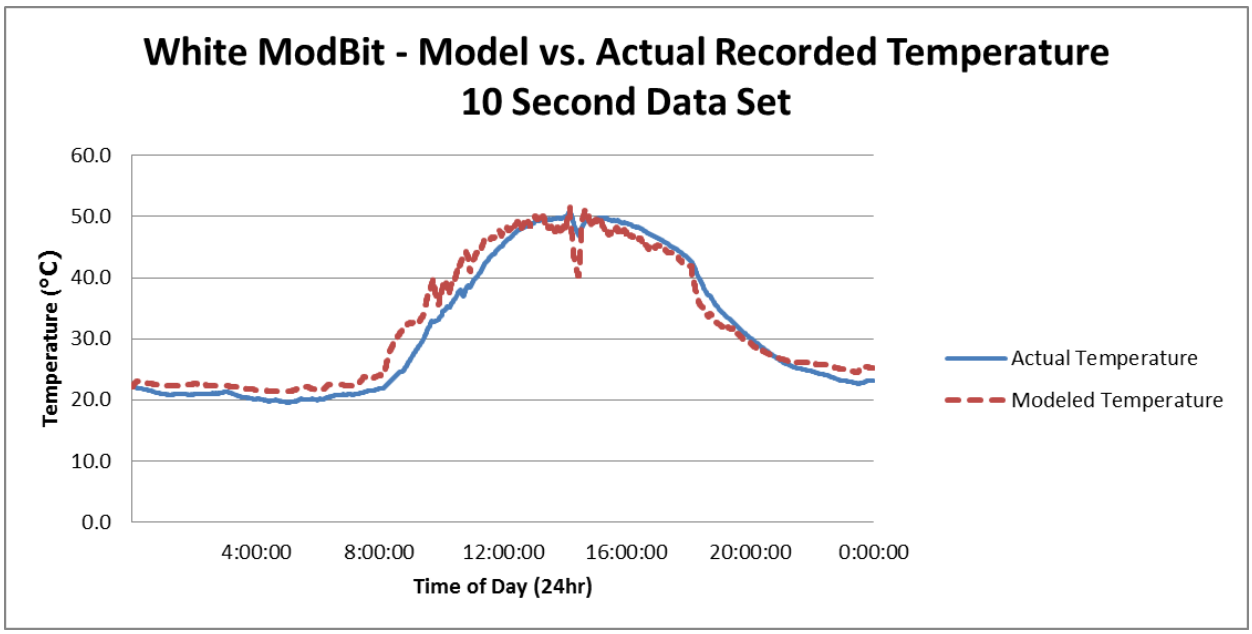
White ModBit - Model vs. Actual Recorded Temperature
10 Second Data Set
Temperature (°C)
60.0
50.0
40.0
30.0
20.0
10.0
0.0
4:00:00
8:00:00
12:00:00
16:00:00
20:00:00
0:00:00
Time of Day (24hr)
Actual Temperature
Modeled Temperature

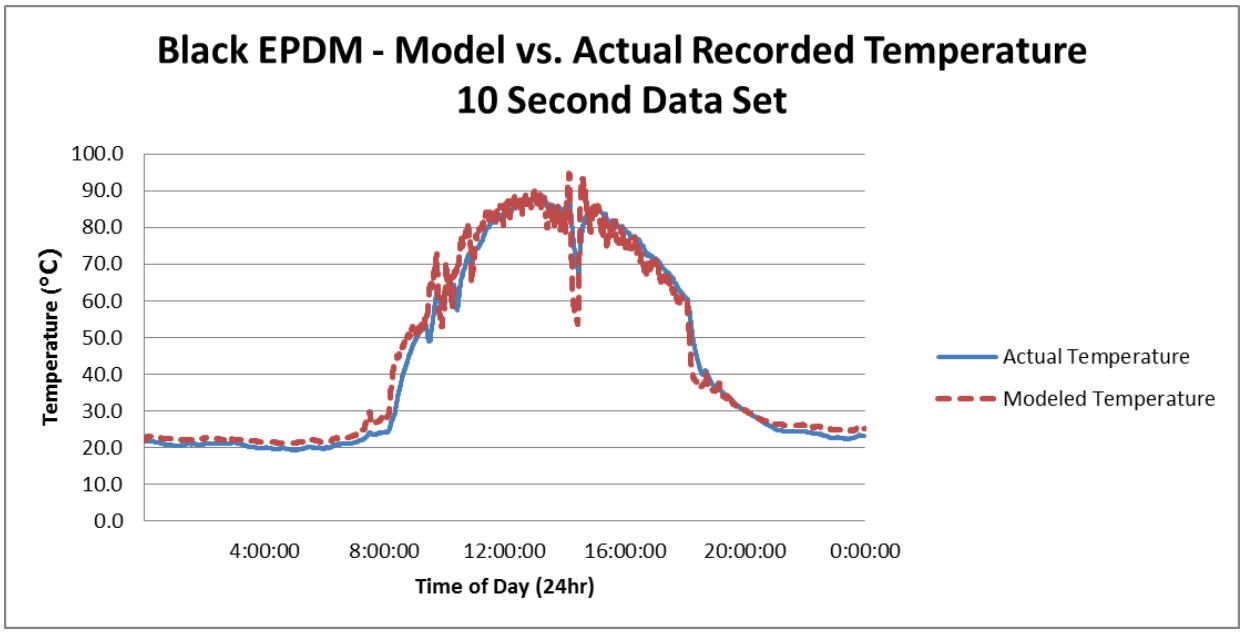
Black EPDM - Model vs. Actual Recorded Temperature
10 Second Data Set
Temperature (°C)
100.0
90.0
80.0
70.0
60.0
50.0
40.0
30.0
20.0
10.0
0.0
4:00:00
8:00:00
12:00:00
16:00:00
20:00:00
0:00:00
Time of Day (24hr)
Actual Temperature
Modeled Temperature

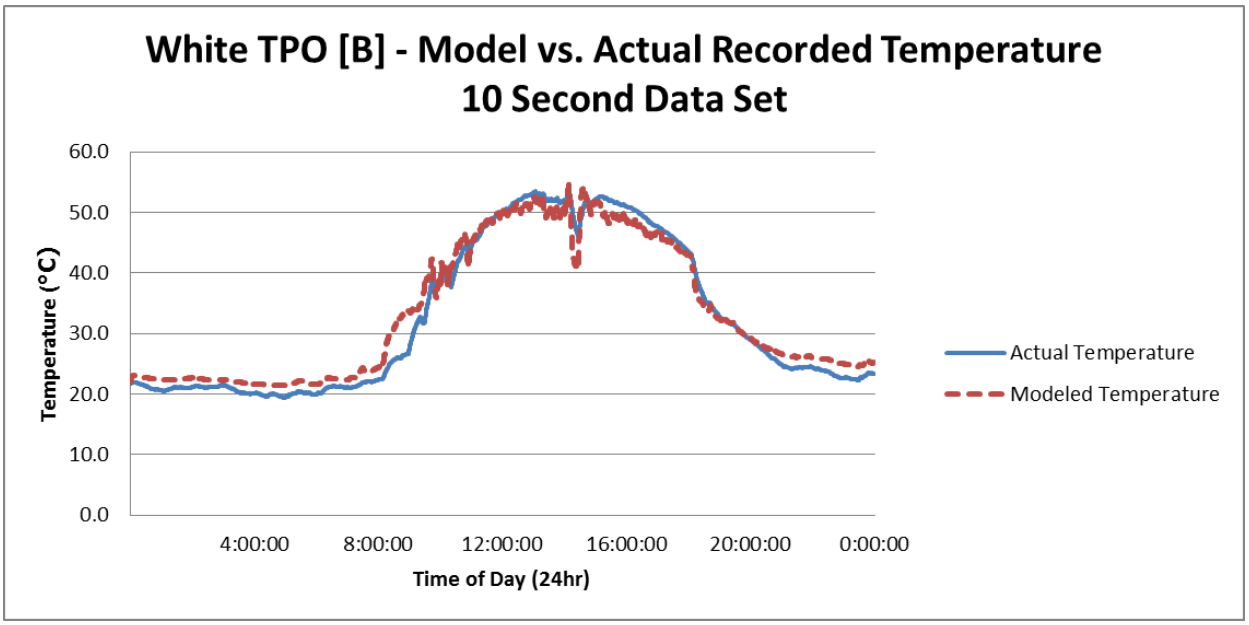
White TPO [B] - Model vs. Actual Recorded Temperature
10 Second Data Set
Temperature (°C)
60.0
50.0
40.0
30.0
20.0
10.0
0.0
4:00:00
8:00:00
12:00:00
16:00:00
20:00:00
0:00:00
Time of Day (24hr)
Actual Temperature
Modeled Temperature

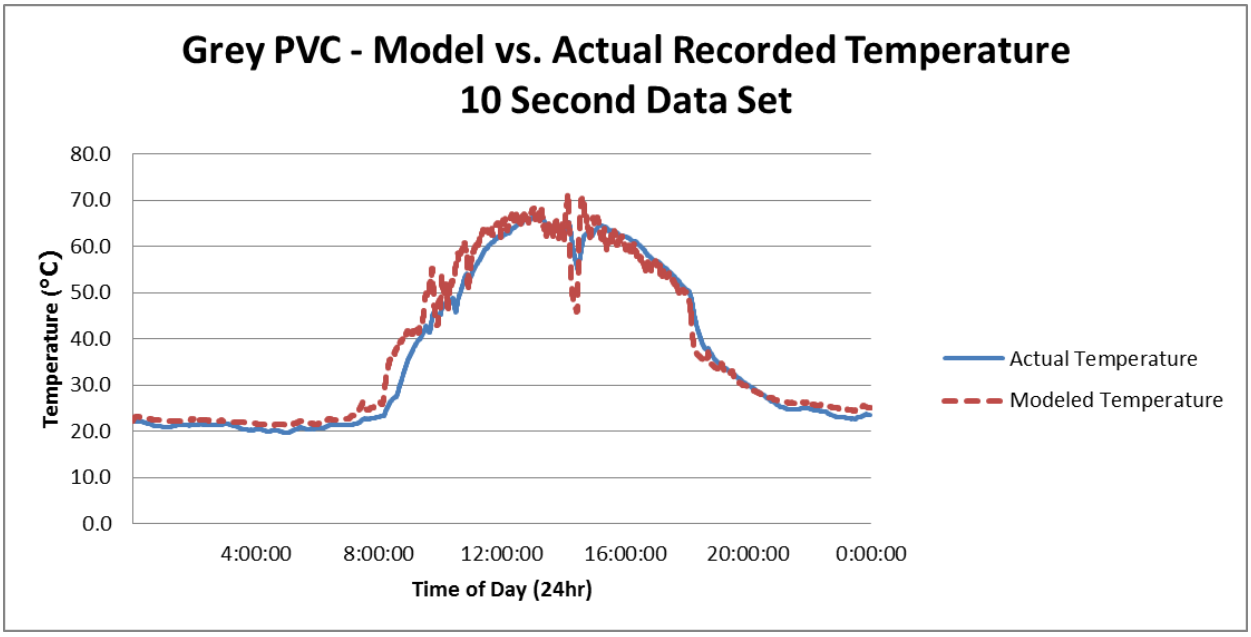
Grey PVC - Model vs. Actual Recorded Temperature
10 Second Data Set
Temperature (°C)
80.0
70.0
60.0
50.0
40.0
30.0
20.0
10.0
0.0
4:00:00
8:00:00
12:00:00
16:00:00
20:00:00
0:00:00
Time of Day (24hr)
Actual Temperature
Modeled Temperature

August 12, 2010

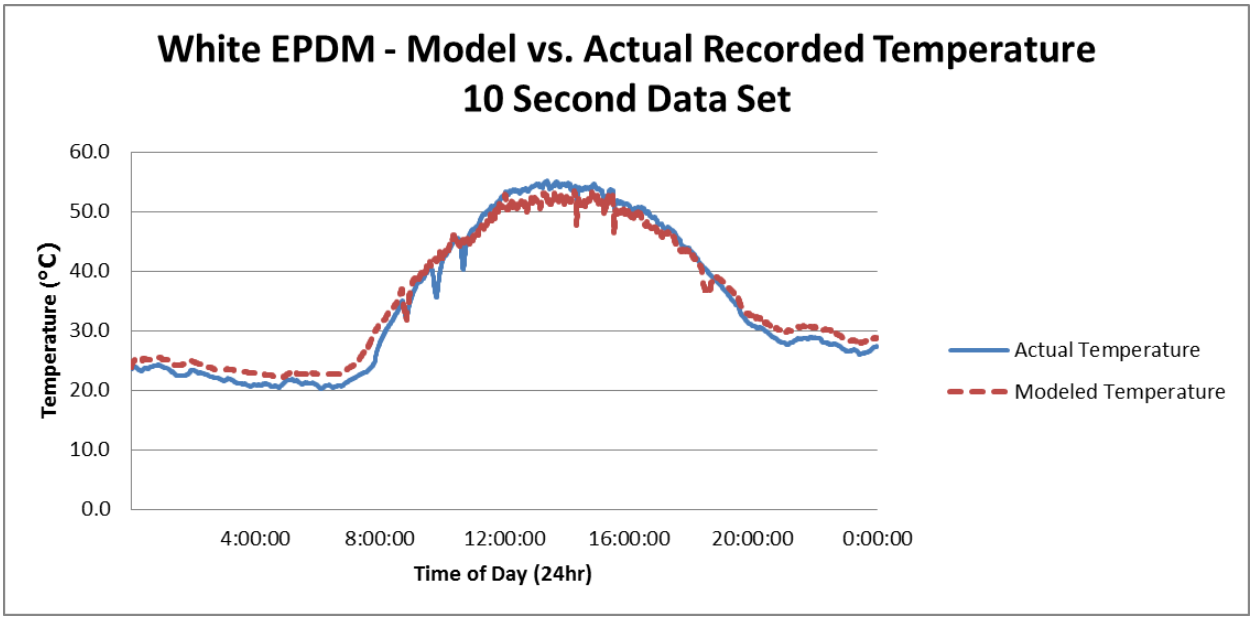
White EPDM - Model vs. Actual Recorded Temperature
10 Second Data Set
Temperature (°C)
60.0
50.0
40.0
30.0
20.0
10.0
0.0
4:00:00
8:00:00
12:00:00
16:00:00
20:00:00
0:00:00
Time of Day (24hr)
Actual Temperature
Modeled Temperature

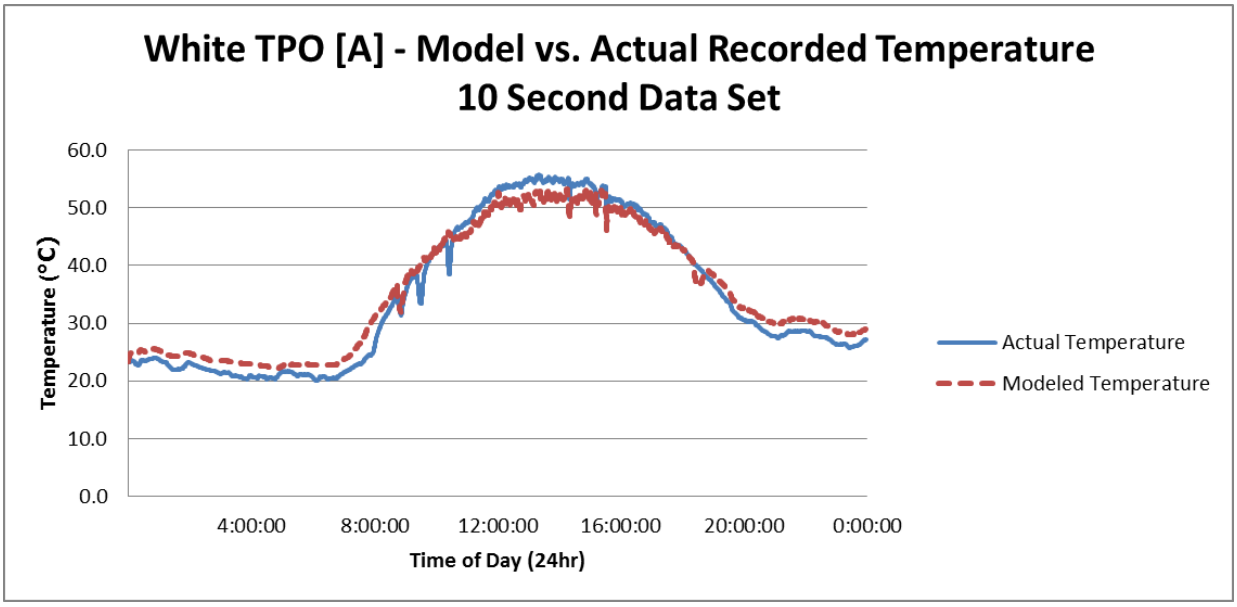
White TPO [A] - Model vs. Actual Recorded Temperature
10 Second Data Set
Temperature (°C)
60.0
50.0
40.0
30.0
20.0
10.0
0.0
4:00:00
8:00:00
12:00:00
16:00:00
20:00:00
0:00:00
Time of Day (24hr)
Actual Temperature
Modeled Temperature

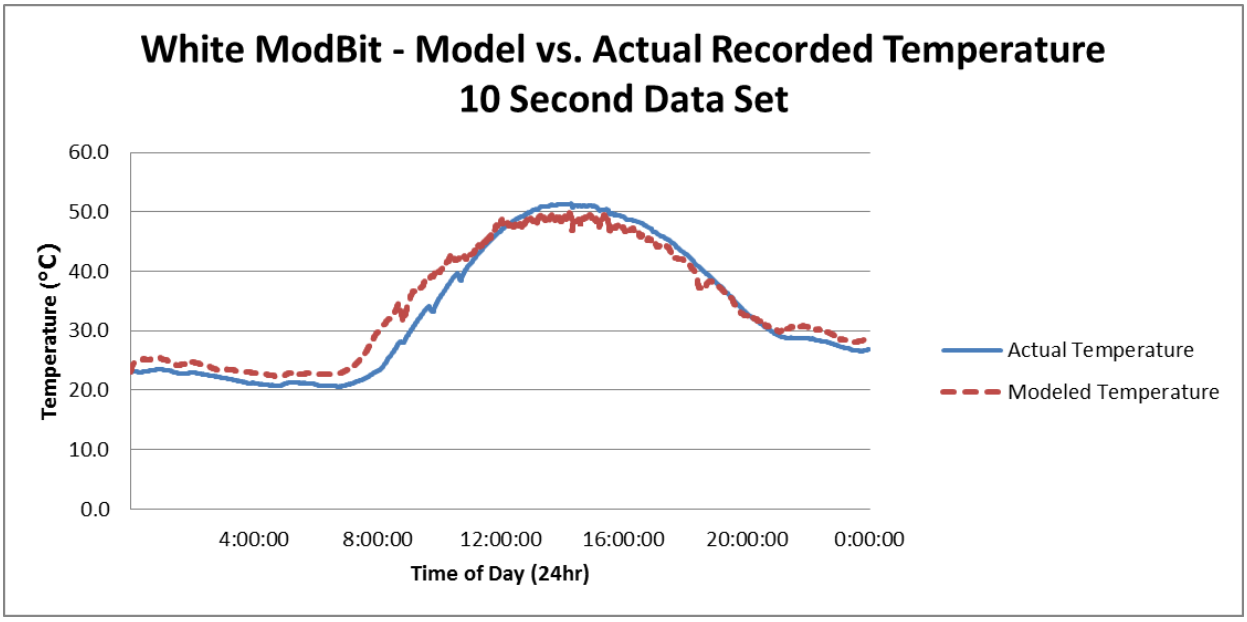
White ModBit - Model vs. Actual Recorded Temperature
10 Second Data Set
Temperature (°C)
60.0
50.0
40.0
30.0
20.0
10.0
0.0
4:00:00
8:00:00
12:00:00
16:00:00
20:00:00
0:00:00
Time of Day (24hr)
Actual Temperature
Modeled Temperature

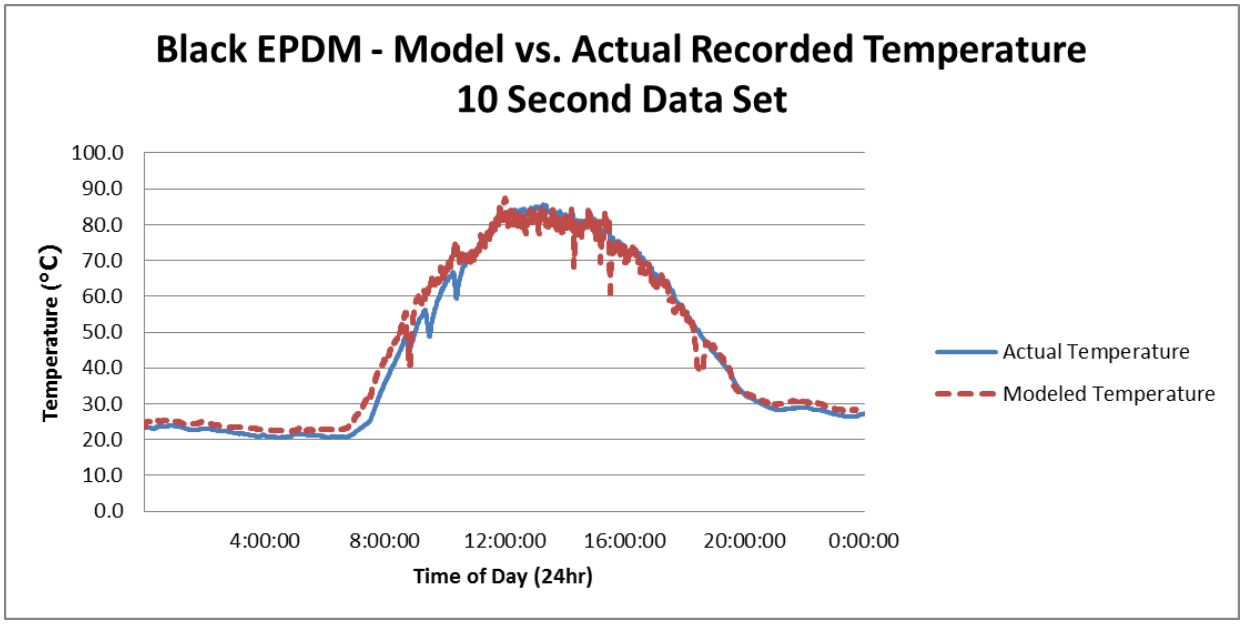
Black EPDM - Model vs. Actual Recorded Temperature
10 Second Data Set
Temperature (°C)
100.0
90.0
80.0
70.0
60.0
50.0
40.0
30.0
20.0
10.0
0.0
4:00:00
8:00:00
12:00:00
16:00:00
20:00:00
0:00:00
Time of Day (24hr)
Actual Temperature
Modeled Temperature

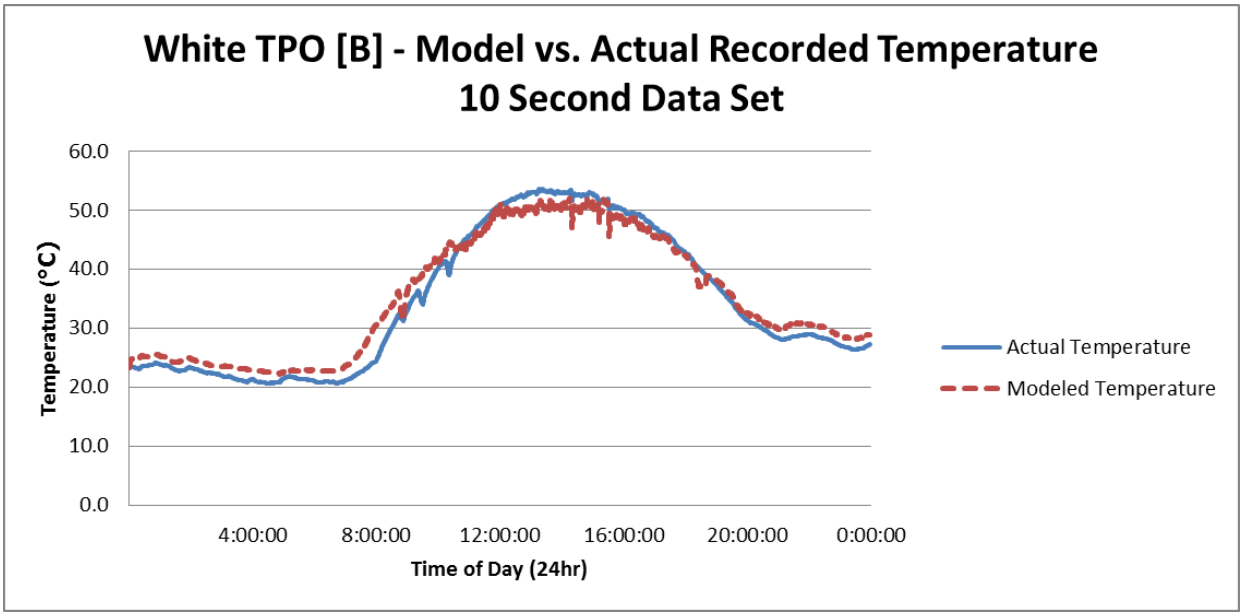
White TPO [B] - Model vs. Actual Recorded Temperature
10 Second Data Set
Temperature (°C)
60.0
50.0
40.0
30.0
20.0
10.0
0.0
4:00:00
8:00:00
12:00:00
16:00:00
20:00:00
0:00:00
Time of Day (24hr)
Actual Temperature
Modeled Temperature

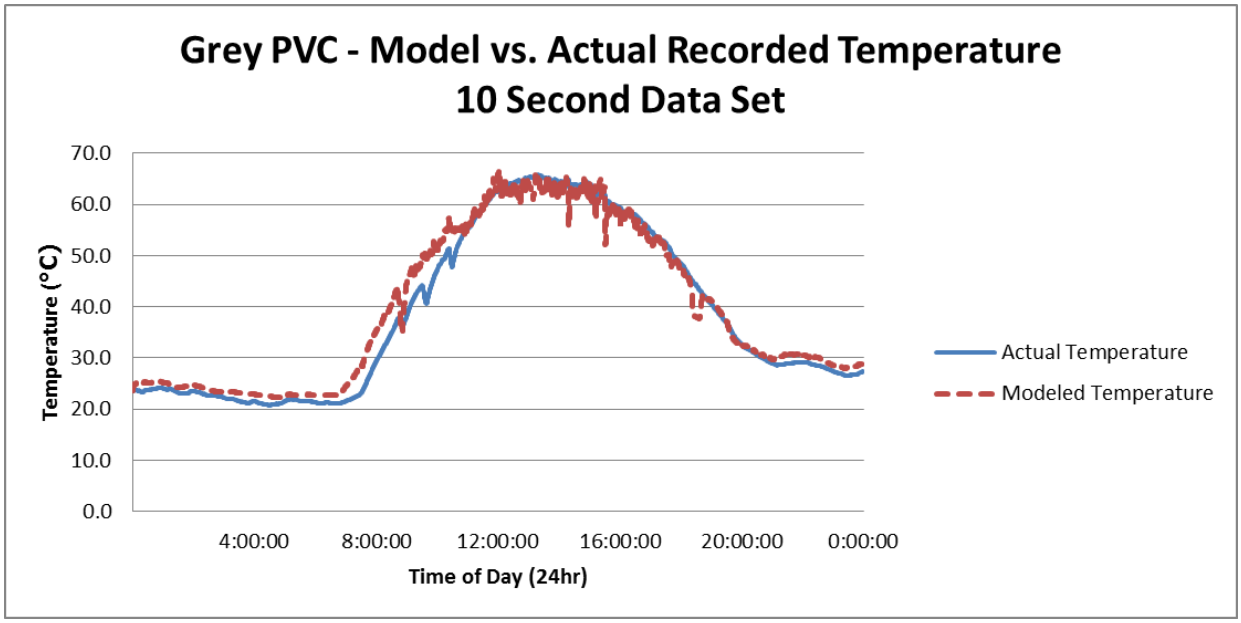
Grey PVC - Model vs. Actual Recorded Temperature
10 Second Data Set
Temperature (°C)
70.0
60.0
50.0
40.0
30.0
20.0
10.0
0.0
4:00:00
8:00:00
12:00:00
16:00:00
20:00:00
0:00:00
Time of Day (24hr)
Actual Temperature
Modeled Temperature

August 13, 2010

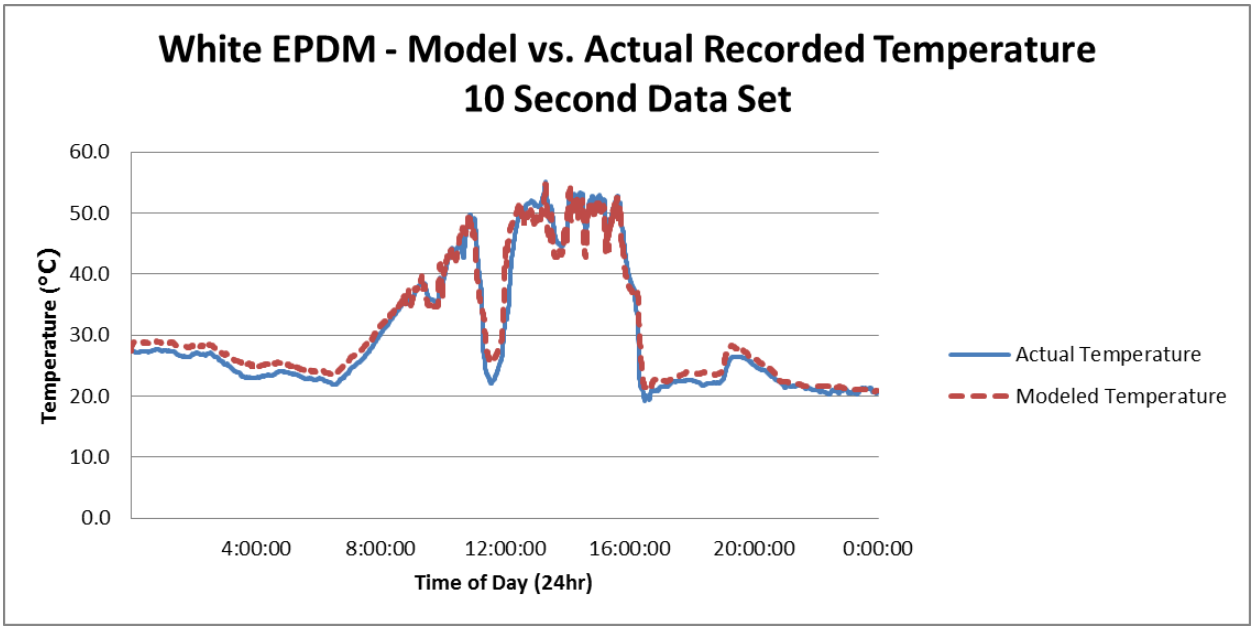
White EPDM - Model vs. Actual Recorded Temperature
10 Second Data Set
60.0
50.0
40.0
30.0
20.0
10.0
0.0
Temperature (°C)
4:00:00
8:00:00
12:00:00
16:00:00
20:00:00
0:00:00
Time of Day (24hr)
Actual Temperature
Modeled Temperature

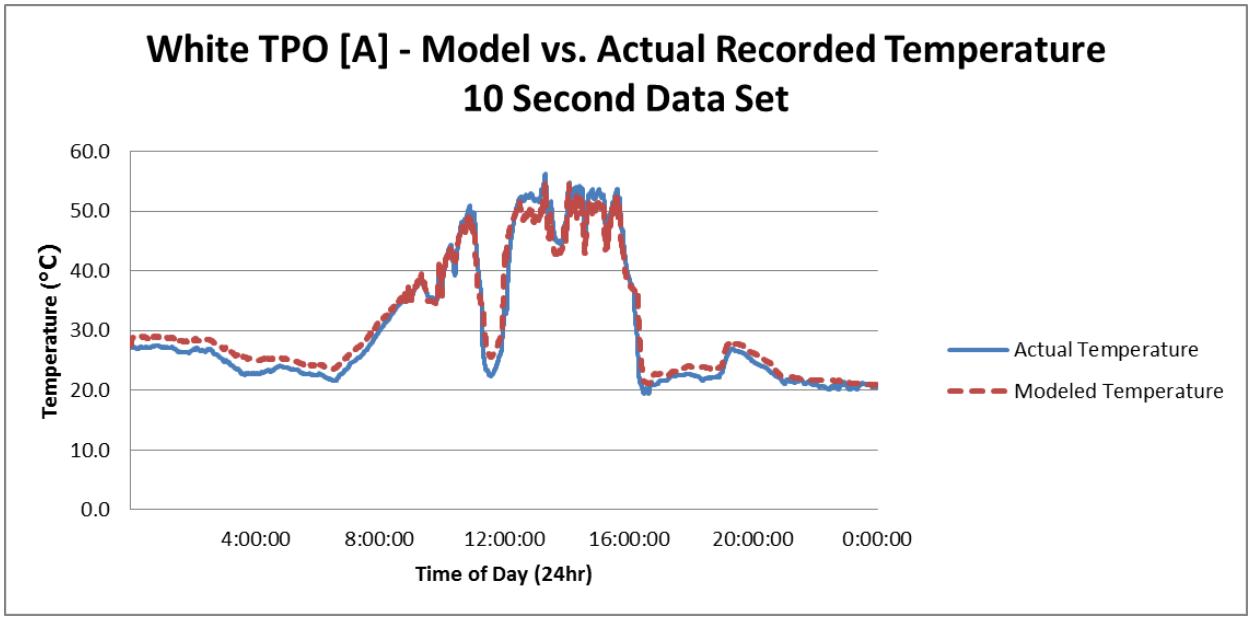
White TPO [A] - Model vs. Actual Recorded Temperature
10 Second Data Set
60.0
50.0
40.0
30.0
20.0
10.0
0.0
Temperature (°C)
4:00:00
8:00:00
12:00:00
16:00:00
20:00:00
0:00:00
Time of Day (24hr)
Actual Temperature
Modeled Temperature

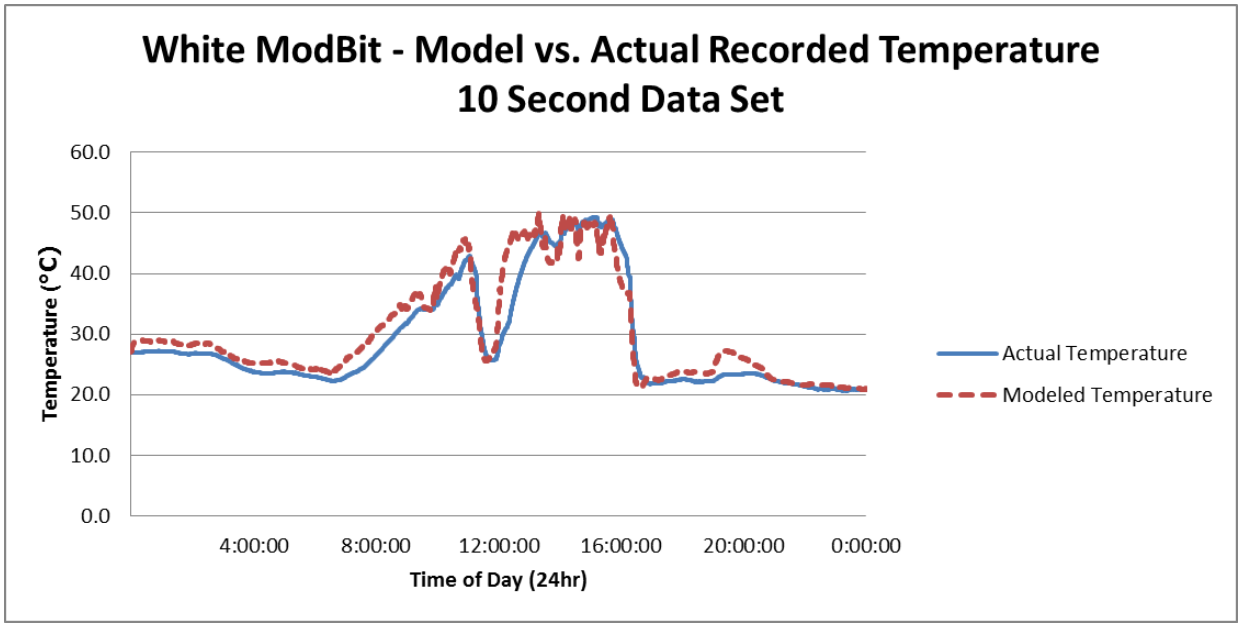
White ModBit - Model vs. Actual Recorded Temperature
10 Second Data Set
Temperature (°C)
60.0
50.0
40.0
30.0
20.0
10.0
0.0
4:00:00
8:00:00
12:00:00
16:00:00
20:00:00
0:00:00
Time of Day (24hr)
Actual Temperature
Modeled Temperature

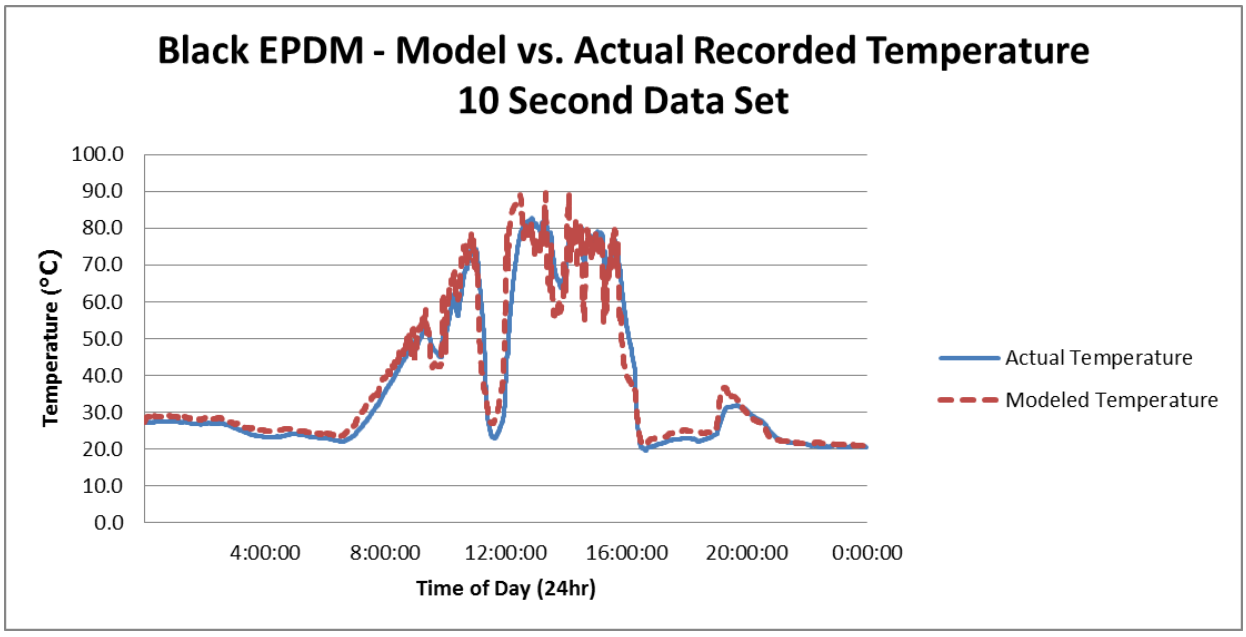
Black EPDM - Model vs. Actual Recorded Temperature
10 Second Data Set
Temperature (°C)
100.0
90.0
80.0
70.0
60.0
50.0
40.0
30.0
20.0
10.0
0.0
4:00:00
8:00:00
12:00:00
16:00:00
20:00:00
0:00:00
Time of Day (24hr)
Actual Temperature
Modeled Temperature

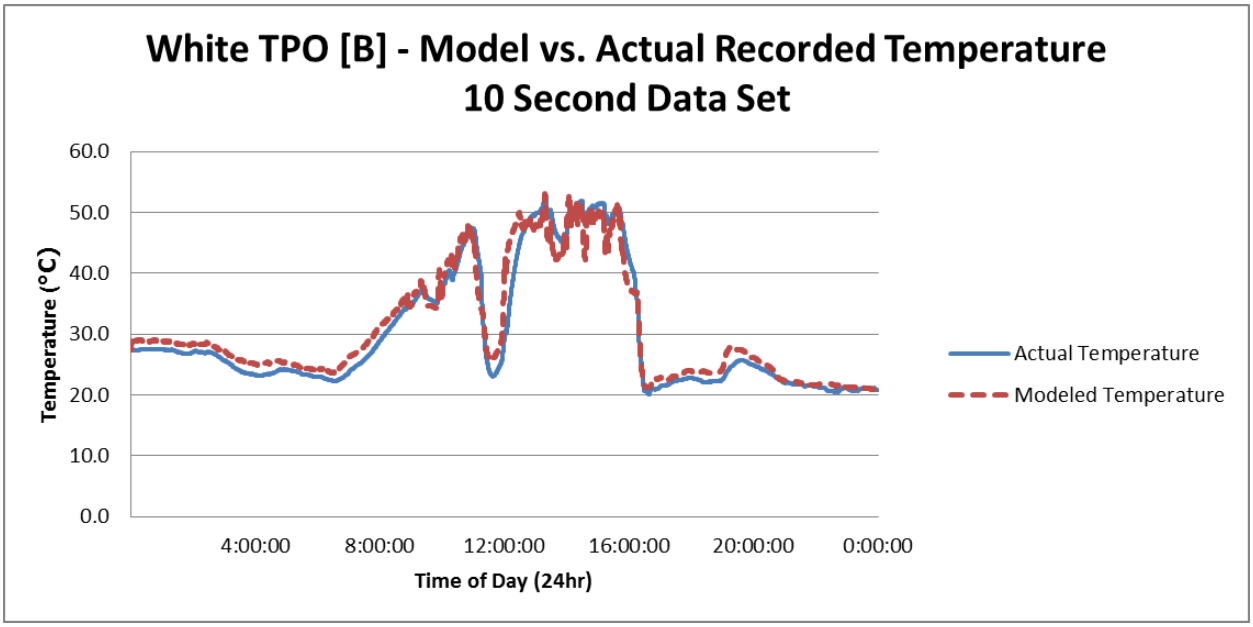
White TPO [B] - Model vs. Actual Recorded Temperature
10 Second Data Set
60.0
50.0
40.0
30.0
20.0
10.0
0.0
Temperature (°C)
4:00:00
8:00:00
12:00:00
16:00:00
20:00:00
0:00:00
Time of Day (24hr)
Actual Temperature
Modeled Temperature

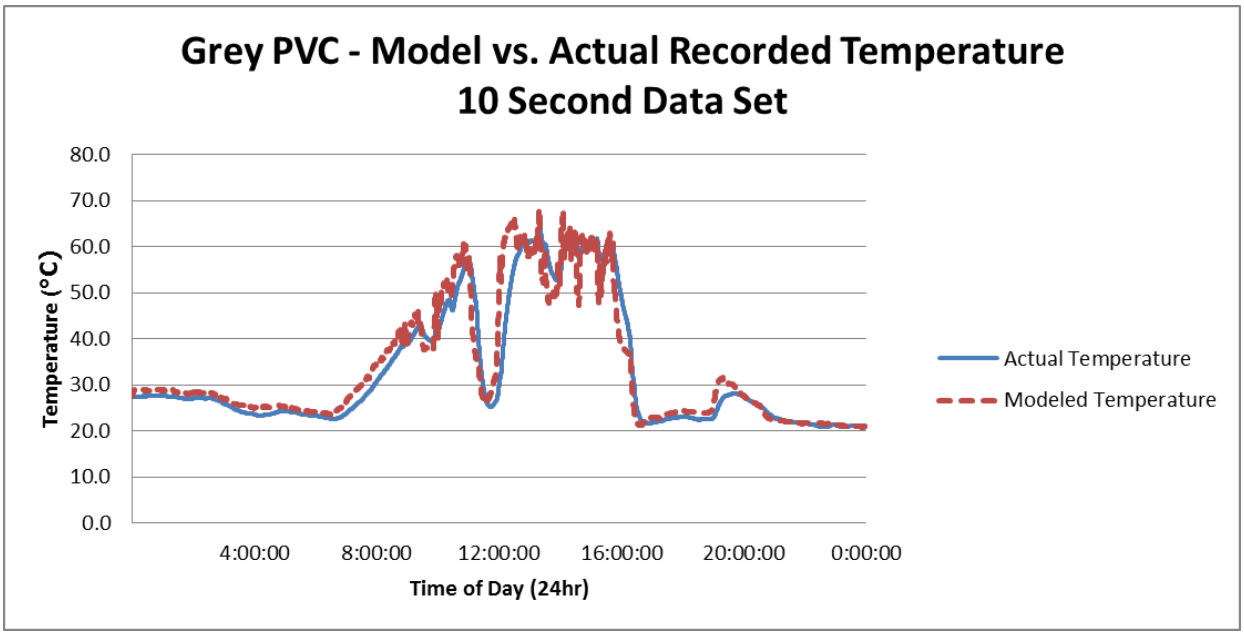
Grey PVC - Model vs. Actual Recorded Temperature
10 Second Data Set
80.0
70.0
60.0
50.0
40.0
30.0
20.0
10.0
0.0
Temperature (°C)
4:00:00
8:00:00
12:00:00
16:00:00
20:00:00
0:00:00
Time of Day (24hr)
Actual Temperature
Modeled Temperature

August 14, 2010

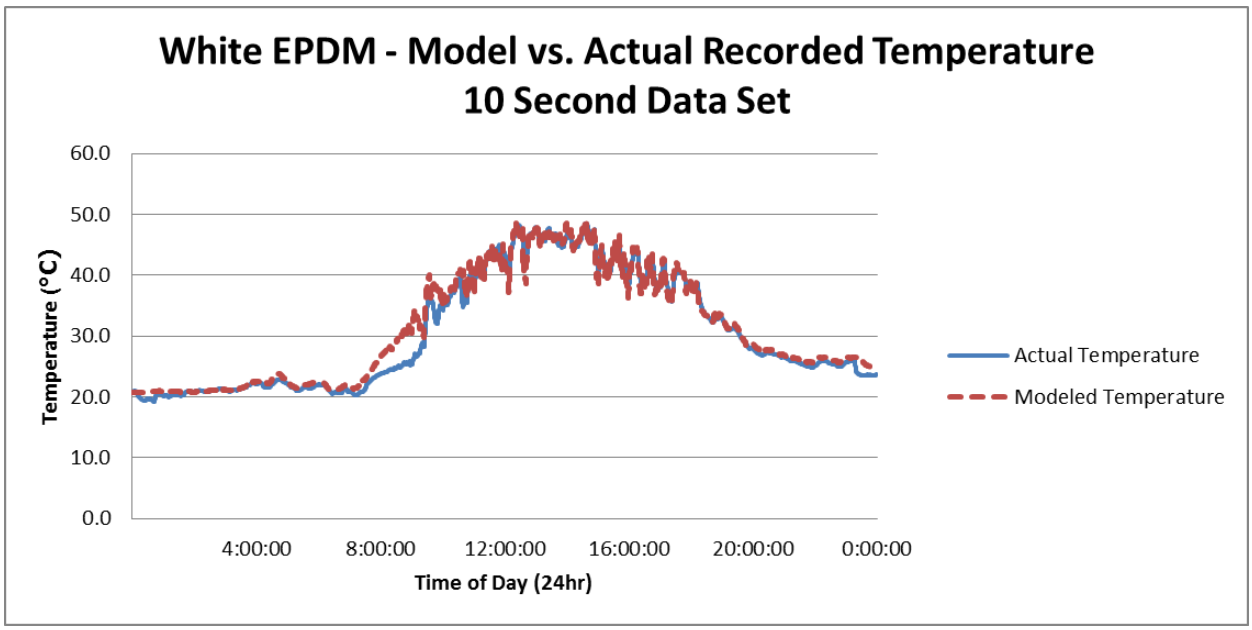
White EPDM - Model vs. Actual Recorded Temperature
10 Second Data Set
60.0
50.0
40.0
30.0
20.0
10.0
0.0
Temperature (°C)
4:00:00
8:00:00
12:00:00
16:00:00
20:00:00
0:00:00
Time of Day (24hr)
Actual Temperature
Modeled Temperature

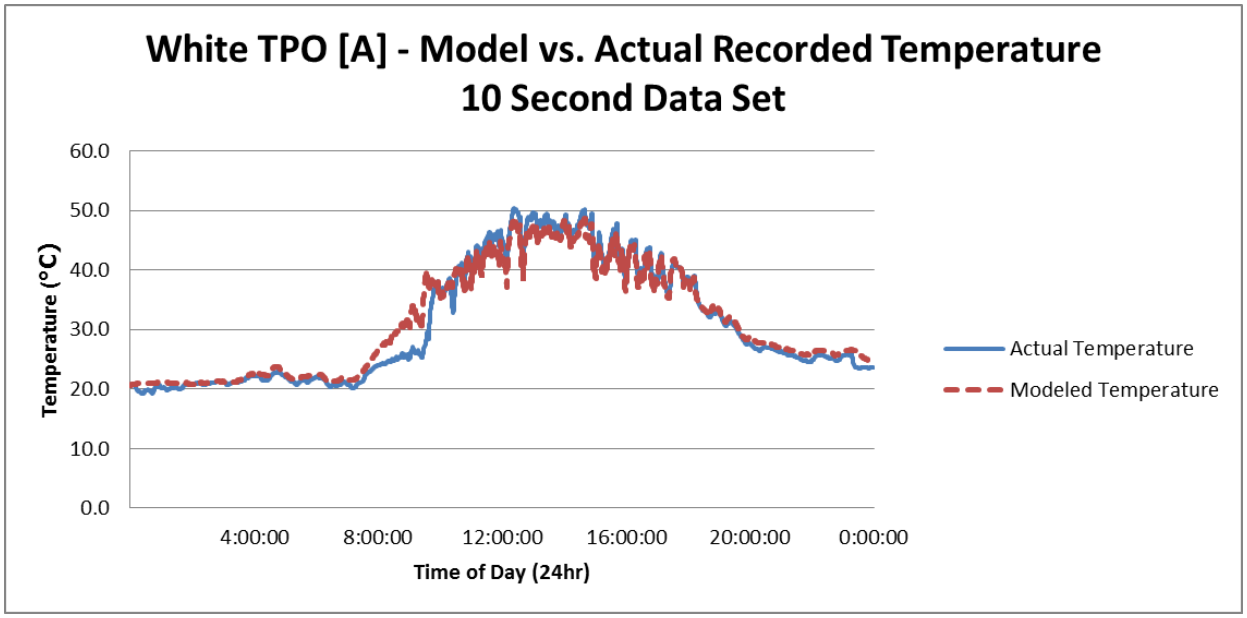
White TPO [A] - Model vs. Actual Recorded Temperature
10 Second Data Set
60.0
50.0
40.0
30.0
20.0
10.0
0.0
Temperature (°C)
4:00:00
8:00:00
12:00:00
16:00:00
20:00:00
0:00:00
Time of Day (24hr)
Actual Temperature
Modeled Temperature

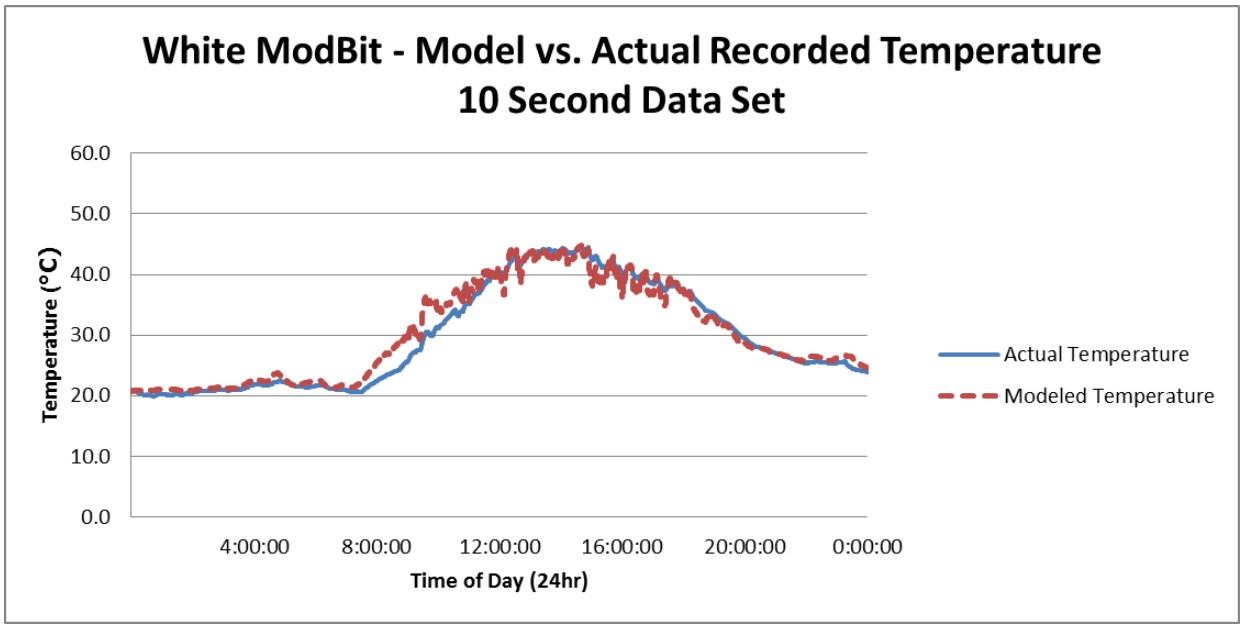
White ModBit - Model vs. Actual Recorded Temperature
10 Second Data Set
Temperature (°C)
60.0
50.0
40.0
30.0
20.0
10.0
0.0
4:00:00
8:00:00
12:00:00
16:00:00
20:00:00
0:00:00
Time of Day (24hr)
Actual Temperature
Modeled Temperature

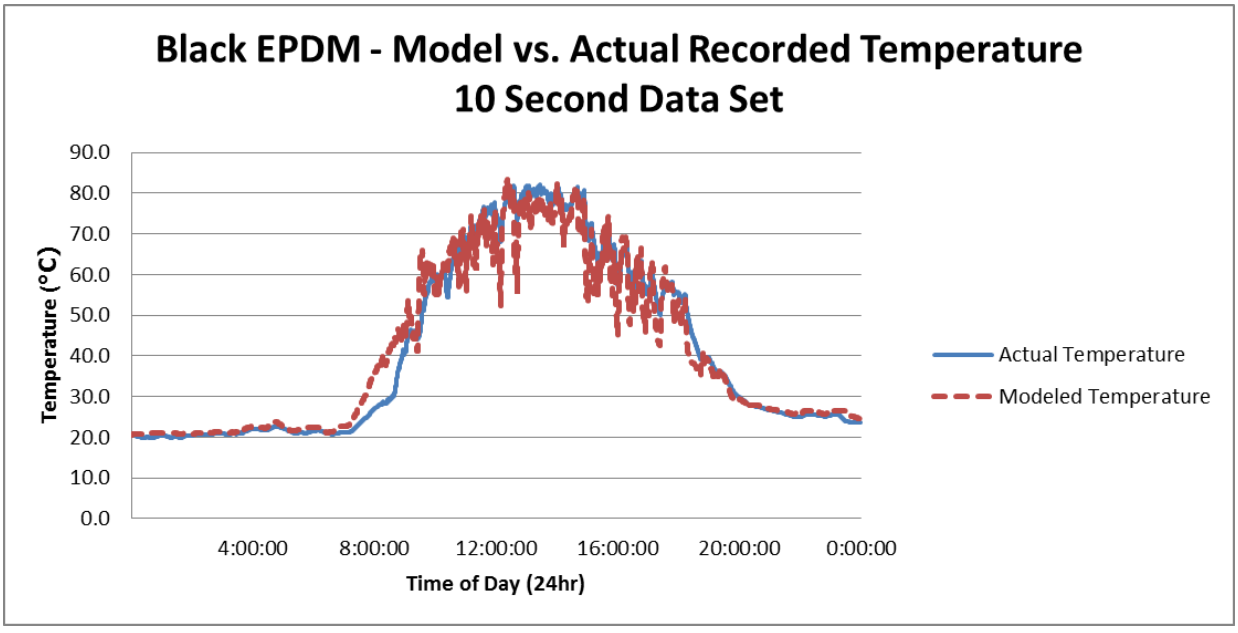
Black EPDM - Model vs. Actual Recorded Temperature
10 Second Data Set
Temperature (°C)
90.0
80.0
70.0
60.0
50.0
40.0
30.0
20.0
10.0
0.0
4:00:00
8:00:00
12:00:00
16:00:00
20:00:00
0:00:00
Time of Day (24hr)
Actual Temperature
Modeled Temperature

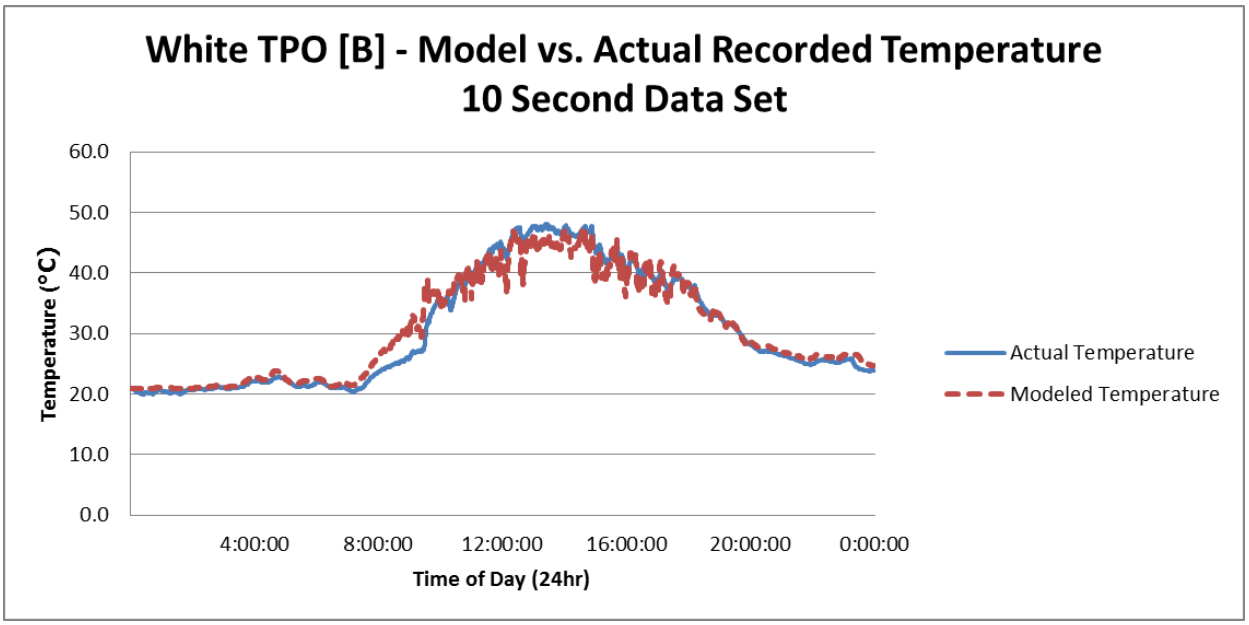
White TPO [B] - Model vs. Actual Recorded Temperature
10 Second Data Set
Temperature (°C)
60.0
50.0
40.0
30.0
20.0
10.0
0.0
4:00:00
8:00:00
12:00:00
16:00:00
20:00:00
0:00:00
Time of Day (24hr)
Actual Temperature
Modeled Temperature

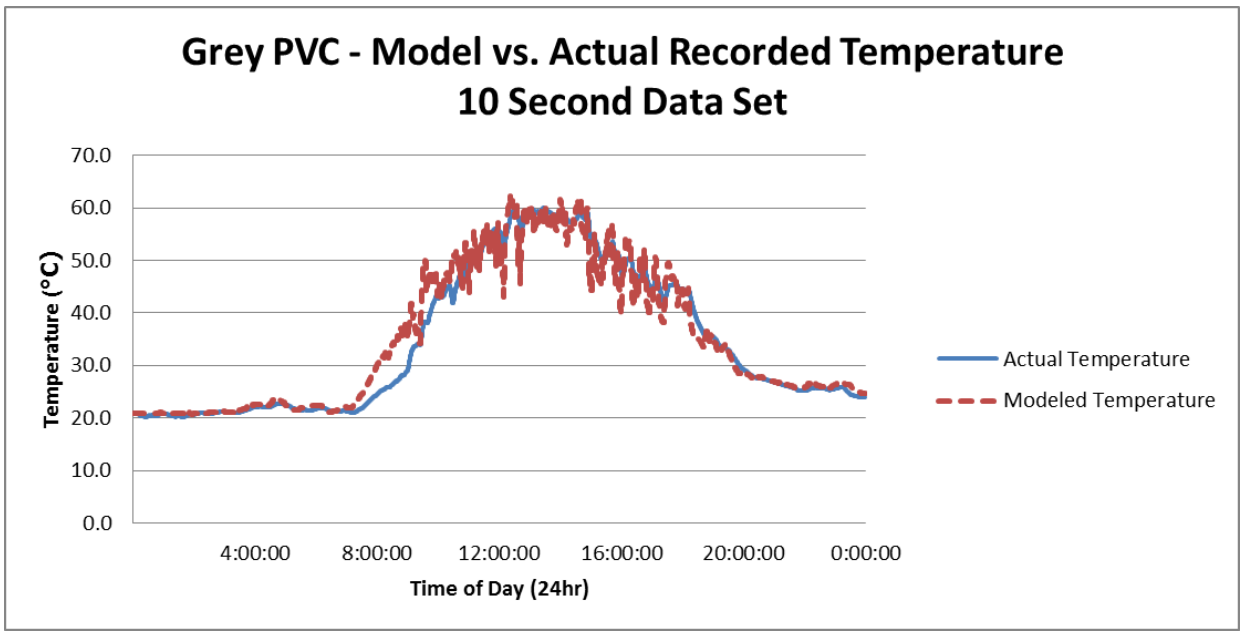
Grey PVC - Model vs. Actual Recorded Temperature
10 Second Data Set
Temperature (°C)
70.0
60.0
50.0
40.0
30.0
20.0
10.0
0.0
4:00:00
8:00:00
12:00:00
16:00:00
20:00:00
0:00:00
Time of Day (24hr)
Actual Temperature
Modeled Temperature

August 15, 2010

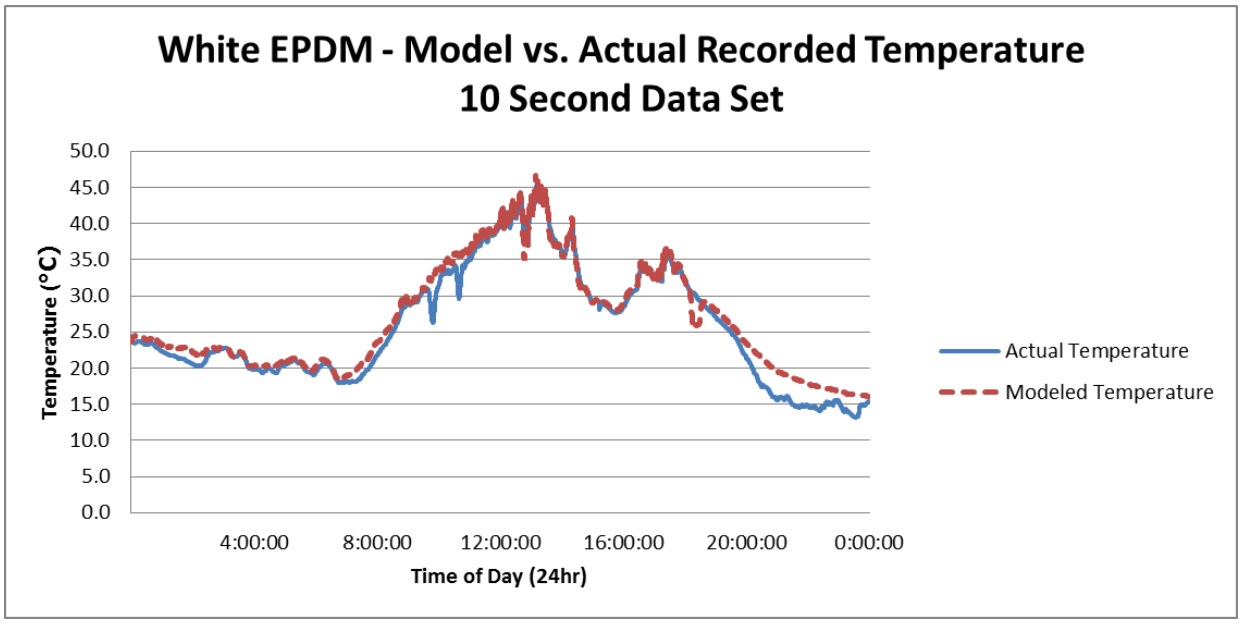
White EPDM - Model vs. Actual Recorded Temperature
10 Second Data Set
Temperature (°C)
50.0
45.0
40.0
35.0
30.0
25.0
20.0
15.0
10.0
5.0
0.0
4:00:00
8:00:00
12:00:00
16:00:00
20:00:00
0:00:00
Time of Day (24hr)
Actual Temperature
Modeled Temperature

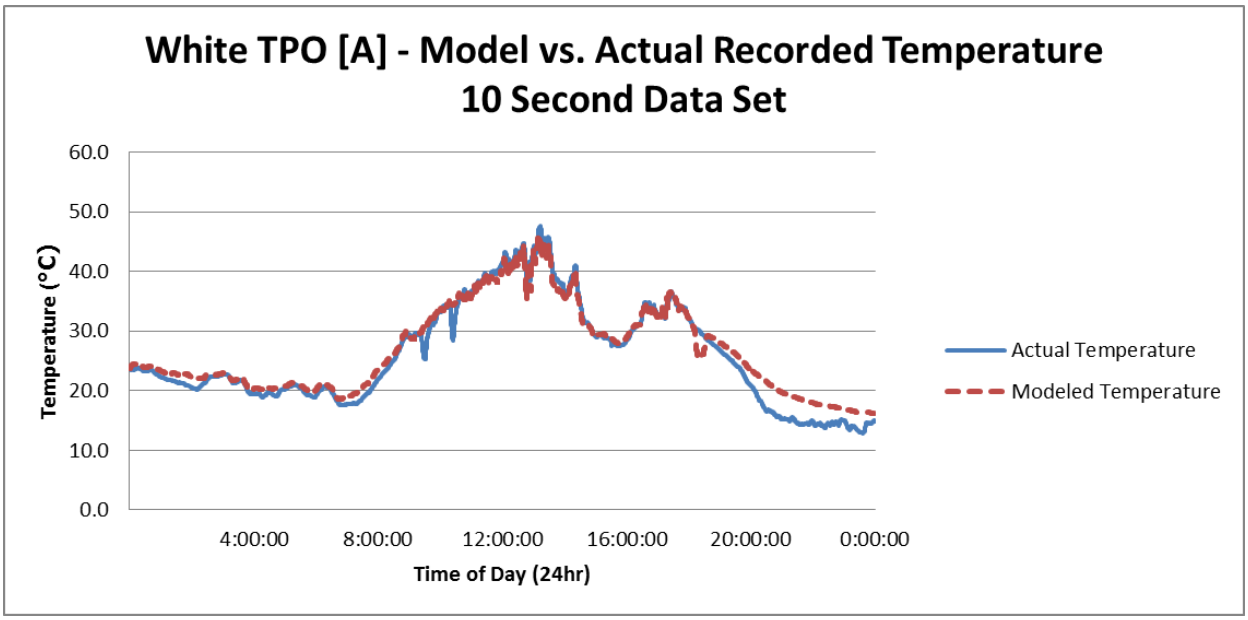
White TPO [A] - Model vs. Actual Recorded Temperature
10 Second Data Set
Temperature (°C)
60.0
50.0
40.0
30.0
20.0
10.0
0.0
4:00:00
8:00:00
12:00:00
16:00:00
20:00:00
0:00:00
Time of Day (24hr)
Actual Temperature
Modeled Temperature

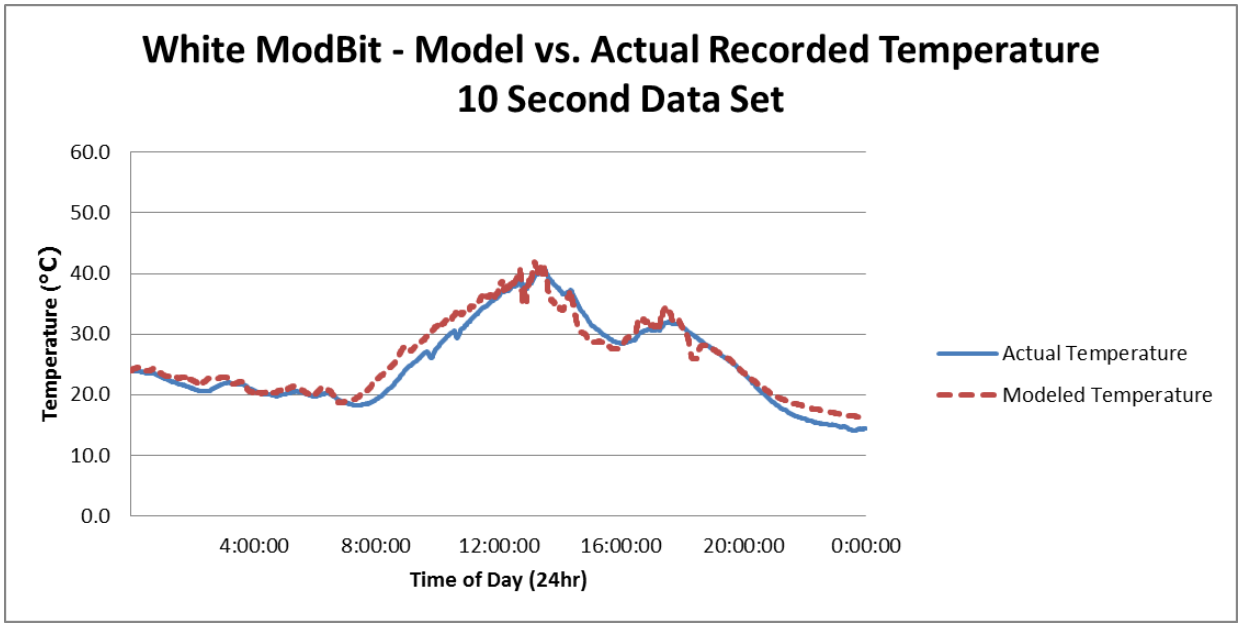
White ModBit - Model vs. Actual Recorded Temperature
10 Second Data Set
Temperature (°C)
60.0
50.0
40.0
30.0
20.0
10.0
0.0
4:00:00
8:00:00
12:00:00
16:00:00
20:00:00
0:00:00
Time of Day (24hr)
Actual Temperature
Modeled Temperature

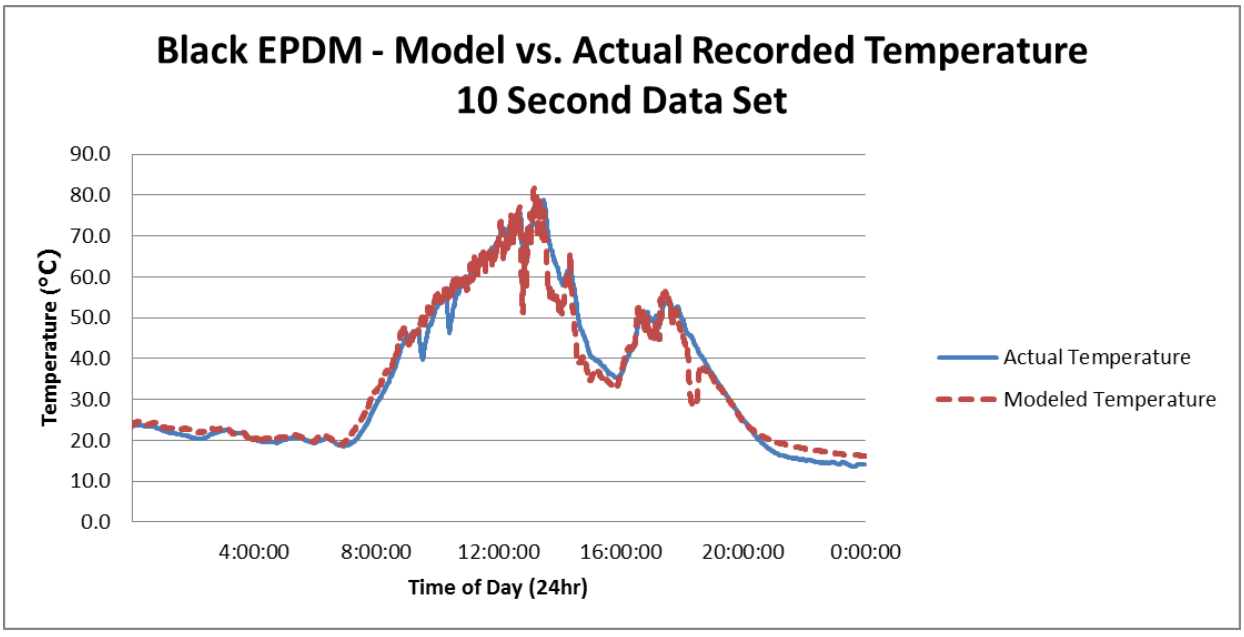
Black EPDM - Model vs. Actual Recorded Temperature
10 Second Data Set
Temperature (°C)
90.0
80.0
70.0
60.0
50.0
40.0
30.0
20.0
10.0
0.0
4:00:00
8:00:00
12:00:00
16:00:00
20:00:00
0:00:00
Time of Day (24hr)
Actual Temperature
Modeled Temperature

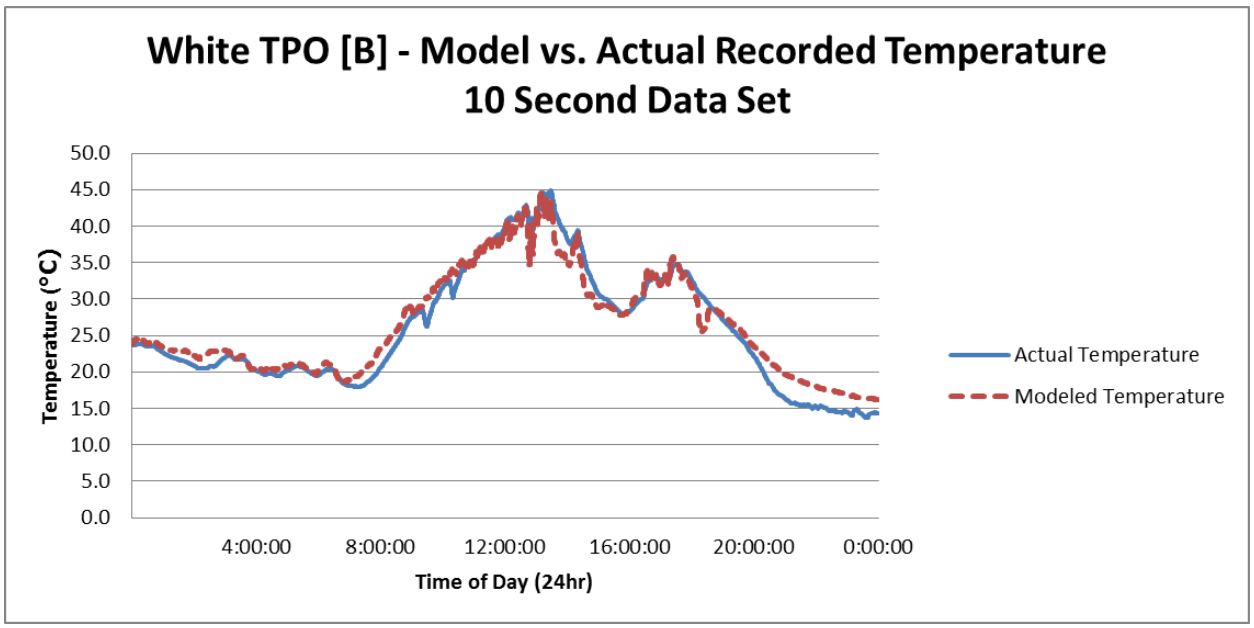
White TPO [B] - Model vs. Actual Recorded Temperature
10 Second Data Set
Temperature (°C)
50.0
45.0
40.0
35.0
30.0
25.0
20.0
15.0
10.0
5.0
0.0
4:00:00
8:00:00
12:00:00
16:00:00
20:00:00
0:00:00
Time of Day (24hr)
Actual Temperature
Modeled Temperature

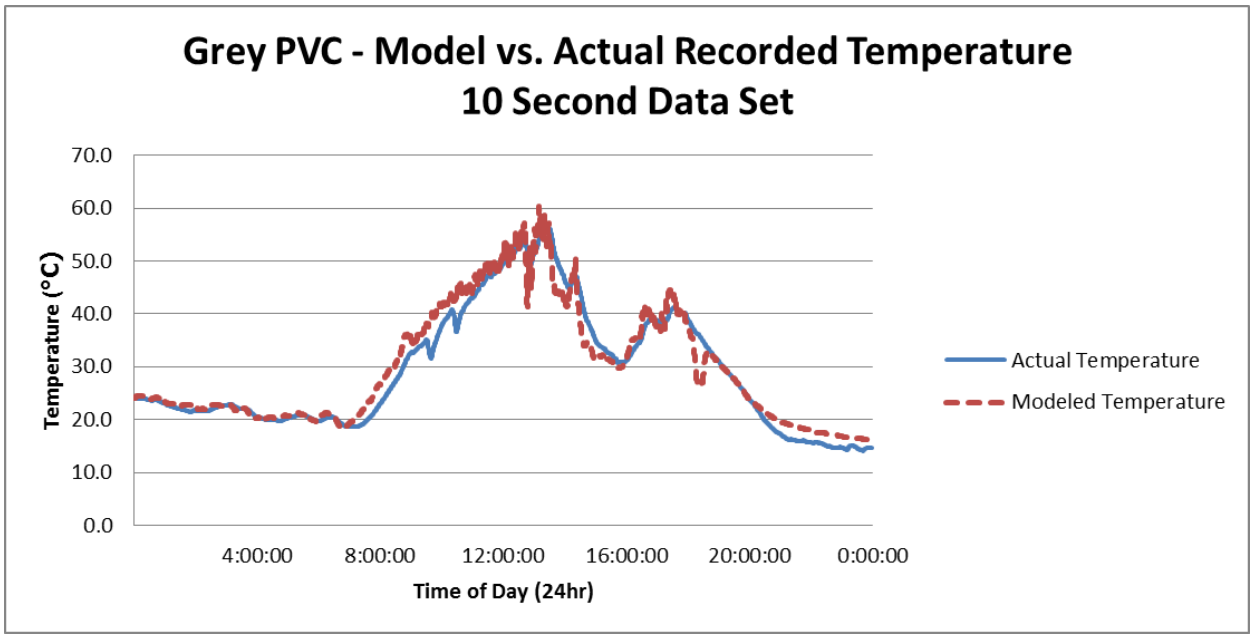
Grey PVC - Model vs. Actual Recorded Temperature
10 Second Data Set
Temperature (°C)
70.0
60.0
50.0
40.0
30.0
20.0
10.0
0.0
4:00:00
8:00:00
12:00:00
16:00:00
20:00:00
0:00:00
Time of Day (24hr)
Actual Temperature
Modeled Temperature

August 16, 2010

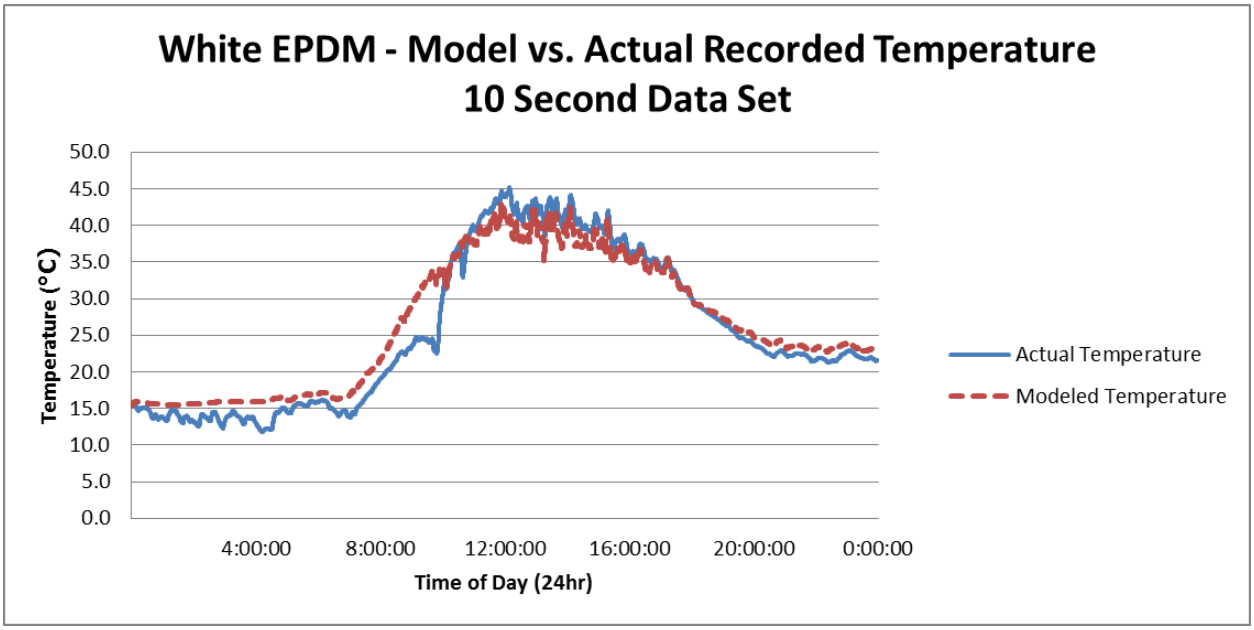
White EPDM - Model vs. Actual Recorded Temperature
10 Second Data Set
Temperature (°C)
50.0
45.0
40.0
35.0
30.0
25.0
20.0
15.0
10.0
5.0
0.0
4:00:00
8:00:00
12:00:00
16:00:00
20:00:00
0:00:00
Time of Day (24hr)
Actual Temperature
Modeled Temperature

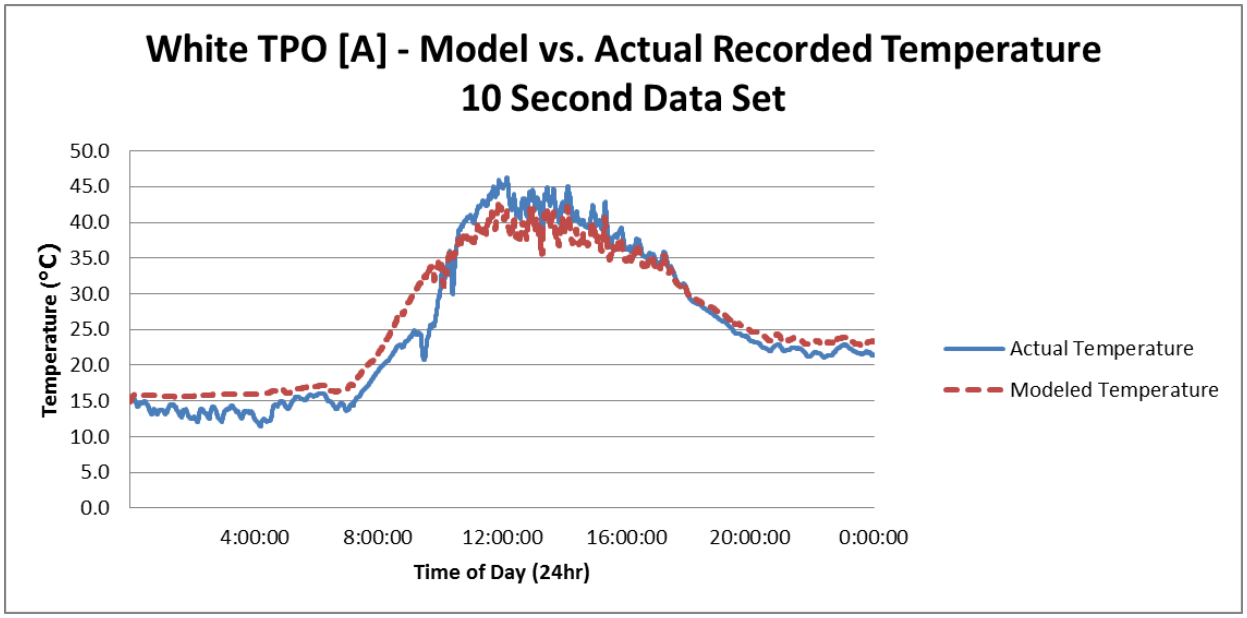
White TPO [A] - Model vs. Actual Recorded Temperature
10 Second Data Set
Temperature (°C)
50.0
45.0
40.0
35.0
30.0
25.0
20.0
15.0
10.0
5.0
0.0
4:00:00
8:00:00
12:00:00
16:00:00
20:00:00
0:00:00
Time of Day (24hr)
Actual Temperature
Modeled Temperature

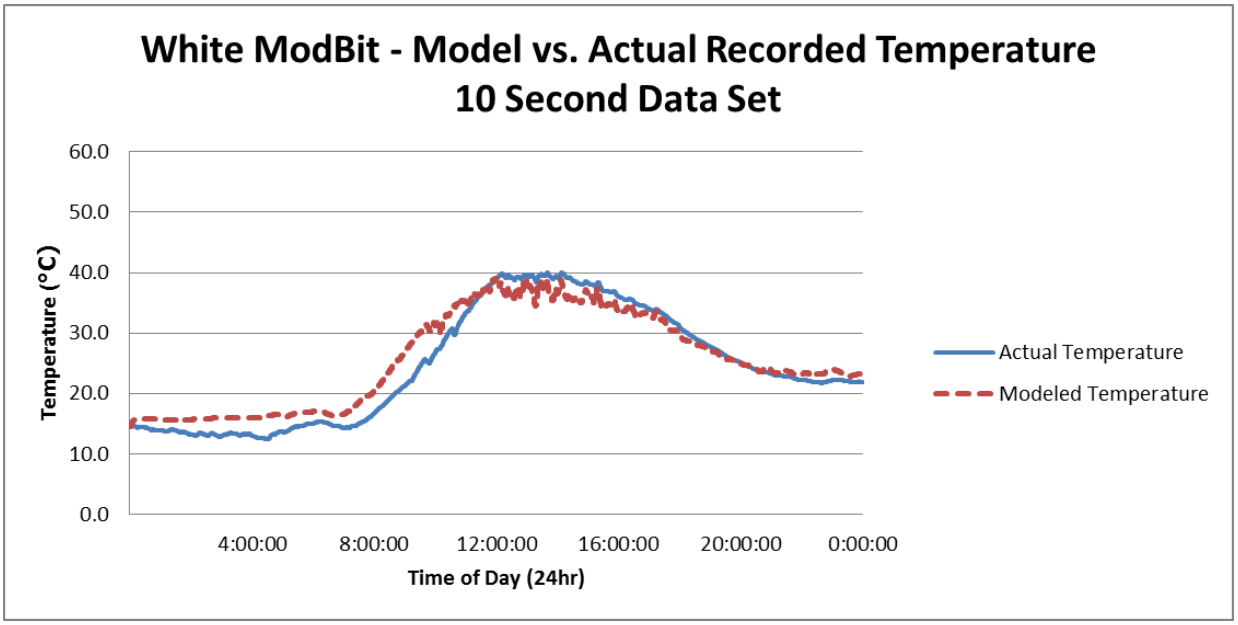
White ModBit - Model vs. Actual Recorded Temperature
10 Second Data Set
Temperature (°C)
60.0
50.0
40.0
30.0
20.0
10.0
0.0
4:00:00
8:00:00
12:00:00
16:00:00
20:00:00
0:00:00
Time of Day (24hr)
Actual Temperature
Modeled Temperature

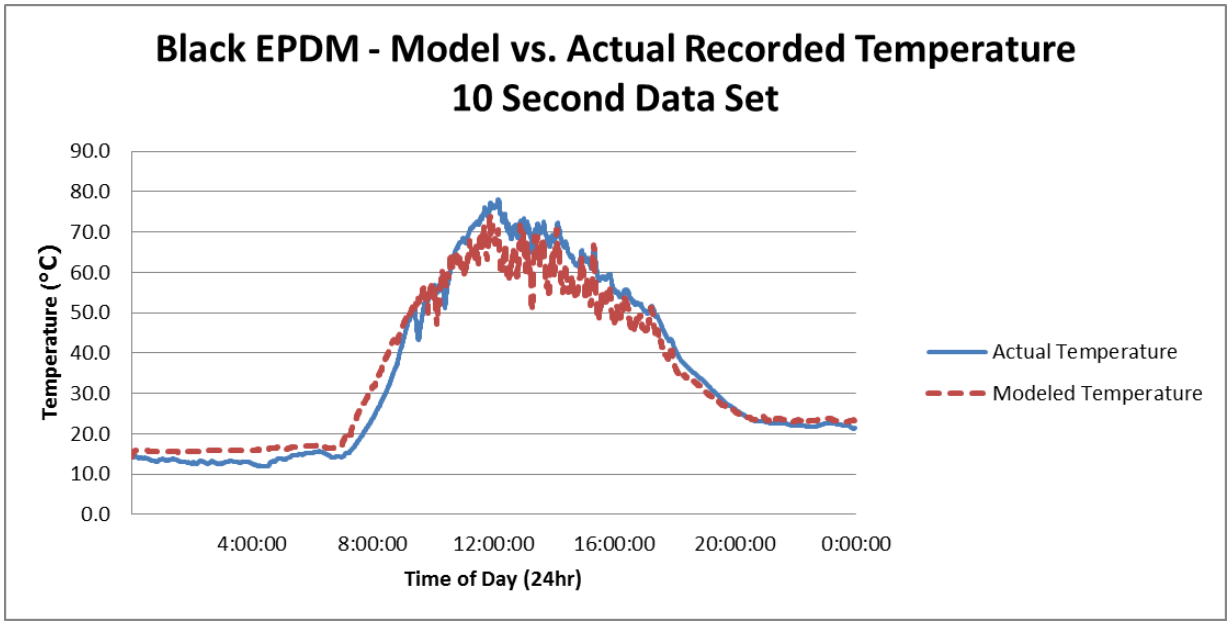
Black EPDM - Model vs. Actual Recorded Temperature
10 Second Data Set
Temperature (°C)
90.0
80.0
70.0
60.0
50.0
40.0
30.0
20.0
10.0
0.0
4:00:00
8:00:00
12:00:00
16:00:00
20:00:00
0:00:00
Time of Day (24hr)
Actual Temperature
Modeled Temperature

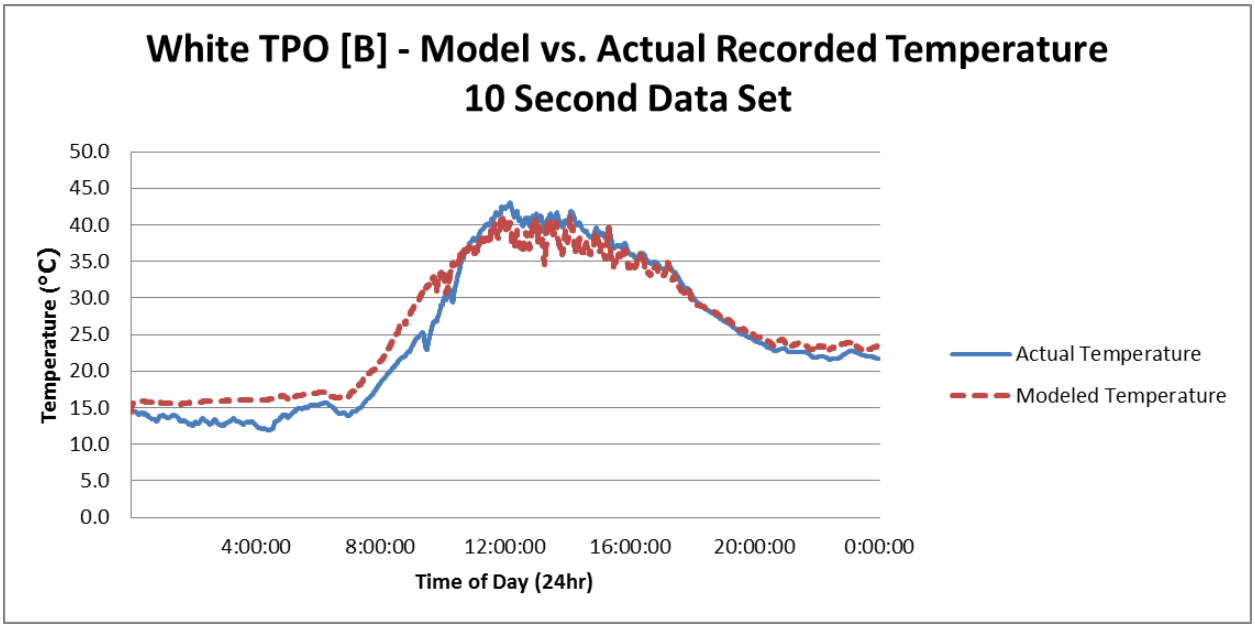
White TPO [B] - Model vs. Actual Recorded Temperature
10 Second Data Set
Temperature (°C)
50.0
45.0
40.0
35.0
30.0
25.0
20.0
15.0
10.0
5.0
0.0
4:00:00
8:00:00
12:00:00
16:00:00
20:00:00
0:00:00
Time of Day (24hr)
Actual Temperature
Modeled Temperature

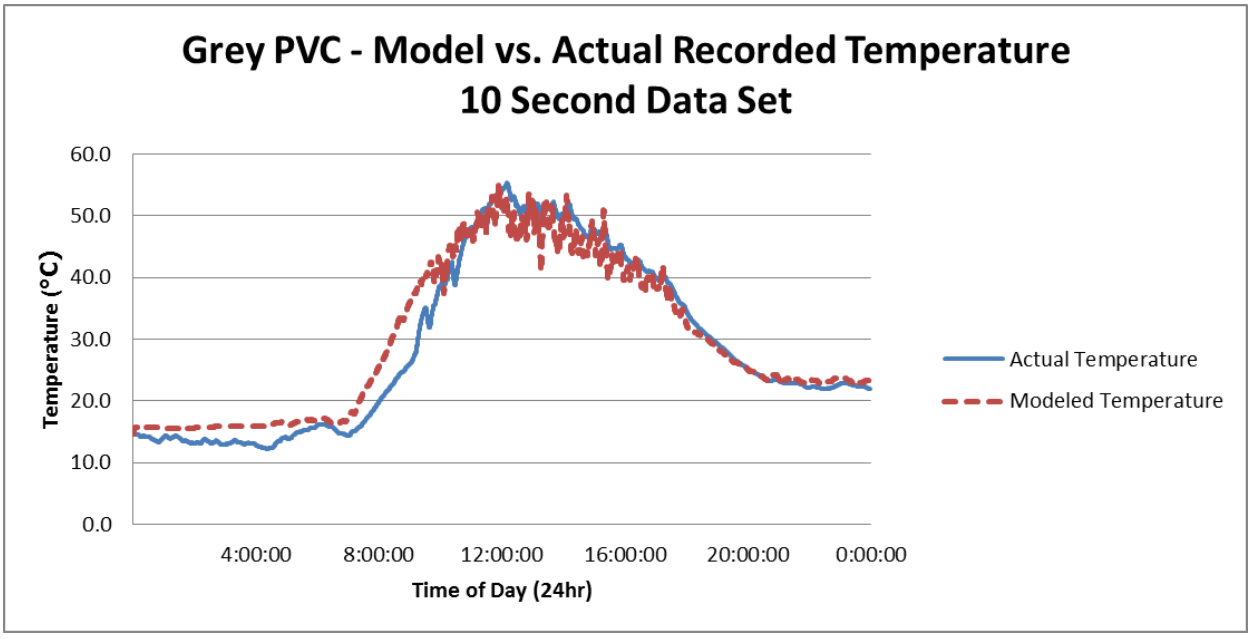
Grey PVC - Model vs. Actual Recorded Temperature
10 Second Data Set
Temperature (°C)
60.0
50.0
40.0
30.0
20.0
10.0
0.0
4:00:00
8:00:00
12:00:00
16:00:00
20:00:00
0:00:00
Time of Day (24hr)
Actual Temperature
Modeled Temperature

August 17, 2010

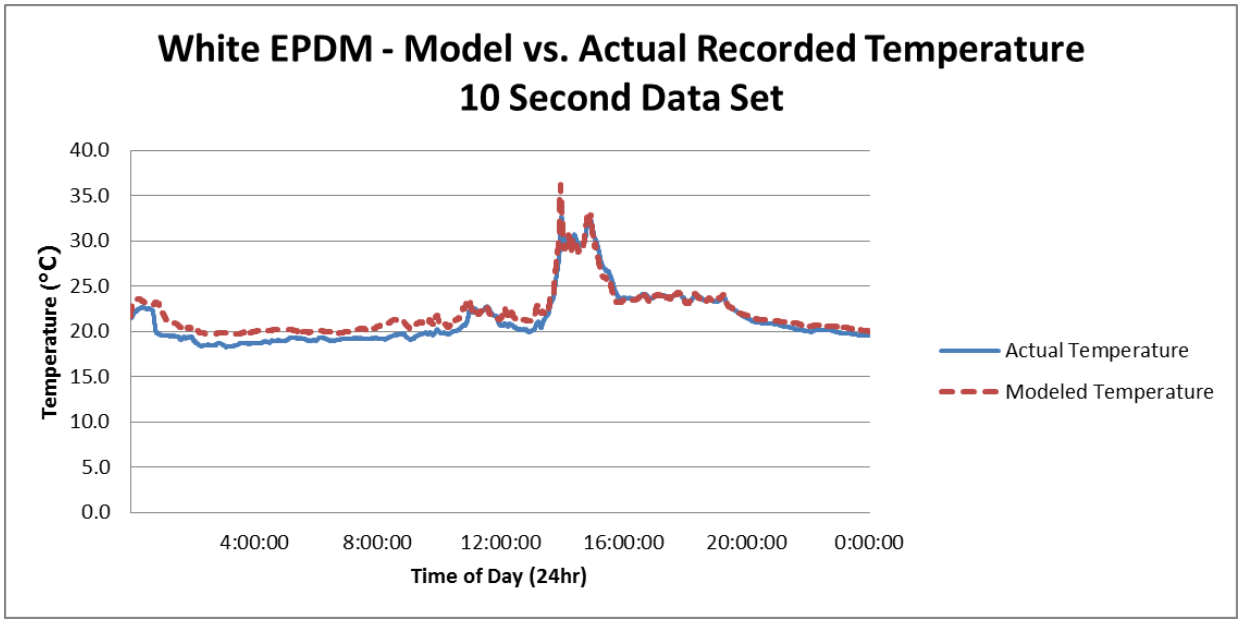
White EPDM - Model vs. Actual Recorded Temperature
10 Second Data Set
Temperature (°C)
40.0
35.0
30.0
25.0
20.0
15.0
10.0
5.0
0.0
4:00:00
8:00:00
12:00:00
16:00:00
20:00:00
0:00:00
Time of Day (24hr)
Actual Temperature
Modeled Temperature

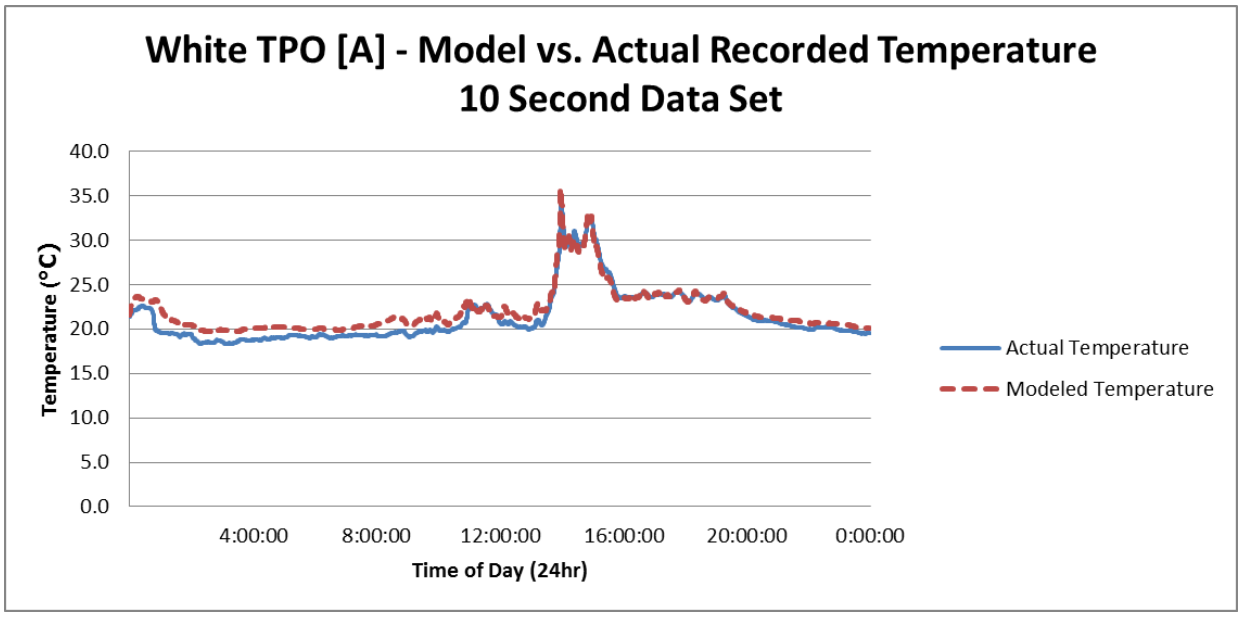
White TPO [A] - Model vs. Actual Recorded Temperature
10 Second Data Set
Temperature (°C)
40.0
35.0
30.0
25.0
20.0
15.0
10.0
5.0
0.0
4:00:00
8:00:00
12:00:00
16:00:00
20:00:00
0:00:00
Time of Day (24hr)
Actual Temperature
Modeled Temperature

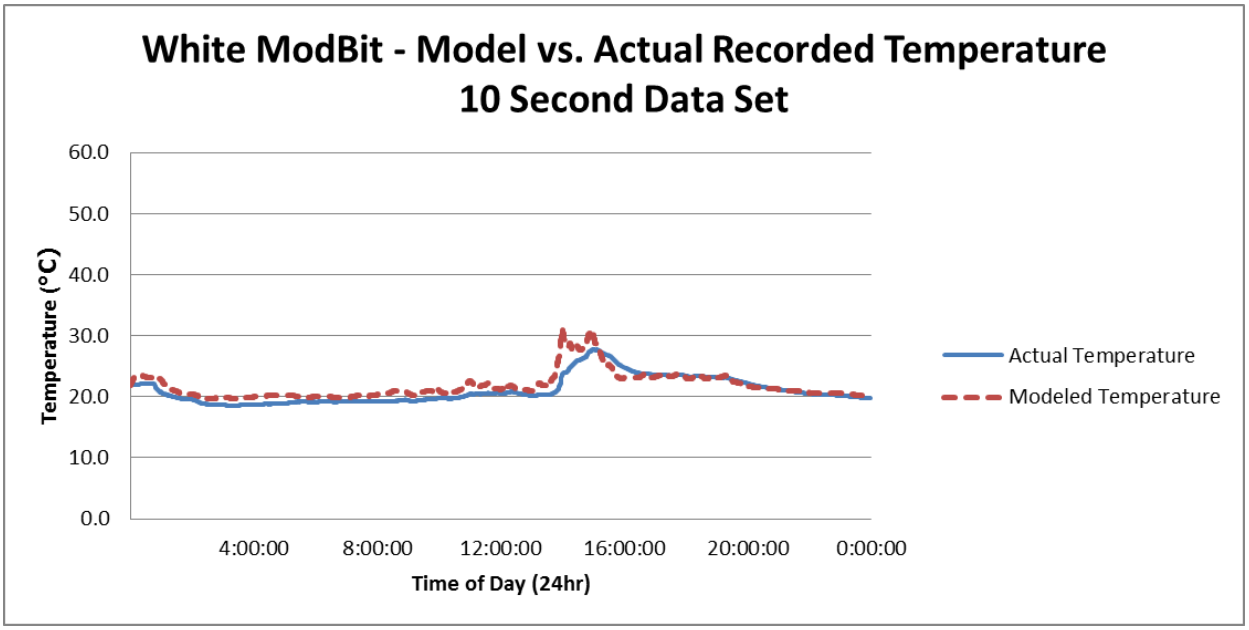
White ModBit - Model vs. Actual Recorded Temperature
10 Second Data Set
60.0
50.0
40.0
30.0
20.0
10.0
0.0
Temperature (°C)
4:00:00
8:00:00
12:00:00
16:00:00
20:00:00
0:00:00
Time of Day (24hr)
Actual Temperature
Modeled Temperature

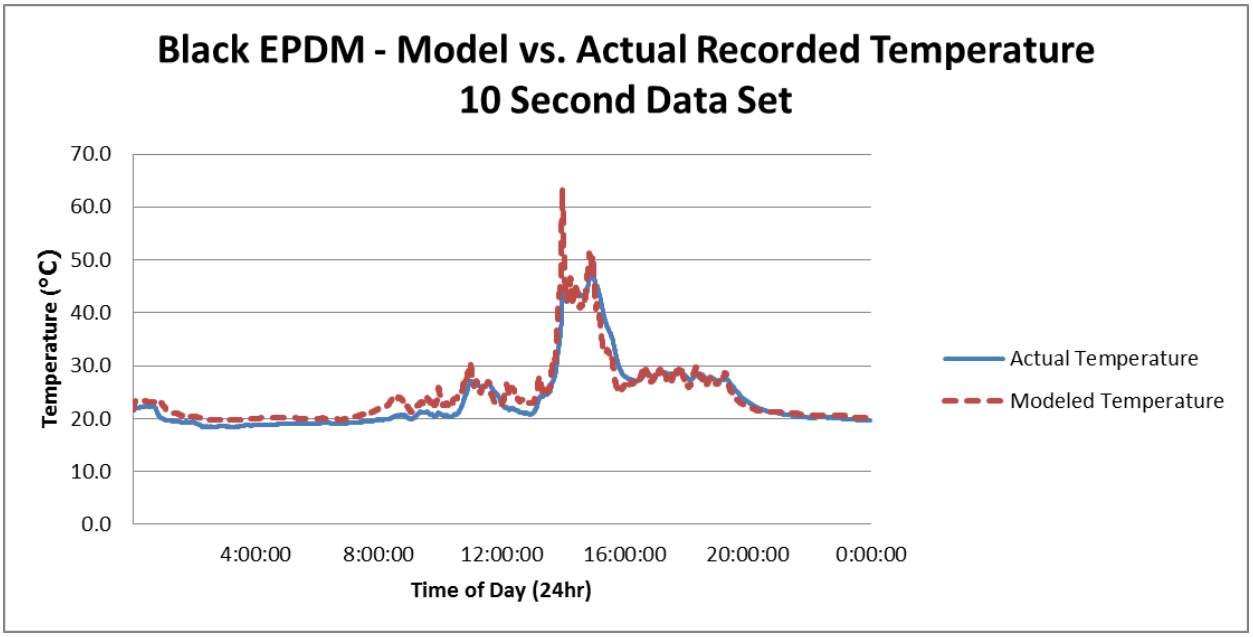
Black EPDM - Model vs. Actual Recorded Temperature
10 Second Data Set
70.0
60.0
50.0
40.0
30.0
20.0
10.0
0.0
Temperature (°C)
4:00:00
8:00:00
12:00:00
16:00:00
20:00:00
0:00:00
Time of Day (24hr)
Actual Temperature
Modeled Temperature

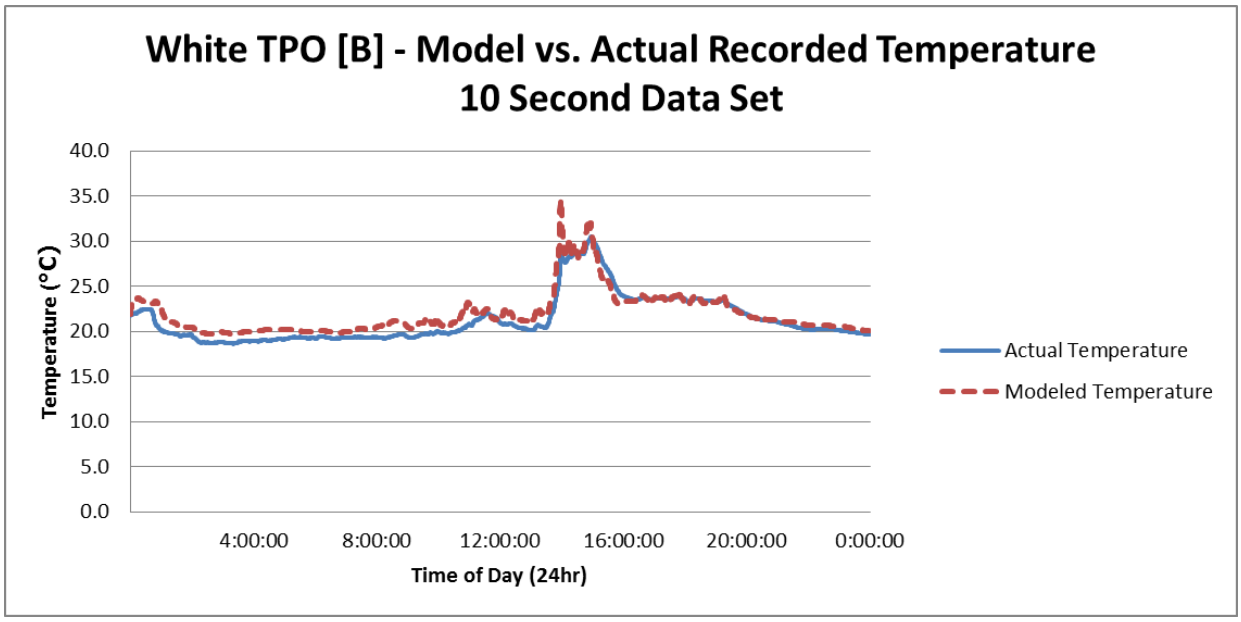
White TPO [B] - Model vs. Actual Recorded Temperature
10 Second Data Set
Temperature (°C)
40.0
35.0
30.0
25.0
20.0
15.0
10.0
5.0
0.0
4:00:00
8:00:00
12:00:00
16:00:00
20:00:00
0:00:00
Time of Day (24hr)
Actual Temperature
Modeled Temperature

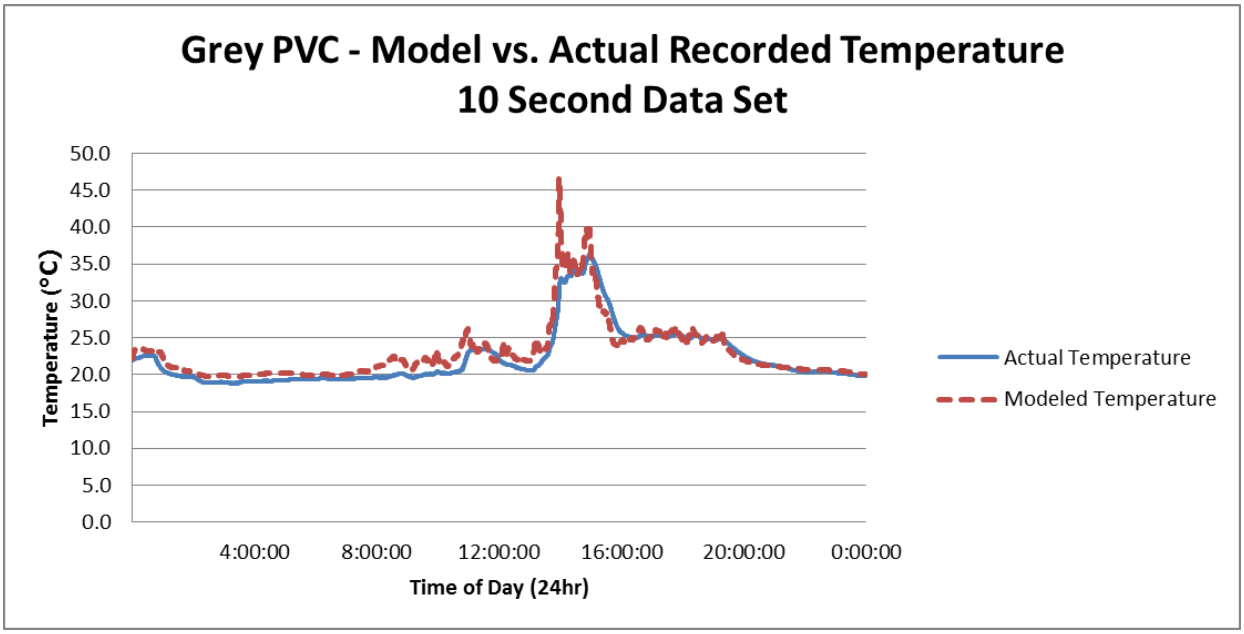
Grey PVC - Model vs. Actual Recorded Temperature
10 Second Data Set
Temperature (°C)
50.0
45.0
40.0
35.0
30.0
25.0
20.0
15.0
10.0
5.0
0.0
4:00:00
8:00:00
12:00:00
16:00:00
20:00:00
0:00:00
Time of Day (24hr)
Actual Temperature
Modeled Temperature

August 18, 2010

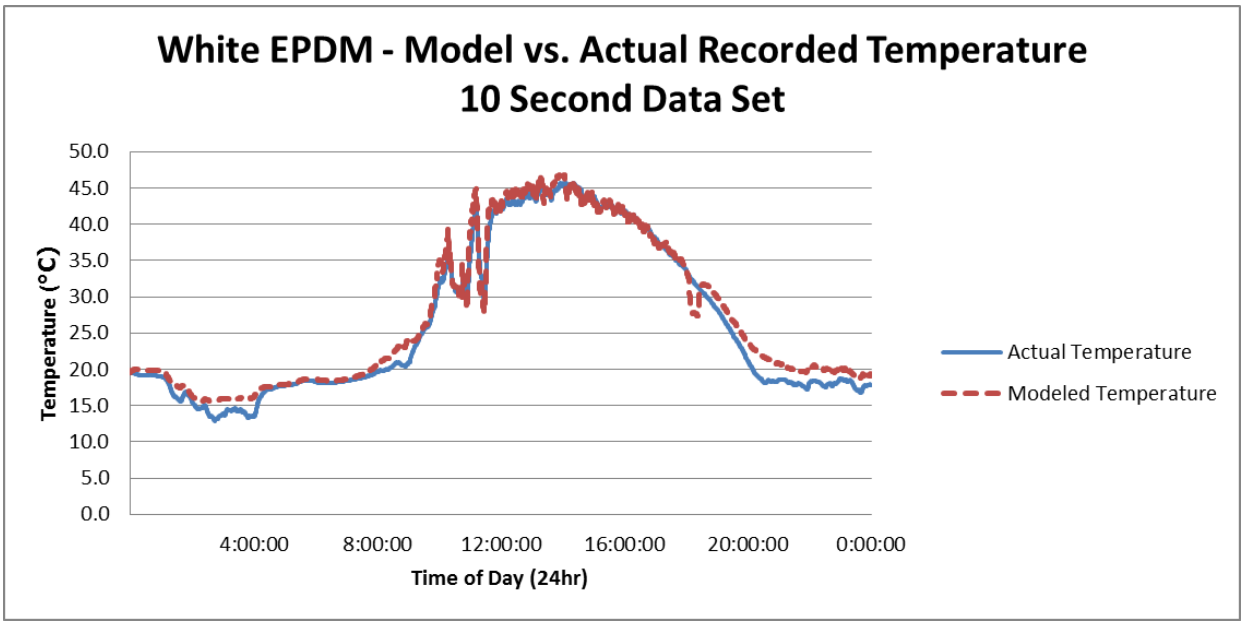
White EPDM - Model vs. Actual Recorded Temperature
10 Second Data Set
Temperature (°C)
50.0
45.0
40.0
35.0
30.0
25.0
20.0
15.0
10.0
5.0
0.0
4:00:00
8:00:00
12:00:00
16:00:00
20:00:00
0:00:00
Time of Day (24hr)
Actual Temperature
Modeled Temperature

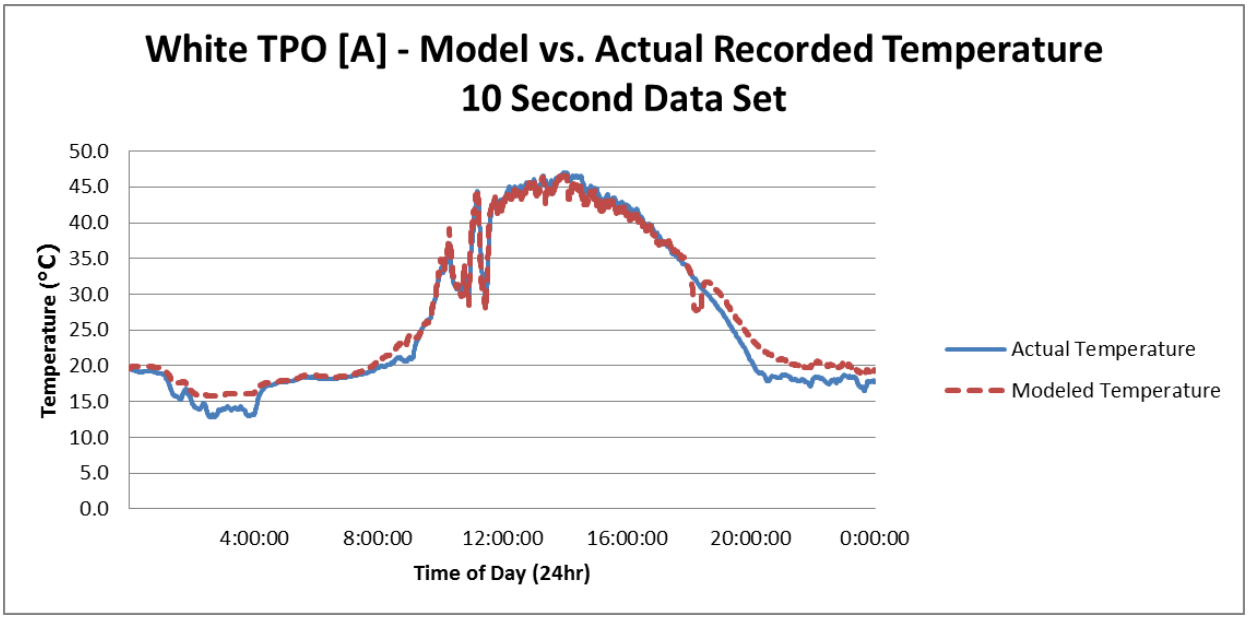
White TPO [A] - Model vs. Actual Recorded Temperature
10 Second Data Set
Temperature (°C)
50.0
45.0
40.0
35.0
30.0
25.0
20.0
15.0
10.0
5.0
0.0
4:00:00
8:00:00
12:00:00
16:00:00
20:00:00
0:00:00
Time of Day (24hr)
Actual Temperature
Modeled Temperature

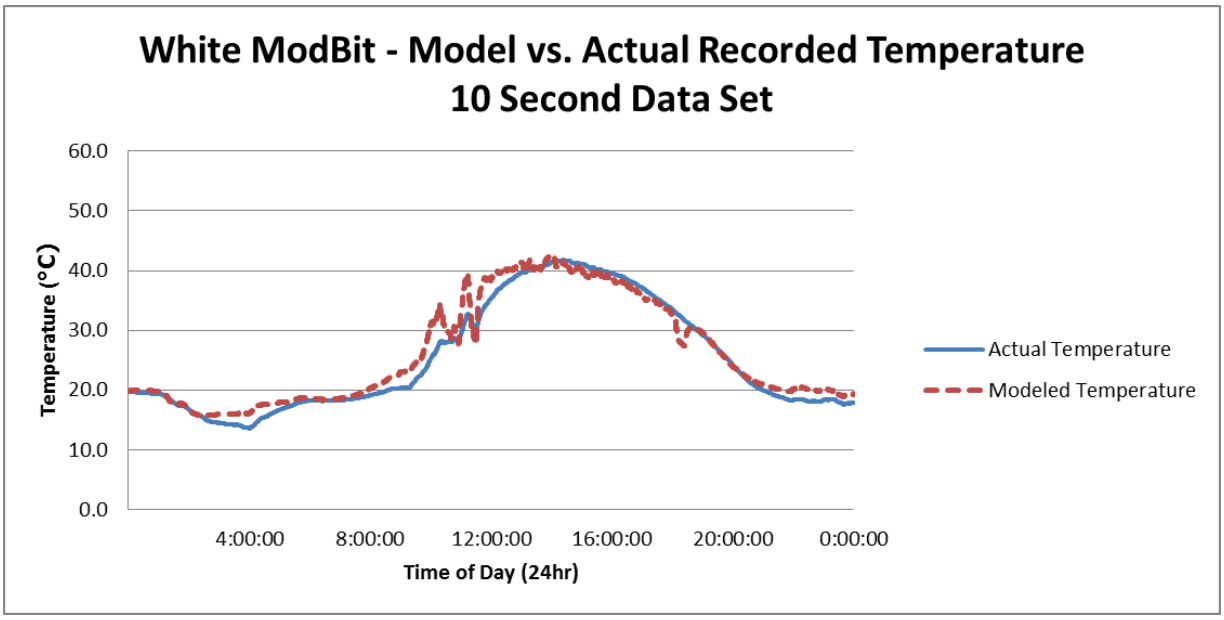
White ModBit - Model vs. Actual Recorded Temperature
10 Second Data Set
Temperature (°C)
60.0
50.0
40.0
30.0
20.0
10.0
0.0
4:00:00
8:00:00
12:00:00
16:00:00
20:00:00
0:00:00
Time of Day (24hr)
Actual Temperature
Modeled Temperature

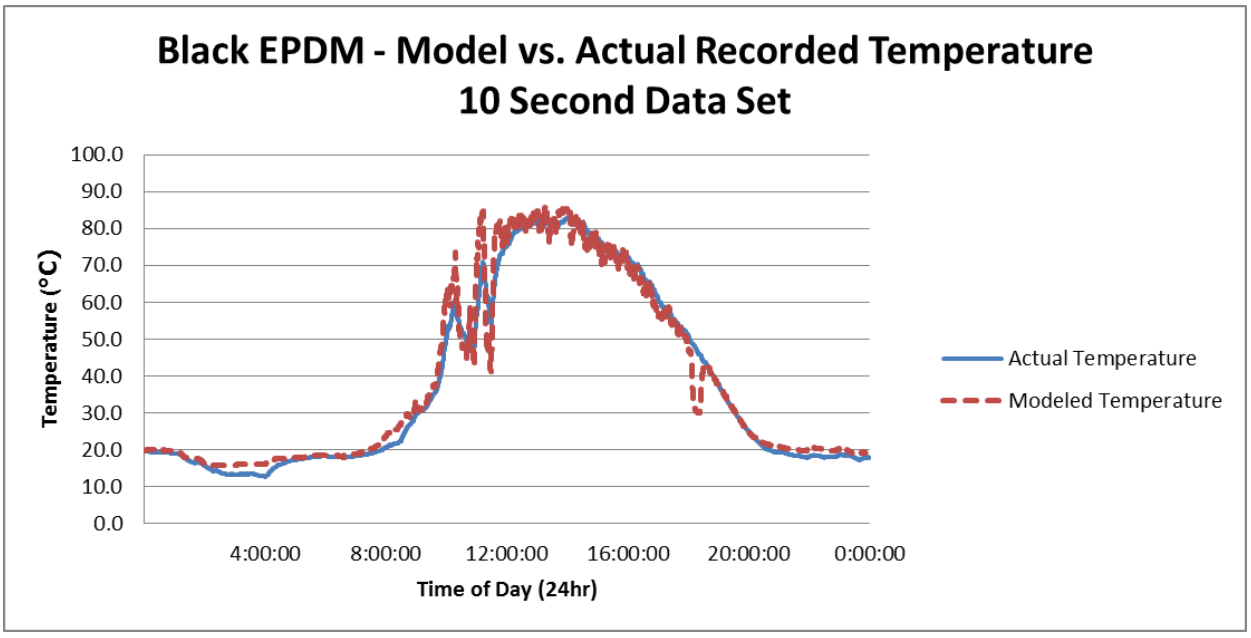
Black EPDM - Model vs. Actual Recorded Temperature
10 Second Data Set
Temperature (°C)
100.0
90.0
80.0
70.0
60.0
50.0
40.0
30.0
20.0
10.0
0.0
4:00:00
8:00:00
12:00:00
16:00:00
20:00:00
0:00:00
Time of Day (24hr)
Actual Temperature
Modeled Temperature

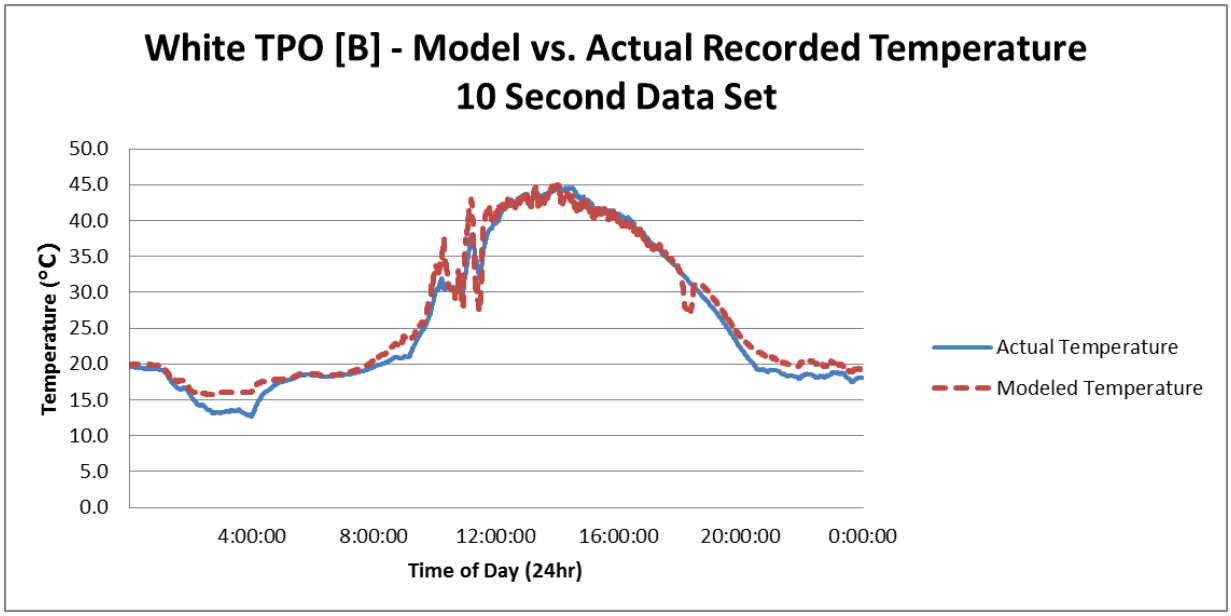
White TPO [B] - Model vs. Actual Recorded Temperature
10 Second Data Set
Temperature (°C)
50.0
45.0
40.0
35.0
30.0
25.0
20.0
15.0
10.0
5.0
0.0
4:00:00
8:00:00
12:00:00
16:00:00
20:00:00
0:00:00
Time of Day (24hr)
Actual Temperature
Modeled Temperature

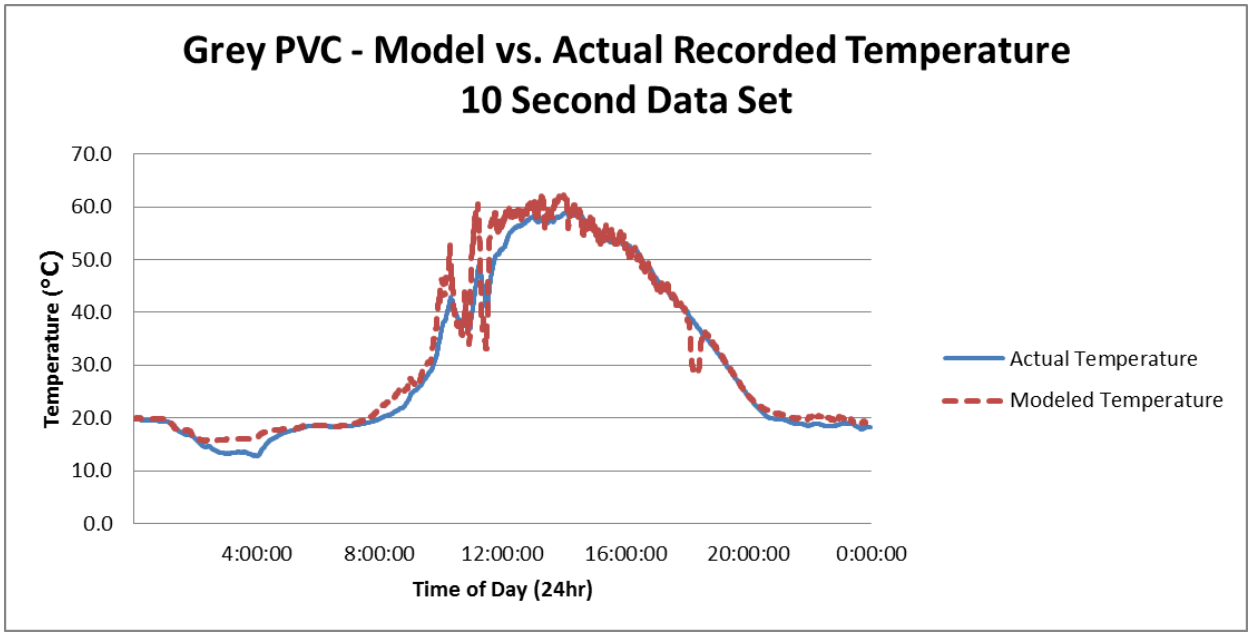
Grey PVC - Model vs. Actual Recorded Temperature
10 Second Data Set
Temperature (°C)
70.0
60.0
50.0
40.0
30.0
20.0
10.0
0.0
4:00:00
8:00:00
12:00:00
16:00:00
20:00:00
0:00:00
Time of Day (24hr)
Actual Temperature
Modeled Temperature

August 19, 2010

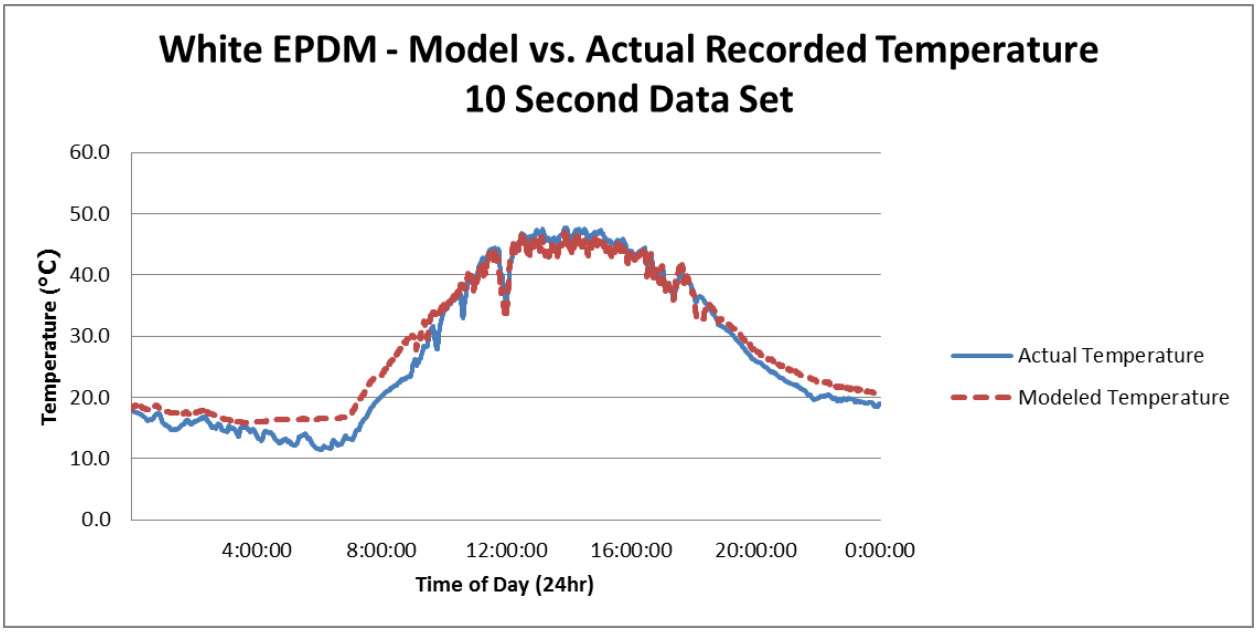
White EPDM - Model vs. Actual Recorded Temperature
10 Second Data Set
Temperature (°C)
60.0
50.0
40.0
30.0
20.0
10.0
0.0
4:00:00
8:00:00
12:00:00
16:00:00
20:00:00
0:00:00
Time of Day (24hr)
Actual Temperature
Modeled Temperature

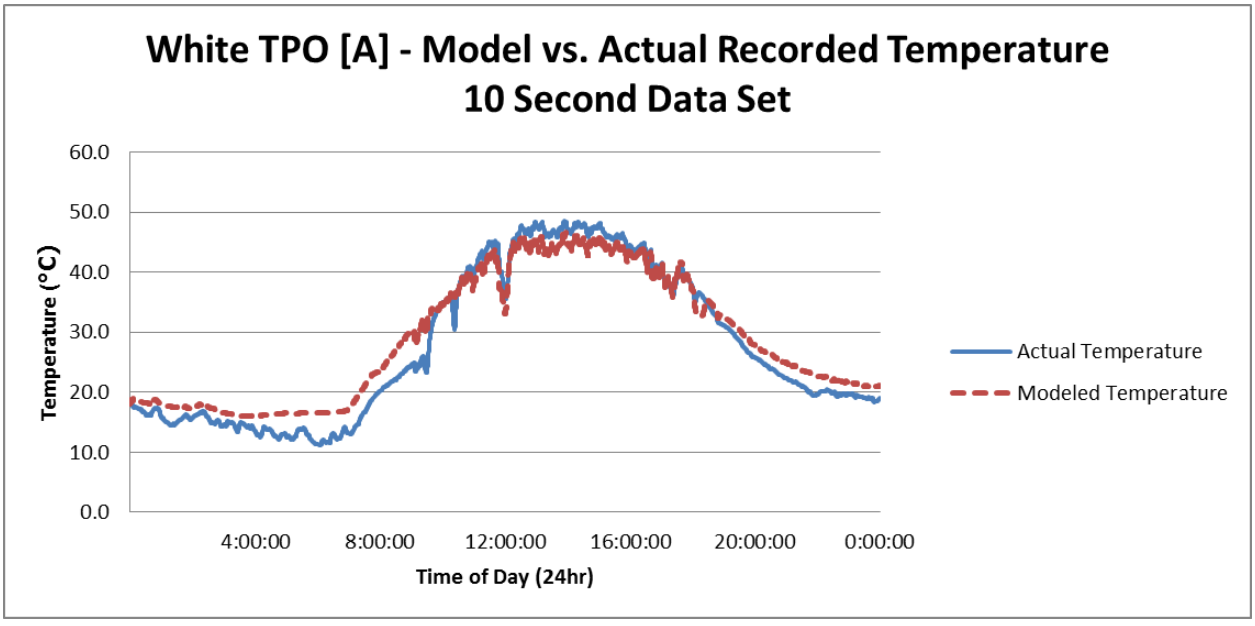
White TPO [A] - Model vs. Actual Recorded Temperature
10 Second Data Set
Temperature (°C)
60.0
50.0
40.0
30.0
20.0
10.0
0.0
4:00:00
8:00:00
12:00:00
16:00:00
20:00:00
0:00:00
Time of Day (24hr)
Actual Temperature
Modeled Temperature

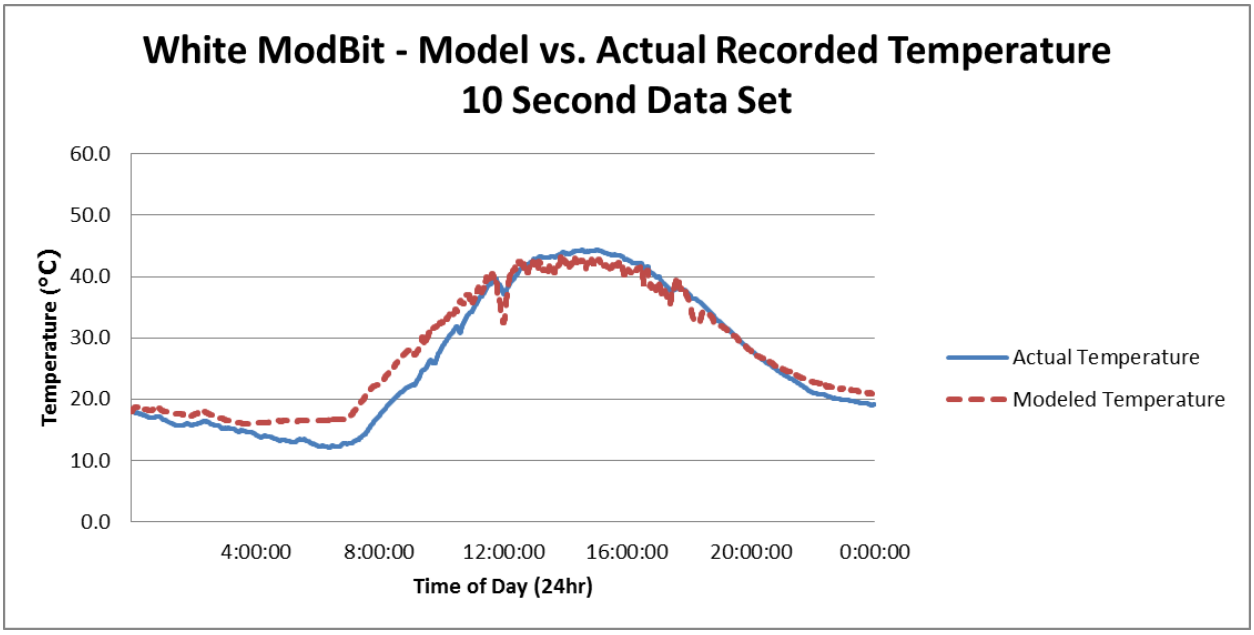
White ModBit - Model vs. Actual Recorded Temperature
10 Second Data Set
Temperature (°C)
60.0
50.0
40.0
30.0
20.0
10.0
0.0
4:00:00
8:00:00
12:00:00
16:00:00
20:00:00
0:00:00
Time of Day (24hr)
Actual Temperature
Modeled Temperature

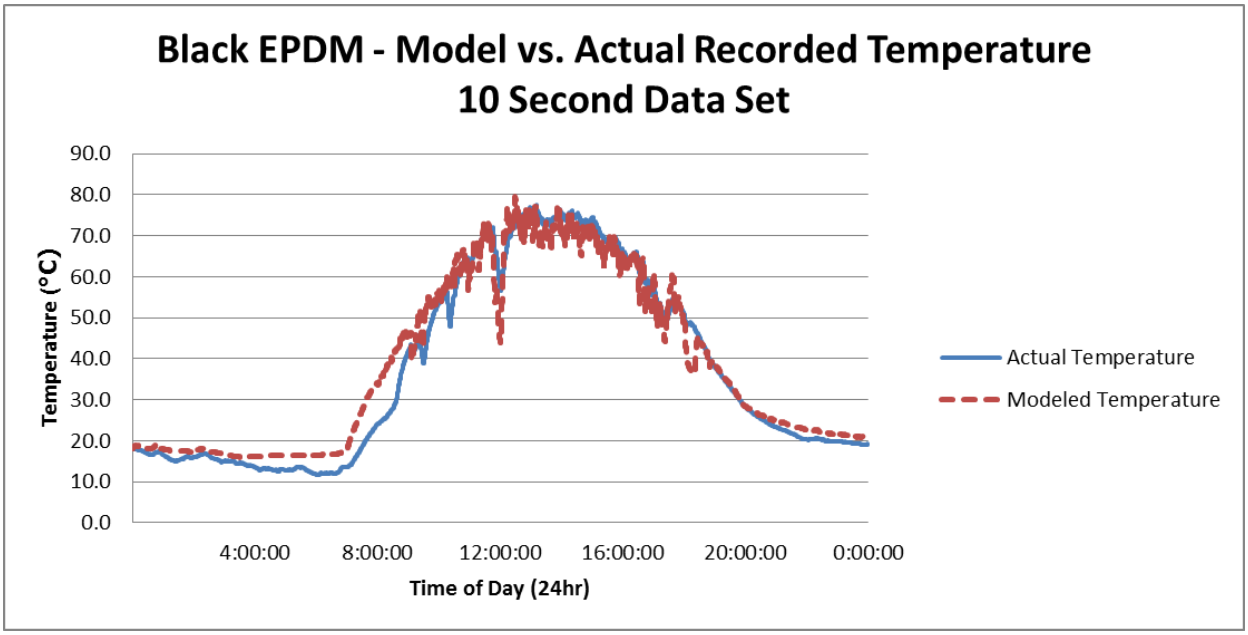
Black EPDM - Model vs. Actual Recorded Temperature
10 Second Data Set
Temperature (°C)
90.0
80.0
70.0
60.0
50.0
40.0
30.0
20.0
10.0
0.0
4:00:00
8:00:00
12:00:00
16:00:00
20:00:00
0:00:00
Time of Day (24hr)
Actual Temperature
Modeled Temperature

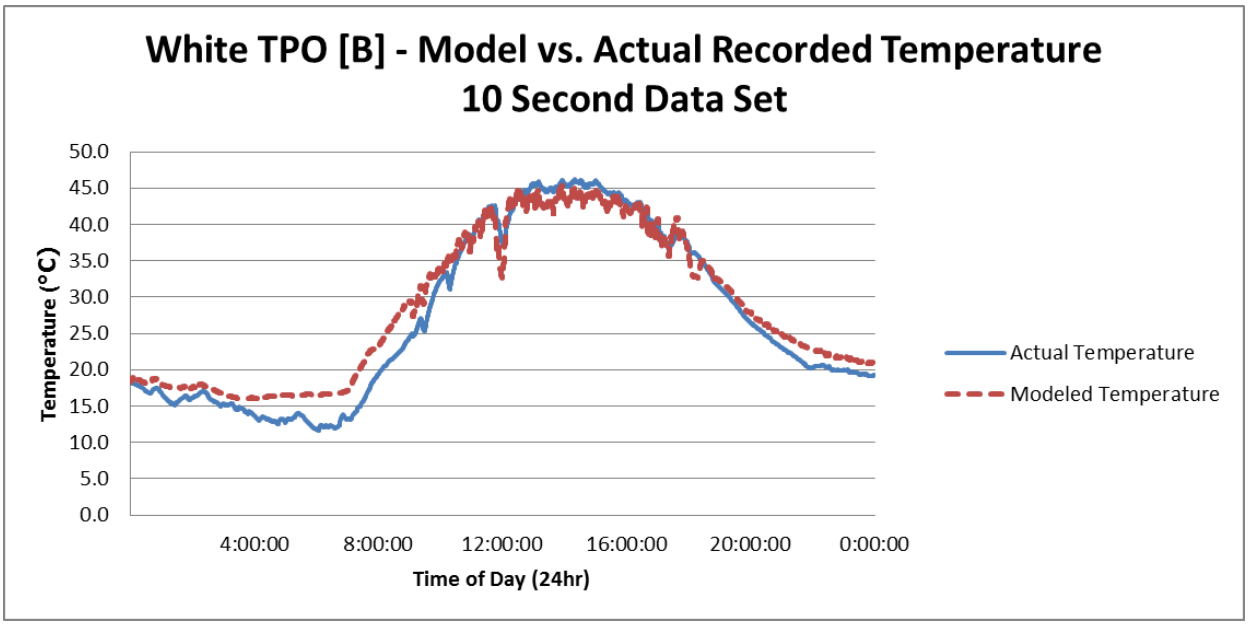
White TPO [B] - Model vs. Actual Recorded Temperature
10 Second Data Set
Temperature (°C)
50.0
45.0
40.0
35.0
30.0
25.0
20.0
15.0
10.0
5.0
0.0
4:00:00
8:00:00
12:00:00
16:00:00
20:00:00
0:00:00
Time of Day (24hr)
Actual Temperature
Modeled Temperature

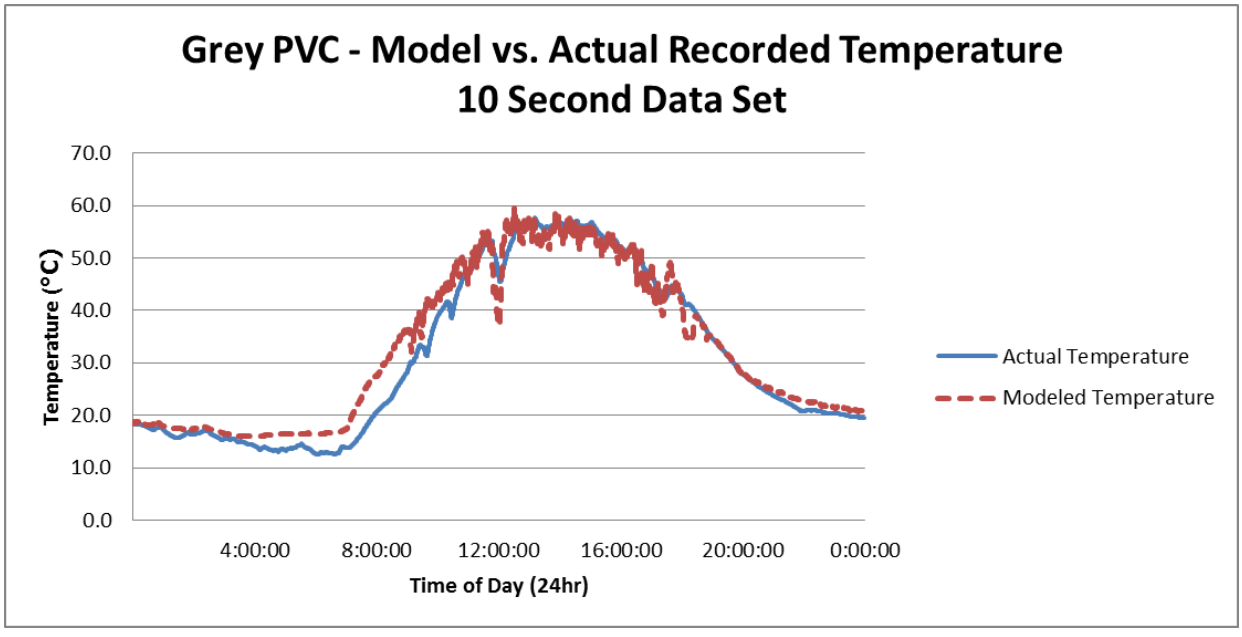
Grey PVC - Model vs. Actual Recorded Temperature
10 Second Data Set
Temperature (°C)
70.0
60.0
50.0
40.0
30.0
20.0
10.0
0.0
4:00:00
8:00:00
12:00:00
16:00:00
20:00:00
0:00:00
Time of Day (24hr)
Actual Temperature
Modeled Temperature

August 20, 2010

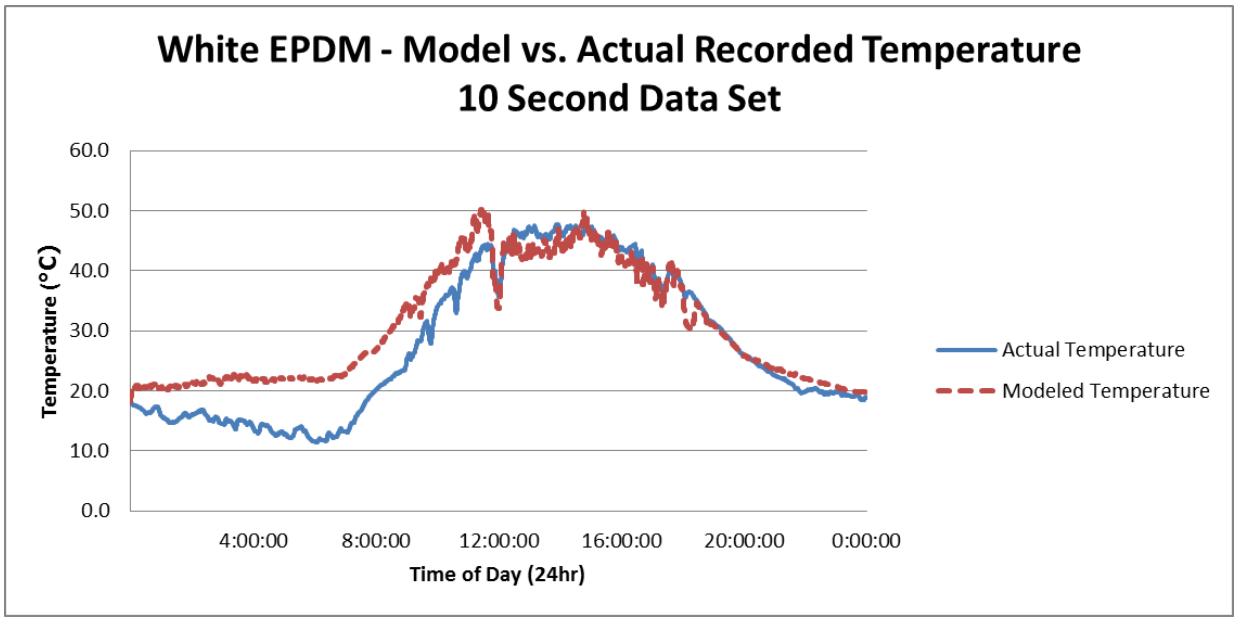
White EPDM - Model vs. Actual Recorded Temperature
10 Second Data Set
60.0
50.0
40.0
30.0
20.0
10.0
0.0
Temperature (°C)
4:00:00
8:00:00
12:00:00
16:00:00
20:00:00
0:00:00
Time of Day (24hr)
Actual Temperature
Modeled Temperature

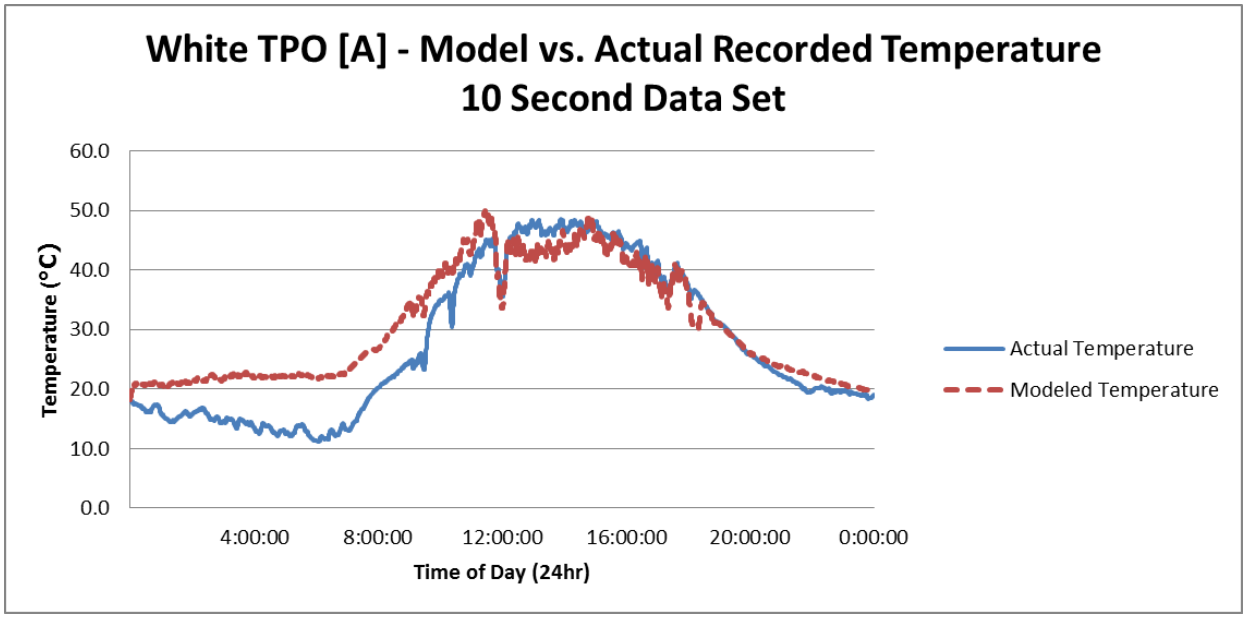
White TPO [A] - Model vs. Actual Recorded Temperature
10 Second Data Set
60.0
50.0
40.0
30.0
20.0
10.0
0.0
Temperature (°C)
4:00:00
8:00:00
12:00:00
16:00:00
20:00:00
0:00:00
Time of Day (24hr)
Actual Temperature
Modeled Temperature

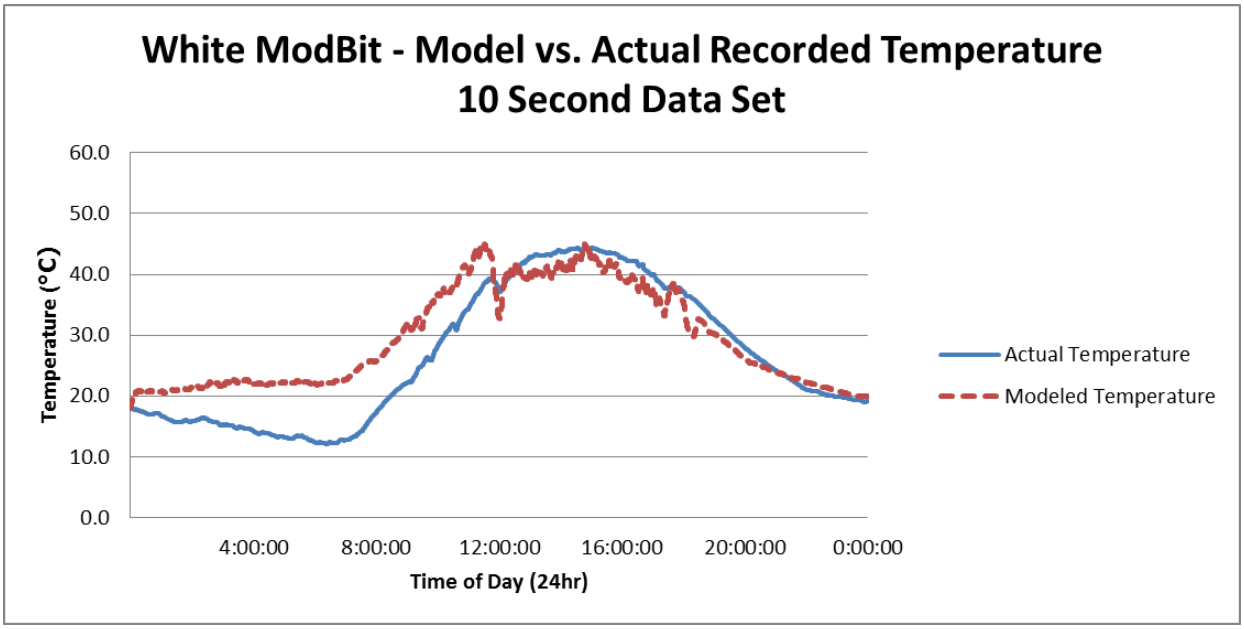
White ModBit - Model vs. Actual Recorded Temperature
10 Second Data Set
Temperature (°C)
60.0
50.0
40.0
30.0
20.0
10.0
0.0
4:00:00
8:00:00
12:00:00
16:00:00
20:00:00
0:00:00
Time of Day (24hr)
Actual Temperature
Modeled Temperature

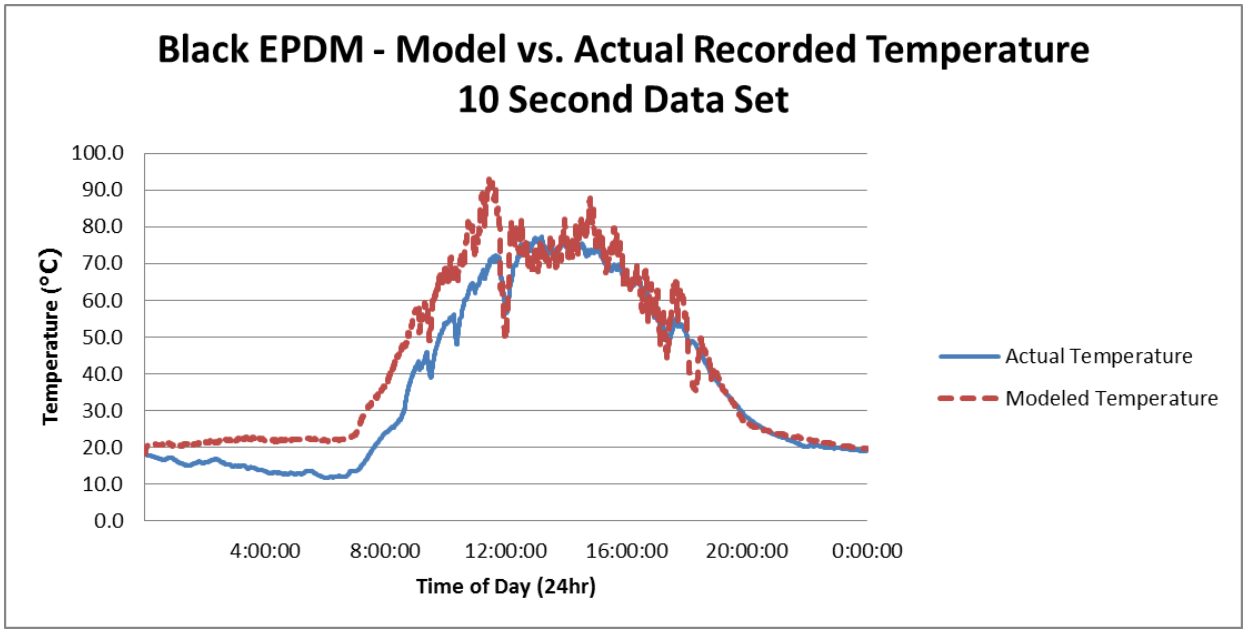
Black EPDM - Model vs. Actual Recorded Temperature
10 Second Data Set
Temperature (°C)
100.0
90.0
80.0
70.0
60.0
50.0
40.0
30.0
20.0
10.0
0.0
4:00:00
8:00:00
12:00:00
16:00:00
20:00:00
0:00:00
Time of Day (24hr)
Actual Temperature
Modeled Temperature

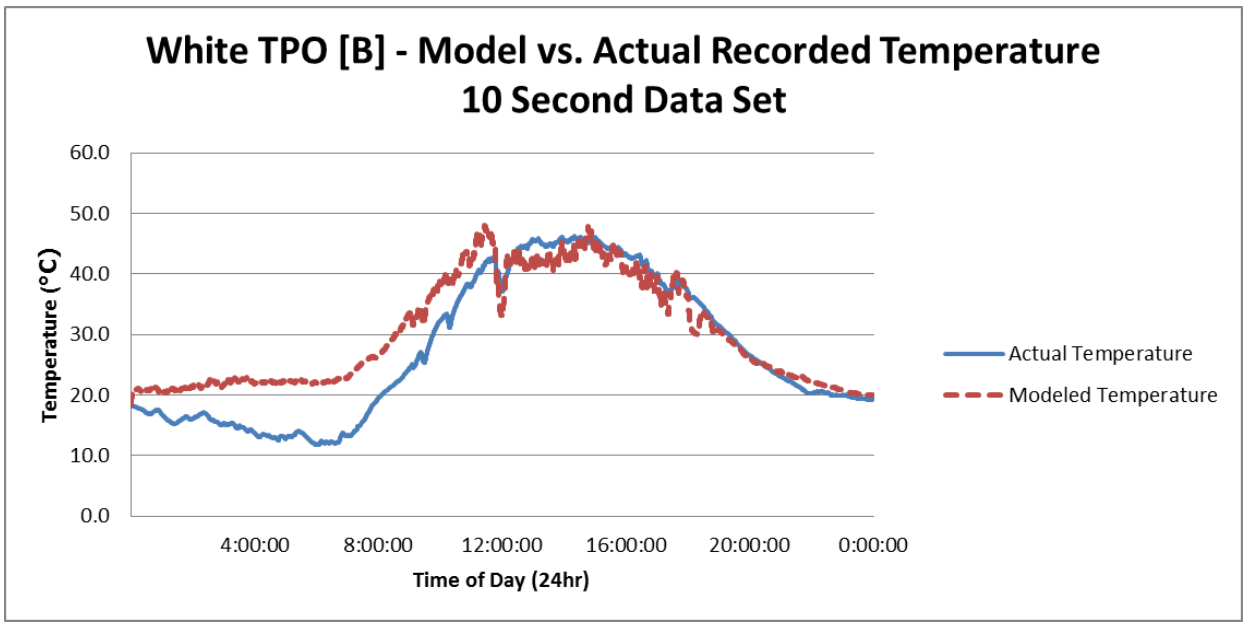
White TPO [B] - Model vs. Actual Recorded Temperature
10 Second Data Set
60.0
50.0
40.0
30.0
20.0
10.0
0.0
Temperature (°C)
4:00:00
8:00:00
12:00:00
16:00:00
20:00:00
0:00:00
Time of Day (24hr)
Actual Temperature
Modeled Temperature

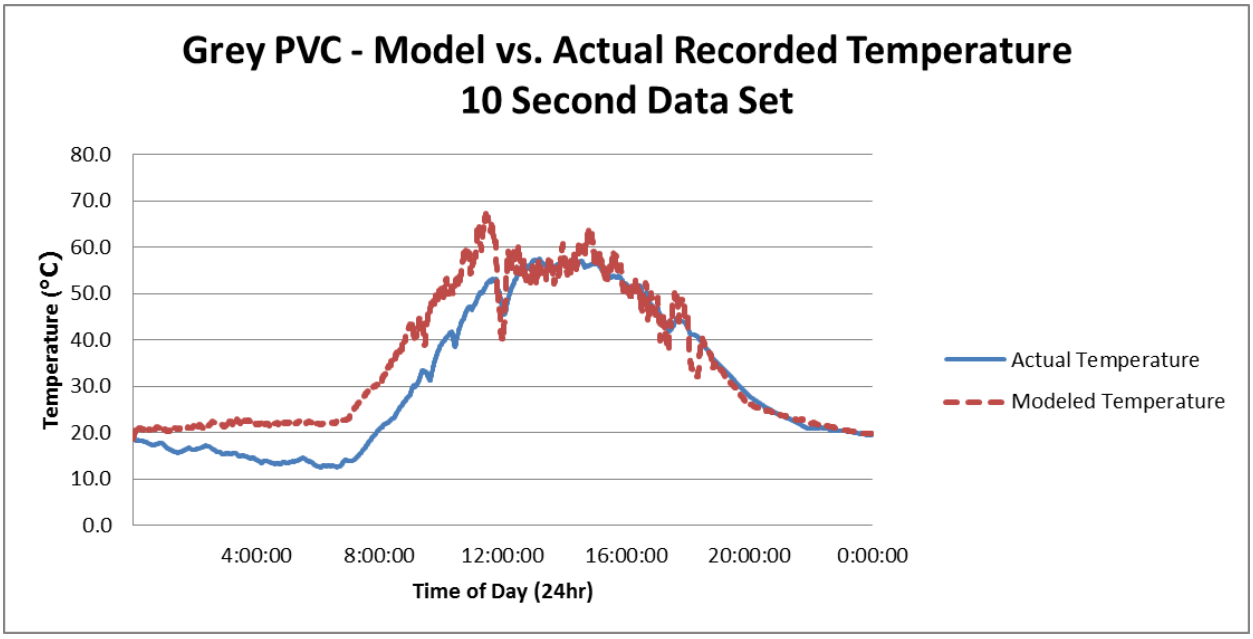
Grey PVC - Model vs. Actual Recorded Temperature
10 Second Data Set
80.0
70.0
60.0
50.0
40.0
30.0
20.0
10.0
0.0
Temperature (°C)
4:00:00
8:00:00
12:00:00
16:00:00
20:00:00
0:00:00
Time of Day (24hr)
Actual Temperature
Modeled Temperature

August 21, 2010

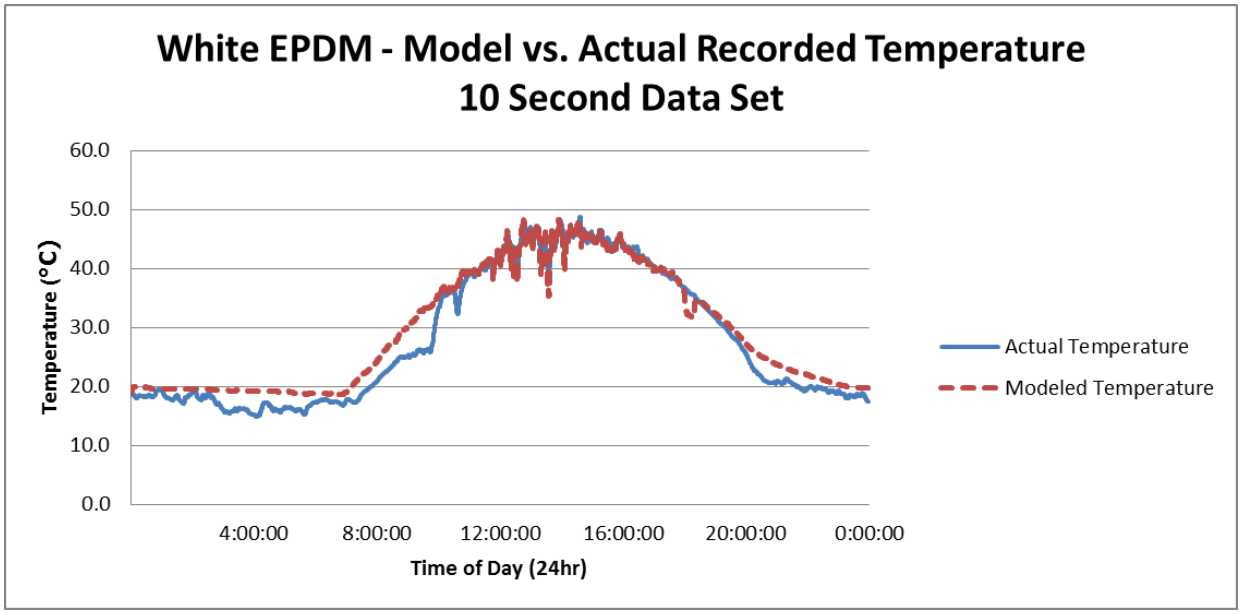
White EPDM - Model vs. Actual Recorded Temperature
10 Second Data Set
Temperature (°C)
60.0
50.0
40.0
30.0
20.0
10.0
0.0
4:00:00
8:00:00
12:00:00
16:00:00
20:00:00
0:00:00
Time of Day (24hr)
Actual Temperature
Modeled Temperature

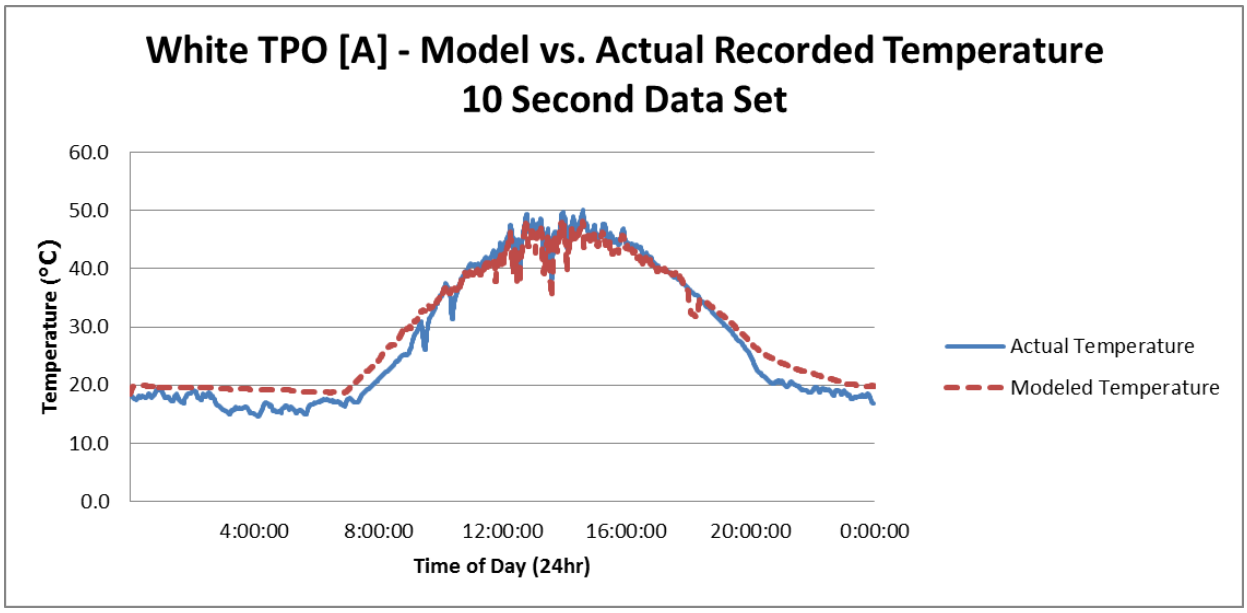
White TPO [A] - Model vs. Actual Recorded Temperature
10 Second Data Set
Temperature (°C)
60.0
50.0
40.0
30.0
20.0
10.0
0.0
4:00:00
8:00:00
12:00:00
16:00:00
20:00:00
0:00:00
Time of Day (24hr)
Actual Temperature
Modeled Temperature

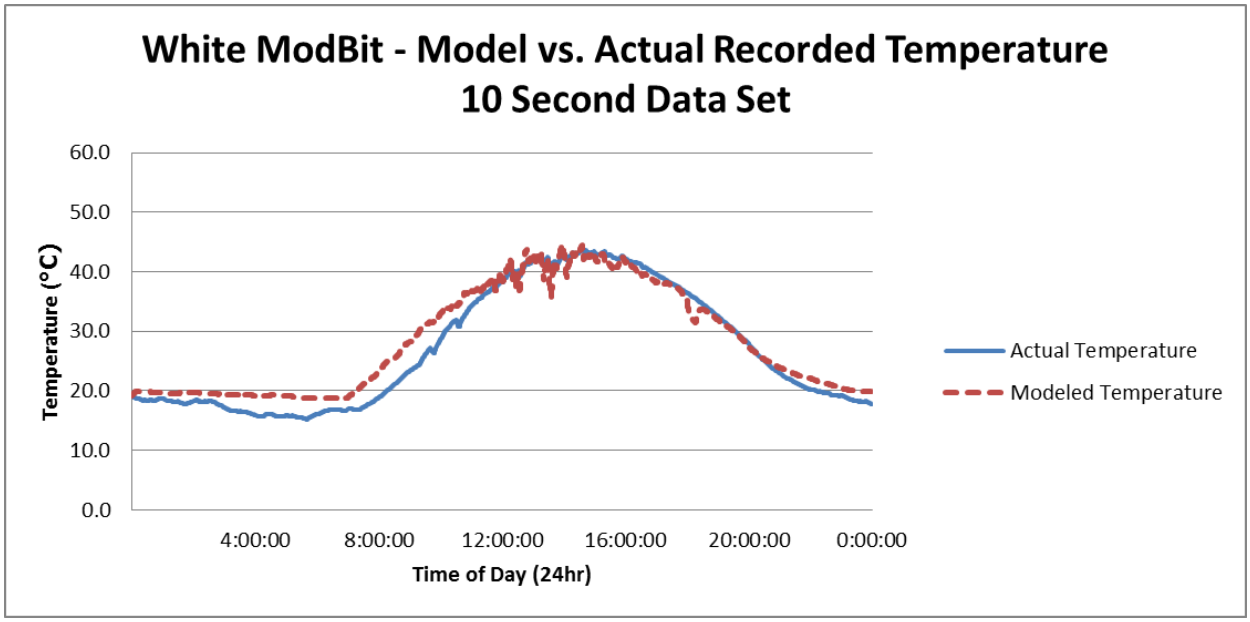
White ModBit - Model vs. Actual Recorded Temperature
10 Second Data Set
Temperature (°C)
60.0
50.0
40.0
30.0
20.0
10.0
0.0
4:00:00
8:00:00
12:00:00
16:00:00
20:00:00
0:00:00
Time of Day (24hr)
Actual Temperature
Modeled Temperature

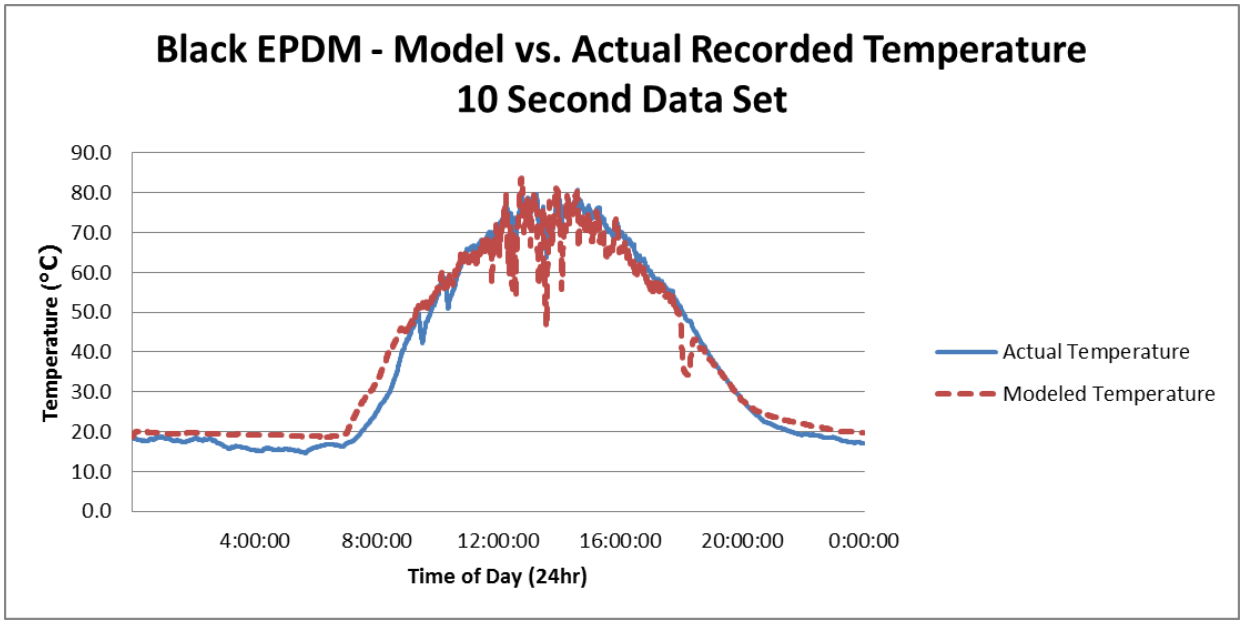
Black EPDM - Model vs. Actual Recorded Temperature
10 Second Data Set
Temperature (°C)
90.0
80.0
70.0
60.0
50.0
40.0
30.0
20.0
10.0
0.0
4:00:00
8:00:00
12:00:00
16:00:00
20:00:00
0:00:00
Time of Day (24hr)
Actual Temperature
Modeled Temperature

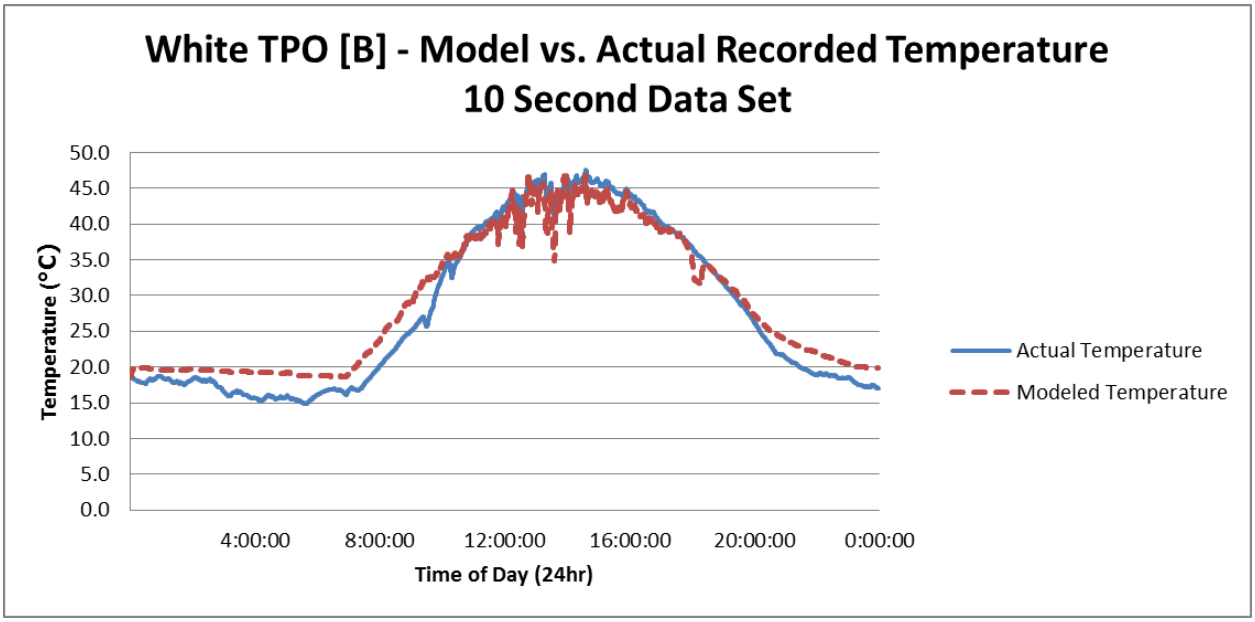
White TPO [B] - Model vs. Actual Recorded Temperature
10 Second Data Set
Temperature (°C)
50.0
45.0
40.0
35.0
30.0
25.0
20.0
15.0
10.0
5.0
0.0
4:00:00
8:00:00
12:00:00
16:00:00
20:00:00
0:00:00
Time of Day (24hr)
Actual Temperature
Modeled Temperature

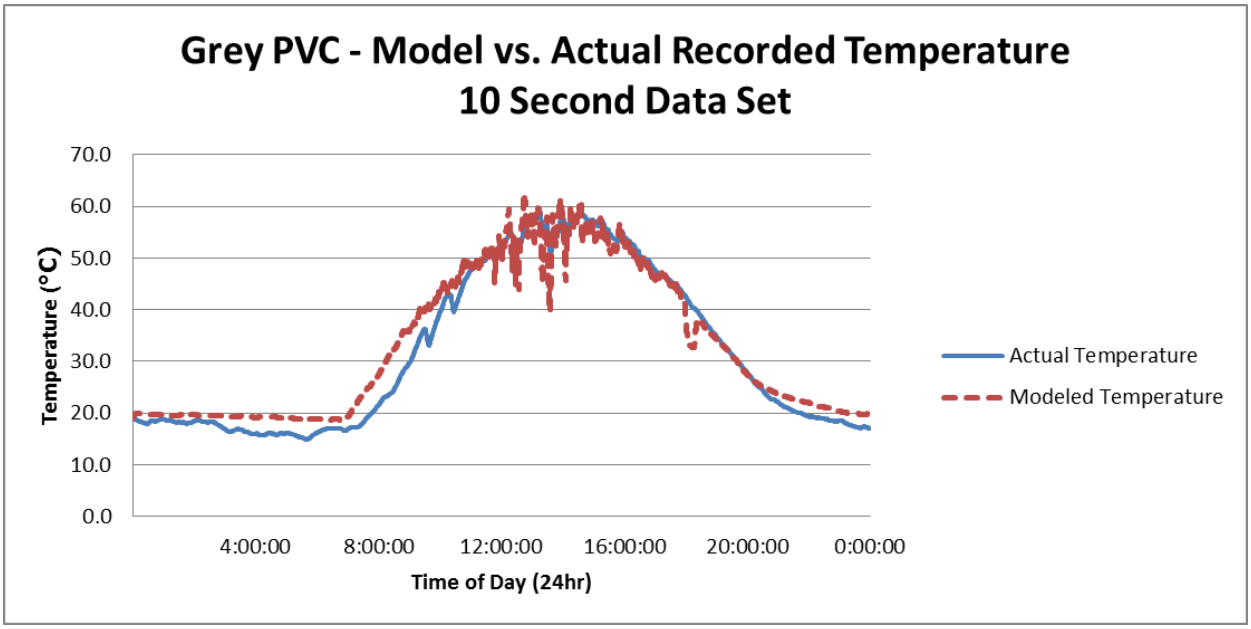
Grey PVC - Model vs. Actual Recorded Temperature
10 Second Data Set
Temperature (°C)
70.0
60.0
50.0
40.0
30.0
20.0
10.0
0.0
4:00:00
8:00:00
12:00:00
16:00:00
20:00:00
0:00:00
Time of Day (24hr)
Actual Temperature
Modeled Temperature

August 22, 2010

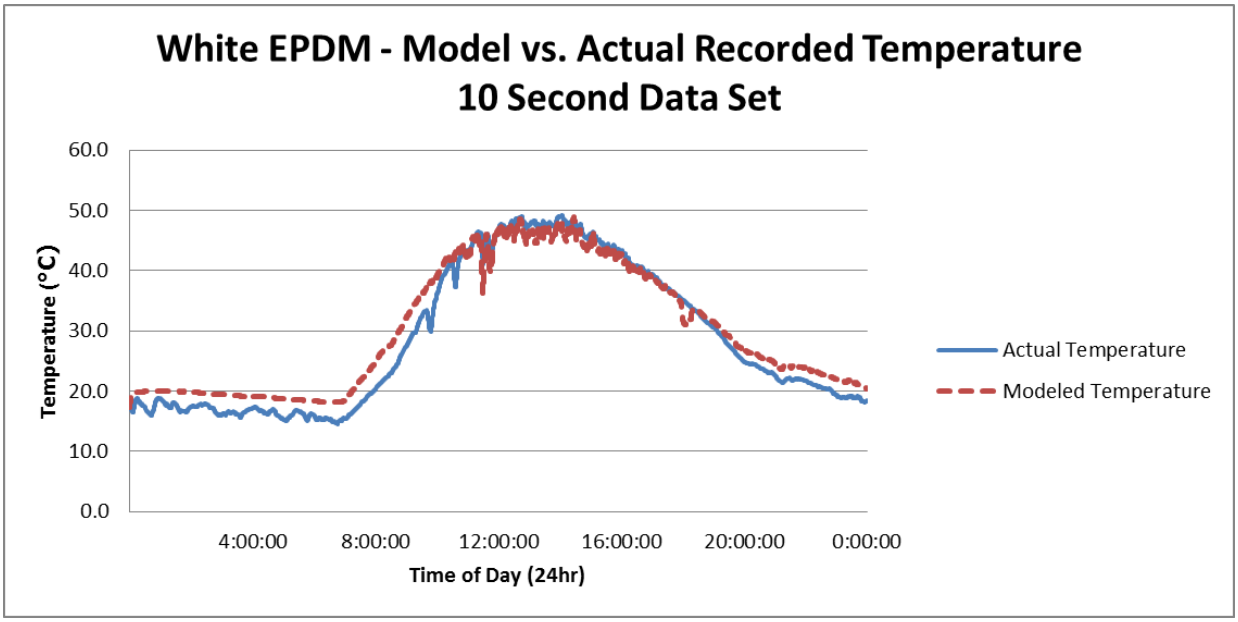
White EPDM - Model vs. Actual Recorded Temperature
10 Second Data Set
60.0
50.0
40.0
30.0
20.0
10.0
0.0
Temperature (°C)
4:00:00
8:00:00
12:00:00
16:00:00
20:00:00
0:00:00
Time of Day (24hr)
Actual Temperature
Modeled Temperature

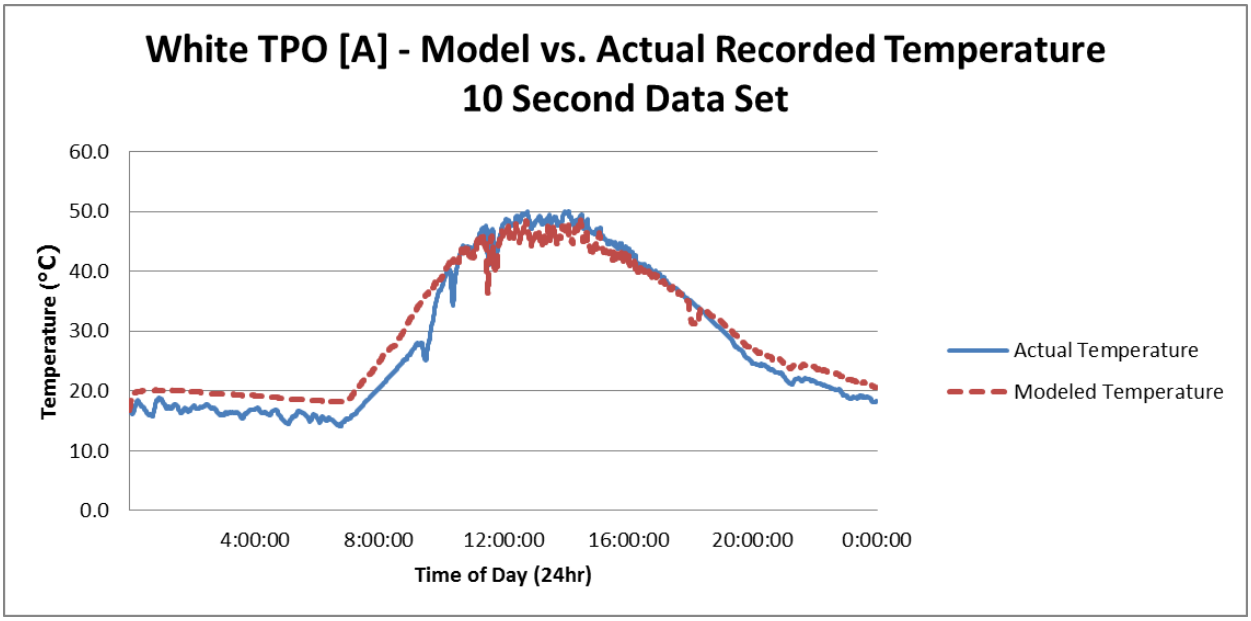
White TPO [A] - Model vs. Actual Recorded Temperature
10 Second Data Set
60.0
50.0
40.0
30.0
20.0
10.0
0.0
Temperature (°C)
4:00:00
8:00:00
12:00:00
16:00:00
20:00:00
0:00:00
Time of Day (24hr)
Actual Temperature
Modeled Temperature

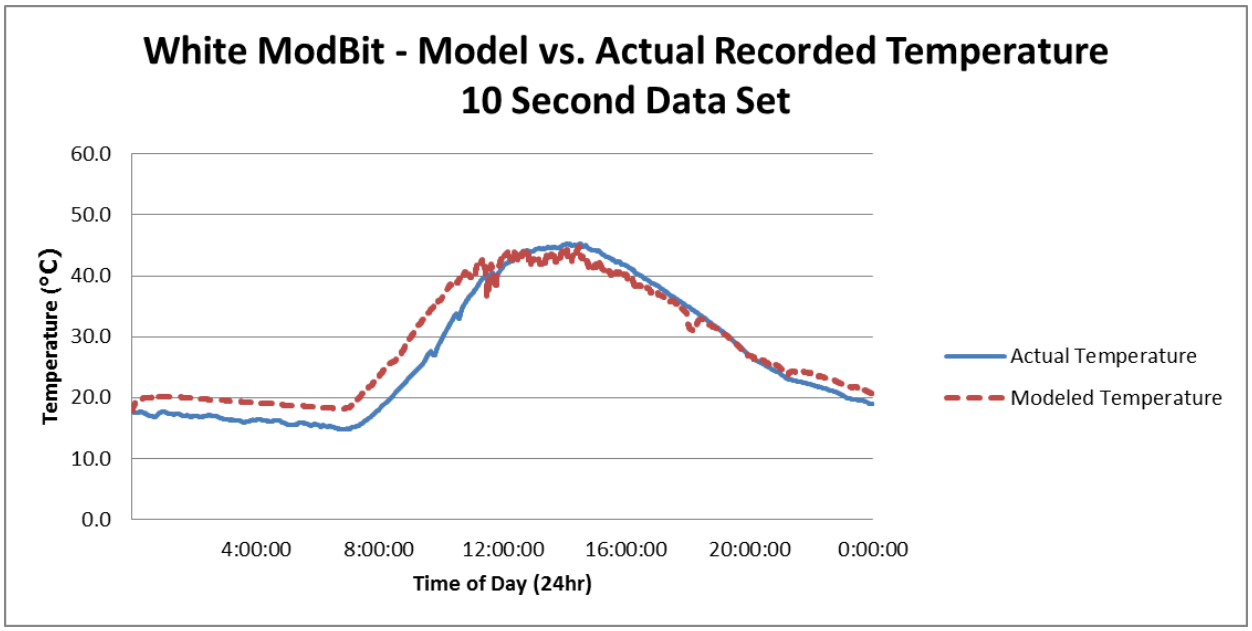
White ModBit - Model vs. Actual Recorded Temperature
10 Second Data Set
Temperature (°C)
60.0
50.0
40.0
30.0
20.0
10.0
0.0
4:00:00
8:00:00
12:00:00
16:00:00
20:00:00
0:00:00
Time of Day (24hr)
Actual Temperature
Modeled Temperature

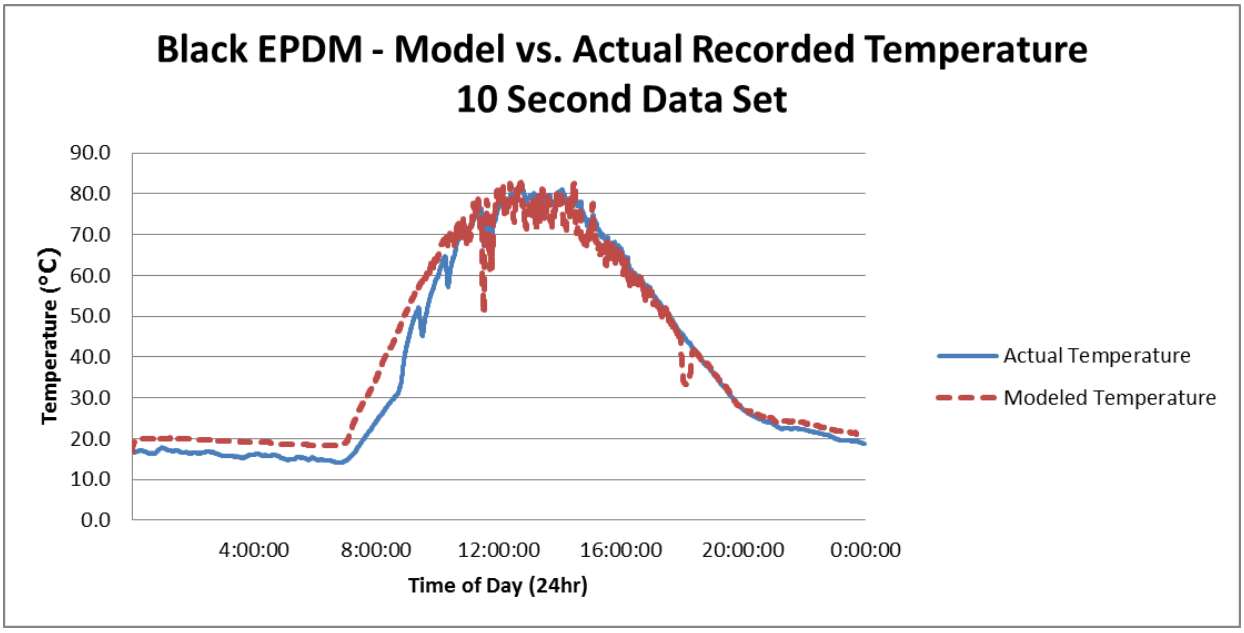
Black EPDM - Model vs. Actual Recorded Temperature
10 Second Data Set
Temperature (°C)
90.0
80.0
70.0
60.0
50.0
40.0
30.0
20.0
10.0
0.0
4:00:00
8:00:00
12:00:00
16:00:00
20:00:00
0:00:00
Time of Day (24hr)
Actual Temperature
Modeled Temperature

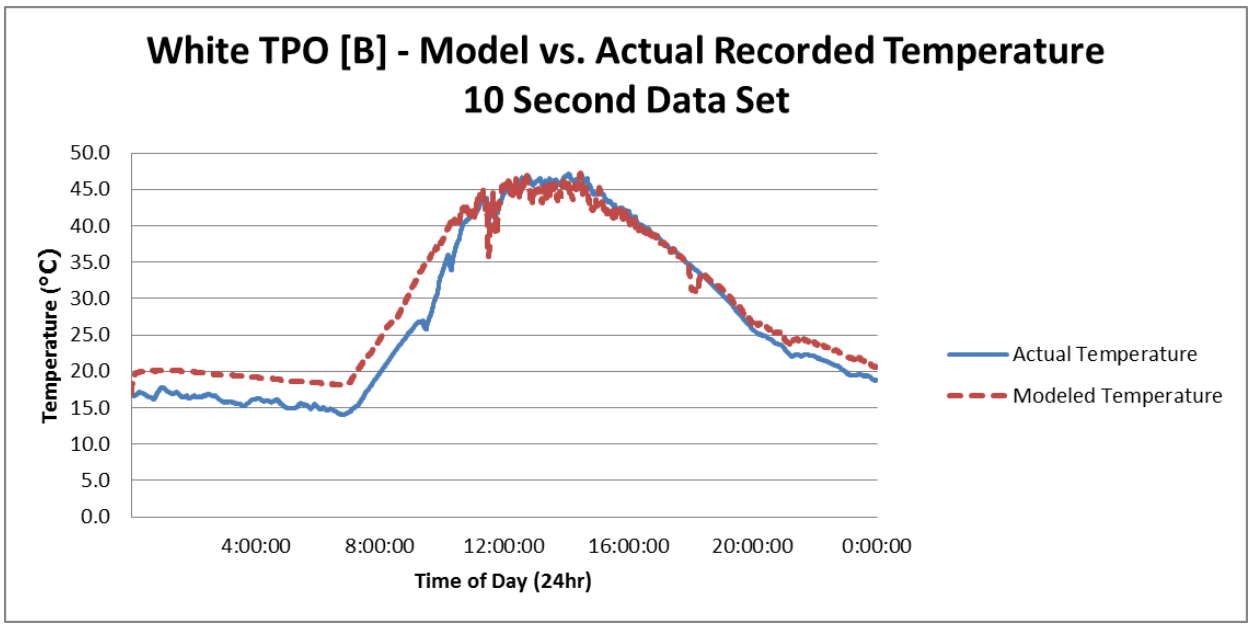
White TPO [B] - Model vs. Actual Recorded Temperature
10 Second Data Set
Temperature (°C)
50.0
45.0
40.0
35.0
30.0
25.0
20.0
15.0
10.0
5.0
0.0
4:00:00
8:00:00
12:00:00
16:00:00
20:00:00
0:00:00
Time of Day (24hr)
Actual Temperature
Modeled Temperature

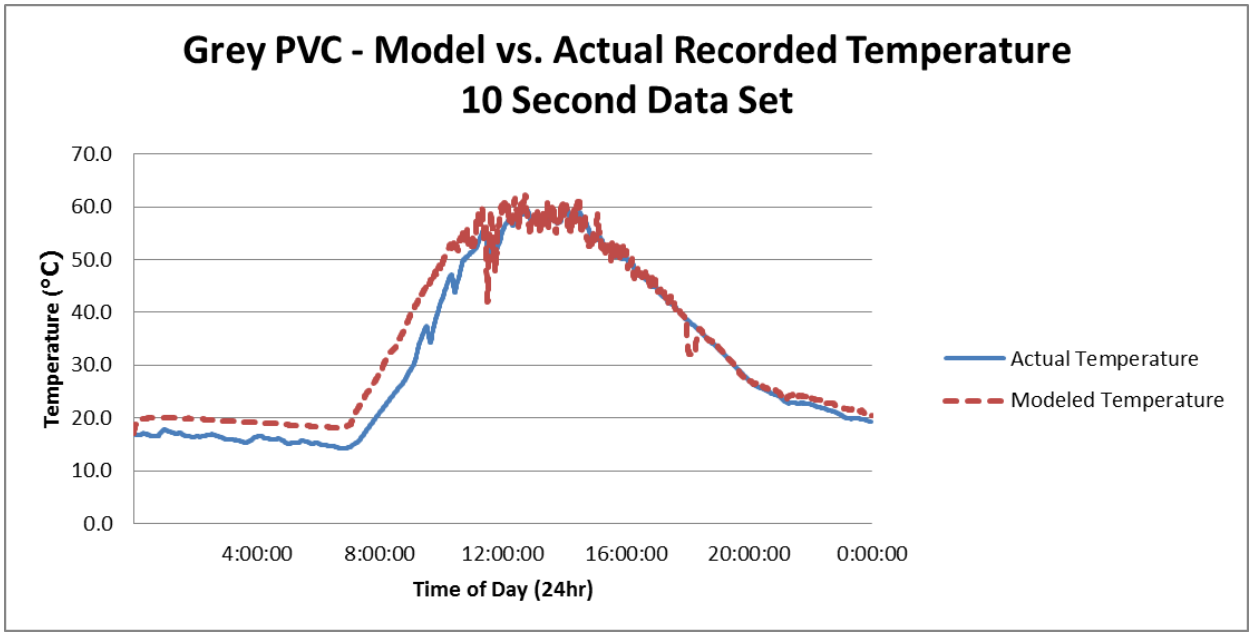
Grey PVC - Model vs. Actual Recorded Temperature
10 Second Data Set
Temperature (°C)
70.0
60.0
50.0
40.0
30.0
20.0
10.0
0.0
4:00:00
8:00:00
12:00:00
16:00:00
20:00:00
0:00:00
Time of Day (24hr)
Actual Temperature
Modeled Temperature

August 23, 2010

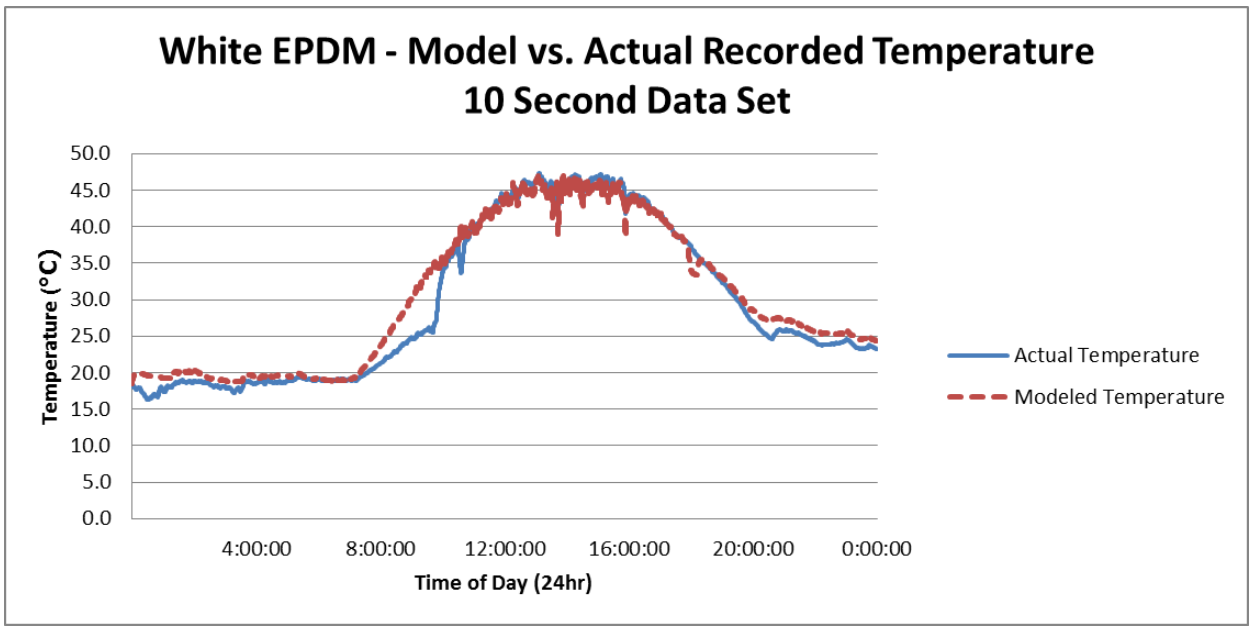
White EPDM - Model vs. Actual Recorded Temperature
10 Second Data Set
Temperature (°C)
50.0
45.0
40.0
35.0
30.0
25.0
20.0
15.0
10.0
5.0
0.0
4:00:00
8:00:00
12:00:00
16:00:00
20:00:00
0:00:00
Time of Day (24hr)
Actual Temperature
Modeled Temperature

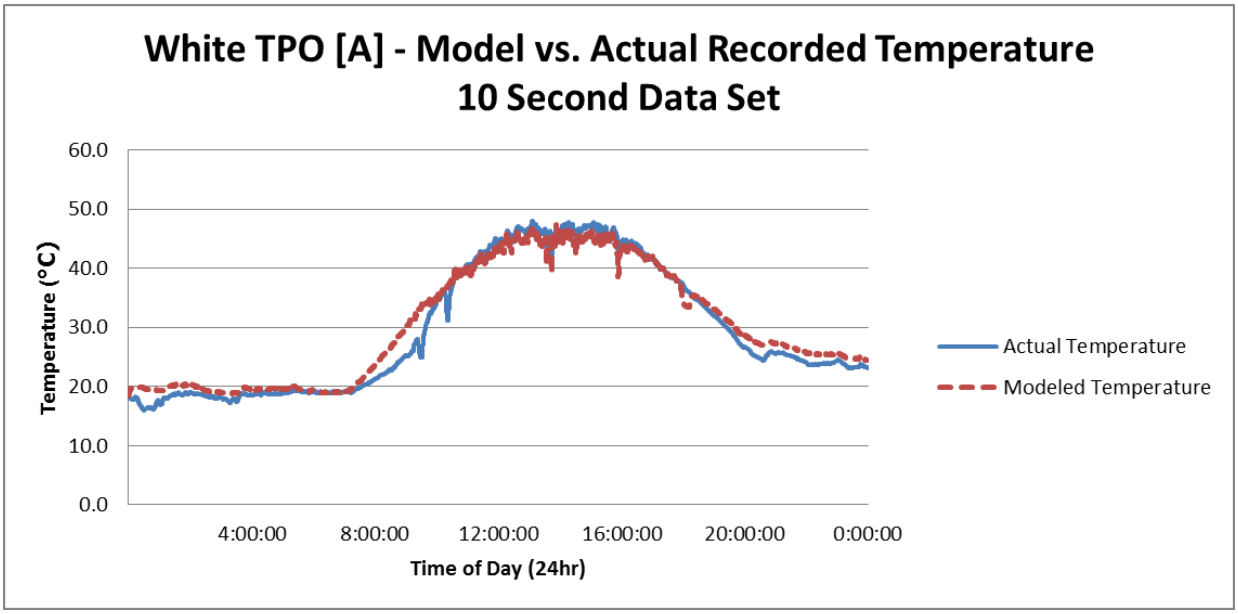
White TPO [A] - Model vs. Actual Recorded Temperature
10 Second Data Set
Temperature (°C)
60.0
50.0
40.0
30.0
20.0
10.0
0.0
4:00:00
8:00:00
12:00:00
16:00:00
20:00:00
0:00:00
Time of Day (24hr)
Actual Temperature
Modeled Temperature

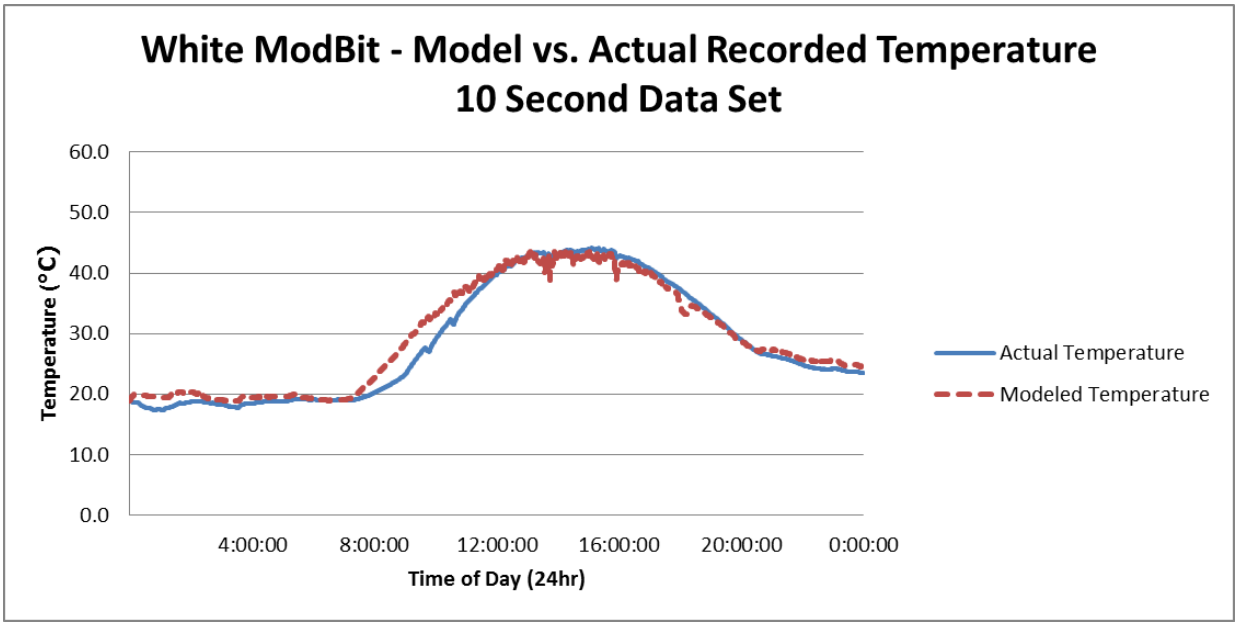
White ModBit - Model vs. Actual Recorded Temperature
10 Second Data Set
Temperature (°C)
60.0
50.0
40.0
30.0
20.0
10.0
0.0
4:00:00
8:00:00
12:00:00
16:00:00
20:00:00
0:00:00
Time of Day (24hr)
Actual Temperature
Modeled Temperature

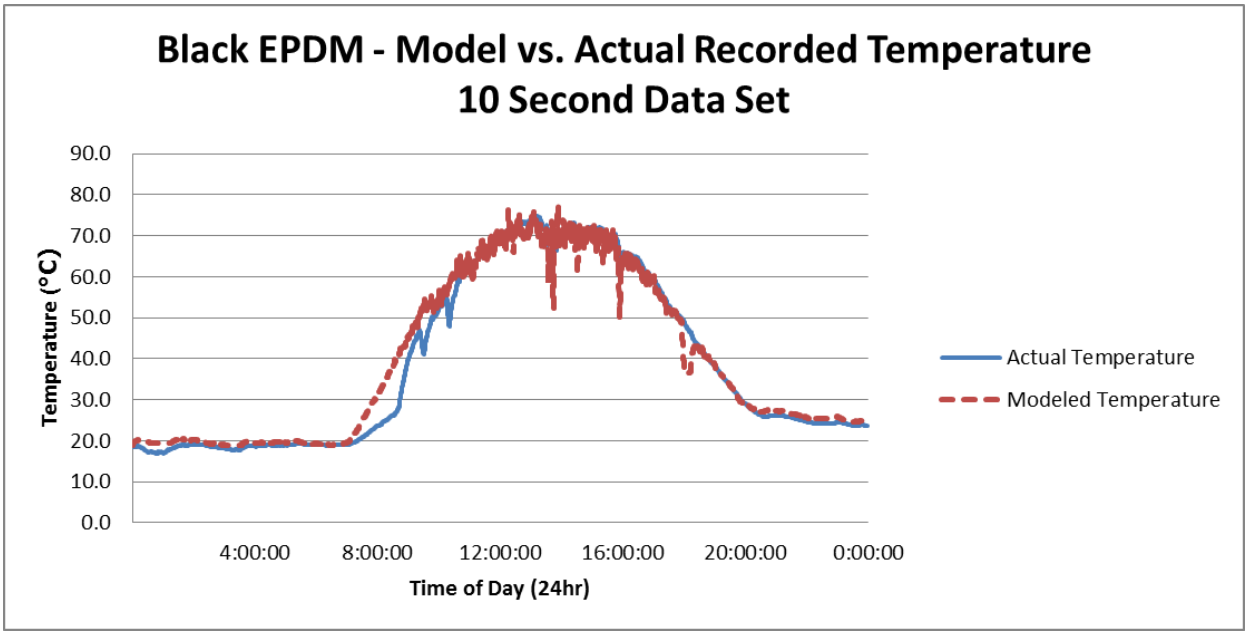
Black EPDM - Model vs. Actual Recorded Temperature
10 Second Data Set
Temperature (°C)
90.0
80.0
70.0
60.0
50.0
40.0
30.0
20.0
10.0
0.0
4:00:00
8:00:00
12:00:00
16:00:00
20:00:00
0:00:00
Time of Day (24hr)
Actual Temperature
Modeled Temperature

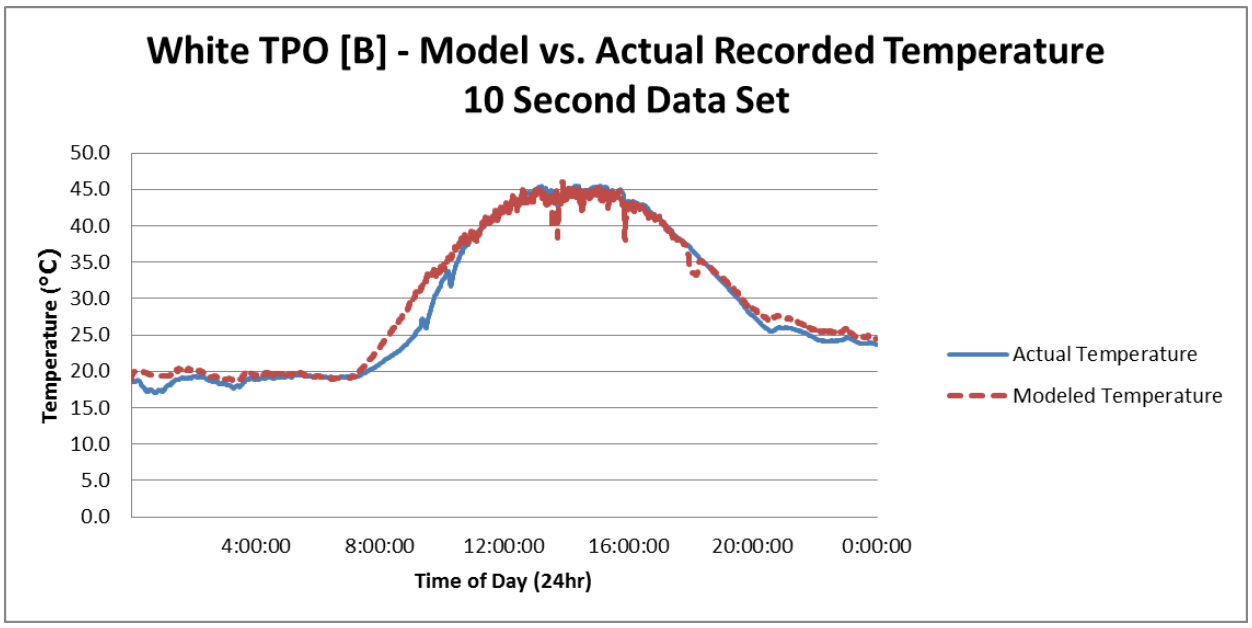
White TPO [B] - Model vs. Actual Recorded Temperature
10 Second Data Set
Temperature (°C)
50.0
45.0
40.0
35.0
30.0
25.0
20.0
15.0
10.0
5.0
0.0
4:00:00
8:00:00
12:00:00
16:00:00
20:00:00
0:00:00
Time of Day (24hr)
Actual Temperature
Modeled Temperature

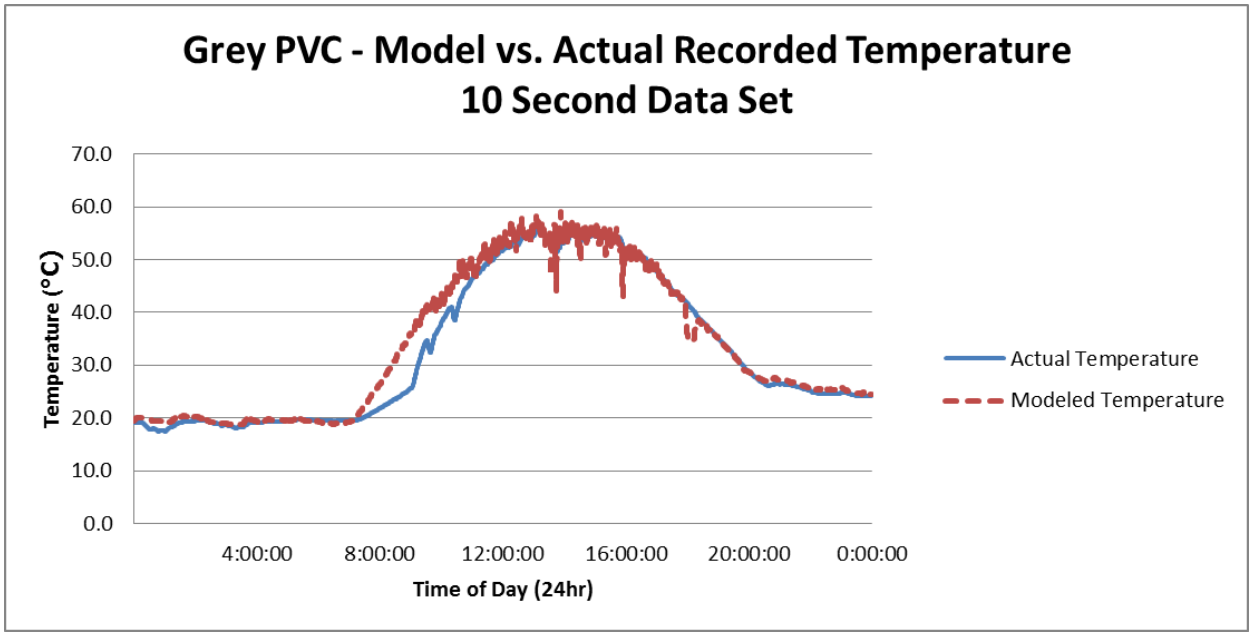
Grey PVC - Model vs. Actual Recorded Temperature
10 Second Data Set
Temperature (°C)
70.0
60.0
50.0
40.0
30.0
20.0
10.0
0.0
4:00:00
8:00:00
12:00:00
16:00:00
20:00:00
0:00:00
Time of Day (24hr)
Actual Temperature
Modeled Temperature

August 24, 2010

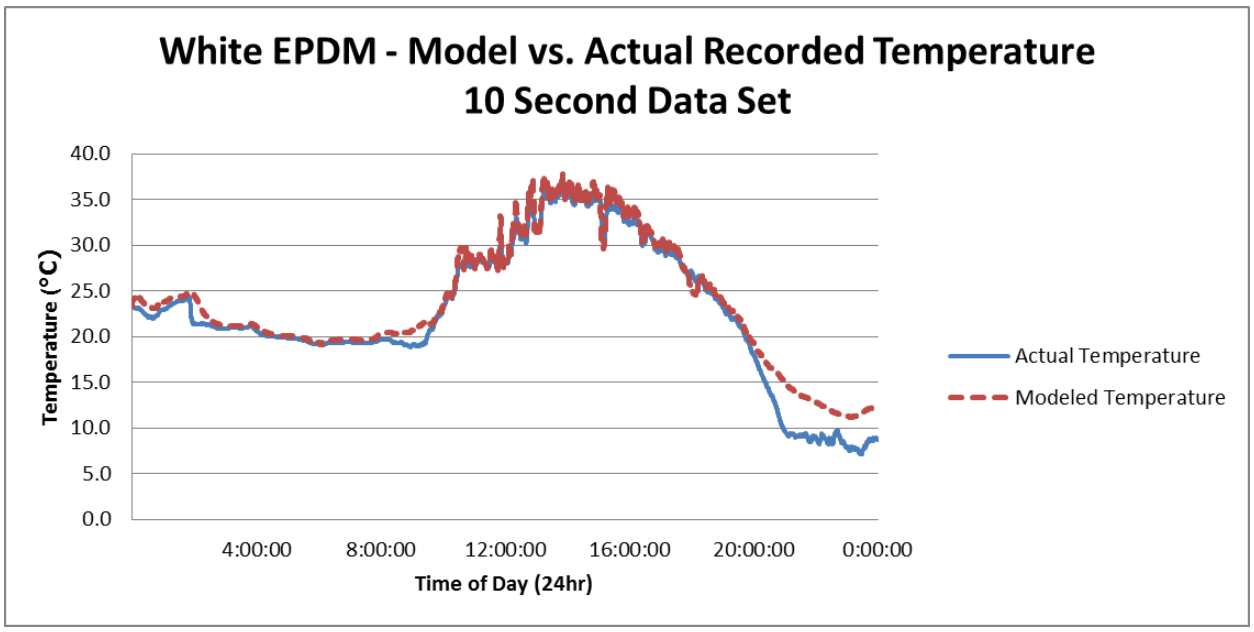
White EPDM - Model vs. Actual Recorded Temperature
10 Second Data Set
Temperature (°C)
40.0
35.0
30.0
25.0
20.0
15.0
10.0
5.0
0.0
4:00:00
8:00:00
12:00:00
16:00:00
20:00:00
0:00:00
Time of Day (24hr)
Actual Temperature
Modeled Temperature

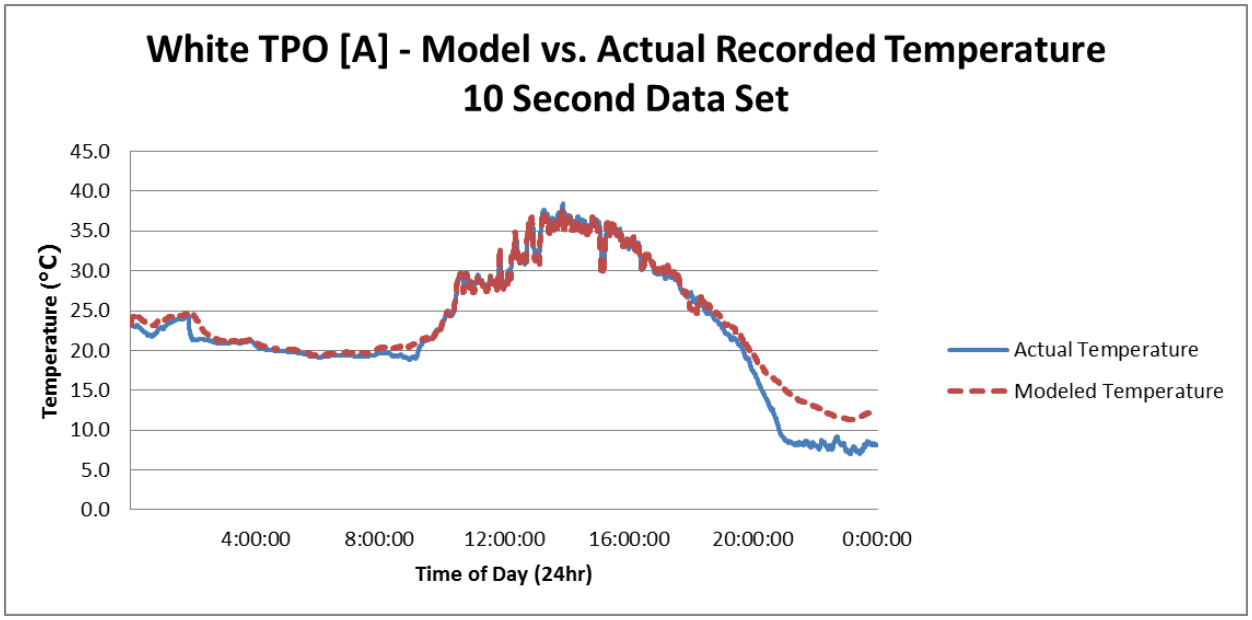
White TPO [A] - Model vs. Actual Recorded Temperature
10 Second Data Set
Temperature (°C)
45.0
40.0
35.0
30.0
25.0
20.0
15.0
10.0
5.0
0.0
4:00:00
8:00:00
12:00:00
16:00:00
20:00:00
0:00:00
Time of Day (24hr)
Actual Temperature
Modeled Temperature

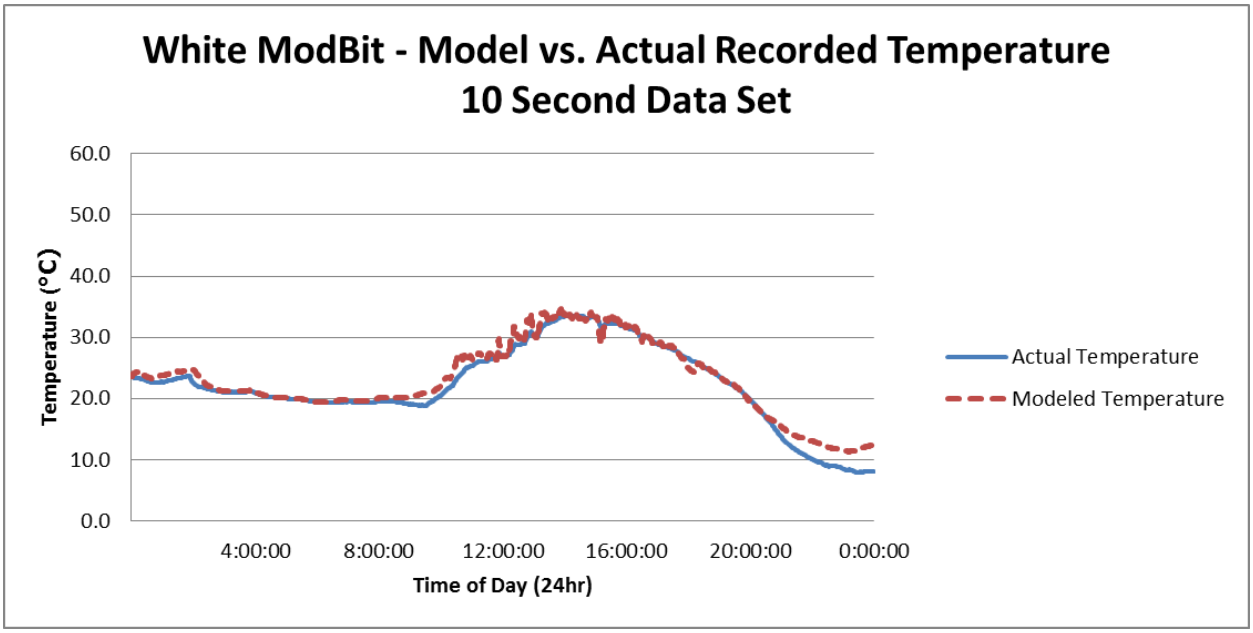
White ModBit - Model vs. Actual Recorded Temperature
10 Second Data Set
60.0
50.0
40.0
30.0
20.0
10.0
0.0
Temperature (°C)
4:00:00
8:00:00
12:00:00
16:00:00
20:00:00
0:00:00
Time of Day (24hr)
Actual Temperature
Modeled Temperature

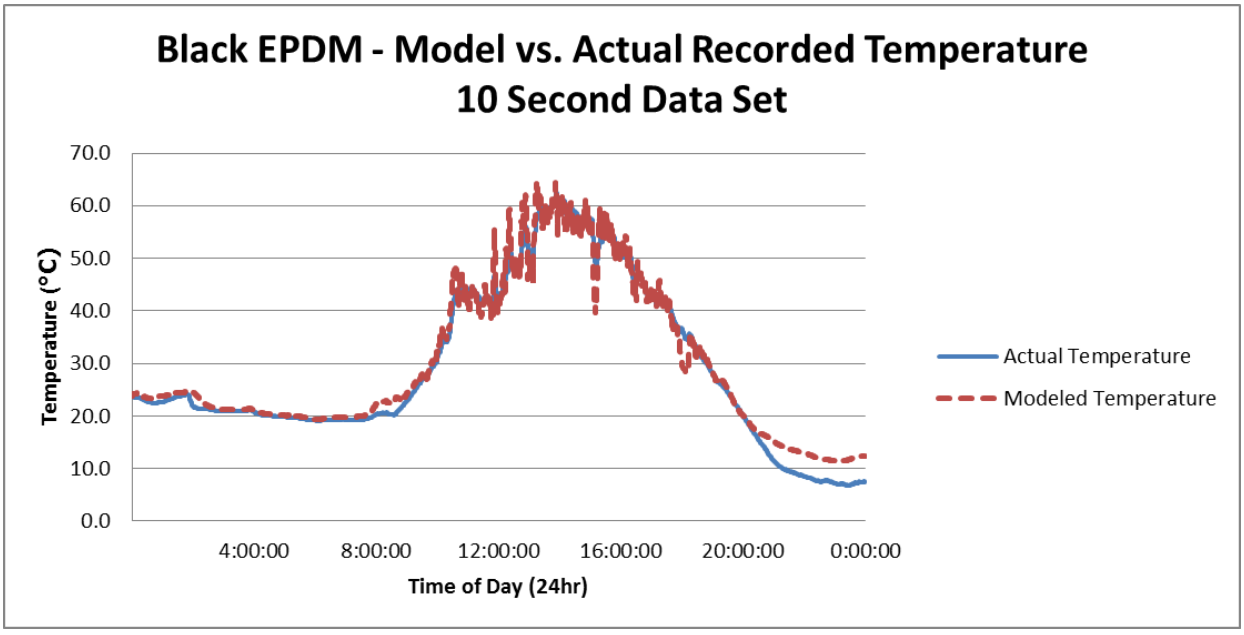
Black EPDM - Model vs. Actual Recorded Temperature
10 Second Data Set
70.0
60.0
50.0
40.0
30.0
20.0
10.0
0.0
Temperature (°C)
4:00:00
8:00:00
12:00:00
16:00:00
20:00:00
0:00:00
Time of Day (24hr)
Actual Temperature
Modeled Temperature

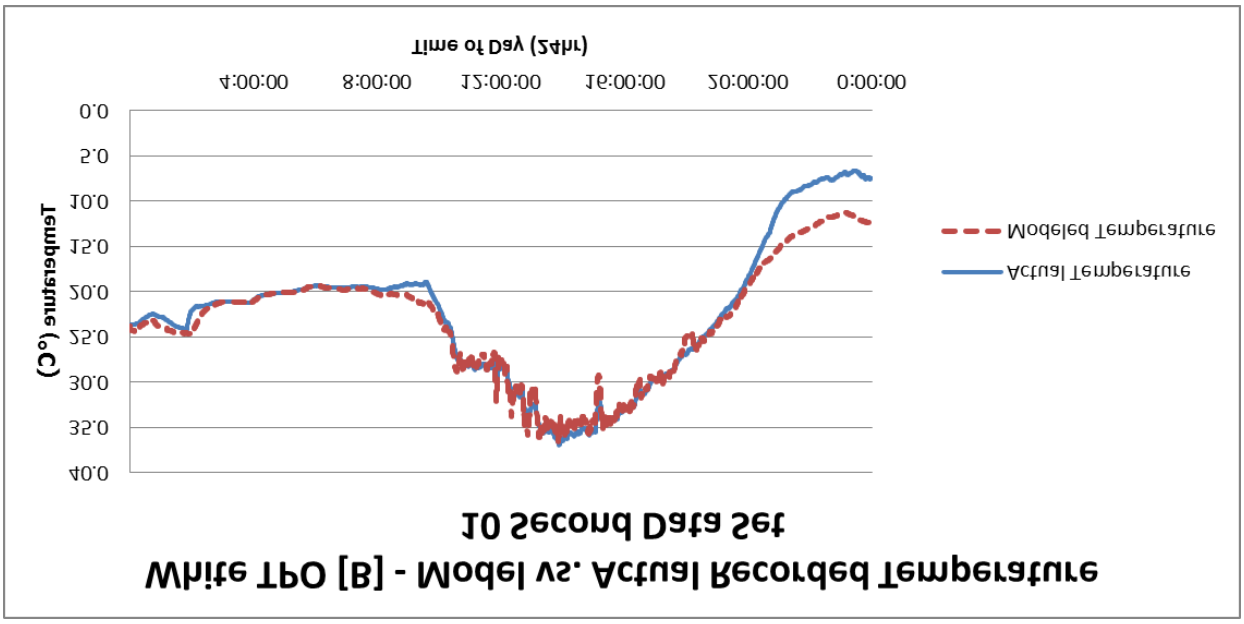
Grey PVC - Model vs. Actual Recorded Temperature
10 Second Data Set
Temperature (°C)
60.0
50.0
40.0
30.0
20.0
10.0
0.0
4:00:00
8:00:00
12:00:00
16:00:00
20:00:00
0:00:00
Time of Day (24hr)
Actual Temperature
Modeled Temperature

August 25, 2010

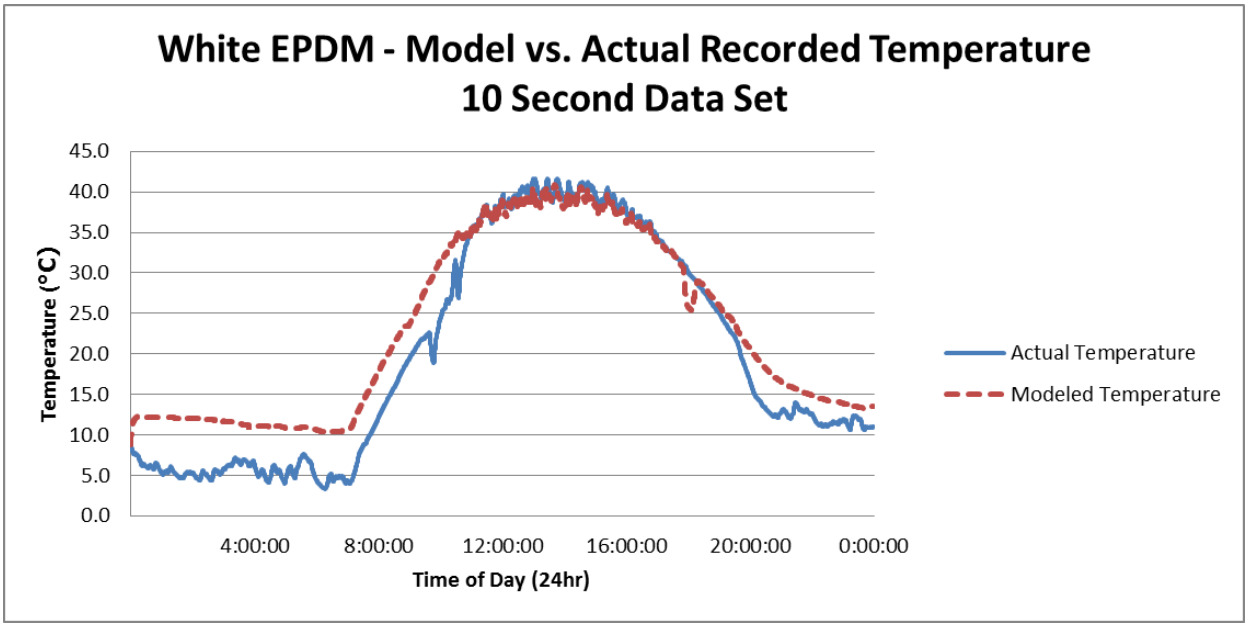
White EPDM - Model vs. Actual Recorded Temperature
10 Second Data Set
Temperature (°C)
45.0
40.0
35.0
30.0
25.0
20.0
15.0
10.0
5.0
0.0
4:00:00
8:00:00
12:00:00
16:00:00
20:00:00
0:00:00
Time of Day (24hr)
Actual Temperature
Modeled Temperature

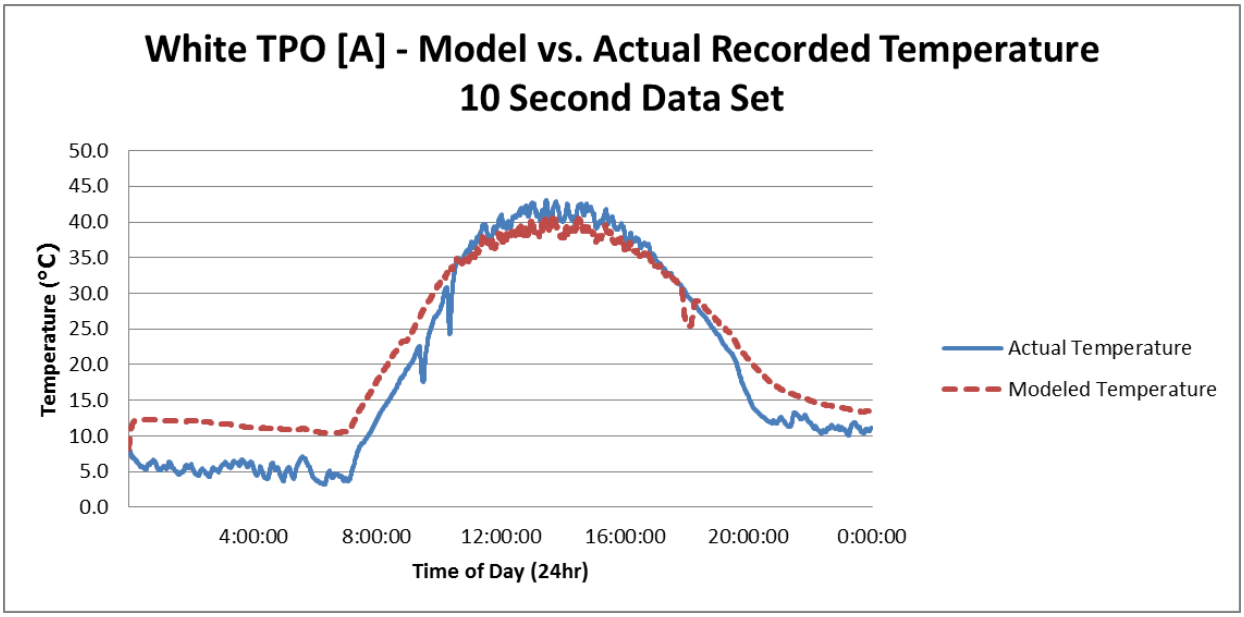
White TPO [A] - Model vs. Actual Recorded Temperature
10 Second Data Set
Temperature (°C)
50.0
45.0
40.0
35.0
30.0
25.0
20.0
15.0
10.0
5.0
0.0
4:00:00
8:00:00
12:00:00
16:00:00
20:00:00
0:00:00
Time of Day (24hr)
Actual Temperature
Modeled Temperature

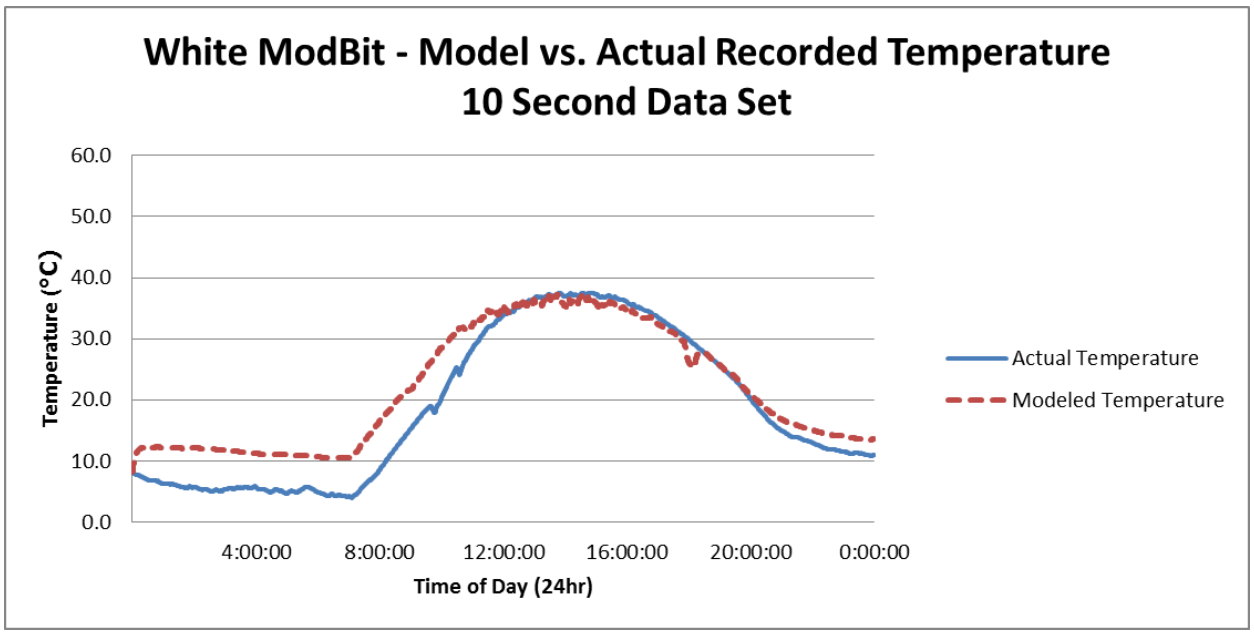
White ModBit - Model vs. Actual Recorded Temperature
10 Second Data Set
Temperature (°C)
60.0
50.0
40.0
30.0
20.0
10.0
0.0
4:00:00
8:00:00
12:00:00
16:00:00
20:00:00
0:00:00
Time of Day (24hr)
Actual Temperature
Modeled Temperature

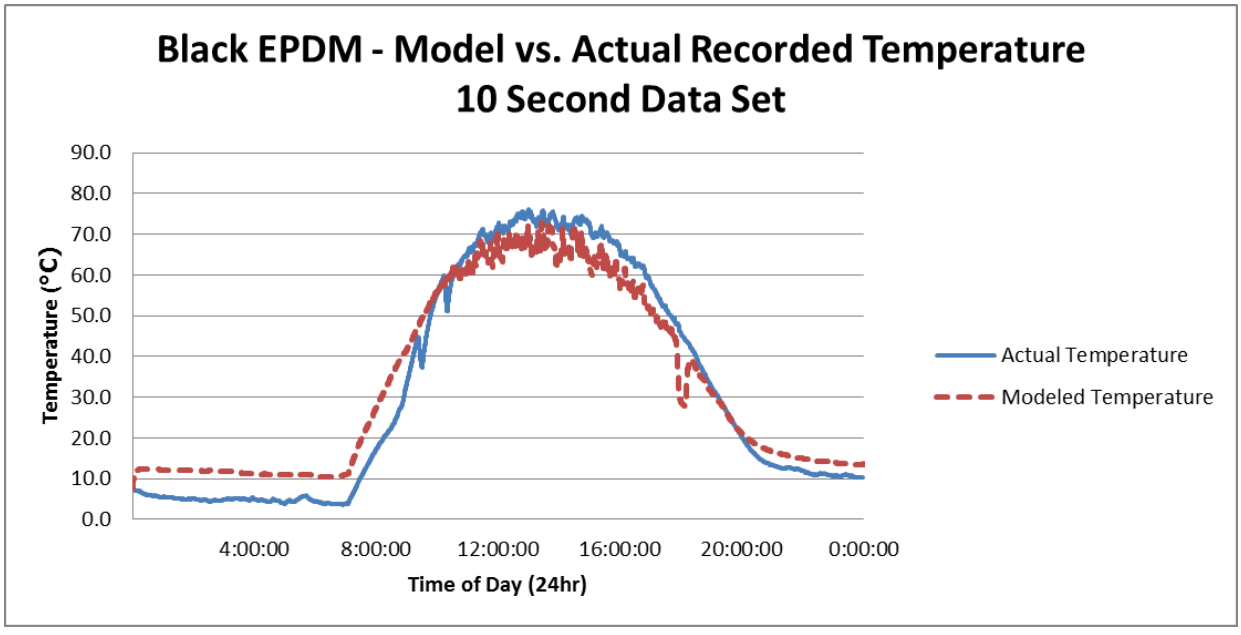
Black EPDM - Model vs. Actual Recorded Temperature
10 Second Data Set
Temperature (°C)
90.0
80.0
70.0
60.0
50.0
40.0
30.0
20.0
10.0
0.0
4:00:00
8:00:00
12:00:00
16:00:00
20:00:00
0:00:00
Time of Day (24hr)
Actual Temperature
Modeled Temperature

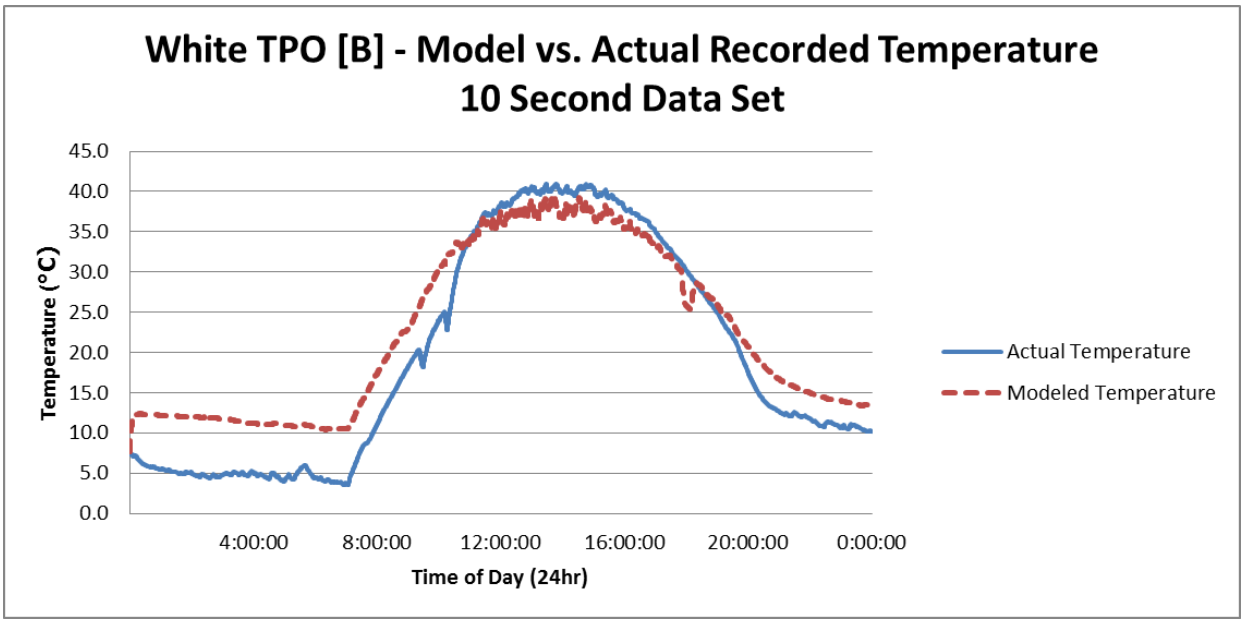
White TPO [B] - Model vs. Actual Recorded Temperature
10 Second Data Set
Temperature (°C)
45.0
40.0
35.0
30.0
25.0
20.0
15.0
10.0
5.0
0.0
4:00:00
8:00:00
12:00:00
16:00:00
20:00:00
0:00:00
Time of Day (24hr)
Actual Temperature
Modeled Temperature

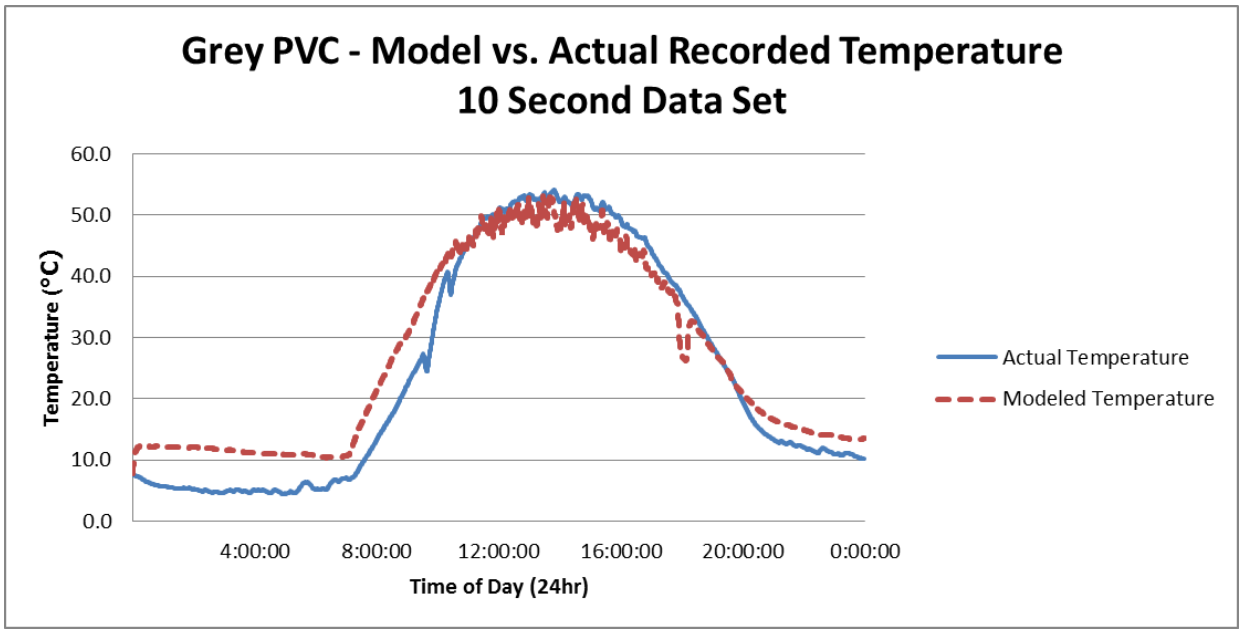
Grey PVC - Model vs. Actual Recorded Temperature
10 Second Data Set
Temperature (°C)
60.0
50.0
40.0
30.0
20.0
10.0
0.0
4:00:00
8:00:00
12:00:00
16:00:00
20:00:00
0:00:00
Time of Day (24hr)
Actual Temperature
Modeled Temperature

August 26, 2010

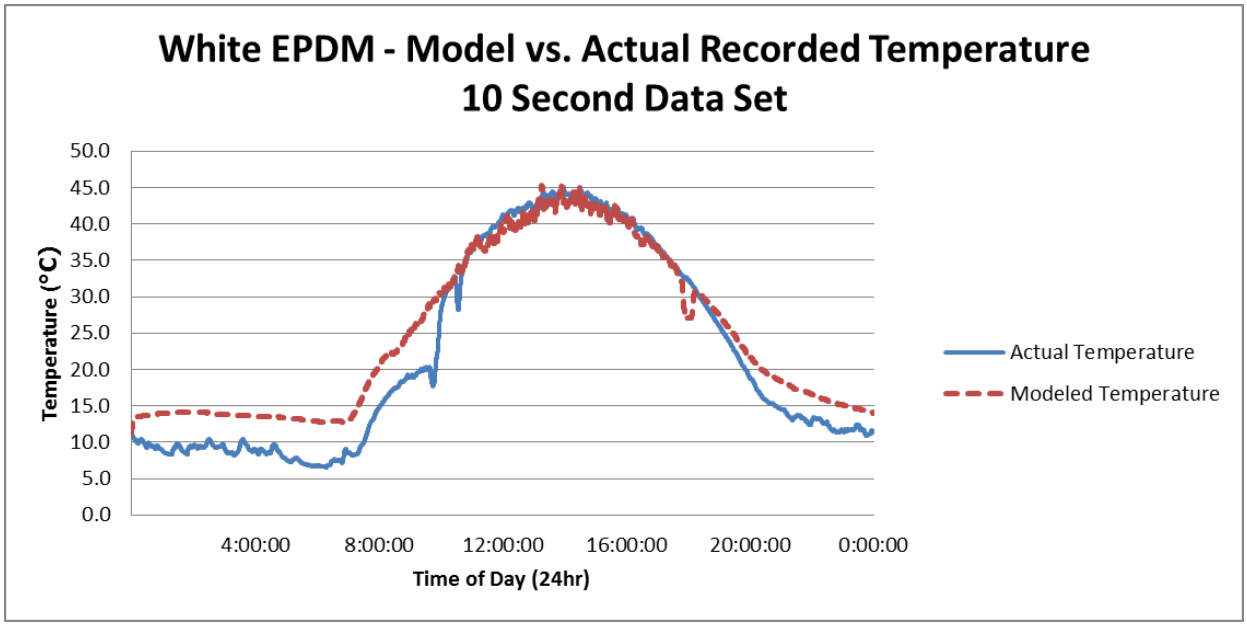
White EPDM - Model vs. Actual Recorded Temperature
10 Second Data Set
Temperature (°C)
50.0
45.0
40.0
35.0
30.0
25.0
20.0
15.0
10.0
5.0
0.0
4:00:00
8:00:00
12:00:00
16:00:00
20:00:00
0:00:00
Time of Day (24hr)
Actual Temperature
Modeled Temperature

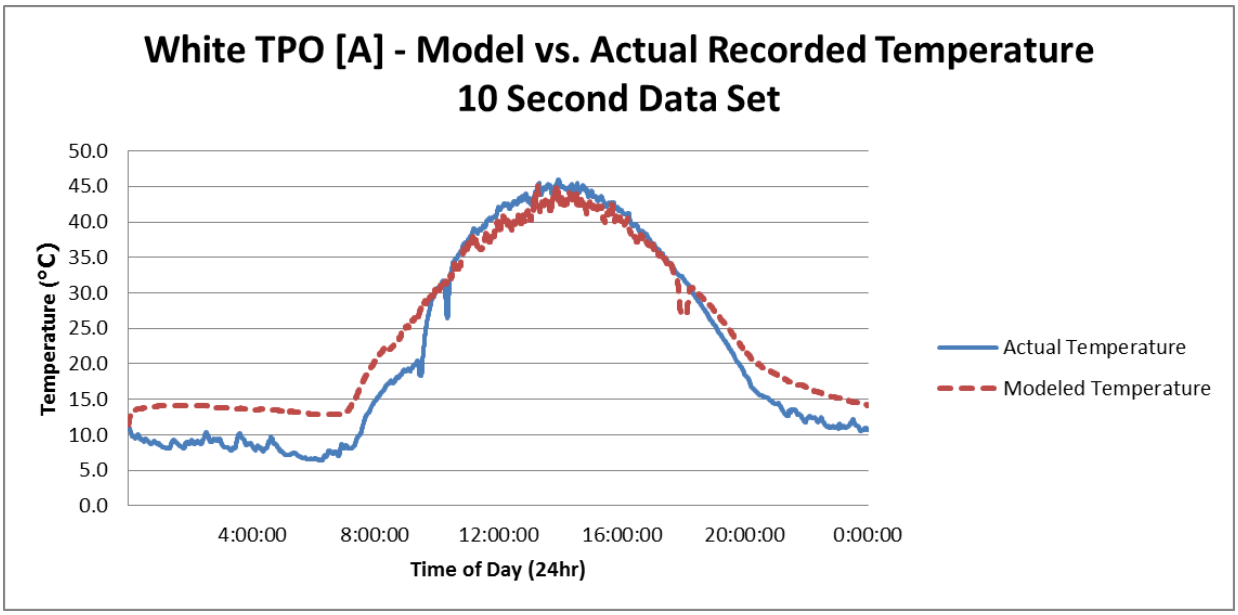
White TPO [A] - Model vs. Actual Recorded Temperature
10 Second Data Set
Temperature (°C)
50.0
45.0
40.0
35.0
30.0
25.0
20.0
15.0
10.0
5.0
0.0
4:00:00
8:00:00
12:00:00
16:00:00
20:00:00
0:00:00
Time of Day (24hr)
Actual Temperature
Modeled Temperature

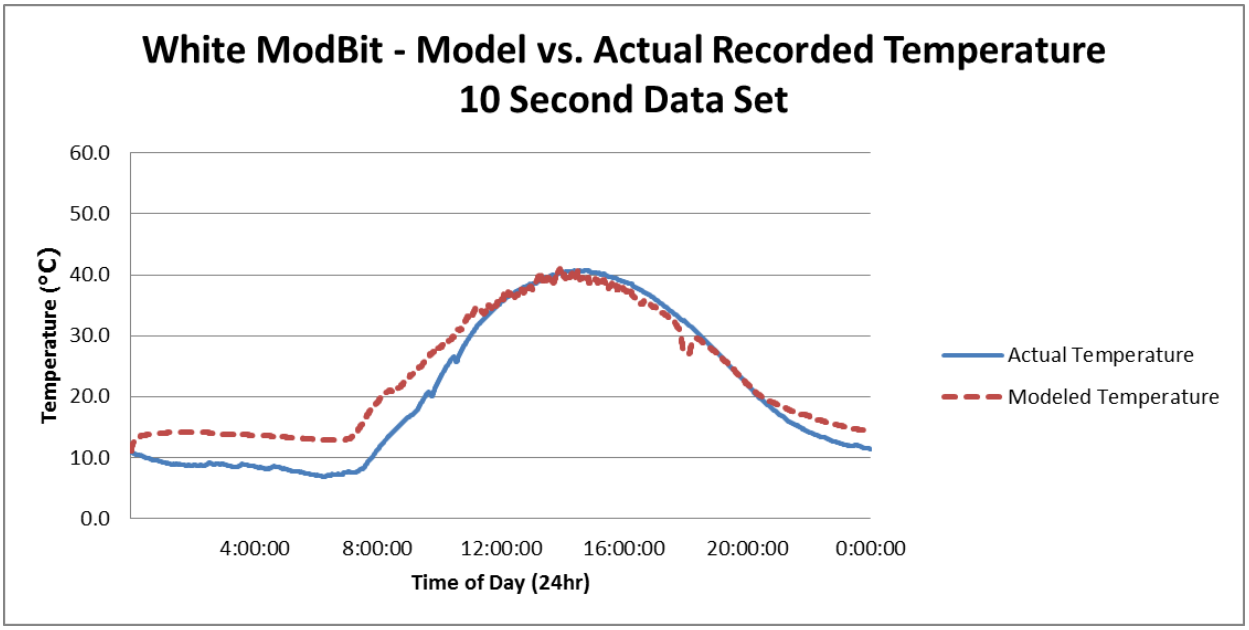
White ModBit - Model vs. Actual Recorded Temperature
10 Second Data Set
60.0
50.0
40.0
30.0
20.0
10.0
0.0
Temperature (°C)
4:00:00
8:00:00
12:00:00
16:00:00
20:00:00
0:00:00
Time of Day (24hr)
Actual Temperature
Modeled Temperature

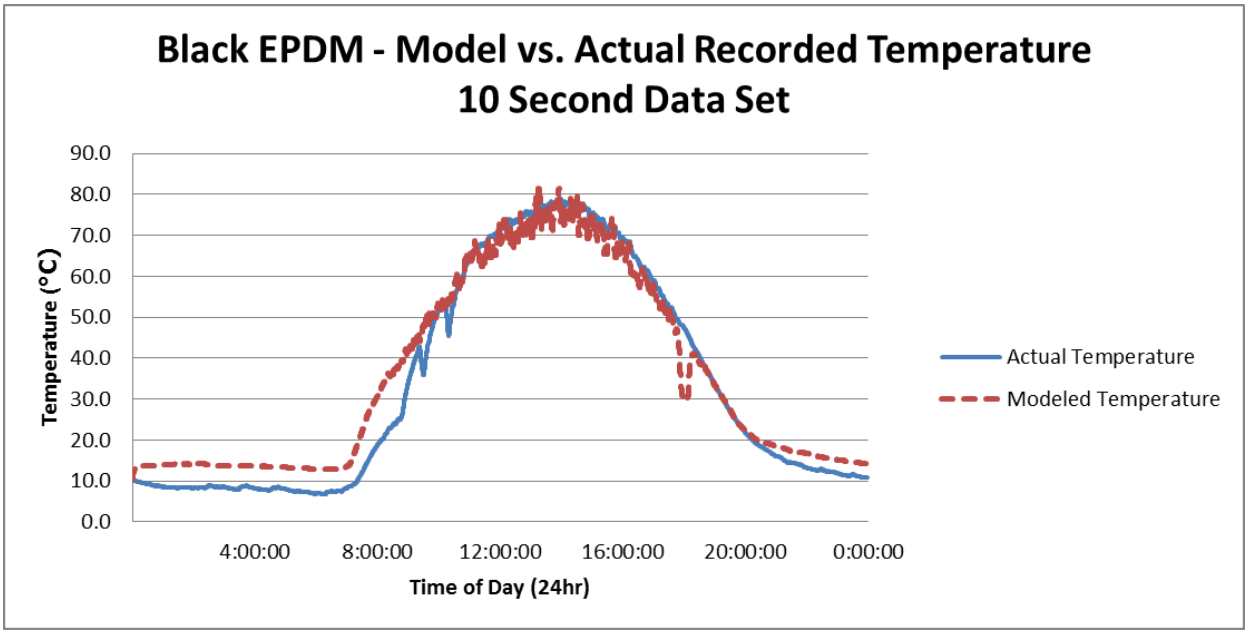
Black EPDM - Model vs. Actual Recorded Temperature
10 Second Data Set
90.0
80.0
70.0
60.0
50.0
40.0
30.0
20.0
10.0
0.0
Temperature (°C)
4:00:00
8:00:00
12:00:00
16:00:00
20:00:00
0:00:00
Time of Day (24hr)
Actual Temperature
Modeled Temperature

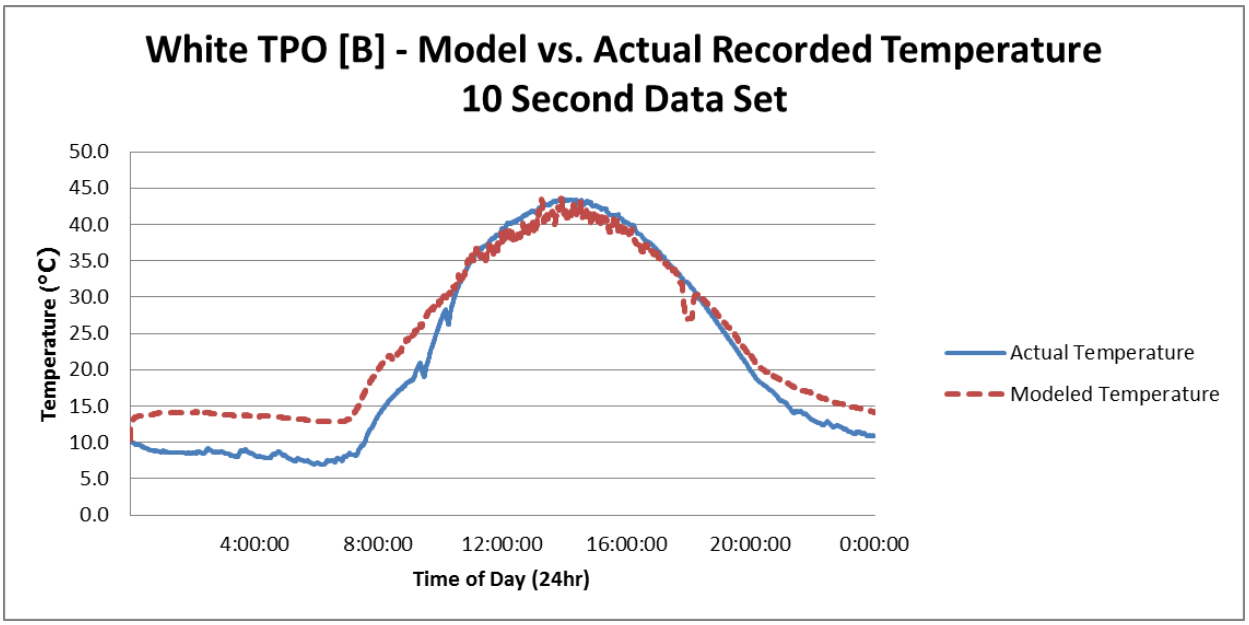
White TPO [B] - Model vs. Actual Recorded Temperature
10 Second Data Set
Temperature (°C)
50.0
45.0
40.0
35.0
30.0
25.0
20.0
15.0
10.0
5.0
0.0
4:00:00
8:00:00
12:00:00
16:00:00
20:00:00
0:00:00
Time of Day (24hr)
Actual Temperature
Modeled Temperature

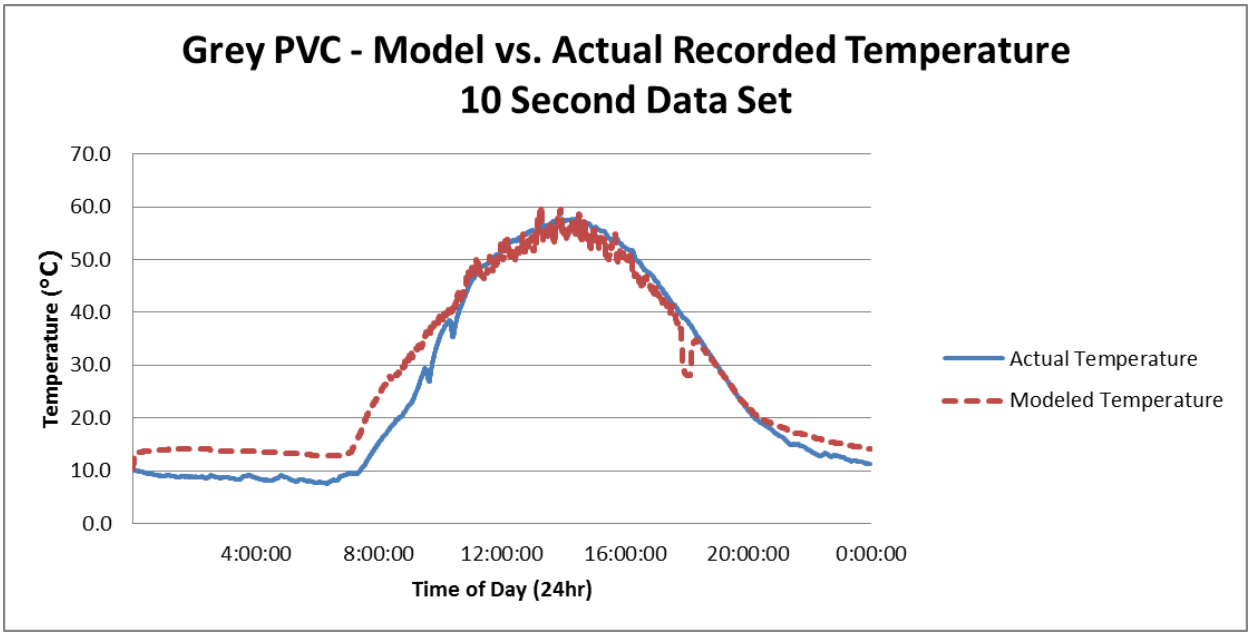
Grey PVC - Model vs. Actual Recorded Temperature
10 Second Data Set
Temperature (°C)
70.0
60.0
50.0
40.0
30.0
20.0
10.0
0.0
4:00:00
8:00:00
12:00:00
16:00:00
20:00:00
0:00:00
Time of Day (24hr)
Actual Temperature
Modeled Temperature

August 27, 2010

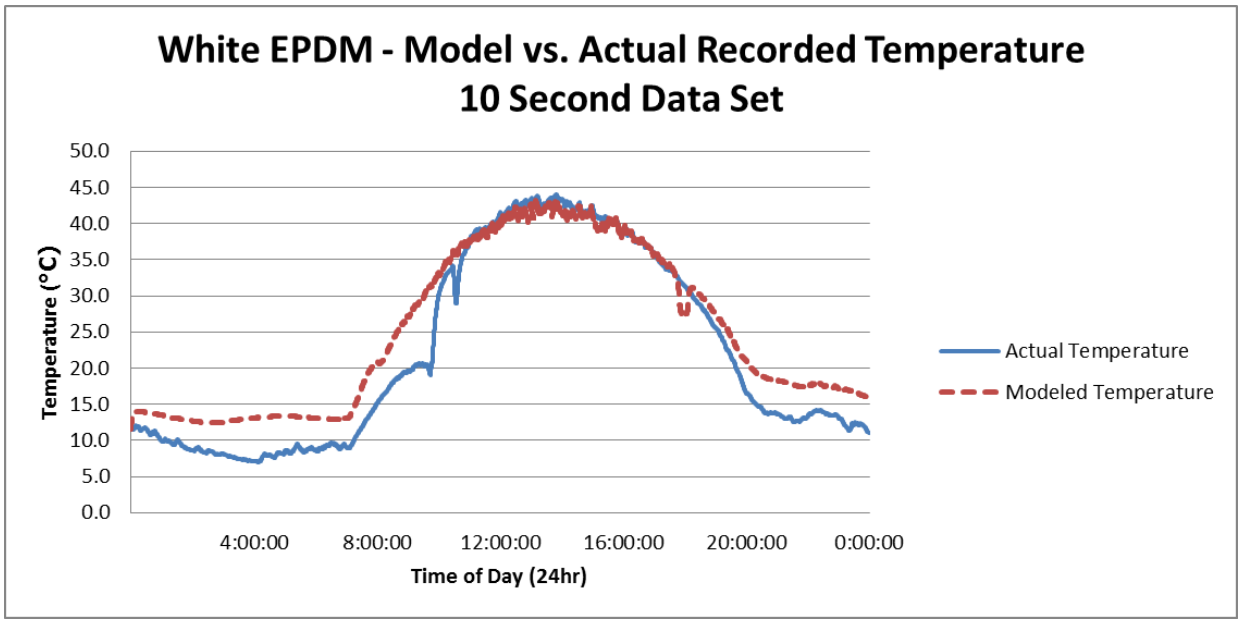
White EPDM - Model vs. Actual Recorded Temperature
10 Second Data Set
Temperature (°C)
50.0
45.0
40.0
35.0
30.0
25.0
20.0
15.0
10.0
5.0
0.0
4:00:00
8:00:00
12:00:00
16:00:00
20:00:00
0:00:00
Time of Day (24hr)
Actual Temperature
Modeled Temperature

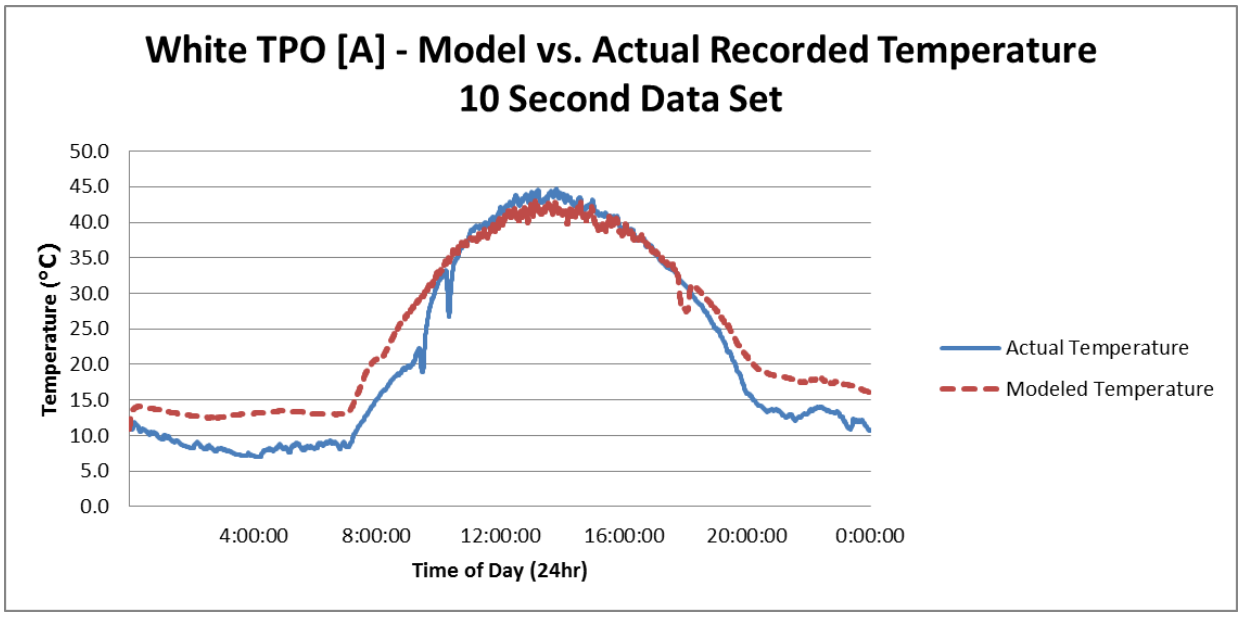
White TPO [A] - Model vs. Actual Recorded Temperature
10 Second Data Set
Temperature (°C)
50.0
45.0
40.0
35.0
30.0
25.0
20.0
15.0
10.0
5.0
0.0
4:00:00
8:00:00
12:00:00
16:00:00
20:00:00
0:00:00
Time of Day (24hr)
Actual Temperature
Modeled Temperature

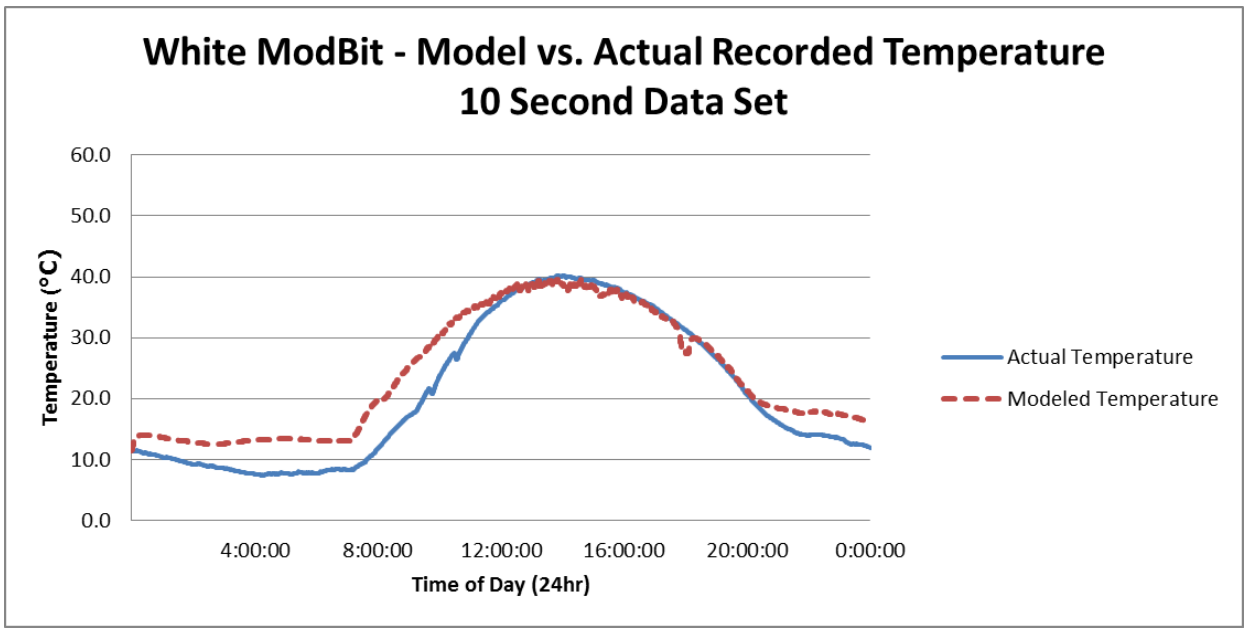
White ModBit - Model vs. Actual Recorded Temperature
10 Second Data Set
60.0
50.0
40.0
30.0
20.0
10.0
0.0
Temperature (°C)
4:00:00
8:00:00
12:00:00
16:00:00
20:00:00
0:00:00
Time of Day (24hr)
Actual Temperature
Modeled Temperature

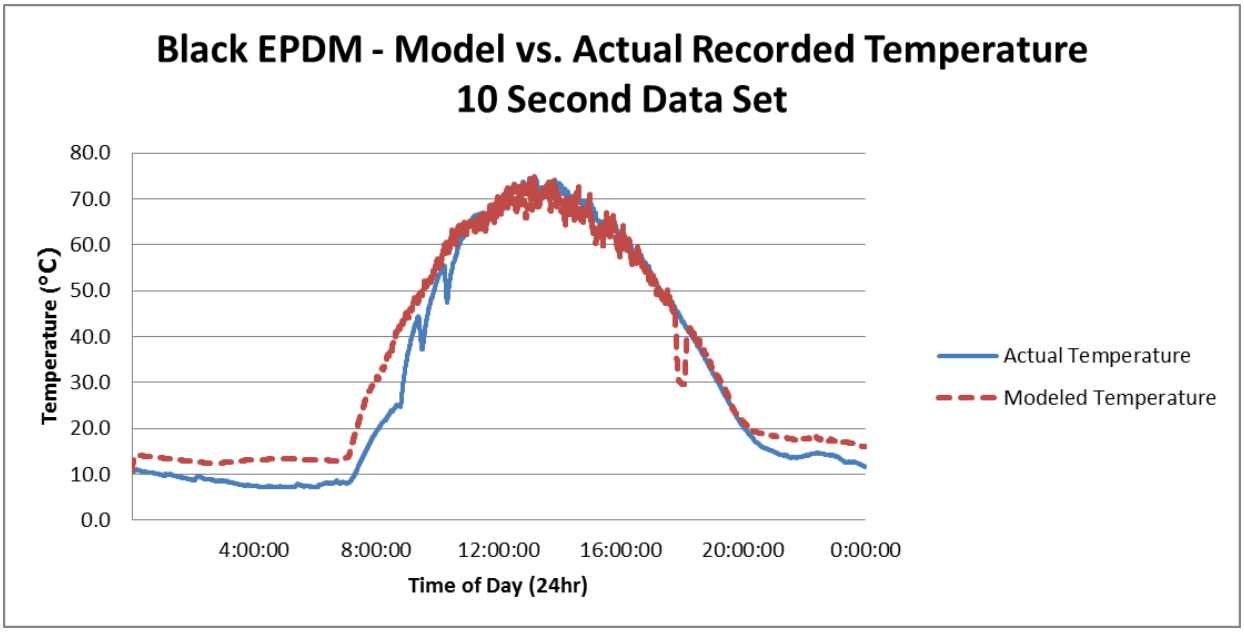
Black EPDM - Model vs. Actual Recorded Temperature
10 Second Data Set
80.0
70.0
60.0
50.0
40.0
30.0
20.0
10.0
0.0
Temperature (°C)
4:00:00
8:00:00
12:00:00
16:00:00
20:00:00
0:00:00
Time of Day (24hr)
Actual Temperature
Modeled Temperature

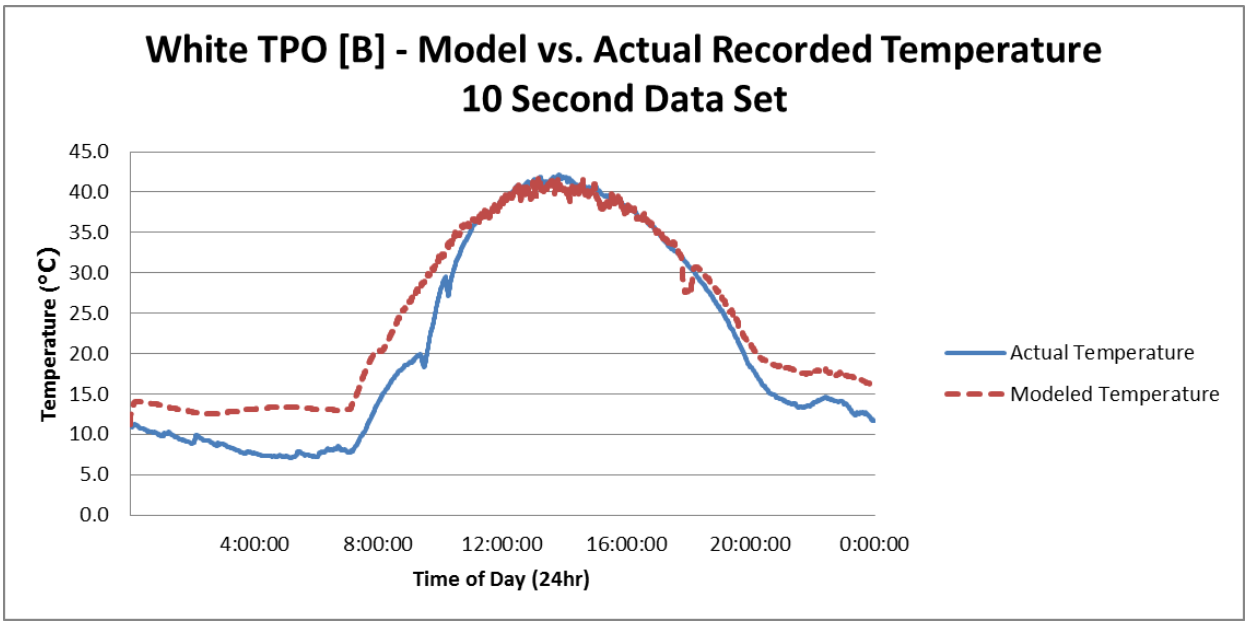
White TPO [B] - Model vs. Actual Recorded Temperature
10 Second Data Set
Temperature (°C)
45.0
40.0
35.0
30.0
25.0
20.0
15.0
10.0
5.0
0.0
4:00:00
8:00:00
12:00:00
16:00:00
20:00:00
0:00:00
Time of Day (24hr)
Actual Temperature
Modeled Temperature

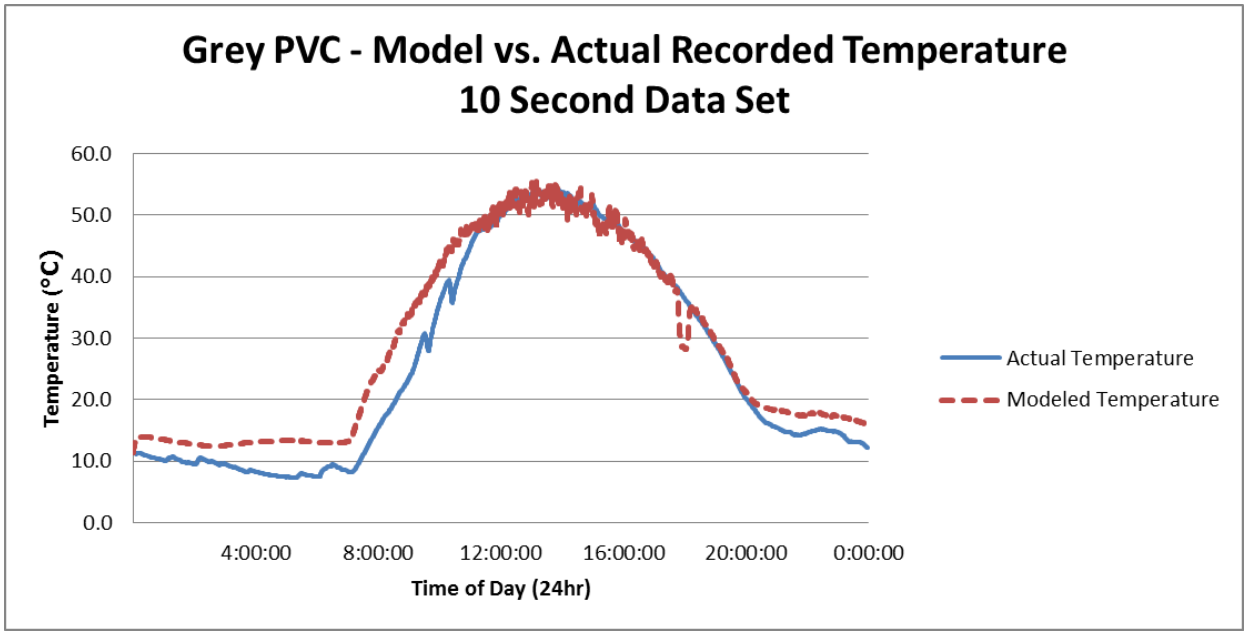
Grey PVC - Model vs. Actual Recorded Temperature
10 Second Data Set
Temperature (°C)
60.0
50.0
40.0
30.0
20.0
10.0
0.0
4:00:00
8:00:00
12:00:00
16:00:00
20:00:00
0:00:00
Time of Day (24hr)
Actual Temperature
Modeled Temperature

August 28, 2010

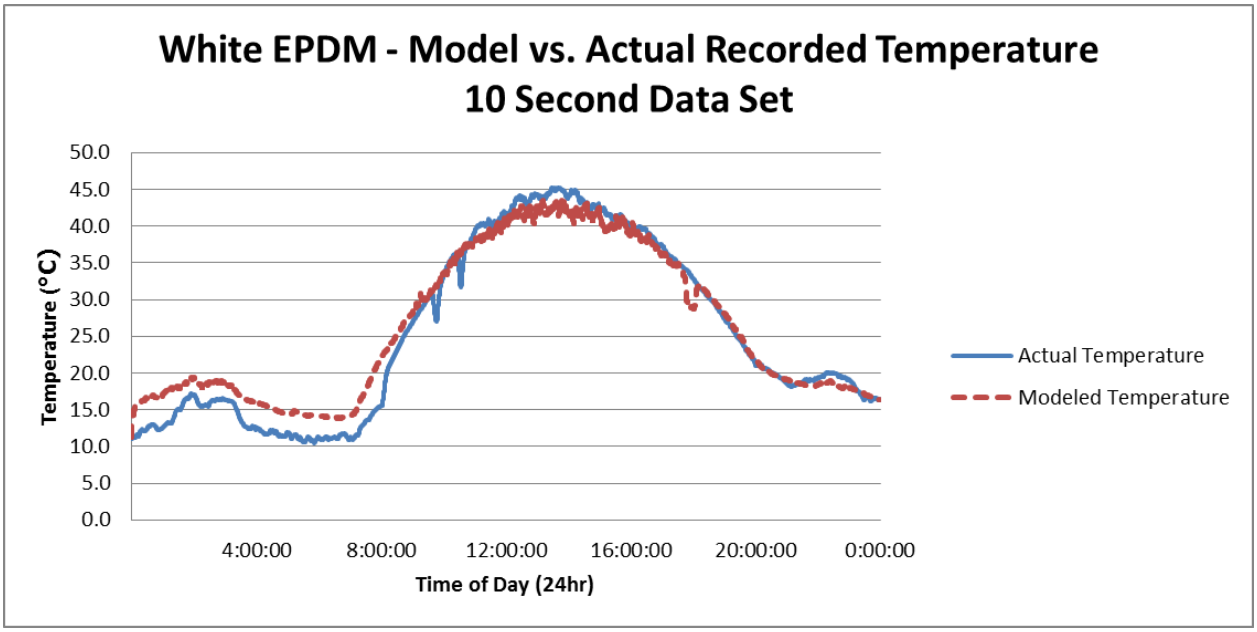
White EPDM - Model vs. Actual Recorded Temperature
10 Second Data Set
Temperature (°C)
50.0
45.0
40.0
35.0
30.0
25.0
20.0
15.0
10.0
5.0
0.0
4:00:00
8:00:00
12:00:00
16:00:00
20:00:00
0:00:00
Time of Day (24hr)
Actual Temperature
Modeled Temperature

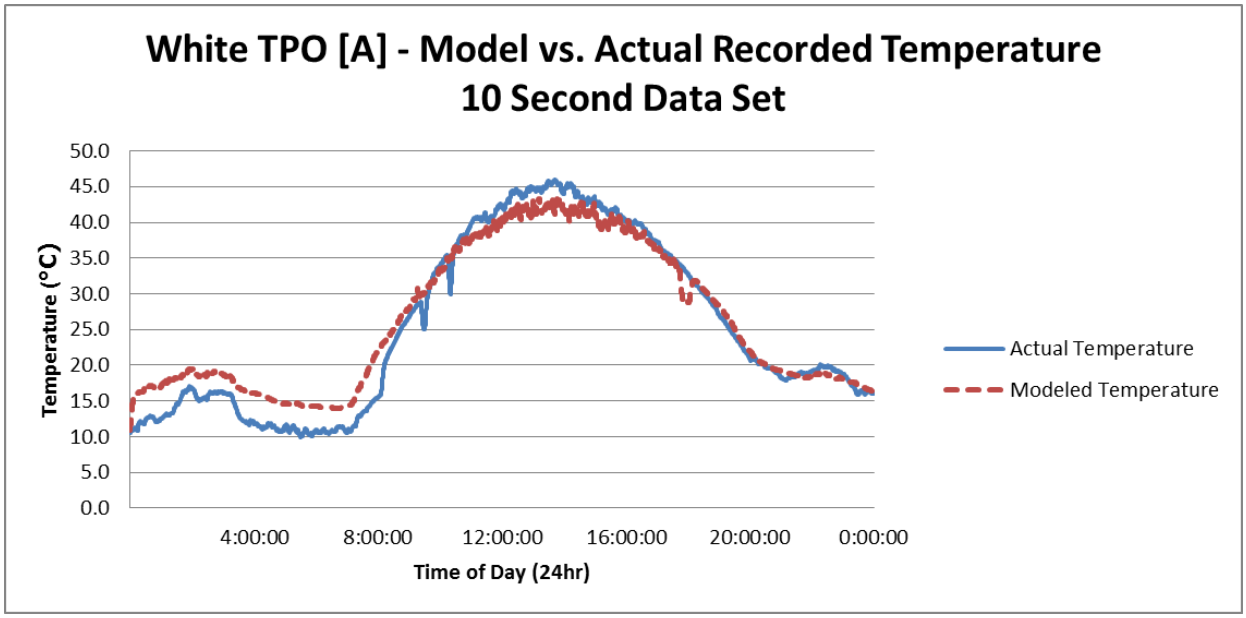
White TPO [A] - Model vs. Actual Recorded Temperature
10 Second Data Set
Temperature (°C)
50.0
45.0
40.0
35.0
30.0
25.0
20.0
15.0
10.0
5.0
0.0
4:00:00
8:00:00
12:00:00
16:00:00
20:00:00
0:00:00
Time of Day (24hr)
Actual Temperature
Modeled Temperature

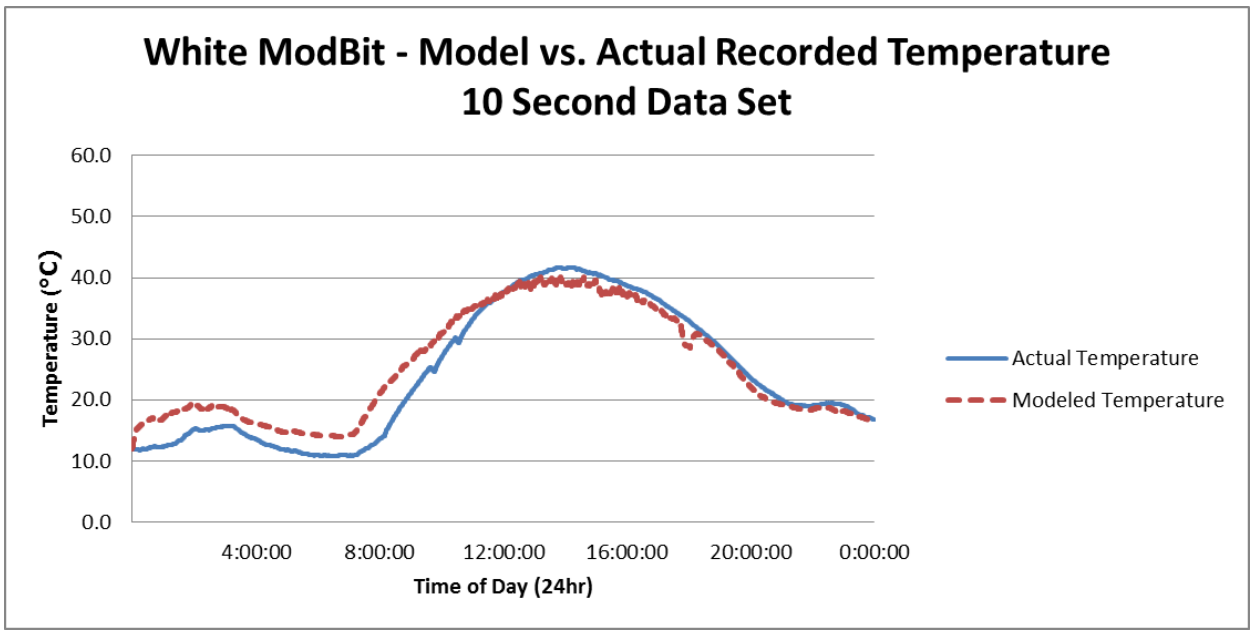
White ModBit - Model vs. Actual Recorded Temperature
10 Second Data Set
Temperature (°C)
60.0
50.0
40.0
30.0
20.0
10.0
0.0
4:00:00
8:00:00
12:00:00
16:00:00
20:00:00
0:00:00
Time of Day (24hr)
Actual Temperature
Modeled Temperature

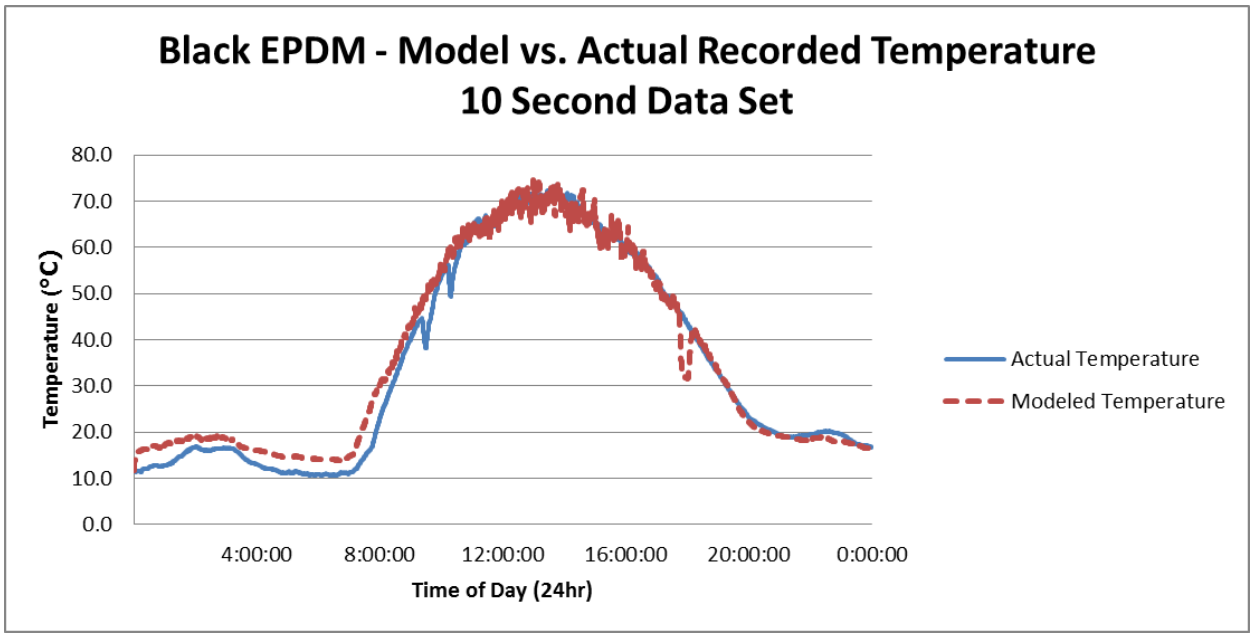
Black EPDM - Model vs. Actual Recorded Temperature
10 Second Data Set
Temperature (°C)
80.0
70.0
60.0
50.0
40.0
30.0
20.0
10.0
0.0
4:00:00
8:00:00
12:00:00
16:00:00
20:00:00
0:00:00
Time of Day (24hr)
Actual Temperature
Modeled Temperature

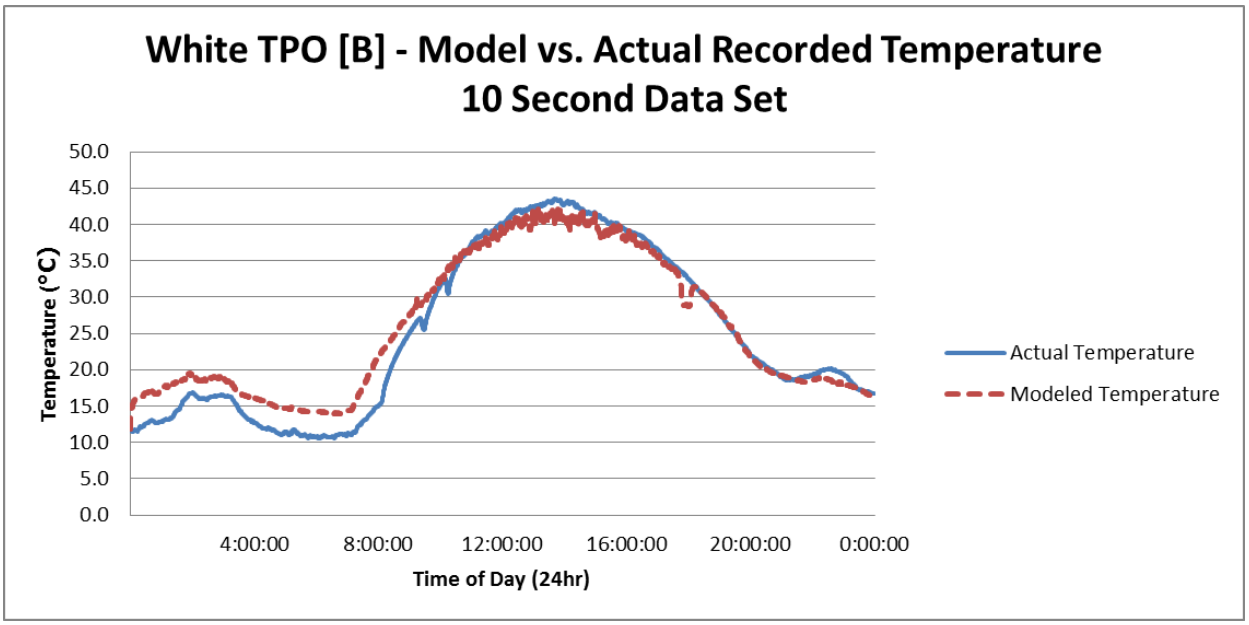
White TPO [B] - Model vs. Actual Recorded Temperature
10 Second Data Set
Temperature (°C)
50.0
45.0
40.0
35.0
30.0
25.0
20.0
15.0
10.0
5.0
0.0
4:00:00
8:00:00
12:00:00
16:00:00
20:00:00
0:00:00
Time of Day (24hr)
Actual Temperature
Modeled Temperature

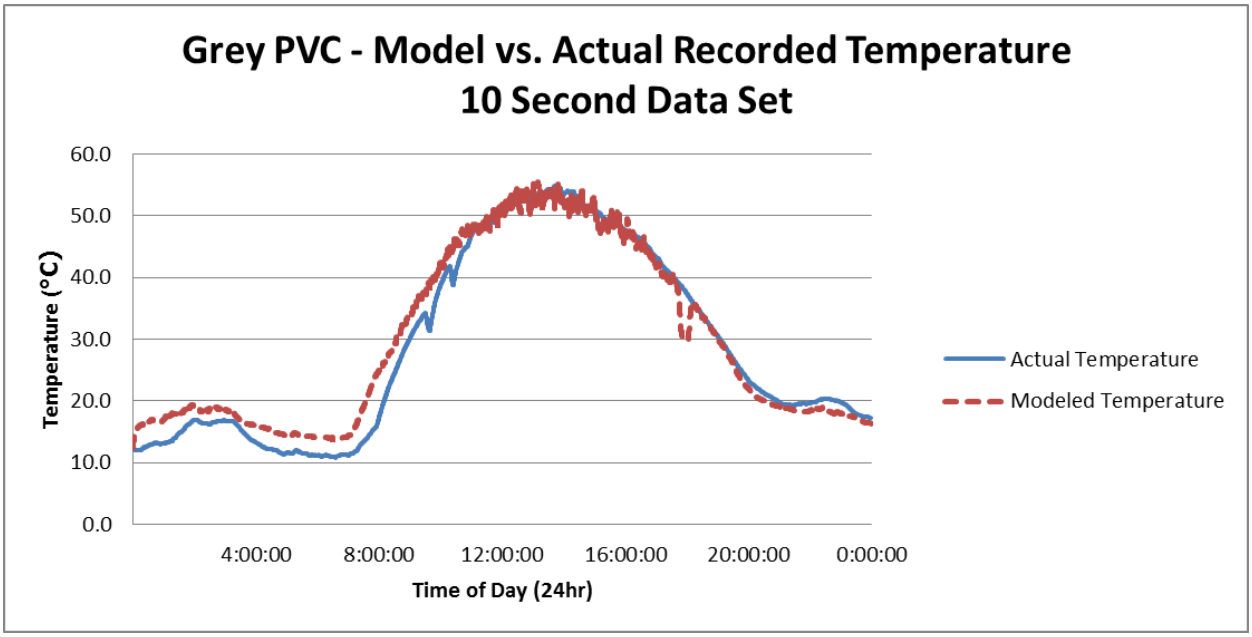
Grey PVC - Model vs. Actual Recorded Temperature
10 Second Data Set
Temperature (°C)
60.0
50.0
40.0
30.0
20.0
10.0
0.0
4:00:00
8:00:00
12:00:00
16:00:00
20:00:00
0:00:00
Time of Day (24hr)
Actual Temperature
Modeled Temperature

August 30, 2010

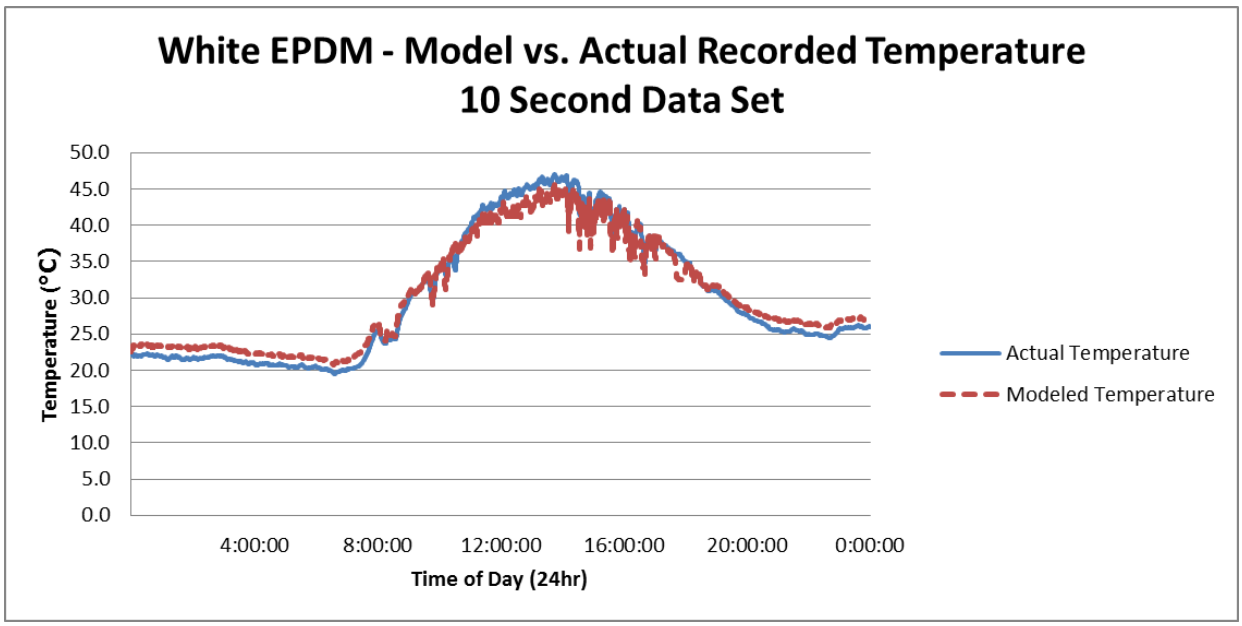
White EPDM - Model vs. Actual Recorded Temperature
10 Second Data Set
Temperature (°C)
50.0
45.0
40.0
35.0
30.0
25.0
20.0
15.0
10.0
5.0
0.0
4:00:00
8:00:00
12:00:00
16:00:00
20:00:00
0:00:00
Time of Day (24hr)
Actual Temperature
Modeled Temperature

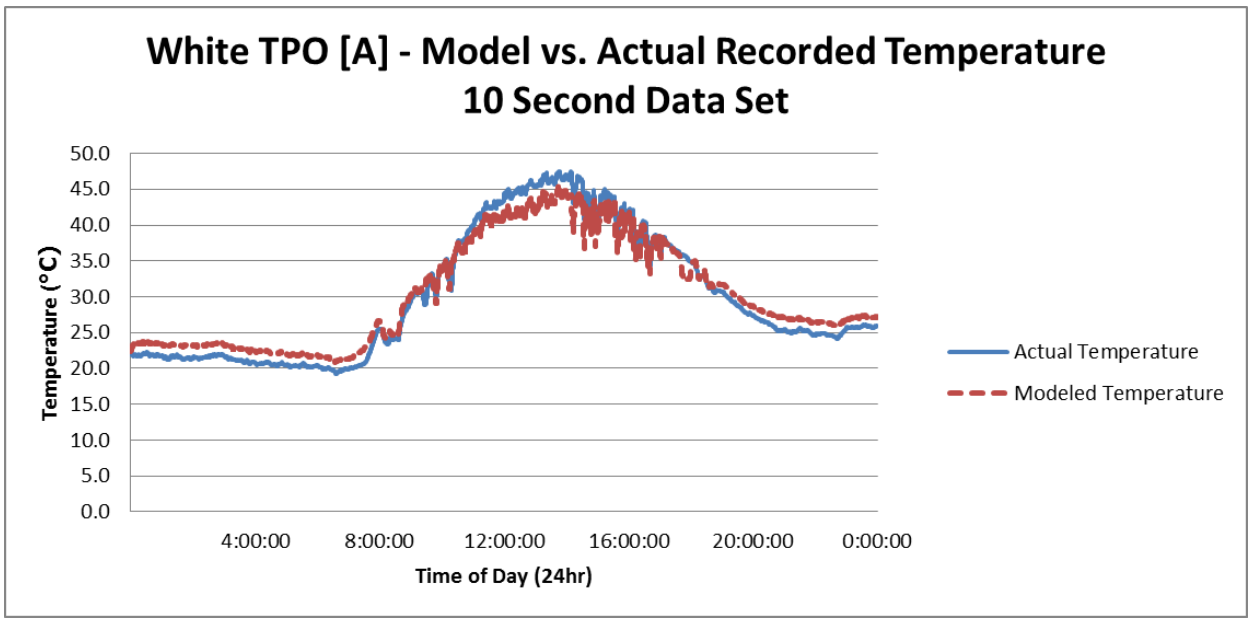
White TPO [A] - Model vs. Actual Recorded Temperature
10 Second Data Set
Temperature (°C)
50.0
45.0
40.0
35.0
30.0
25.0
20.0
15.0
10.0
5.0
0.0
4:00:00
8:00:00
12:00:00
16:00:00
20:00:00
0:00:00
Time of Day (24hr)
Actual Temperature
Modeled Temperature

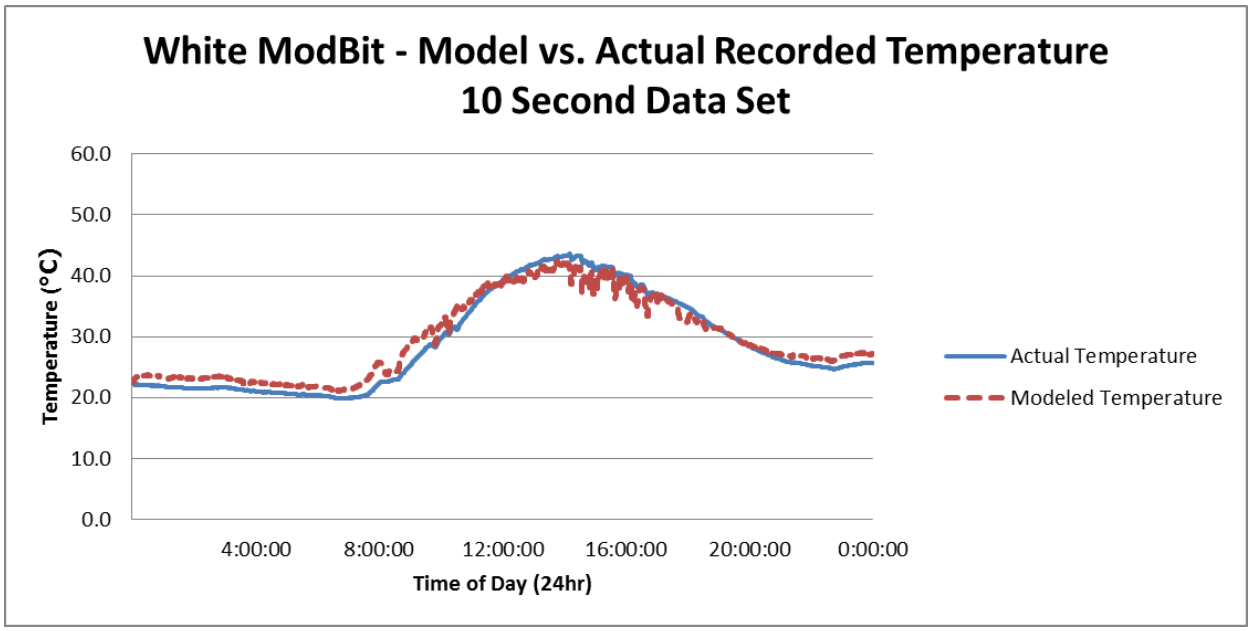
White ModBit - Model vs. Actual Recorded Temperature
10 Second Data Set
Temperature (°C)
60.0
50.0
40.0
30.0
20.0
10.0
0.0
4:00:00
8:00:00
12:00:00
16:00:00
20:00:00
0:00:00
Time of Day (24hr)
Actual Temperature
Modeled Temperature

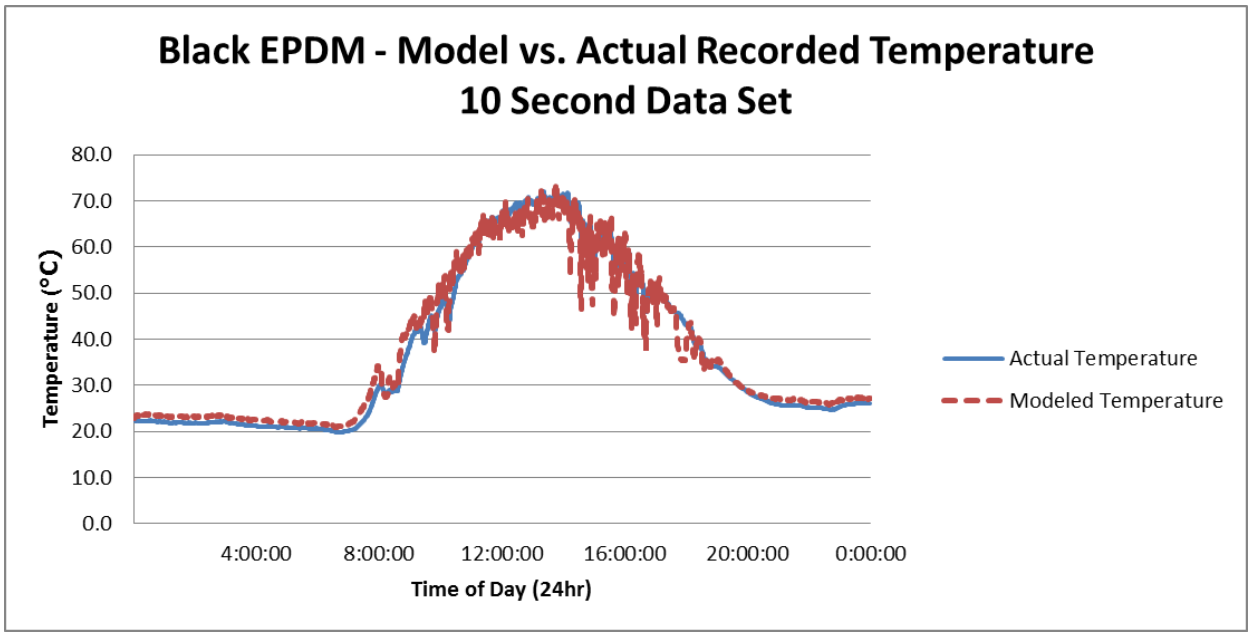
Black EPDM - Model vs. Actual Recorded Temperature
10 Second Data Set
Temperature (°C)
80.0
70.0
60.0
50.0
40.0
30.0
20.0
10.0
0.0
4:00:00
8:00:00
12:00:00
16:00:00
20:00:00
0:00:00
Time of Day (24hr)
Actual Temperature
Modeled Temperature

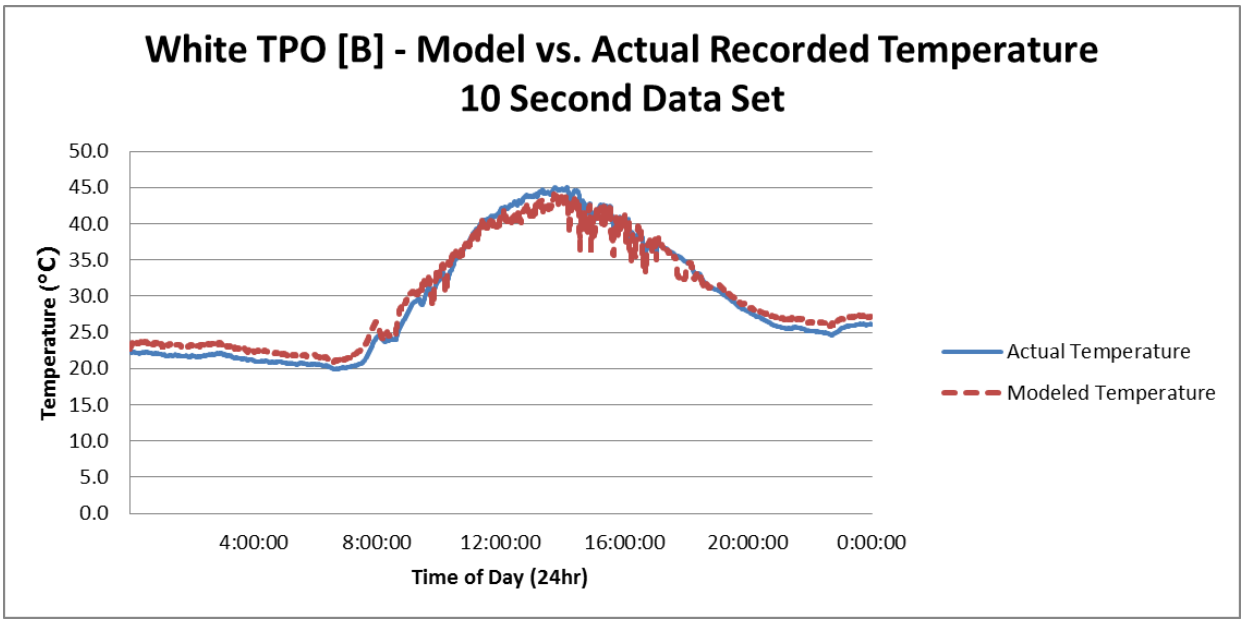
White TPO [B] - Model vs. Actual Recorded Temperature
10 Second Data Set
Temperature (°C)
50.0
45.0
40.0
35.0
30.0
25.0
20.0
15.0
10.0
5.0
0.0
4:00:00
8:00:00
12:00:00
16:00:00
20:00:00
0:00:00
Time of Day (24hr)
Actual Temperature
Modeled Temperature

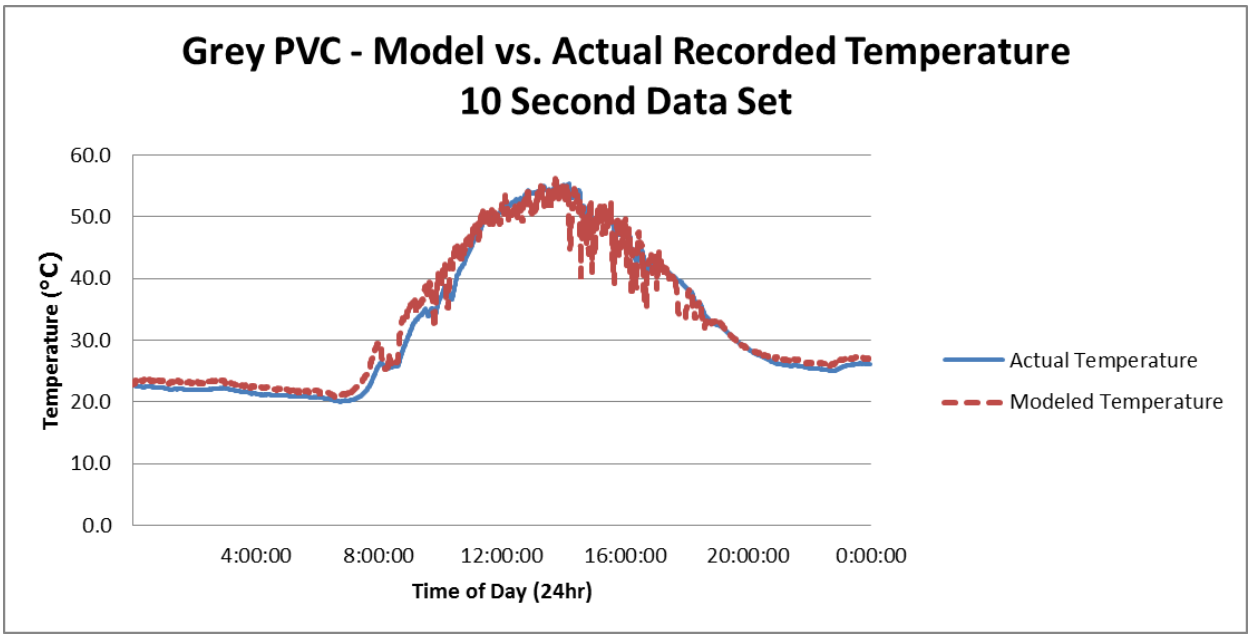
Grey PVC - Model vs. Actual Recorded Temperature
10 Second Data Set
Temperature (°C)
60.0
50.0
40.0
30.0
20.0
10.0
0.0
4:00:00
8:00:00
12:00:00
16:00:00
20:00:00
0:00:00
Time of Day (24hr)
Actual Temperature
Modeled Temperature

August 31, 2010

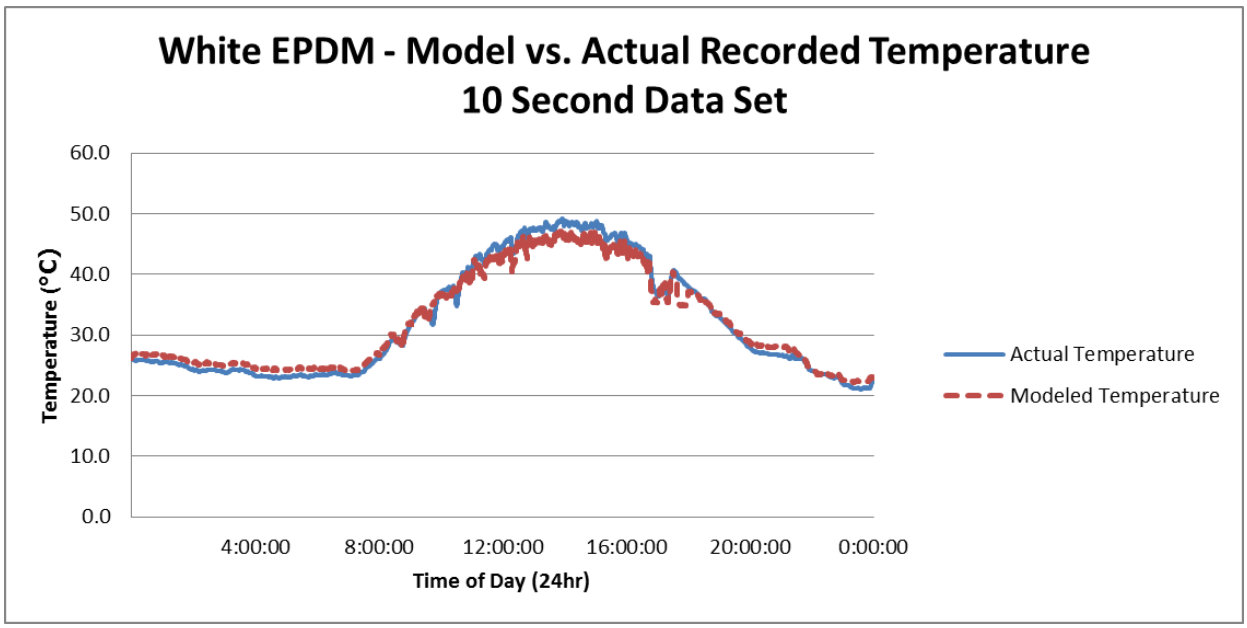
White EPDM - Model vs. Actual Recorded Temperature
10 Second Data Set
60.0
50.0
40.0
30.0
20.0
10.0
0.0
Temperature (°C)
4:00:00
8:00:00
12:00:00
16:00:00
20:00:00
0:00:00
Time of Day (24hr)
Actual Temperature
Modeled Temperature

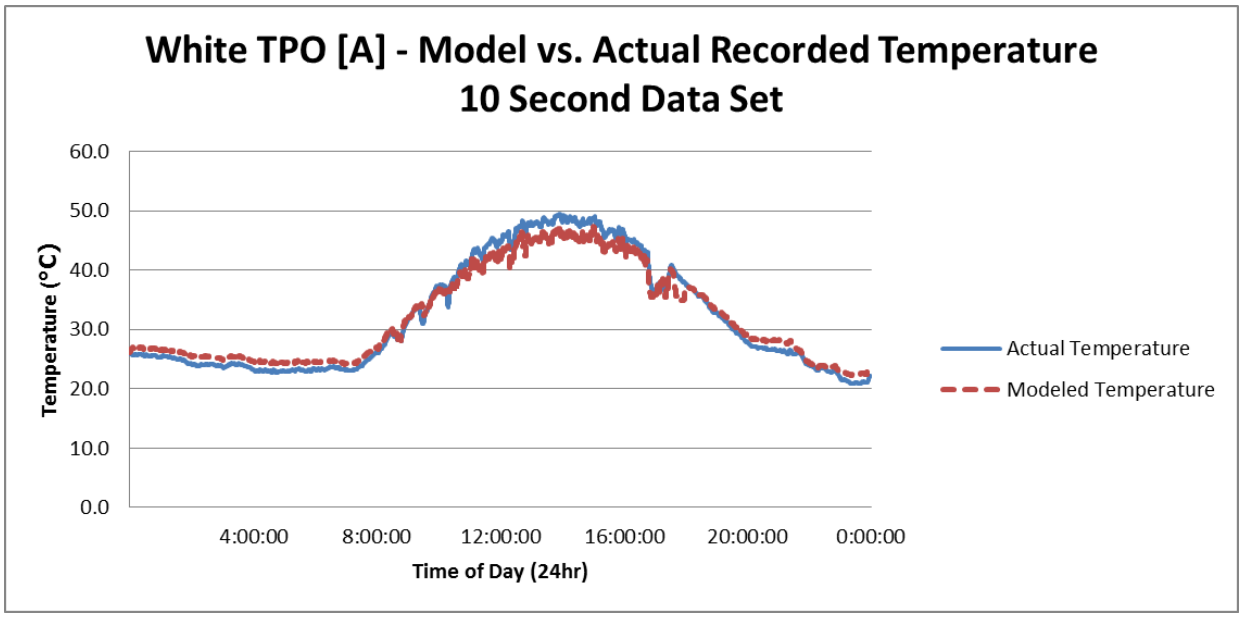
White TPO [A] - Model vs. Actual Recorded Temperature
10 Second Data Set
60.0
50.0
40.0
30.0
20.0
10.0
0.0
Temperature (°C)
4:00:00
8:00:00
12:00:00
16:00:00
20:00:00
0:00:00
Time of Day (24hr)
Actual Temperature
Modeled Temperature

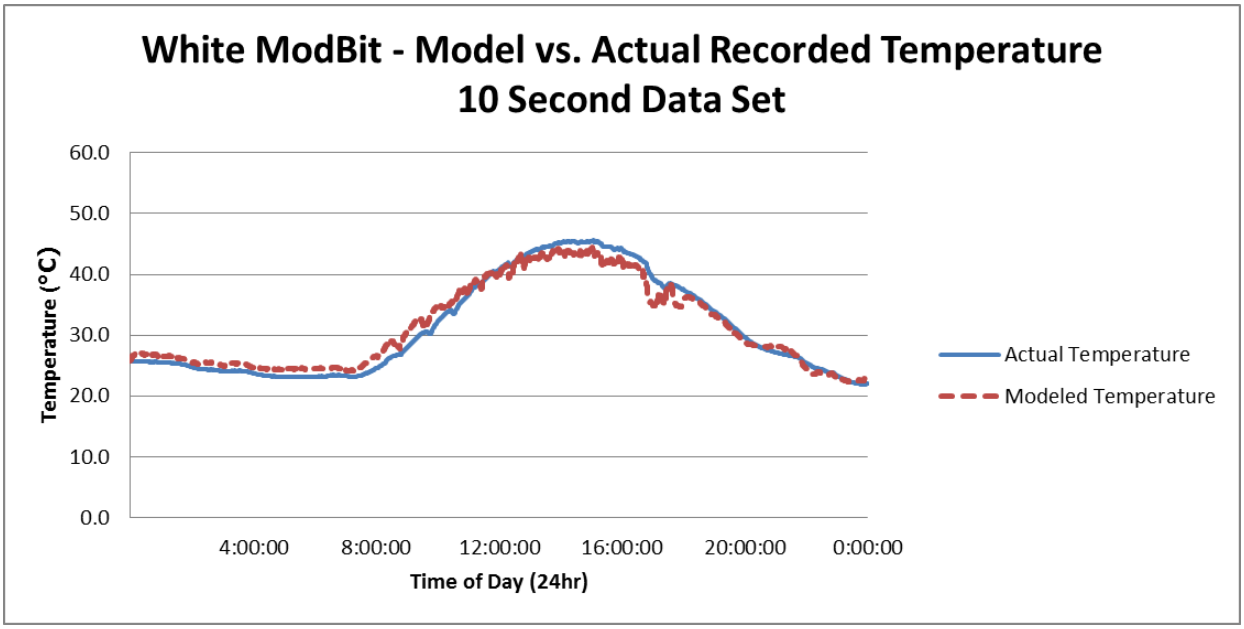
White ModBit - Model vs. Actual Recorded Temperature
10 Second Data Set
60.0
50.0
40.0
30.0
20.0
10.0
0.0
Temperature (°C)
4:00:00
8:00:00
12:00:00
16:00:00
20:00:00
0:00:00
Time of Day (24hr)
Actual Temperature
Modeled Temperature

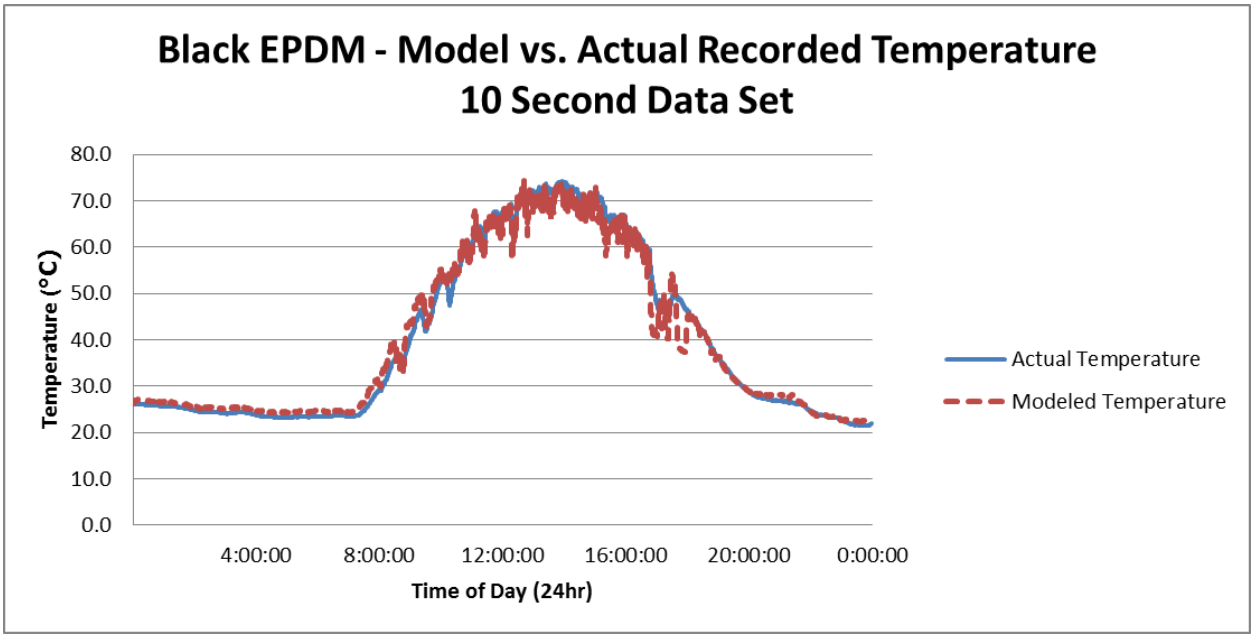
Black EPDM - Model vs. Actual Recorded Temperature
10 Second Data Set
80.0
70.0
60.0
50.0
40.0
30.0
20.0
10.0
0.0
Temperature (°C)
4:00:00
8:00:00
12:00:00
16:00:00
20:00:00
0:00:00
Time of Day (24hr)
Actual Temperature
Modeled Temperature

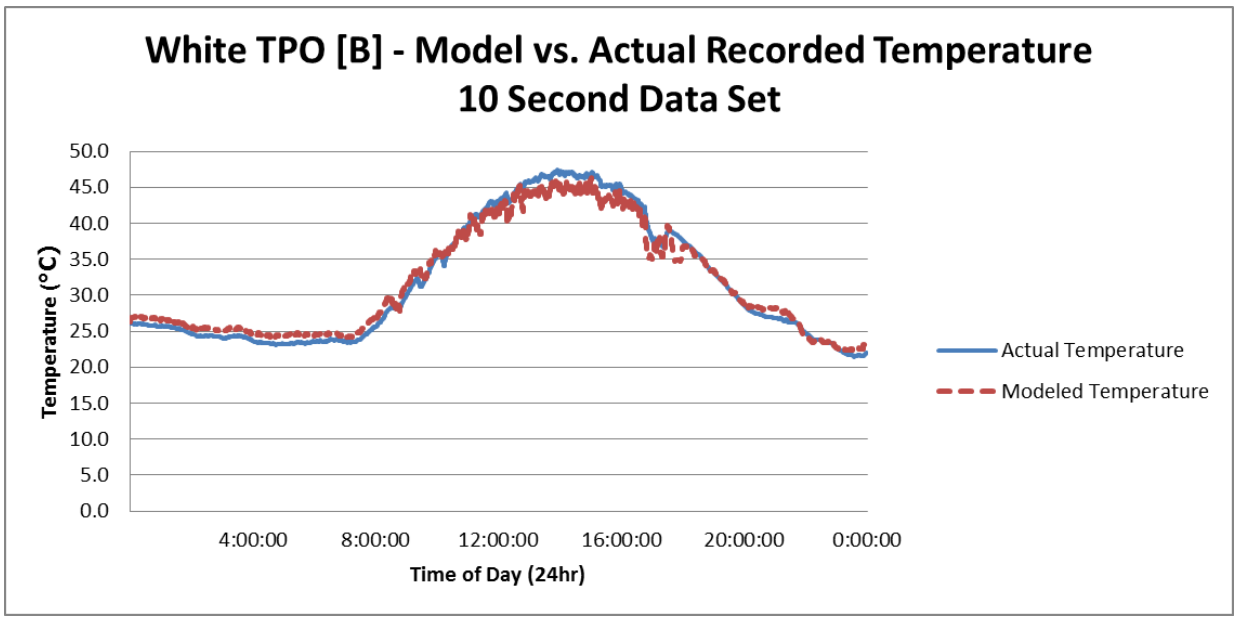
White TPO [B] - Model vs. Actual Recorded Temperature
10 Second Data Set
Temperature (°C)
50.0
45.0
40.0
35.0
30.0
25.0
20.0
15.0
10.0
5.0
0.0
4:00:00
8:00:00
12:00:00
16:00:00
20:00:00
0:00:00
Time of Day (24hr)
Actual Temperature
Modeled Temperature

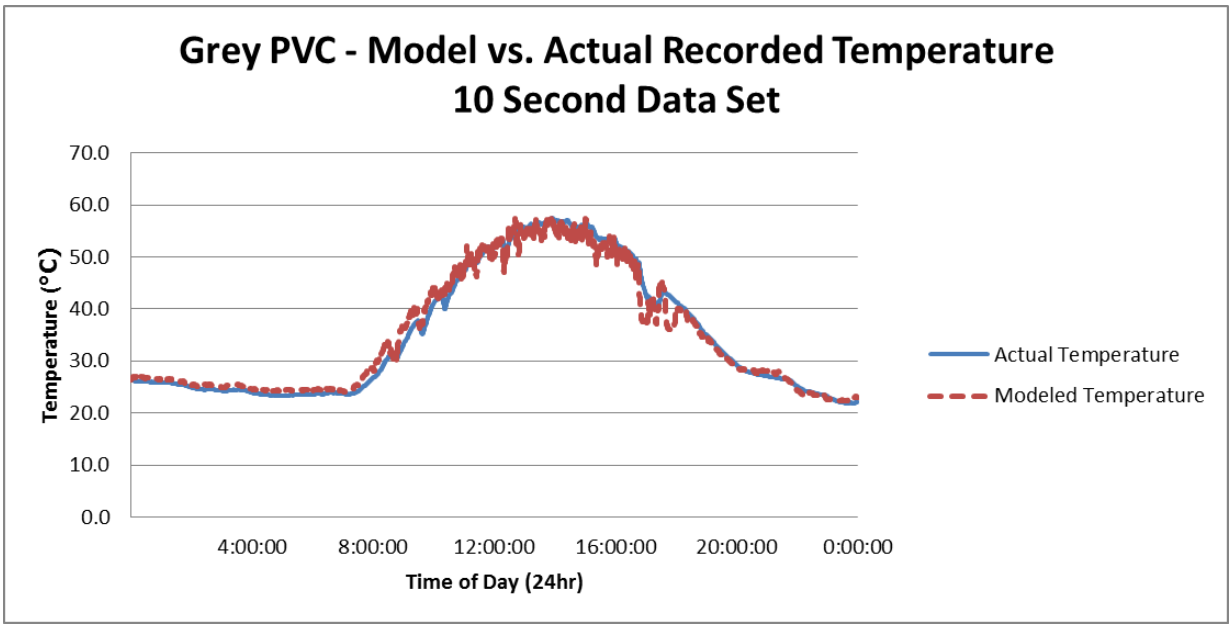
Grey PVC - Model vs. Actual Recorded Temperature
10 Second Data Set
Temperature (°C)
70.0
60.0
50.0
40.0
30.0
20.0
10.0
0.0
4:00:00
8:00:00
12:00:00
16:00:00
20:00:00
0:00:00
Time of Day (24hr)
Actual Temperature
Modeled Temperature

Appendix C

Discussion of Precipitation and Membrane Surface Condensation

This appendix discusses the issue of precipitation and roof membrane surface condensation.

There are 29 viable days of data in the August 2010 population. Within this population there are subsets of data. These subsets are days with measured precipitation, days with suspected roof membrane surface condensation, and days without precipitation or suspected roof membrane surface condensation. Suspected roof membrane condensation is more commonly referred to as dew. The precipitation, in the month of August, was almost certainly rain.

Rain and dew bring new variables into the roof membrane temperature model. The rain falls on the roof with, almost certainly, a different temperature than the temperature of the roof membrane and causes a convective heat transfer. While we did have a rain gauge present on the metrological station that reports a rainfall rate (cm/hr), there is no data for the temperature of the falling rain. Research has been made into this area[1]. However, accounting for this variable is not possible without knowing the temperature or dwell time (time a volume of rain water stays on the roof and is able to transfer heat energy).

The formation of dew on roof membranes is a common nighttime occurrence. The condensation and evaporation of dew on the roof membrane creates heat energy changes from the latent heats. Because it was impossible to entirely account for these latent heats and the augmentation of radiative properties, there is some uncertainty in the heat energy accounting.

The presence of dew on the roof was determined by calculating the dew point temperature from the modified Magnus-Tetens formula, shown in Equation 7-2. This equation was solved using the Air Temperature (T_A) and the Relative Humidity (RH) from the metrological data. The temperature calculated from this equation was then compared to the roof membrane Surface Temperature (T_S). If the roof membrane temperature was found to be equal to or lower than the calculated dew point temperature, there was a risk of dew formation.

$$T_{D=} \frac{237.7\left(\ln(RH) + \frac{17.27T_A}{237.7 + T_A}\right)}{17.27 - \left(\ln(RH) + \frac{17.27T_A}{237.7 + T_A}\right)}$$

Equation 7-2 the Magnus-Tetens formula solved for dew point temperature

The risk of dew formation was calculated in the spreadsheets. This is not a confirmation of dew formation. Nor does this calculation create an ability to determine when the condensed dew evaporated off of the surface of the roof. The only thing that can be said from this calculation is the possibility of dew formation existed if the roof membrane temperature was lower than the dew point.

Given the inability to directly determine the formation of dew and the heat transfer caused by precipitation, the impact of these events is ignored in the validation and experimental analysis for the roof membrane temperature model. Table 7-1 shows the tally of days with clear conditions, as well as the potential dew formation and recorded precipitation, along with the averaged percent error for those days within the subset. The presence of these phenomena and their potential impact is acknowledged, but will be set aside for this study. The experimental analysis is conducted with the full population of 29 days of data.

	Clear	Dew	Precipitation
Average Percent Error (%)	0.57	0.82	0.51
Days	10	17	2

Table 7-1 Effect of potential dew formation and recorded precipitation within days on model accuracy.

Reference:

1. Beyers, *Measurement of Rain Tempertaure.* Journal of Meteorology, 1949. **6**(Febuary 1949): p. 51-55.